Part II
Future Climate Change

Projected Change—Atmosphere

5

Wilhelm May, Anette Ganske, Gregor C. Leckebusch, Burkhardt Rockel, Birger Tinz and Uwe Ulbrich

Abstract

Several aspects describing the state of the atmosphere in the North Sea region are considered in this chapter. These include large-scale circulation, means and extremes in temperature and precipitation, cyclones and winds, and radiation and clouds. The climate projections reveal several pronounced future changes in the state of the atmosphere in the North Sea region, both in the free atmosphere and near the surface: amplification and an eastward shift in the pattern of NAO variability in autumn and winter; changes in the storm track with increased cyclone density over western Europe in winter and reduced cyclone density on the southern flank in summer; more frequent strong winds from westerly directions and less frequent strong winds from south-easterly directions; marked mean warming of 1.7–3.2 °C for different scenarios, with stronger warming in winter than in summer and a relatively strong warming over southern Norway; more intense extremes in daily maximum temperature and reduced extremes in daily minimum temperature, both in strength and frequency; an increase in mean precipitation during the cold season and a reduction during the warm season; a pronounced increase in the intensity of heavy daily precipitation events, particularly in winter; a considerable increase in the intensity of extreme hourly precipitation in summer; an increase (decrease) in cloud cover in the northern (southern) part of the North Sea region, resulting in a decrease (increase) in net solar radiation at the surface.

W. May (✉)
Research and Development Department, Danish Meteorological Institute (DMI), Copenhagen, Denmark
e-mail: wm@dmi.dk

W. May
Centre for Environmental and Climate Research, Lund University, Lund, Sweden
e-mail: wilhelm.may@cec.lu.se

A. Ganske
Federal Maritime and Hydrographic Agency (BSH), Hamburg, Germany
e-mail: Anette.Ganske@bsh.de

G.C. Leckebusch
School of Geography, Earth and Environmental Sciences, University of Birmingham, Birmingham, UK
e-mail: G.C.Leckebusch@bham.ac.uk

B. Rockel
Institute of Coastal Research, Helmholtz-Zentrum Geesthacht, Geesthacht, Germany
e-mail: burkhardt.rockel@hzg.de

B. Tinz
German Meteorological Service (DWD), Hamburg, Germany
e-mail: Birger.Tinz@dwd.de

U. Ulbrich
Institute of Meteorology, Freie Universität Berlin, Berlin, Germany
e-mail: ulbrich@met.fu-berlin.de

M. Quante and F. Colijn (eds.), *North Sea Region Climate Change Assessment*, Regional Climate Studies, DOI 10.1007/978-3-319-39745-0_5

5.1 Introduction

Wilhelm May

Projections of future climate change are obtained from simulations with global coupled as well as regional climate models (GCMs and RCMs, respectively). In these projections, concentrations or emissions of the well-mixed greenhouse gases and of the anthropogenic aerosol load are prescribed according to different scenarios, which take different possibilities for future developments into account. For the Fourth Assessment Report (AR4) of the Intergovernmental Panel on Climate Change (IPCC), these scenarios were based on the assumptions of the Special Report on Emission Scenarios (SRES; Nakićenović et al. 2000), while for the Fifth Assessment Report (AR5) the newly developed Representative Concentration Pathways (RCPs; Moss et al. 2010; van Vuuren et al. 2011) were applied. The RCP scenarios differ from the SRES scenarios in that they assume different pathways to specific targets of the radiative forcing by the end of the 21st century. The two families of scenarios were also applied in the Coupled Model Intercomparison Project (CMIP), the SRES scenarios in phase 3 (CMIP3; Meehl et al. 2007a) and the RCP scenarios in phase 5 of the project (CMIP5; Taylor et al. 2012).

In the contributions of IPCC Working Group I to AR4, the projections of future climate change based on the SRES scenarios are presented in two different chapters, one addressing the global aspects of climate change (Meehl et al. 2007b) and one covering the regional aspects (Christensen et al. 2007). In the latter, the projected changes in climate are described separately for different continents and/or regions, including Europe. In 2012, the AR4 was complemented by the IPCC Special Report on climate extremes (SREX), where among others the observed and projected future changes in different kinds of extreme climate events were assessed (Seneviratne et al. 2012). In Table 3.3 of the latter report, the projected future changes in temperature and precipitation extremes were summarised for different regions, including northern, central and southern Europe. Also in 2012, the European Environment Agency (EEA) published a report on climate change, impacts and vulnerability in Europe, covering several aspects of climate and climate change (EEA 2012). In particular, the report includes references to several scientific publications based on future climate projections originating from a multi-model ensemble of RCM simulations for Europe performed within the ENSEMBLES project (Van der Linden and Mitchell 2009). The SRES scenarios were applied in these simulations. Recently, a new set of future climate projections for Europe has become available within the World Climate Research Programme (WCRP) Coordinated Regional Downscaling Experiment (CORDEX; Giorgi et al. 2009), with the aim to increase both the number of RCMs and the number of driving coupled climate models compared to the ENSEMBLES project. These scenario simulations are based on the RCP scenarios, with the driving coupled climate model data taken from CMIP5. As for Europe, a specific set of climate scenarios at a horizontal resolution of 12.5 km has become available within the CORDEX initiative, with seven different RCMs to date (Jacob et al. 2014). In ENSEMBLES, the finest horizontal resolution of the climate scenarios was 25 km.

In the contributions of IPCC Working Group I to AR5, the global aspects of the projections of future climate change based on the RCP scenarios are presented in a specific chapter (Collins et al. 2013), while the regional aspects were covered differently to AR4. In AR5, future changes in the characteristics of a number of prominent climate phenomena, i.e., monsoon systems, the El Niño-Southern Oscillation, annular and dipolar modes and large-scale storm systems, and their relevance for regional climate change were assessed (Christensen et al. 2013a), with the regional changes in climate presented in the form of an atlas for as many as 18 different regions distributed over the globe (IPCC 2013). As for Europe, the northern and central parts of the continent and the Mediterranean region were distinguished. The regional aspects of the projections of future climate change were also considered in the contributions of Working Group II to AR5 (Hewitson et al. 2014a, b), again distinguishing between the aforementioned three parts of Europe. A detailed assessment of the impacts of the projected changes in climate for Europe, as for several other regions, is presented in a specific chapter of this part of AR5 (Kovats et al. 2014a, b).

Adaptation strategies are needed in response to the observed as well as to the projected changes in climate (Noble at el. 2014) and these are currently developed at the national and local level in many countries. This is typically done on the basis of national climate scenarios, which are already available for several countries and are likely to become more widespread in the future. Both the Netherlands (KNMI 2014) and Denmark (DMI 2014), for instance, have recently published reports on future climate scenarios for their countries. In Germany, future climate scenarios have even become available at a regional level through so-called regional climate offices, which cover different parts of the country. Despite their high value for the development of adaptation strategies for a particular country or part of a country, these national climate scenarios cannot easily be combined to give a consistent scenario for a larger area, such as the North Sea region. While the climate scenarios for Denmark follow closely the scenarios used in AR4 and AR5 (DMI 2014), the future climate scenarios for the Netherlands were developed by combining numerous climate scenarios originating from different climate models in accordance with the simulated rate of global warming and the simulated

change in the large-scale circulation over western Europe (KNMI 2014). This distinction resulted in four categories of climate scenario: one with moderate warming (about 1.5 °C by the end of the 21st century) and a weak influence of circulation change (i.e. a small change in the frequency of the dominant circulation patterns relative to present-day conditions); one with moderate warming and a strong influence of circulation change (i.e. a large change in the frequency of the dominant circulation patterns); one with strong warming (about 3.5 °C by the end of the 21st century) and a weak influence of circulation change; and one with strong warming and a strong influence of circulation change. The dominant circulation patterns are characterised by prevailing westerly winds during winter and prevailing easterly winds in association with high surface pressure during summer, respectively.

In this chapter, the projected changes in the atmosphere in the North Sea region are assessed on the basis of the existing literature, including the recent assessment reports referred to above. Typically, these changes have been projected for the end of the 21st century using conditions at the end of the 20th century as the baseline, but in the last few years several projections have also become available for the middle of the 21st century. Because few studies have focussed specifically on the North Sea region, most of the results described here have been extracted from climate projections for Europe (based on RCM scenario simulations from ENSEMBLES or CORDEX) or even from projections covering the whole globe (based on GCM scenario simulations from CMIP3 or CMIP5). Several aspects describing the state of the atmosphere in the North Sea region have been considered, such as features of the large-scale circulation (Sect. 5.2), the mean and extremes, primarily at daily time scales, in temperature (Sect. 5.3) and precipitation (Sect. 5.4), cyclones and winds (Sect. 5.5), and radiation and clouds (Sect. 5.6).

5.2 Large-Scale Circulation

Uwe Ulbrich, Birger Tinz, Wilhelm May

5.2.1 Prominent Climate Phenomena

Regional climate is affected by various kinds of climate phenomena. Their change under rising greenhouse gas concentrations is thus relevant for future regional climate change (e.g. Christensen et al. 2013a). Prominent climate phenomena include the monsoon systems in different parts of the tropics, the El Niño-Southern Oscillation, different annual or dipolar modes, and blocking and large-scale storm systems. The interannual variability of the climate in the North Atlantic region and specifically the North Sea region is mainly affected by two modes of variability: the North Atlantic Oscillation (NAO) and its hemispheric counterpart, the Northern Annular Mode (NAM) or Arctic Oscillation (e.g. Itoh 2008). Other large-scale factors affecting the climate in the Atlantic-European sector are atmospheric blocking and the strength and position of the Atlantic jet stream. These factors are all related to the strength and location of the Atlantic storm track and in turn to the NAO.

5.2.2 Modes of Interannual Variability

The NAO is a dipolar mode of climate variability, characterised by opposite variations in sea-level pressure between the Atlantic sub-tropical High and the Icelandic Low (e.g. Hurrell et al. 2003). Through its direct effect on westerly air flow into Europe, its link with Atlantic cyclones and atmospheric blocking, it strongly affects the climate over the North Atlantic Ocean and the surrounding continents (e.g. Hurrell and Deser 2009). The NAO can be established throughout the entire year, despite different physical mechanisms initiating and maintaining this mode of variability during winter and summer (e.g. Folland et al. 2009).

The CMIP5 simulations for the intermediate RCP4.5 scenario (i.e. 75 simulations with 37 different global climate models) show an overall amplification of the NAO up to the end of the 21st century in all seasons, with the greatest increase in autumn (Gillett and Fyfe 2013). That is, the pressure difference between the Azores High and the Icelandic Low is projected to increase in these scenario simulations. This is consistent with earlier results from the CMIP3 simulations (Miller et al. 2006). These trends, however, are generally small compared to the natural climate variability (Deser et al. 2012). It should be noted that Gillett and Fyfe's (2013) use of a particular index to define the NAO might have had an effect on the magnitude of the projected change in the NAO, as the respective centres of action over the northern and southern parts of the North Atlantic might have different positions under a changing climate. For instance, Dong et al. (2011) found a poleward and eastward shift in the pattern of NAO variability in response to greenhouse gas forcing, in line with previous findings by Ulbrich and Christoph (1999). Both the future changes in the troposphere and the stratosphere as a direct response to the prescribed greenhouse gas forcing and the associated changes in sea surface temperatures in the North Atlantic contribute to the aforementioned changes in the NAO. In a recent study, Davini and Cagnazzo (2013) pointed at the possibility of misinterpreting the NAO signals in current climate models. This is because some of the models were not able to realistically simulate the physical processes connected to the NAO, namely atmospheric

blocking and interaction with the Atlantic jet stream. This is particularly the case for those models that strongly underestimate the frequency of atmospheric blocking in the Greenland area. These shortcomings might affect studies analysing the NAO under different mean climate states, i.e. for future climate scenarios.

The NAO has been interpreted as the manifestation of an annular mode in sea-level pressure, the NAM, over the North Atlantic region (e.g. Thompson and Wallace 2000). Similar to their findings for the NAO, Gillett and Fyfe (2013) also found an overall amplification of the NAM under future climate conditions in all seasons. The increase is greatest in autumn and winter and smallest in summer. Furthermore, none of the climate models simulated a significant decrease in the NAM in any season.

5.2.3 Atmospheric Blocking

Atmospheric blocking is typically associated with persistent stationary or slowly moving high-pressure systems in the extratropics, interrupting the prevailing westerly winds and the usual track of eastward moving cyclones at these latitudes. Blocking occurs most frequently in the exit regions of the storm tracks in both hemispheres and is characterised by marked seasonal variability with high frequencies during winter and spring and low frequencies during summer and autumn (e.g. Wiedenmann et al. 2002; Masato et al. 2013). In the Atlantic-European sector blocking occurs more frequently over the North Atlantic in winter but more frequently over Europe in summer (e.g. Tyrlis and Hoskins 2008). Blocking is a major contributor to intraseasonal variability in the extratropics and can lead to seasonal climate anomalies over large parts of Europe (e.g. Trigo et al. 2004) as well as to climate extremes like cold spells in winter (e.g. Cattiaux et al. 2010) or heat waves in summer (e.g. Matsueda 2011). As previously mentioned, atmospheric blocking in the Atlantic-European sector during winter is strongly related to the NAO (Croci-Maspoli et al. 2007).

The CMIP5 simulations for the high RCP8.5 scenario show an overall decrease in the frequency of atmospheric blocking in the Atlantic-European sector in both winter (Cattiaux et al. 2013; Dunn-Sigouin and Son 2013; Masato et al. 2013) and summer (Dunn-Sigouin and Son 2013; Masato et al. 2013). The decrease in summer is accompanied by an increase on its eastern flank, leading to an eastward shift of the area with high blocking frequencies (Masato et al. 2013). While the decrease in winter is a consistent finding, regardless of how many different simulations from CMIP5 are considered or which method is used to define a blocking event, the situation is less clear in summer. In contrast to the findings of Dunn-Sigouin and Son (2013) and Masato et al. (2013), Cattiaux et al. (2013) found an increase in the frequency of blocking events in the Atlantic-European sector during summer for most of the 19 CMIP5 models considered. The other two studies considered simulations from fewer CMIP5 models and used various indices to define blocking, while Cattiaux et al. (2013) used an approach based on weather regimes, with blocking being one of them. No noticeable changes, however, were found regarding the duration of individual blocking events (Dunn-Sigouin and Son 2013). These results are consistent with findings based on the CMIP3 simulations, which show a significant decrease in blocking frequency, particularly during winter (Barnes and Hartmann 2010; Barnes et al. 2012), but are somewhat less clear. According to Woollings (2010) the effect of greenhouse gas forcing on blocking might to a large extent reflect changes in the mean state of the atmosphere rather than dynamical processes directly associated with blocking. Barnes and Hartmann (2010) demonstrated, for instance, that a poleward shift in the Atlantic jet stream could lead to a decreased frequency of atmospheric blocking in winter due to a reduction in poleward Rossby-wave breaking.

5.2.4 Sea-Level Pressure

The AR5 reported an increase in mean sea-level pressure (MSLP) over western Europe and the adjacent part of the North Atlantic in winter, with a centre over the Mediterranean region, for RCP2.6, RCP4.5 and RCP8.5 (Collins et al. 2013). Further north the MSLP is markedly reduced. In summer, on the other hand, MSLP is reduced over Europe but increased over the North Atlantic, with a centre west of the British Isles. In both cases, the magnitude of the changes in MSLP follows the strength of the radiative forcing with the smallest (largest) changes in MSLP associated with the weakest (strongest) scenario. Van den Hurk et al. (2014) obtained similar results, when regressing changes in MSLP in the Atlantic-European region on the corresponding changes in global mean temperature for a total of 245 climate change simulations from CMIP5, covering 37 different global climate models, four scenarios (including RCP6.0) and ensemble simulations for some of the models. For spring and autumn, the authors found increases in MSLP over much of the North Atlantic and western Europe and decreases further north over the Arctic, but in contrast to winter, the maximum increases are centred over the North Atlantic during the transition seasons. The projected changes in MSLP contribute to the positive trend in the NAO and the NAM mentioned in Sect. 5.2.2, particularly in autumn.

5.2.5 Jet Stream

The CMIP5 simulations show a small (about 1° for the multi-model ensemble means) poleward shift in the position of the Atlantic jet stream for the RCP8.5 scenario, while its speed remains nearly constant (Barnes and Polvani 2013). The poleward shift in the position of the Atlantic jet steam was found to reduce its north-south wobble as well as to enhance the variability of its speed (i.e. more of a pulsing of the jet stream). Woollings and Blackburn (2012) obtained consistent results based on the CMIP3 simulations, both with regard to a poleward shift in the mean position of the Atlantic jet stream and to considerable variations between individual models, particularly in winter. The poleward shifts were often small compared to the errors in the simulation of the jet stream position. Moreover, Woollings and Blackburn (2012) found that the NAO in combination with the East Atlantic pattern (EA) of the large-scale circulation can describe both the climatological changes and the inter-annual variations of both the position and strength of the Atlantic jet stream at the tropopause level. It is largely the NAO that describes shifts in the position of the jet, whereas the NAO and EA are both associated with changes in the strength of the jet.

The mechanisms underlying a poleward shift in the jet stream are still not fully understood. Changes in the activity of large-scale planetary waves or in the characteristics of the synoptic-scale transient wave activity have been suggested to contribute to the poleward shift (e.g. Collins et al. 2013). Haarsma et al. (2013) found an eastward extension to the zonal winds at 500 hPa over the eastern Atlantic Ocean and western Europe, primarily related to changes in the tropospheric temperature profile. The temperature changes in two regions were found to be important for forcing the changes in mean zonal flow: the relatively strong upper-tropospheric warming in the subtropics and the reduced surface warming in the mid-latitudes. Inter-model differences in the projected changes in mean zonal flow over the eastern Atlantic Ocean and western Europe could be partly attributed to uncertainties in the response of the North Atlantic Ocean to the anthropogenic forcing in both the CMIP3 and CMIP5 models.

5.2.6 Summary

Both the CMIP3 and CMIP5 simulations project marked future changes in various aspects of the large-scale circulation over the Atlantic-European region, of which the North Sea region is part. These changes are expected to affect the near-surface climate of the North Sea region, particularly in terms of weather and climate extremes. Examples include the impact of changes in the distribution of the phases of the NAO on the occurrence of climate extremes in Europe (e.g. Scaife at el. 2008), and the role of atmospheric blocking over the North Atlantic on the occurrence of cold winter temperatures in Europe (Sillmann et al. 2011).

5.3 Temperature

Wilhelm May

5.3.1 Global Mean Temperature

The CMIP5 simulations project a global warming with respect to the present day (1986–2005) of between 1.0 (RCP2.6) and 2.0 °C (RCP8.5) by the mid-21st century and between 1.0 (RCP2.6) and 3.7 °C (RCP8.5) by the end of the 21st century for the multi-model ensemble means (see Table 5.1). The projected changes in temperature vary considerably between models, with the uncertainty ranges depending on the magnitude of the projected multi-model changes. For the RCP2.6 scenario 90 % of the projected changes by the middle of the 21st century fall in the range 0.4–1.6 °C (the smallest mean change) and in the range 2.6–4.8 °C by the end of the 21st century for RCP8.5 (the greatest mean change). Assuming a present-day (1986–2005) global warming of 0.61 °C with respect to the pre-industrial period (1850–1900; see Collins et al. 2013), means that under the RCP2.6 scenario global warming is most likely to stay below the internationally agreed target of limiting warming to less than 2 °C with respect to pre-industrial levels throughout the 21st century, while it is most unlikely that global warming will stay below this threshold over the course of the 21st century under the RCP8.5 scenario.

5.3.2 Regional Mean Temperatures

According to Knutti and Sedláček (2012), the CMIP5 multi-model ensemble projects a so-called 'highly robust' mean surface warming in the North Sea region during both winter and summer. Part of this robust warming pattern is

Table 5.1 Projected change in annual global mean surface air temperature (°C) by the mid- and end of the 21st century relative to present day (1986–2005) for RCP2.6 (32 models), RCP4.5 (42 models) and RCP8.5 (39 models) obtained from the CMIP5 multi-model ensemble as well as the 5–95 % ranges from the models' distribution

Period	RCP2.6	RCP4.5	RCP8.5
2046–2065	1.0 (0.4–1.6)	1.4 (0.9–2.0)	2.0 (1.4–2.6)
2081–2100	1.0 (0.3–1.7)	1.8 (1.1–2.6)	3.7 (2.6–4.8)

Adapted from Collins et al. (2013, their Table 12.2)

Table 5.2 Projected changes in mean surface air temperature (°C) by the mid- and end of the 21st century relative to present day (1986–2005) for northern Europe (see Seneviratne et al. 2012, their Fig. 3.1) for RCP4.5 (42 models) and RCP8.5 (39 models) obtained from the CMIP5 simulations, in terms of winter (December through February; DJF), summer (June through August; JJA) and annual means

Period	Season	RCP4.5	RCP8.5
2046–2065	DJF	2.7 (1.8–3.5)	3.4 (2.9–4.7)
	JJA	1.8 (1.2–2.5)	2.5 (1.9–3.2)
	ANN	2.0 (1.6–2.8)	2.9 (2.4–3.5)
2081–2100	DJF	3.4 (2.6–4.4)	6.1 (5.3–7.5)
	JJA	2.2 (1.6–3.0)	4.5 (3.5–5.8)
	ANN	2.7 (2.1–3.5)	5.0 (4.3–6.3)

Data represent the median of the multi-model ensemble results and the 25th and 75th percentiles of the individual model responses. Adapted from Christensen et al. (2013a, their Table 14.1) and Christensen et al. (2013b, their Table 14.SM.1c), respectively

weaker warming over the North Sea than over the adjacent land areas, particularly in winter. This tendency is also evident in the climate change projections for northern and central Europe based on the CMIP5 multi-model ensemble presented in Annex I of AR5 (IPCC 2013). For the RCP4.5 scenario, the ensemble-mean future warming by the end of the 21st century during winter is 1–2 °C over the North Sea and 3–4 °C over eastern Scandinavia. During summer, on the other hand, future warming is 2–3 °C for the entire northern and central European land areas compared to 1–2 °C over the North Sea. The regional patterns of future warming in the North Sea region are characterised by a west-east gradient with the strongest warming in the east during winter and a north-south gradient with the strongest warming in the south during summer. Averaged over northern Europe as a whole, the annual mean warming is between 2.0 °C (RCP4.5) and 3.4 °C (RCP8.5) by the middle of the 21st century and between 2.7 °C (RCP4.5) and 5.0 °C (RCP8.5) by the end of the 21st century (see Table 5.2). The strength of future warming over northern Europe varies between seasons with stronger warming during winter (6.1 °C) than during summer (4.5 °C), for RCP8.5 by the end of the 21st century (see Table 5.2).

The characteristic warming patterns over Europe are also revealed in a multi-model ensemble based on scenario simulations at high horizontal resolution (~12.5 km) with 11 different RCMs for the RCP4.5 and RCP8.5 scenarios (Jacob et al. 2014). In summer (JJA), for instance, projected warming is 1.5–2 °C adjacent to the North Sea except for southern Norway, where the warming exceeds 2 °C (Fig. 5.1). In winter (DJF), on the other hand, warming is 1.5–2 °C in western Europe, 2–2.5 °C in central Europe and over 2.5 °C in northern Europe. In spring (MAM), warming shows a very similar pattern to that for winter, but with slightly (by ~0.5 °C) weaker warming, while in autumn (SON) warming is 2–2.5 °C over the entire area adjacent to the North Sea. Averaged over the Atlantic region, which comprises the North Sea region except for southern Norway but including Ireland, France and the north-eastern part of the Iberian Peninsula (Metzger et al. 2005), the 11 climate scenarios give an annual mean warming of 1.7 °C (RCP4.5) to 3.2 °C (RCP8.5) by the end of the 21st century (see Table 5.3). These estimates of regional warming are somewhat lower than the corresponding estimates for northern Europe (see Table 5.2), which can be explained by northern Europe extending further north than the Atlantic region and not including south-western Europe.

The national climate scenarios also show marked future warming in the respective countries in response to anthropogenic forcing. For Denmark, the CMIP5 multi-model ensemble projects a future annual mean warming of 1.0 (RCP2.6), 1.8 (RCP4.5), and 3.7 °C (RCP8.5) by the end of the 21st century (DMI 2014). These estimates are about 30 % lower than the corresponding estimates for northern Europe (see Table 5.2). For the Netherlands, the projected change in annual mean temperature by the end of the 21st century varies between 1.3 °C for the scenario with moderate warming and a weak influence of circulation change to 3.7 °C for the scenario with strong warming and a strong influence of circulation change (KNMI 2014). The projected annual mean temperature changes for the Netherlands by the mid-21st century are markedly weaker, at 1.0–2.3 °C. Similarly, a multi-model ensemble of climate projections for Germany for the mid-21st century on the basis of seven combinations of RCMs and driving GCMs, gives a warming of 1.0–1.5 °C for northern Germany under the SRES A1B scenario (Wagner et al. 2013).

5.3.3 Temperature Extremes

Changes in long-term averages for variables such as seasonal or annual mean temperature provide insight into relatively slow climatic change. However, in terms of impacts it is changes in the variability of temperature at much shorter time scales that are most relevant. For instance, weather and climate extremes at daily time scales or, in the case of extended warm spells and heat waves, at time scales of

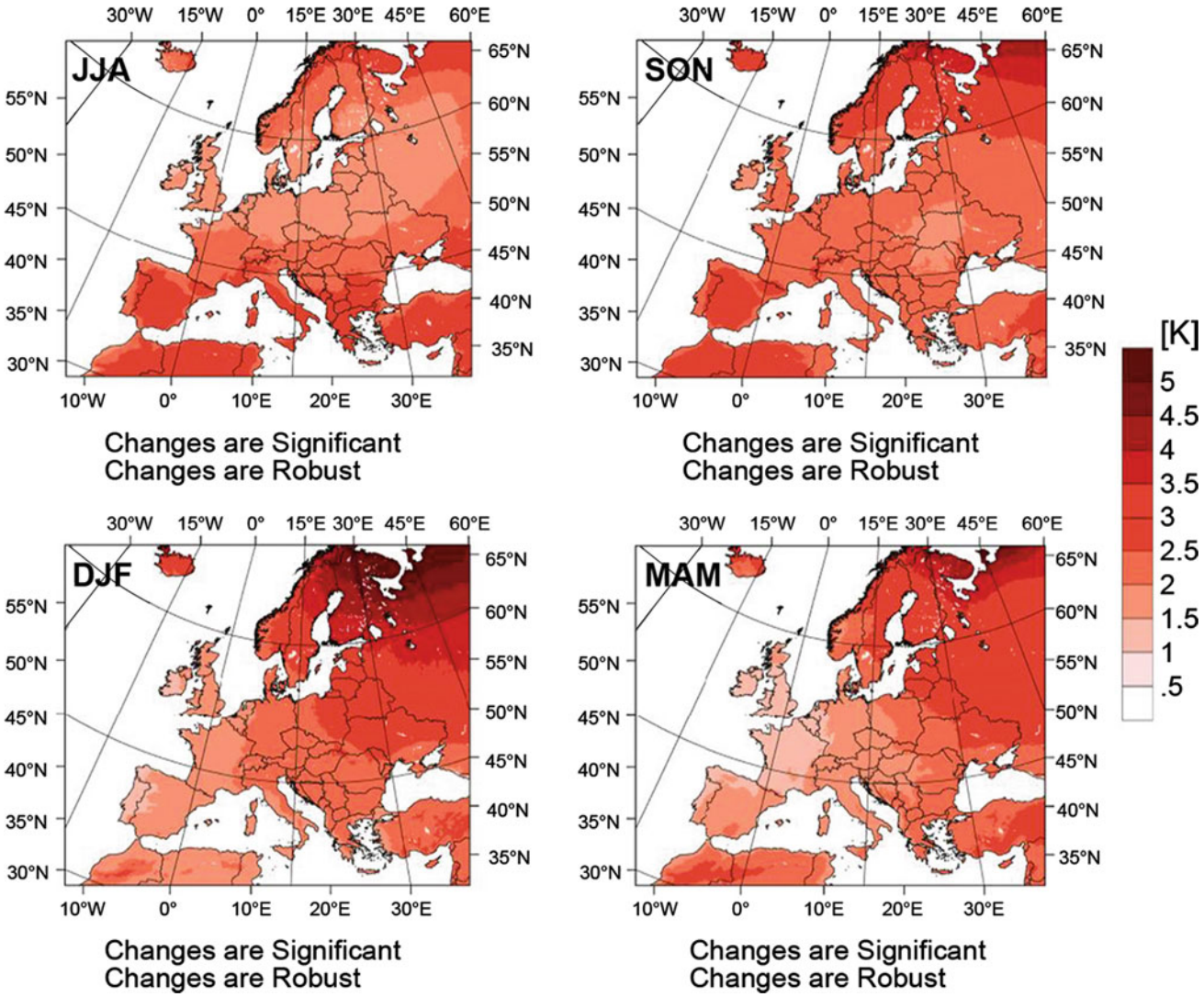

Fig. 5.1 Projected seasonal changes in surface air temperature (K) based on the RCP4.5 scenario for the end of the 21st century (2071–2100) relative to present day (1971–2000). All changes are both robust and statistically significant. From the supplementary material of Jacob et al. (2014)

Table 5.3 Projected changes in selected temperature-related climate variables and indices by the end of the 21st century (2071–2100, with respect to 1971–2000) averaged over the Atlantic region (according to Metzger et al. 2005) for RCP4.5 (eight RCM simulations) and RCP8.5 (nine RCM simulations)

Temperature-related climate indices	RCP4.5	RCP8.5
Annual mean temperature (°C)	1.7 (1.4 to 2.1)	3.2 (2.7 to 3.6)
Frost days per year	−28 (−30 to −15)	−40 (−50 to −26)
Summer days per year	11 (6 to14)	24 (22 to 28)
Tropical nights per year	3 (1 to 5)	7 (3 to 12)
Growing season length (days per growing season)	39 (27 to 43)	58 (47 to 68)
Warm spell duration index (days per year)	21 (19 to 34)	67 (47 to 92)
Cold spell duration index (days per year)	−4 (−5 to −4)	−5 (−6 to −4)

Data represent the median of the multi-model ensemble results and the likely range in these changes, defined to include 66 % of all projected changes around the ensemble median. Adapted from Kovats et al. (2014b, their Table SM23-3)

several days to weeks. A number of indices describing climate extremes have been developed based on some of the characteristics of the respective distributions of daily data. In a first attempt to coordinate and standardise the definition of such extremes, Frich et al. (2002) proposed five different indices concerning daily temperature data. Zhang et al. (2011) extended this list of extreme temperature indices to 15, also revising some of the definitions of Frich et al. (2002). In particular, these indices often focus on relative thresholds that describe the tails in the distribution rather than on specific physically-based thresholds. The indices of Zhang et al. (2011) capture both moderately extreme events that typically occur several times per year and extreme events that occur less often (once a year or less). In recognition of the strong impact of weather and climate extremes the IPCC published a special report on managing the risks of extreme events and disasters to advance climate change adaptation (SREX; IPCC 2012).

Kovats et al. (2014b) reported on projected changes in the characteristics of seven different temperature-related extremes based on the multi-model ensemble of high-resolution RCM simulations for the RCP4.5 and RCP8.5 scenarios (Jacob et al. 2014). In Table 5.3 these changes are presented for the end of the 21st century averaged over the Atlantic region. The indices were defined in accordance with Zhang et al. (2011), that is, the number of frost days were defined as the annual count of days when the daily minimum temperature drops below 0 °C, the number of summer days as the annual count of days when the daily maximum temperature exceeds 25 °C, the number of tropical nights as the annual count of days when the daily minimum temperature exceeds 20 °C, growing season length as the annual count between the first span of at least six days with daily mean temperatures above 5 °C and the first span after 1 July of six days with daily mean temperatures below 5 °C, the warm spell duration index as the annual count of days with at least six consecutive days when the daily maximum temperature exceeds the respective 90th percentile, and the cold spell duration index as the annual count of days with at least six consecutive days when the daily minimum temperature drops below the respective 10th percentile.

The projected changes in these indices reveal the overall tendency of a future amplification of the extremes related to daily maximum temperature and a future reduction of the extremes related to daily minimum temperature. The number of summer days by the end of the 21st century, for instance, is increased by 11 (24) for RCP4.5 (RCP8.5), while the number of frost days is reduced by 28 (40) (see Table 5.3). The changes are generally stronger for RCP8.5 than for RCP4.5, and for some indices the likelihood ranges based on individual models for the two scenarios do not show any overlap. This is the case for the number of summer days, growing season length and the warm spell duration index. For the cold spell duration index, on the other hand, the likelihood ranges are similar for the two scenarios. The relatively large likelihood ranges for some indices indicate strong variation between the eight (RCP4.5) and nine (RCP8.5) projections with different RCMs that have been considered, and hence a high degree of uncertainty in the projected changes.

Kovats et al. (2014a) presented the geographical distributions of the projected change in the number of heat waves during May through September at the end of the 21st century on the basis of the same set of RCM simulations for the RCP4.5 and RCP8.5 scenarios. Heat waves were defined as periods of more than five consecutive days with daily maximum temperatures exceeding the mean daily maximum temperature for the reference period (1971–2000) by at least 5 °C. For the North Sea region, the only area with notably more frequent heat waves was in southwestern Norway for RCP8.5, for RCP4.5 the number of heat waves does not change in that region. Jacob et al. (2014) defined heat waves differently, in this case as periods of more than three consecutive days with daily maximum temperatures exceeding the 99th percentile of the daily maximum temperature for the same reference period, and found markedly more heat waves over the North Sea region under RCP8.5 at the end of the 21st century, with increases in the number of heat waves ranging from 10 to 15 for the Netherlands, northern Germany and Denmark, and exceeding 30 in southern Norway.

The CMIP5 simulations have also been used to assess the projected change in various temperature-related extremes in several studies, with some of these assessments being included in AR5 (Collins et al. 2013). Sillmann et al. (2013), for instance, presented global maps of the projected change in annual minimum and maximum temperatures (i.e. the minimum of the daily minimum temperatures and the maximum of the daily maximum temperatures occurring in the course of a year), in the number of frost days and in the number of tropical nights, in the number of cold nights (with daily minimum temperatures below the respective 10th percentile) and in the number of warm nights (with daily maximum temperatures exceeding the respective 90th percentile), as well as in the cold and warm spell duration indices at the end of the 21st century for the RCP2.6, RCP4.5 and RCP8.5 scenarios. Sillmann et al. (2013) also found notable future increases in both the annual minimum and maximum temperatures over western, central and northern Europe. Strong increases in annual minimum temperature of about 9–11 °C for RCP8.5 occur in northern Europe, presumably associated with retreating snow cover in this region. The strongest increases in annual maximum temperature, on the other hand, occur in central and eastern Europe, reaching about 6–8 °C for RCP8.5. Corresponding to these increases in annual temperature extremes, the number of frost days is markedly lower in central and

northern Europe, while the number of tropical nights is much higher over southern Europe. In much of the North Sea region the number of tropical nights rises by about 10 days under RCP4.5 and by more than 20 days under RCP8.5, with tropical nights hardly ever occurring in this region under the present-day climate. Similarly, cold spells are projected to become shorter in the North Sea region, by about 3 days for RCP4.5 and about 4–6 days for RCP8.5. Warm spells are projected to become markedly longer in the North Sea region, by about 30 days for RCP4.5 and by 60–120 days for RCP8.5. The national climate change assessment for the Netherlands also considers change in temperature-related extremes (KNMI 2014). In winter, for instance, the number of frost days is projected to decrease by 35–80 % (with respect to 38 days for the reference period 1981–2000) at the end of the 21st century, with the weakest change for the scenario with moderate warming and weak influence of circulation change and the strongest change for the scenario with strong warming and strong influence of circulation change. For the scenarios with strong warming, the differences between a weak and strong influence of circulation change account for 20 % of the projected fall in the number of frost days. The number of summer days, on the other hand, is projected to increase by 30–130 % (relative to 21 days for the reference period 1981–2000), again depending on the overall strength of the scenario.

Kharin et al. (2013) used 20-year return levels to assess future changes in annual extremes of daily temperature at the end of the 21st century for the RCP2.6, RCP4.5 and RCP8.5 scenarios on the basis of the CMIP5 simulations for the entire globe. In the North Sea region, the multi-model ensemble projects increases in the 20-year return levels of the annual minimum temperatures of 4–8 °C for RCP4.5 and 8–12 °C for RCP8.5. The projected increases in the 20-year return levels for annual maximum temperature in the North Sea region are somewhat weaker, at 2–4 °C for RCP4.5 and 6–8 °C for RCP8.5. Nikulin et al. (2011) used 20-year return levels to assess future change in annual extremes of daily temperature in Europe at the end of the 21st century on the basis of an ensemble of six scenario simulations with one particular RCM forced by six different GCMs applying the SRES A1B scenario (Fig. 5.2). According to these scenario simulations, the 20-year return levels for annual minimum temperature increase by about 4–10 °C over most of the North Sea region, while the respective return levels for the annual maximum temperature increase only by about 2–4 °C. Nevertheless, waiting times for a 20-year event of the annual maximum temperature during the reference period (1961–1990) are reduced to 2–5 years in the North Sea region, meaning that at the end of the 21st century such an event is expected to occur every two to five years.

Schoetter et al. (2014) assessed changes in the characteristics of western European heat waves projected in the CMIP5 ensemble at the end of the 21st century. In this case heat waves were defined as periods of three consecutive days, during which at least 30 % of western Europe is affected by extremely high temperatures (exceeding the 98th percentile of the daily maximum temperatures for the period May through October). The study covers the UK, Belgium, the Netherlands and northern Germany as parts of the North Sea region. Heat waves in western Europe become more frequent and of greater duration, increase in extent and

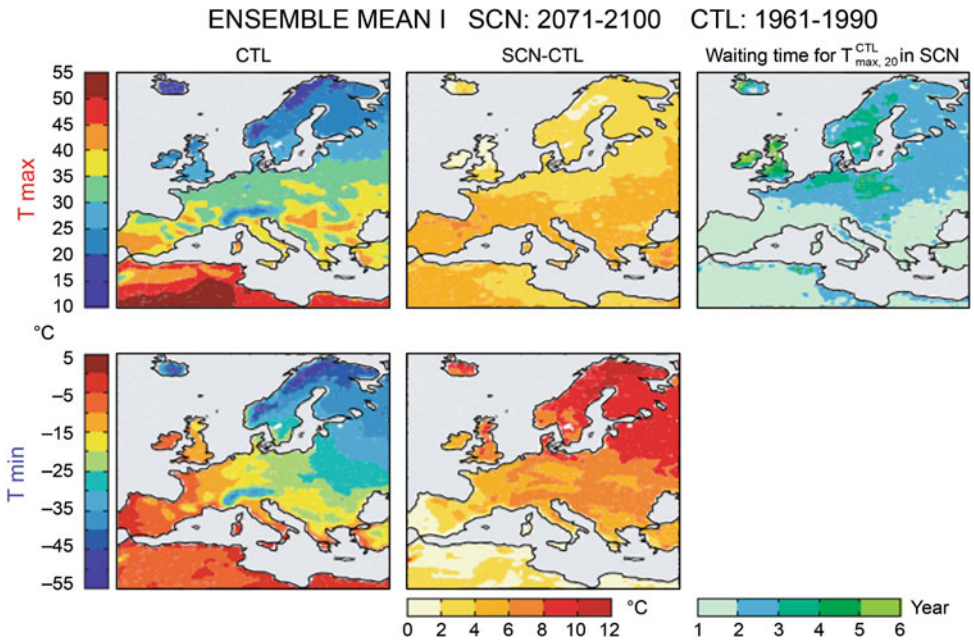

Fig. 5.2 *Left-hand panels* The ensemble mean of (*upper panel*) the 20-year return level of daily maximum temperature ($T_{max,20}$) and (*lower panel*) the 20-year return level of daily minimum temperature ($T_{min,20}$) for 1961–1990 and (*middle panel*) the respective changes of $T_{max,20}$ and $T_{min,20}$ in 2071–2100 relative to 1961–1990 (°C). Only differences significant at the 10 % significance level are shown. *Right-hand Panel* Waiting times (years) of the 1961–1990 $T_{max,20}$ in 2071–2100 (Nikulin et al. 2011)

become more intense. Heat waves that are similar to or stronger than the one observed across Europe in 2003 remain rare under RCP2.6 and RCP4.5, but become the norm under RCP8.5. For the latter, heat waves with five times the severity of the 2003 heat wave were simulated. The severity of heat waves is described by the so-called cumulative heat wave severity, which is defined as the product of the number of heat waves during a 30-year period and the mean severity of the individual heat waves. The latter is defined as the product of the duration, the mean extent and the mean intensity of the respective heat wave. Most of the changes in the temperature-related extremes during summer are partly associated with corresponding changes in the variation in temperature over the course of a day (diurnal cycle) as well as variations in temperature from day to day. According to Cattiaux et al. (2015), both diurnal variability and day-to-day variability in summer temperature increase under the different RCP scenarios, with extremely strong variations over both time scales occurring more frequently. In western Europe, for instance, diurnal and day-to-day variability both increase by about 10 % under the RCP8.5 scenario, with weaker increases over northern Europe of up to 6 %. The increases in variability are primarily linked to a future decrease in surface evapotranspiration as a consequence of drier European summers.

Several extremes related to daily temperature were identified in the SREX report with high confidence for northern Europe (Seneviratne et al. 2012). For instance, the frequency of warm days is very likely to increase, but not as much as in central and southern Europe (Fischer and Schär 2010), there are very likely to be fewer cold days (with daily maximum temperatures below the respective 10th percentile) and a likely increase in the 20-year return levels of annual maximum temperature. There are very likely to be fewer cold nights (Kjellström et al. 2007; Sillmann and Roeckner 2008) and more warm nights (Tebaldi et al. 2006). Heat waves and warm spells are likely to occur more often, last for longer and/or be more intense, but the changes in northern Europe are smaller than in southern Europe, while Scandinavia shows little change at all (Beniston et al. 2007; Koffi and Koffi 2008; Fischer and Schär 2010; Orlowsky and Seneviratne 2012).

5.4 Precipitation

Wilhelm May

5.4.1 Mean Precipitation

At a global scale, the CMIP5 simulations project increases in precipitation in the tropics as well as at mid and high latitudes, and a decrease in the sub-tropics (Knutti and Sedláček 2012). For the North Sea region, the multi-model ensemble projects an increase in winter and a decrease in summer except for Denmark and southern Norway. This tendency is also evident in the projected changes in precipitation for northern and central Europe based on the CMIP5 simulations presented in Annex I of AR5 (IPCC 2013) for the cold (October through March) and warm (April through September) seasons. For the cold season, the RCP4.5 scenario is characterised by increases of up to 10 % in the North Sea region at the end of the 21st century, and the changes projected exceed natural variability over the entire region. For the warm season, on the other hand, precipitation is projected to decrease by up to 10 % in England, Belgium, the Netherlands and northern Germany and to increase by up to 10 % in Denmark and southern Norway. However, the changes projected during the warm season do not exceed natural climate variability anywhere across the region. Averaged over northern Europe, the projected increase in precipitation during the cold season ranges from 8 % (RCP4.5) to 11 % (RCP8.5) for the mid-21st century and from 11 % (RCP4.5) to 20 % (RCP8.5) at the end of the 21st century (see Table 5.4). Precipitation averaged over northern Europe during the warm season is increased, ranging from 3 to 4 % for the mid-21st century and 5–8 % at the end of the century.

Table 5.4 Projected relative changes in mean precipitation (%) by the mid- and end of the 21st century (2046–2065 and 2081–2100, with respect to 1986–2005) for northern Europe (see Seneviratne et al. 2012, their Fig. 3.1) for RCP4.5 (42 models) and RCP8.5 (39 models) obtained from the CMIP5 simulations, distinguishing between the cold season (October through March; ONDJFM) and warm season (April through September; AMJJAS)

Period	Season	RCP4.5	RCP8.5
2046–2065	ONDJFM	8 (3–11)	11 (8–15)
	AMJJAS	3 (2–8)	4 (1–10)
2081–2100	ONDJFM	11 (7–14)	20 (15–29)
	AMJJAS	5 (2–8)	8 (2–12)

Data represent the median of the multi-model ensemble of changes and the 25th and 75th percentiles of the individual model responses. Adapted from Christensen et al. (2013a, their Table 14.1) and Christensen et al. (2013b, their Table 14.SM.1c), respectively

During winter some precipitation in the North Sea region falls as snow. As conditions warm, the fraction falling as snow is expected to decrease. According to Brutel-Vuilmet et al. (2013) the CMIP5 simulations are characterised by several snow-related changes in the mid-latitudes of the northern hemisphere at the end of the 21st century. Between 40° and 60°N the RCP scenarios project a decrease in solid precipitation of about 10 % (RCP2.6) to 30 % (RCP8.5), despite a marked rise in total precipitation at these latitudes. Consistent with this, snow depth declines by about 10 % (RCP2.6) to 40 % (RCP8.5), and the snow season shortens with the decrease ranging from up to a fortnight (RCP2.6) to a month or more (RCP8.5). Räisänen and Eklund (2012) presented consistent results for northern Europe based on an ensemble of regional climate scenarios applying the SRES A1B scenario from the ENSEMBLES project (e.g. van der Linden and Mitchell 2009). They identified future decreases in snowfall and snow depth across all low-altitude parts of northern Europe, including Denmark and southern Norway as part of the North Sea region.

The characteristic changes in precipitation over Europe were also revealed in the multi-model ensemble of high-resolution RCM simulations for Europe used by Jacob et al. (2014). For the RCP4.5 scenario, seasonal mean precipitation in the North Sea region increases in winter and spring by about 10–15 % at the end of the 21st century (Fig. 5.3). In summer and autumn, on the other hand, precipitation increases (exceeding 5 %) in south-western Norway, but there is little change in the rest of the North Sea region, ranging between a slight decrease (of less than 5 %) in the south to a slight increase (of less than 5 %) in the north. Averaged over the Atlantic region, annual mean precipitation increases slightly (1 %) for RCP4.5 and more notably for RCP8.5 (see Table 5.5). For the RCP4.5

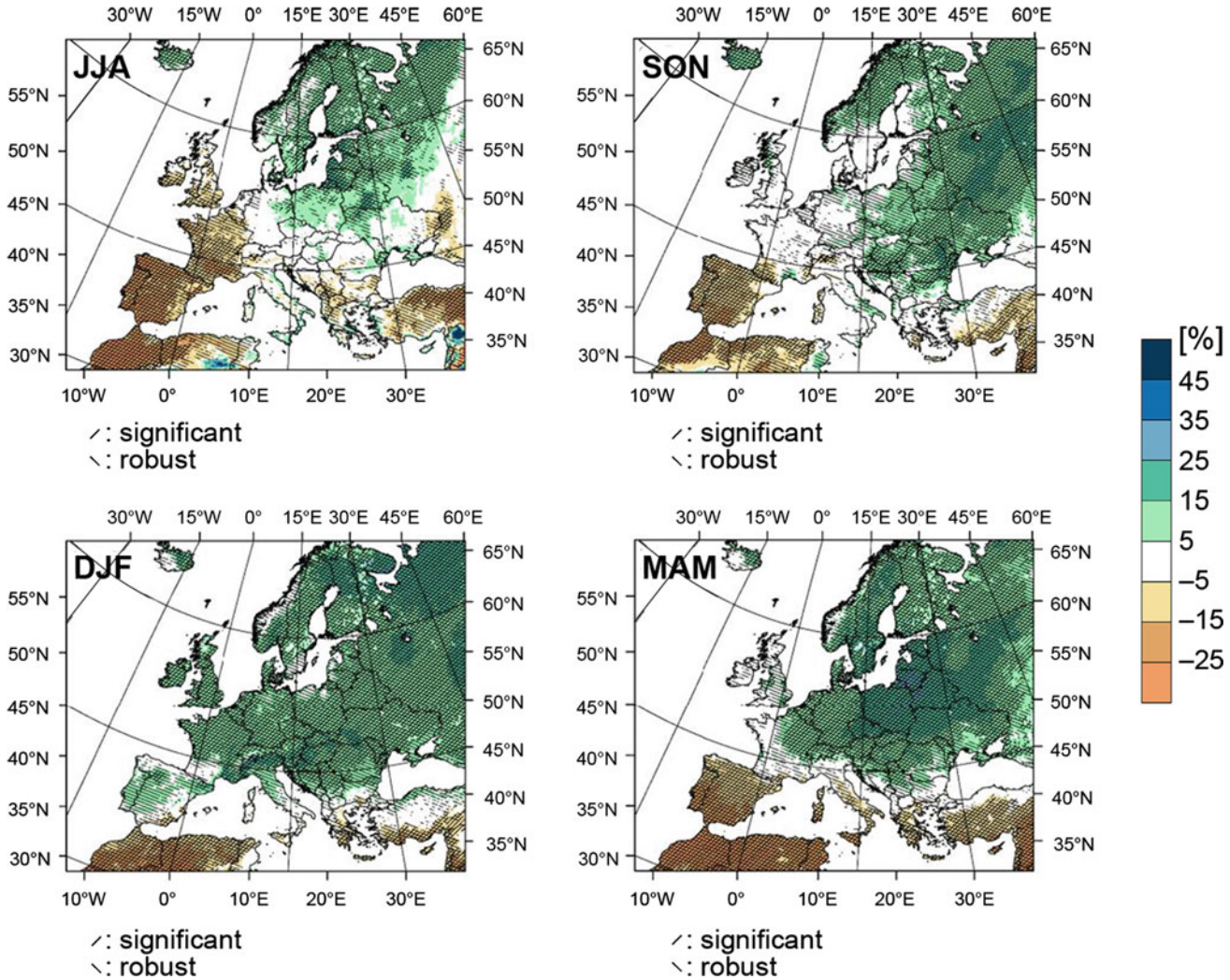

Fig. 5.3 Projected seasonal change in precipitation (%) based on the RCP4.5 scenario for the period 2071–2100 relative to 1971–2000. Hatched areas indicate regions with robust and/or statistically significant change. From the supplementary material of Jacob et al. (2014)

Table 5.5 Projected change in precipitation-related variables and indices for the end of the 21st century (2071–2100 with respect to 1971–2000) averaged over the Atlantic region for the RCP4.5 (eight RCM simulations) and RCP8.5 (nine RCM simulations) scenarios

	RCP4.5	RCP8.5
Annual total precipitation (%)	1 (−1 to 6)	4 (1 to 7)
Annual total precipitation where daily precipitation exceeds the 99th percentile in 1971–2000 (%)	21 (13 to 44)	43 (32 to 68)

The data represent the median of the multi-model ensemble of changes and the likely range of these changes, defined to include 66 % of all projected changes around the ensemble median. Adapted from Kovats et al. (2014b, their table SM23-3)

scenario, however, one sixth of the different RCM simulations are actually characterised by decreasing precipitation across the Atlantic region.

In Denmark the CMIP5 simulations project increases in seasonal mean precipitation at the end of the 21st century in all seasons except summer (DMI 2014). For summer, the RCP8.5 scenario projects a decrease of about 17 % but with an inter-model standard deviation of 21 %. This scenario projects the strongest increase in winter (18 %), and change in the transition seasons are 10 and 11 %, respectively. For annual mean precipitation, the RCP8.5 scenario projects a future increase of about 7 %, which is slightly larger than the inter-model standard deviation. Consistent with this, the high-resolution RCM simulations used by Wagner et al. (2013) project future increases in annual mean precipitation of 2–6 % in northern Germany. For the Netherlands, the projections are characterised by an increase in annual mean precipitation of 5–7 % with little dependence on the strength of impact of the circulation change (KNMI 2014). This is, however, not the case for changes in the seasonal means, where the scenarios with a strong influence of circulation change project stronger changes in precipitation. In winter, the scenarios with strong warming rate project an increase of 30 % by the end of the 21st century in combination with a strong influence of circulation change and 11 % in combination with a weak impact. In summer, on the other hand, the scenarios with strong warming project reductions of 17 and 4.5 %, respectively.

5.4.2 Precipitation Extremes

Similar to temperature, changes in the variability of precipitation at time scales of up to a season are more relevant in terms of impact than changes in seasonal or annual precipitation. Examples are heavy rainfall at sub-daily or daily time scales, wet spells of several days duration and extended dry periods lasting from one to several weeks or months. On the basis of daily time series of precipitation, Frich et al. (2002) proposed five different indices describing climate extremes related to precipitation in order to coordinate and standardise the definition of such extremes. Zhang et al. (2011) extended this list of extreme precipitation indices to 12, also revising some of the definitions of Frich et al. (2002). These indices often focus on relative thresholds that describe the tails of the distribution rather than on physically-based thresholds.

Kovats et al. (2014b) reported on projected changes in the fraction of the annual precipitation originating from extremely wet days (exceeding the 99th percentile of daily precipitation; Zhang et al. 2011). Averaged over the Atlantic region, this is projected to increase by 21 % (RCP4.5) to 43 % (RCP8.5) at the end of the 21st century (see Table 5.5).

Jacob et al. (2014) considered projected change in precipitation on very wet days (exceeding the 95th percentile of daily precipitation; Zhang et al. 2011), distinguishing between seasons. At the end of the 21st century both the RCP4.5 (Fig. 5.4) and RCP8.5 scenarios project significant increases in the intensity of heavy precipitation events over the entire North Sea region and in all seasons. For RCP4.5 the projected increases are typically 5–15 %, while for RCP8.5 the increases are 15–25 % in all seasons except summer. Jacob et al. (2014) also considered future change in very long lasting droughts (defined as the 95th percentile of the length of dry spells) and found no change in the North Sea region for RCP4.5 and a very small increase of 1–2 days in western Europe for RCP8.5.

The CMIP5 simulations have also been used to project change in various precipitation-related extremes, with some referred to in AR5 (Collins et al. 2013). For instance, Sillmann et al. (2013) presented global maps of future change in very high daily precipitation, defined as the 95th percentile of precipitation on wet days. They found pronounced increases in the intensity of heavy precipitation events over western, central and northern Europe at the end of the 21st century for all RCP scenarios considered, with the smallest increases (about 20 %) for RCP2.6 and the largest (40–70 %) for RCP8.5. The magnitude of the relative changes in the intensity of heavy precipitation events is considerably greater than the corresponding changes in the average intensity of daily precipitation on all wet days. In south-western Europe, the intensity of heavy precipitation events is projected to increase despite a projected decrease in average intensity. Consistent with this, Scoccimarro et al. (2013) projected a relatively strong increase in the fraction of precipitation originating from daily precipitation events in the range between the 90th and 99th percentile in western, central and northern Europe. In winter, the contributions of

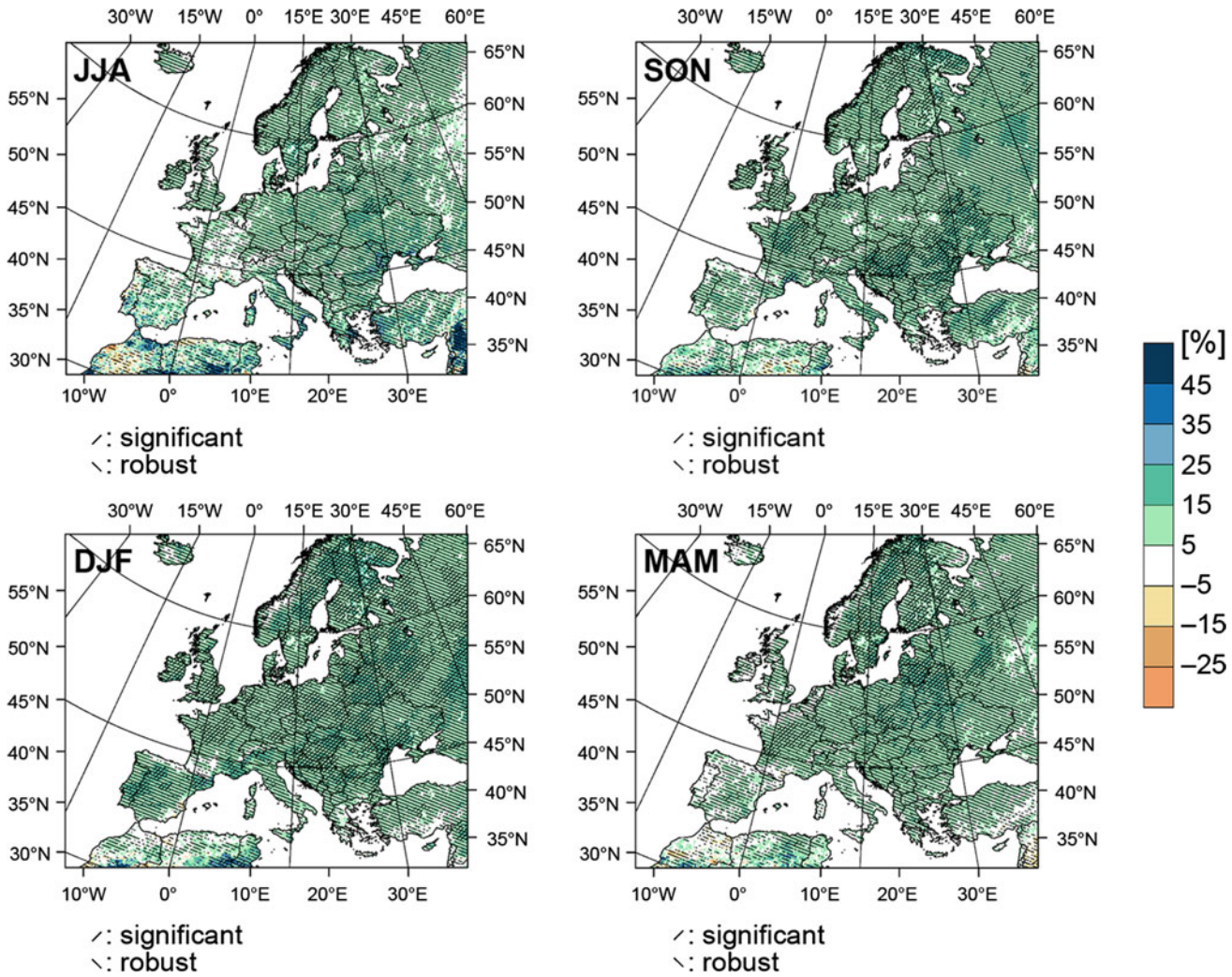

Fig. 5.4 Projected seasonal change in heavy precipitation (%) based on the RCP4.5 scenario for the period 2071–2100 compared to 1971–2000. Hatched areas indicate regions with robust and/or statistically significant change (Jacob et al. 2014)

the heavy daily precipitation events increase by more than 20 % in these areas of Europe, in summer the increases are typically 10–20 % for RCP8.5. It is only in summer that the intensity of heavy precipitation events increases in those parts of western, central and northern Europe, where average intensity decreases. In winter, the intensity of heavy daily precipitation events and the average intensity both increase in western, central and northern Europe.

Another way to depict the projected changes in heavy daily precipitation events is in terms of the number of days for which future daily precipitation exceeds a particular high threshold for the reference period. Applying this approach to an ensemble of RCM simulations, Wagner et al. (2013) found that for more than 5 % of days, the amounts of daily precipitation exceeded the 95th percentile for the reference period in north-western Germany in the mid-21st century. Instead of a variable threshold, another approach is to consider a particular amount of daily precipitation. Sillmann et al. (2013), for instance, analysed future change in the number of days with at least 10 mm precipitation and projected an increase in western, central and northern Europe, ranging from about two additional days (RCP2.6) to about six additional days (RCP8.5) at the end of the 21st century. In contrast to Sillmann et al. (2013), who based their analysis on data covering the entire year, KNMI (2014) distinguished between winter and summer and used different thresholds for the two seasons, 10 mm in winter and 20 mm in summer. In winter, KNMI (2014) found more days with at least 10 mm precipitation in the Netherlands, with increases of 14–24 % for the two scenarios with moderate future warming and 30–60 % for the two scenarios with strong future warming. For each of the two rates of future warming the strongest increases are associated with a strong influence of circulation change (i.e. a more predominantly westerly

flow). In summer, however, the situation is different, with more days with at least 20 mm precipitation for the two scenarios with a weak influence of circulation change. In the case of a strong influence of circulation change (i.e. a more predominantly easterly flow), the increase in the number of days with at least 20 mm precipitation is less pronounced in some parts of the Netherlands and the number of such days is even reduced in others.

Over the last couple of years, change in precipitation at sub-daily time scales has also become the subject of scientific study. Lenderink and van Meijgaard (2008), for instance, investigated the potential future change in various extremes of hourly and daily precipitation in central Europe during summer in a scenario simulation with a state-of-the-art RCM. As well as identifying much stronger relative increases in hourly precipitation extremes (19–39 % for different percentiles) than in daily precipitation extremes (9–20 % for different percentiles) they found that the projected increases in hourly precipitation extremes exceeded 7 % per degree of warming, which would be expected according to the Clausius-Clapeyron equation, that is, about 14 % per °C for the 99.9th percentile of hourly precipitation. According to KNMI (2014) the summer maximum hourly precipitation is projected to increase by 8–19 % for the two moderate warming scenarios and by 19–45 % for the two strong warming scenarios by the end of the 21st century. In this case, the difference in the influence of circulation change had little effect. The magnitude of the projected absolute changes in extreme hourly precipitation typically simulated by RCMs, however, is probably smaller than what can actually be expected in the future. Kendon et al. (2014) demonstrated that a numerical model operated at a spatial resolution of 1.5 km, which is typical for numerical weather prediction, gives much stronger changes in hourly precipitation extremes during summer than a model operated at a coarser resolution of 12 km. Nevertheless, the relative increases in extreme hourly precipitation of 45 % for the warm scenario combined with a strong impact of the circulation change are of the same order of magnitude as the relative increases projected over the southern part of the UK by Kendon et al. (2014).

Kharin et al. (2013) depicted future changes in extreme daily precipitation events on the basis of the CMIP5 simulations by means of the 20-year return levels for annual maximum daily precipitation. At the end of the 21st century they found an increase in the 20-year return levels of about 10–20 % in the North Sea region for RCP8.5. This means that the annual maximum daily precipitation amounts with a return period of 20 years under present-day climate conditions are likely to occur about every 10–14 years in the future. Nikulin et al. (2011) analysed future changes in 20-year return levels for maximum daily precipitation in winter and summer, when computing the 20-year return levels combining six RCM simulations for Europe. In summer they found changes in the 20-year return level in the range 10–20 % in the North Sea region at the end of the 21st century, and in winter values of 15–30 %. As a consequence, waiting times for a 20-year event under present-day climate conditions are notably more reduced in winter (about 8–12 years) than summer (about 12–16 years).

The projected intensification of heavy daily precipitation in the North Sea region is accompanied by an increase in the mean duration of periods with consecutive dry days. According to Sillmann et al. (2013), the average length of periods with consecutive dry days increases by 1–5 days for the North Sea region under RCP8.5. For RCP4.5, however, there is little change in the average length of periods with consecutive dry days. This is consistent with the findings of Wagner et al. (2013), who identified only very small changes in the average length of periods with consecutive dry days (in this case lasting more than five days) in northern Germany for the mid-21st century under the SRES A1B scenario.

The SREX report (Seneviratne et al. 2012) identified with high confidence very likely increases in both the intensity and frequency of heavy daily precipitation events in northern Europe, accompanied by increases in the fraction of the days with precipitation, for which the daily precipitation exceeds 10 mm, north of 45°N in winter (Frei et al. 2006; Beniston et al. 2007; Kendon et al. 2008). The report also identified a likely increase in the 20-year return levels of daily precipitation in northern Europe.

5.5 Cyclones and Winds

Anette Ganske, Gregor C. Leckebusch, Wilhelm May

5.5.1 Cyclones

Zappa et al. (2013) analysed future projections of the occurrence of extratropical cyclones in the North Atlantic-European sector on the basis of 19 CMIP5 model simulations for both the RCP4.5 and RCP8.5 scenarios. In this study, cyclones were identified and tracked using the objective feature tracking algorithm developed by Hodges (1999). During winter (December through February) the authors identified a tri-polar pattern over Europe with an increase in storm track density over the eastern North Atlantic centred over the British Isles and the North Sea and decreases centred around Iceland and over the Mediterranean Sea (Fig. 5.5). These changes indicate an extension of the Atlantic storm track to the northeast in combination with a narrowing of the storm track over western Europe. These results are in line with the corresponding changes in storm track density on the

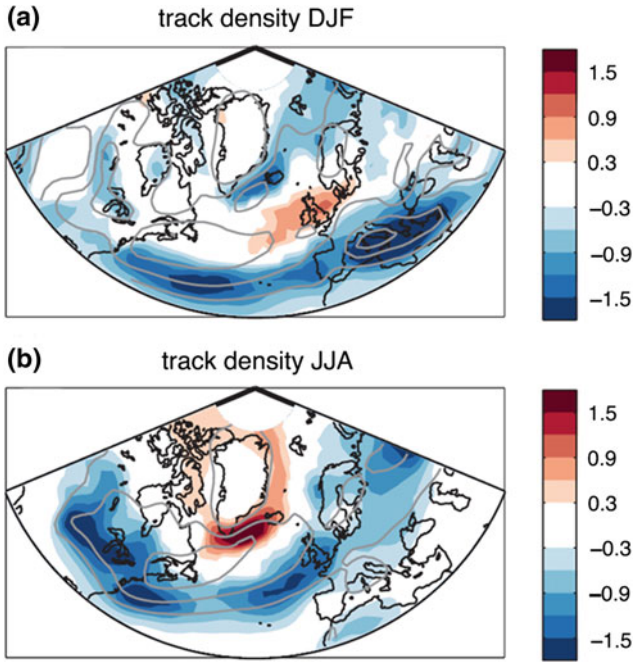

Fig. 5.5 Projected change in mean track density for winter (December through February, DJF; *upper panel*) and summer (June through August, JJA; *lower panel*) based on the RCP8.5 scenario from 19 CMIP5 simulations. Units are number of cyclones per month per unit area. Only responses statistically significant at the 5 % level are shown (Zappa et al. 2013)

basis of the CMIP3 simulations (Ulbrich et al. 2008). The RCP8.5 scenario gives increases in the range 0.6–1.2 cyclones per month in winter at the end of the 21st century over the British Isles, the North Sea and Denmark and only small changes over western Europe. For the RCP4.5 scenario the corresponding changes range between 0.3 and 0.9 cyclones per month. Considering only intense cyclones with pressures below 980 hPa during their lifetimes, Mizuta (2012) found increases of about 0.1 cyclones per month centred over the British Isles for the RCP4.5 scenario on the basis of 11 CMIP5 model simulations. During summer (June through August), on the other hand, Zappa et al. (2013) found an increase in storm track intensity centred between Iceland and southern Greenland and a decrease centred west of the British Isles extending further into the North Sea region (Fig. 5.5). This decrease indicates a marked reduction in the number of cyclones at the southern flank of the storm track over western Europe. For the RCP8.5 scenario the number of cyclones in summer is projected to decrease by 0.6–1.5 cyclones per month over the North Sea and by 0.6–0.9 cyclones per month over western and northern Europe. The RCP4.5 scenario gives increases in the range 0.3–0.6 cyclones per month over the North Sea and about 0.3 cyclones per month over western Europe.

Harvey et al. (2012) assessed the magnitude of projected changes in the Atlantic storm track for both the CMIP3 (SRES A1B scenario) and CMIP5 (RCP4.5 scenario) simulations relative to its typical interannual variations. The storm track was defined via band-pass filtered (2–6 days) variations in the daily surface pressure fields. The authors found that the multi-model ensemble changes in the Atlantic storm track in winter largely agree between the CMIP3 and CMIP5 simulations, when scaling with the respective changes in global mean temperature. The changes simulated by individual models, however, typically have a magnitude similar to the variability at decadal time scales and are locally as strong as the interannual variability. In some parts of the North Atlantic, up to 40 % of the climate models considered were characterised by a positive change in storm track density, exceeding half the magnitude of the interannual variability. With respect to the projected changes in cyclone track density, Ulbrich et al. (2013) noted that part of the uncertainty regarding regional trends in cyclone activity can be related to the choice of a particular method for identification and tracking of cyclones. While different methodologies gave consistent results for intense cyclones, i.e., an increase in the number of cyclones over western Europe in winter, they led to opposing results for weak cyclones with either an increase or decrease in the number of cyclones. According to Chang et al. (2012), the overall tendency of a poleward shift of the Atlantic storm track under future climate conditions is accompanied by an upward extension of the storm track into the upper troposphere and lower stratosphere under the projected global warming, again consistent for the CMIP3 and the CMIP5 simulations.

In a recent review on storminess over the North Atlantic and north-western Europe, Feser et al. (2015) summarised projected changes in both storm frequency and storm intensity on the basis of numerous recent studies that assessed potential future change in these two aspects of storms on the basis of climate scenario simulations with different kinds of models. For the North Sea region, the review considered results from 16 studies published between 1997 and 2013 based on GCMs (either coupled to an ocean model or atmosphere-only) and RCMs with different scenarios for anthropogenic greenhouse gas forcing prescribed. Most of these studies (9 out of 11) showed a future increase in storm frequency, while two found a decrease. Likewise, 10 out of 11 studies showed a future increase in storm intensity; no trend was found in the remaining study. The same trends were also identified over the North Atlantic south of about 60°N, while over northern and central Europe about the same number of studies projected either increases or decreases in storm frequency.

5.5.2 Mean Wind Speeds

The mean winds near the surface (at 10 m height) in the North Sea region are characterised by a clear gradient between the North Sea and the adjacent land areas with considerably higher wind speeds over the ocean than over land, particularly during winter (e.g. Kjellström et al. 2011).

In contrast to other meteorological variables such as precipitation and temperature, very few studies have assessed potential future changes in near-surface winds in response to anthropogenic climate forcing on the basis of scenario simulations originating from GCMs. McInnes et al. (2011) analysed future changes in mean wind speeds at 10 m at a global scale on the basis of the CMIP3 simulations based on the SRES A1B scenario and found an increase in mean wind speeds over both the North Sea and the adjacent land areas in winter at the end of the 21st century, while in summer a notable increase was found over the North Sea only. On an annual basis, mean wind speeds are projected to increase over the entire North Sea region; with the projected changes in mean wind speed typically exceeding 10 %. Despite an overall tendency of increasing mean wind speed in the North Sea region, McInnes et al. (2011) identified marked variations between individual models regarding the sign of the change, particularly in the southern North Sea region. In a recent study, Sterl et al. (2015) analysed projected change in annual mean wind speeds at 10 m over the southern North Sea region for the RCP4.5 and RCP8.5 scenarios using one GCM. In contrast to the overall tendency obtained from the CMIP3 simulations, Sterl et al. (2015) found decreases in annual mean wind speed over the entire region, with little difference between the two scenarios.

More studies exist in which potential future changes in near-surface winds in response to anthropogenic climate forcing for selected regions or continents have been assessed on the basis of scenario simulations with RCMs. The finer spatial resolution not only adds regional detail to the simulations, which is important when looking at the North Sea region, but also affects the magnitude of the projected changes, particularly regarding extreme wind speeds (Winterfeldt and Weisse 2009). This is especially the case when RCMs are applied at very high horizontal resolution. Pryor et al. (2012) showed, for instance, that for the RCA3 RCM an increase in horizontal resolution from 50 to 6.25 km leads to an overall increase in simulated mean near-surface wind speed of 5 % averaged over southern Scandinavia, while the 50-year return level of wind speeds and wind gusts increases by over 10 and 24 %, respectively.

Kjellström et al. (2011) analysed potential future change in mean wind speed on the basis of an ensemble of simulations with the RCA3 RCM driven by six different GCMs for the SRES A1B scenario. These projections are characterised by a small (up to 0.25 ms^{-1}) increase in mean wind speed in the North Sea region in winter but a decrease over land areas and a small increase over the southern part of the North Sea. In particular in winter, the regional distributions of the projected changes vary considerably, both in sign and in strength between the RCA simulations driven by different GCMs. In a similar type of study based on an ensemble of climate projections with the HIRHAM RCM driven by three different GCMs for either the SRES B2 or the SRES A1B scenario, Debernard and Røed (2008) found increases in annual mean wind speed in the North Sea region, reaching up to 2 % over ocean areas.

5.5.3 Wind Extremes

For extremes of near-surface winds, defined via the 99th percentile of daily mean wind speed, the CMIP3 simulations show an overall slight increase (up to 5 %) in the North Sea region during winter and an overall slight decrease (up to 5 %) during summer (McInnes et al. 2011). In this, the projected changes in extreme wind speed are markedly less pronounced than the corresponding changes in mean wind speed when normalised with the climatological values for present-day climate conditions. De Winter et al. (2013) analysed projected changes in annual maximum near-surface wind speed based on scenario simulations with 12 GCMs from CMIP5 for both the RCP4.5 and RCP8.5 scenarios. In contrast to McInnes et al. (2011), they analysed the scenarios from each GCM separately instead of the multi-model ensemble mean. The different GCMs simulated very different changes in the North Sea region, with some models giving either increases or decreases in the intensity of wind extremes over most of the North Sea region and others giving increases over the northern part of the North Sea region and decreases in the southern part. For the RCP8.5 scenario the projected changes typically vary in the range -1.5 to 1.5 ms^{-1}. The individual GCMs simulate not only very different future changes in the intensity of extreme winds, but also very different distributions of the intensity of extreme winds, both with regard to the location of the peak and with regard to the width of the respective probability density functions aggregated over the North Sea.

Donat et al. (2011) presented the projected changes in the intensity of wind extremes (defined via the 98th percentile of daily maximum wind speed) for six different GCMs from CMIP3 for the SRES A1B scenario individually, finding very different changes in the intensity of extreme winds in the North Sea region. The multi-model ensemble mean showed intensified extreme winds in the range 0.25–0.75 ms^{-1} in the North Sea region at the end of the 21st century. Donat et al. (2011) also considered a number of

scenario simulations with different RCMs driven by these GCMs, which were part of the ENSEMBLES project (Van der Linden and Mitchell 2009). They found that dynamical downscaling contributed to the uncertainty of the projected changes, as RCMs driven with identical large-scale boundary conditions simulated quite different changes in the intensity of wind extremes.

Nikulin et al. (2011), on the other hand, considered six different scenario simulations with one particular RCM (RCA3) driven by global scenario simulations with six different GCMs for the SRES A1B scenario. Consistent with the studies above, Nikulin et al. (2011) also found very different changes in the 20-year return levels of daily maximum wind speeds in the North Sea region at the end of the 21st century for the individual RCM simulations. The multi-model ensemble means were characterised by a general tendency of more intense wind extremes in the North Sea region. Similarly, Gaslikova et al. (2013) analysed four different scenario simulations with the CCLM RCM driven by four different global scenario simulations with one particular GCM (two realisations of both the SRES B1 and the SRES A1B scenarios). The projected changes in the intensity of extreme winds (defined as the 99th percentile of annual maximum daily wind speeds) over the North Sea were also found to vary considerably between the four scenarios. This was particularly the case for the scenarios driven by the two realisations of the global simulations, where one realisation gave weaker wind extremes over the northern part of the North Sea. The A1B scenario resulted in notably stronger increases in the intensity of extreme winds than the B1 scenario. The multi-model ensemble means are characterised by more intense wind extremes to the south of 58°N, ranging between 0.2 and 0.4 ms^{-1} over most of the area at the end of the 21st century.

The differences between the two realisations over the North Sea are also revealed in the time series of the change in the intensity of wind extremes at different locations in the North Sea for the four different scenario simulations (Fig. 5.6). At the central North Sea location two of the realisations (A1B_2 and B1_2) simulated weaker wind extremes during the entire 21st century, while at the two locations in the German Bight this tendency is only apparent during the first half of the 21st century. The other two realisations (A1B_1 and B1_1), on the other hand, simulated stronger wind extremes during the course of the 21st century. The time series also illustrate the marked internal variability at multi-decadal time scales, making it difficult to identify systematic differences between the SRES A1B and B1 scenario simulations at these locations. For individual 30-year periods, however, marked differences between the A1B and B1 scenarios can occur, i.e., the two realisations A1B_1 and B1_1 at the end of the 21st century.

5.5.4 Wind Direction

McInnes et al. (2011) analysed projected changes in the direction of the mean winds at a global scale on the basis of the CMIP3 simulations. For the North Sea region, they found very small changes in mean wind direction in winter but in summer anticlockwise changes across the entire region, exceeding 15° in the southern areas. The

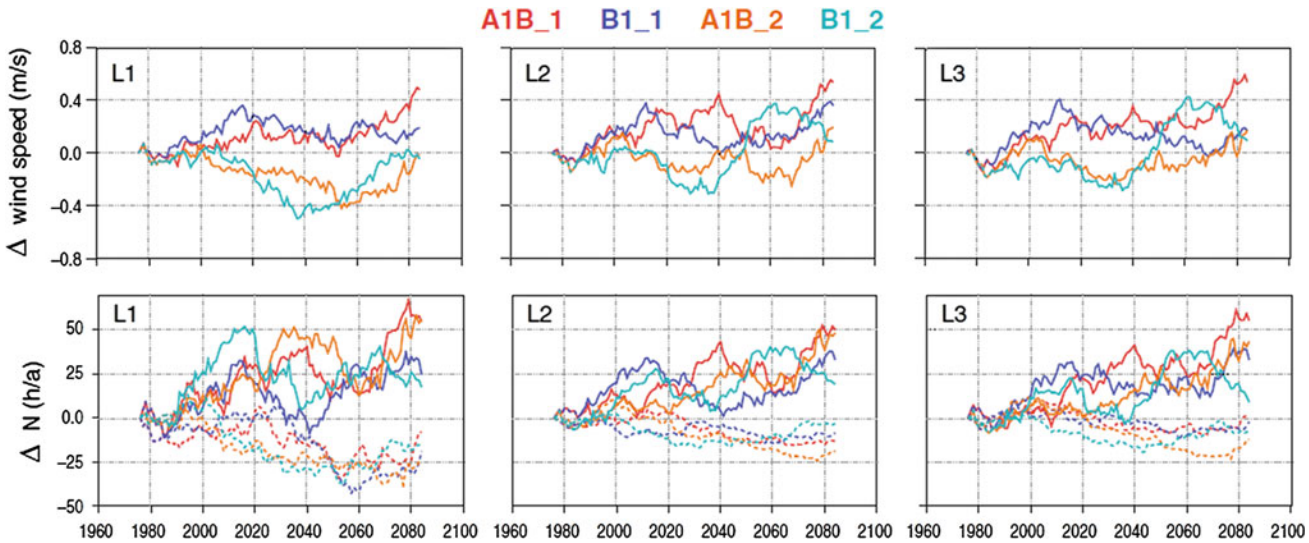

Fig. 5.6 Changes in 30-year running means with respect to 1961–1990 for four different RCM scenario simulations for the annual 99th percentile wind speeds (*upper row*) and (*lower row*) the annual frequencies of strong (≥17.2 ms^{-1}) westerly winds (165–345°; *solid lines*) and strong easterly winds (345–165°; *dashed lines*) at a site in the central North Sea (L1) and two sites in the German Bight (L2 and L3) (adapted from Gaslikova et al. 2013, their Fig. 8)

anticlockwise changes in mean wind direction in the southern North Sea region are consistent between most of the scenario simulations considered.

De Winter et al. (2013), on the other hand, analysed projected changes in the direction of strong winds over the North Sea on the basis of 12 GCMs contributing to CMIP5 for both the RCP4.5 and RCP8.5 scenarios. Strong winds were defined as the annual maxima of daily mean wind speeds and two areas were distinguished, one in the northern part of the North Sea and the other in the southern part. The authors found a common tendency towards less frequent strong winds from south-eastern directions and more frequent strong winds from south-western and western directions in the latter half of the 21st century in both regions for both scenarios. However, it should be noted that due to the rarity of strong wind events the wind direction statistics are characterised by a high degree of variability, which affects the robustness of the projected changes. These changes in the predominant wind directions are consistent with the findings of Donat et al. (2010), who considered storm days (based on daily maximum wind speeds) over western Europe on the basis of six GCMs contributing to CMIP3 for the SRES A1B scenario, and by Sterl et al. (2009) on the basis of a multi-member ensemble of scenario simulations for the SRES A1B scenario with one particular GCM. The projected changes from south-easterly to more south-westerly and westerly winds could indicate a poleward shift in the storm track, because in the North Sea region a storm following a northern track is associated with predominantly westerly winds, while a storm following a more southern track mainly produces south-easterly winds. Both the CMIP3 and CMIP5 simulations are characterised by corresponding changes in the storm track in the North Sea region (e.g. Harvey et al. 2012; Zappa et al. 2013).

Gaslikova et al. (2013) used an ensemble of four different scenario simulations with the CCLM RCM driven by four different global scenario simulations with one particular GCM (two realisations of both the SRES B1 and SRES A1B scenarios) to analyse projected changes in the direction of wind speeds of at least 17.2 ms^{-1} (corresponding to 8 Bft) at several locations in the North Sea region. They found a general tendency of more frequent strong westerly winds and of less frequent easterly winds in the central North Sea as well as in the German Bight in the course of the 21st century (Fig. 5.6). The decreases in the frequency of strong easterly winds are more pronounced in the German Bight than in the central North Sea, while increases in the frequency of strong westerly winds are similar at all locations. The time series of the projected changes for the four scenario simulations reveal both strong temporal variability at multi-decadal time scales and notable differences between the individual scenario simulations, illustrating the important role of internal variability for regional assessments of future change in the characteristics of storms.

5.6 Radiation and Clouds

Burkhardt Rockel, Wilhelm May

Few recent publications describe projected changes in radiation and clouds. Also, the RCMs and GCMs used to derive these projections, the emission scenarios used in the projections, and the time periods analysed are quite diverse. The projected changes are presented separately for solar and terrestrial radiation as well as for cloud cover, with similarities between these changes highlighted. The numbers presented in this section are typically estimated from the geographical distributions that cover a much larger area than the North Sea region, such as the globe or the entire European continent.

5.6.1 Solar Radiation

For annual mean net downward solar radiation at the surface, all studies show a distinct pattern with a decrease in the northern North Sea region and an increase in the south. This tendency is found regardless of which climate model or scenario is used or which time period is considered and so can be considered a robust result. The magnitude of the projected changes in the two areas varies between studies, however.

With increasing numbers of climate scenario simulations available from different coupled climate models, estimates based on a multi-model ensemble are often taken into account. Henschel (2013), for instance, considered results from 39 GCMs from CMIP5 for the RCP8.5 scenario and found a median decrease of about 0.1 Wm^{-2} per year for the southern part of the North Sea region for the multi-model ensemble, corresponding to a decrease of about 4 Wm^{-2} by the middle of the 21st century. In contrast, Henschel (2013) did not find any significant trend for the northern North Sea region (north of about 58°N) until the middle of the 21st century and so did not give any estimate of the change at that point in time.

Trenberth and Fasullo (2009) and Zhou et al. (2009) both considered results from multi-model climate simulations for the SRES A1B scenario to assess projected change until the end of the 21st century. However, the two studies considered different time periods and different parts of the atmosphere. Trenberth and Fasullo (2009) analysed projected change in annual mean net solar radiation at the top of the atmosphere and found an increase in absorbed solar radiation of up to 6 Wm^{-2} in the southern North Sea region and a decrease of

up to 1.5 Wm^{-2} in the northern region in the period 2000–2100. Zhou et al. (2009) analysed solar radiation at the surface and found an increase in net surface solar radiation of up to 4 Wm^{-2} in the southern North Sea region and a decrease of up to 6 Wm^{-2} in the north for 2080–2099 relative to 1900–1919.

Ruosteenoja and Räisänen (2013) analysed projected changes in solar radiation from the CMIP3 multi-model ensemble for the SRES A1B scenario by the end of the 21st century, distinguishing between seasons. In their supplemental material, Ruosteenoja and Räisänen (2013) also presented changes by the end of the 21st century for the SRES A2 and B1 scenarios as well as changes by the middle of the 21st century (2020–2049) for the SRES A1B scenario. In contrast to the previously mentioned studies, Ruosteenoja and Räisänen (2013) presented changes relative to the present-day climate (1971–2000) rather than absolute changes. According to their estimates, a relative reduction of 15 % at about 60°N corresponds to a decrease of less than 3 Wm^{-2}. According to their results, the pattern of projected changes at the middle of the 21st century varies little with season except for winter with a decrease in solar radiation over almost the entire North Sea region and a strongest decrease of about 5 %. During summer, on the other hand, solar radiation is increased almost everywhere, with a strongest increase of about 2.5 %. The variations between season are more pronounced at the end of the 21st century than for the mid-century. During both summer and autumn the characteristic north-south structure is evident with a decrease in solar radiation in the northern part (about 5 %) of the North Sea region and an increase in the south (about 10 %; Fig. 5.7). During winter, on the other hand, solar radiation is reduced across the entire North Sea region, particularly in the eastern part with reductions of about 10 %, and over 15 % in the north-eastern part. Consistent with this seasonal variation in the projected changes in solar radiation, KNMI (2014) reported pronounced increases in solar radiation in the Netherlands during summer, of 5.5–9.5 % at the end of the 21st century for the scenarios with a strong influence of circulation change (i.e. scenarios with more frequent high-pressure systems). The projected changes in annual mean solar radiation in the Netherlands are small, ranging from −0.8 to 1.4 % for the different scenarios.

Ruosteenoja and Räisänen (2013) found very similar changes for the SRES A2 scenario, for which in contrast to the A1B scenario forcing by anthropogenic sulphate aerosol is not reduced during the latter half of the 21st century, while the water vapour content of the atmosphere is further enhanced due to the stronger global warming. This led the authors to conclude that the projected changes in solar radiation are mainly caused by changes in meteorological conditions, principally changes in cloudiness.

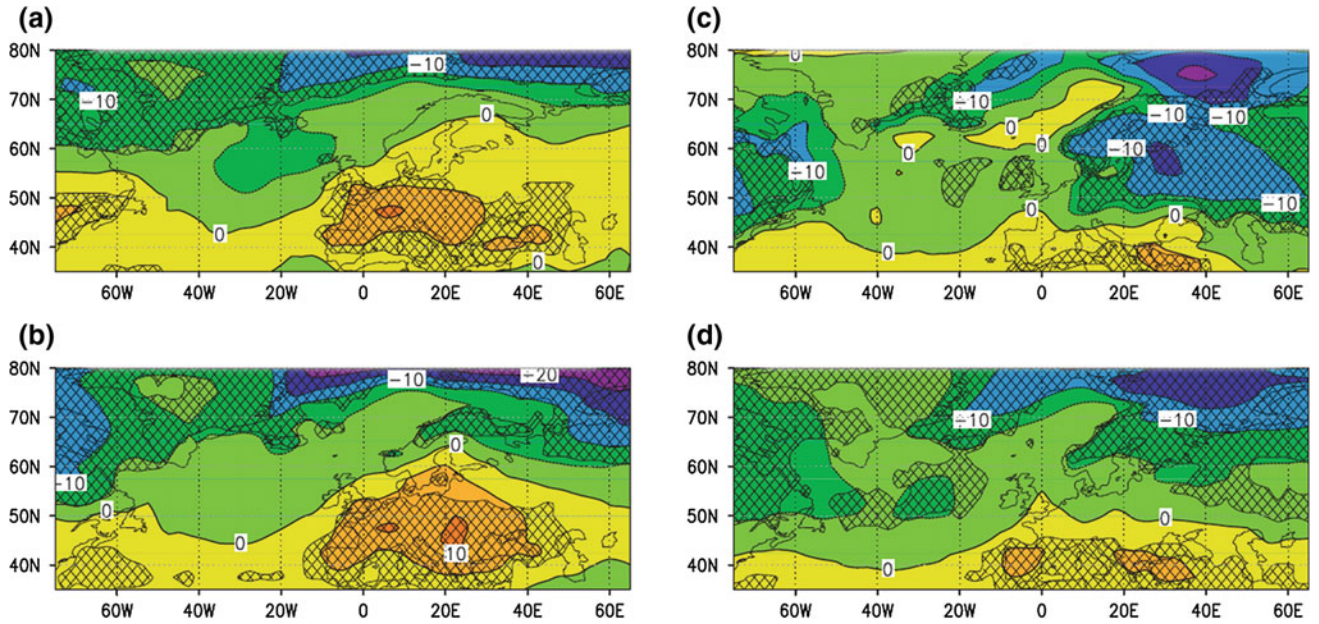

Fig. 5.7 Seasonal change in incident solar radiation (%) from 1971–2000 to 2070–2099 under the SRES A1B scenario as an average of 18 GCMs: **a** summer, **b** autumn, **c** winter, and **d** spring. Areas where more than 85 % of the models (at least 16 of 18 GCMs) agree on the sign of the change are hatched. The contour interval is 5 Wm^{-2}; negative changes are marked by warm colours (*yellow*, *orange* and *red*) and positive changes by cold colours (*green*, *blue* and *purple*) (Ruosteenoja and Räisänen 2013)

5.6.2 Terrestrial Radiation

Compared to solar radiation there are even fewer studies assessing projected changes in terrestrial radiation. This could be considered surprising, since terrestrial radiation plays an important role in the greenhouse effect. Zhou et al. (2009) found, for instance, an increase in annual mean terrestrial radiation across the entire North Sea region, with the increase ranging from 14 Wm^{-2} in the western part to 21 Wm^{-2} in the eastern part by the end of the 21st century. Wild et al. (1997) found a similar pattern with increases of 5–10 Wm^{-2}. Trenberth and Fasullo (2009), who in contrast to other studies considered changes in radiation at the top of the atmosphere, found a decrease in annual mean outgoing terrestrial radiation of about 1.5 Wm^{-2} over the North Sea and about 3 Wm^{-2} over adjacent land areas.

5.6.3 Cloud Cover

Consistent with the projected changes in annual mean net solar radiation at the surface, the aforementioned studies show a distinct pattern with a projected increase in cloud cover over the northern part of the North Sea region and a decrease over the southern part. This can be taken as a robust result, given the different climate models, scenarios and time periods considered. Nevertheless, the magnitude of the projected changes in these two areas does vary between studies. This finding is also supported by the recent RCP scenario simulations. As shown by Collins et al. (2013), both the RCP4.5 and RCP8.5 scenarios give a decrease in the annual mean cloud cover fraction, of up to 5 % in the southern part of the North Sea region by the end of the 21st century for RCP8.5. Moreover, the projected changes are generally weaker (and less significant) over the North Sea itself than over the adjacent land areas.

Zhou et al. (2009) and Trenberth and Fasullo (2009) found a less pronounced effect on cloud cover in the northern part of the North Sea region than in the south. They found a slight increase of up to 0.5 and 0.75 %, respectively, in the northern part, and a considerably stronger decrease of up to 3 % in the southern part. Wild et al. (1997) and Henschel (2013), on the other hand, found a similar amount of change in both areas; about a 2 % increase (decrease) in cloud cover over the northern (southern) part of the North Sea region by the mid-21st century. As these changes are the median from 39 GCMs for the RCP8.5 scenario, these estimates may be considered robust, with two-thirds of the climate models agreeing on a reduction in cloud cover over the southern part of the North Sea region. Consistent with the projected changes in solar radiation, Henschel (2013) did not find any significant trends in cloud cover north of 58°N.

A study by Räisänen et al. (2003) permits a closer look at the North Sea region, as it is based on a set of regional climate simulations for Europe with the RCAO RCM, with lateral boundary conditions originating from two different GCMs for both the SRES A2 and B2 scenarios. By the end of the 21st century they found an increase in annual mean cloud cover of up to 8 % in the northern part of the North Sea region and a decrease of up to 8 % in the southern part. The projected changes in cloud cover are particularly strong during summer, with a typical reduction of 12–20 % in the southern part of the North Sea region, depending on the driving GCM and the scenario used. In the northern part, on the other hand, cloud cover typically increases by 4–12 %. In this, the projected future changes during summer are considerably stronger than during winter. Furthermore, the general structure of the patterns of projected change varies little between the different simulations in summer, emphasising the robustness of these projections. In winter, on the other hand, the patterns of simulated changes in cloud cover are strongly affected by the choice of driving GCM. While the simulations driven by HadAM2H project an increase in cloud cover over all land areas with the exception of the British Isles, the simulations driven by ECHAM4/OPYC project a slight decrease in most of this area. The only exception is the respective simulation for the SRES B2 scenario with enhanced cloud cover over western Europe. According to these results, the projected changes in cloud cover during winter are not as robust as those during summer, presumably owing to the greater uncertainty in the projected changes in the large-scale circulation over Europe due to natural climate variability.

5.6.4 Summary

Considering all the results reported here, a line of zero change can be roughly drawn from the Firth of Forth to the Skagerrak with a tendency for net solar radiation to decrease (increase) in the region to the north (south) of this line. Consistent with this the same zero-line separates areas with an increase (decrease) in cloud cover in the northern (southern) part of the region.

As mentioned in the introductory paragraph, the actual numbers given here for the North Sea region have been estimated from the corresponding geographical part presented in the respective studies, with most of them covering the entire globe. A study on the projected changes in radiation and clouds focusing on the North Sea region is still missing. With the multi-model ensemble of regional climate simulations for Europe, which have become available through CORDEX (Jacob et al. 2014), such a study might be undertaken in the future. Ruosteenoja and Räisänen (2013)

took a first step in this direction by considering the changes of the solar radiation for northern and southern Europe separately. Given the importance of the projected changes in cloud cover in the North Sea region, further investigations on the changes in specific cloud properties, i.e. the vertical distribution with low-, mid and high-level clouds or the phase of the clouds (liquid and ice), might help to understand the physical mechanisms behind the projected changes.

5.7 Conclusions

Wilhelm May

The climate projections considered in this chapter reveal changes in the state of the atmosphere in the North Sea region, both in the free atmosphere and near the surface. The changes mostly concern conditions at the end of the 21st century (with the end of the 20th century or the turn of the 20th and the 21st centuries as the baseline), although some relate to the mid-21st century. They comprise:

- Amplification and an eastward shift in the pattern of NAO variability in autumn and winter.
- Changes in the storm track with increased cyclone density over western Europe in winter and reduced cyclone density on the southern flank in summer.
- More frequent strong winds from westerly directions and less frequent strong winds from south-easterly directions.
- A marked mean warming of 1.7–3.2 °C for different scenarios, with stronger warming in winter than in summer and relatively strong warming over southern Norway.
- Intensified extremes related to daily maximum temperature and reduced extremes related to daily minimum temperature, both in terms of strength and frequency.
- An increase in mean precipitation during the cold season and a reduction during the warm season.
- A pronounced increase in the intensity of heavy daily precipitation events, particularly in winter.
- A considerable increase in the intensity of extreme hourly precipitation in summer.
- An increase (decrease) in cloud cover in the northern (southern) part of the North Sea region, resulting in a decrease (increase) in net solar radiation at the surface.

It should be noted that the uncertainty ranges of the future changes projected by the climate scenarios vary between the different meteorological variables. The uncertainty range is particularly large for the projected changes in wind speed and in wind direction, both for mean winds and for wind extremes. Hence, the projected changes in wind characteristics are typically within the range of natural variability and can even have opposite signs for different scenarios either simulated by different climate models or for different future periods.

The projected changes in future climate presented here for the North Sea region have typically been extracted from geographical distributions for either the entire globe, when scenario simulations with GCMs are considered, or for Europe, when scenario simulations with RCMs are used. In some of the respective studies, however, different parts of Europe were considered separately, typically distinguishing between northern and southern Europe. With the multi-model ensemble of regional climate simulations for Europe, which have become available through CORDEX (Jacob et al. 2014), such studies with a special focus on the North Sea region could become available in the near future. The studies considered here vary widely in the choice of underlying scenarios for anthropogenic climate forcing, namely the different SRES scenarios and RCP scenarios. There is, however, a tendency to focus on the SRES A1B scenario in previous studies and the RCP4.5 and RCP8.5 scenarios, respectively, in the most recent studies. Also, the studies vary considerably in the time periods chosen, both for the present-day and future climate conditions, which can make it difficult to directly compare the magnitude of corresponding projected changes between studies. In particular, some studies focus on projections to the middle of the 21st century instead of the end of the 21st century, while some consider projections for both periods. This chapter mostly reports on changes projected at the end of the 21st century. This is mainly because for most of the forcing scenarios the projected changes are stronger at the end of the century, which means there is a higher probability of the projected regional changes exceeding the range of internal variability at that point. Moreover, the differences between RCP scenarios, in particular between the RCP2.6 and RCP4.5 scenarios, develop during the latter half of the century.

Several factors contribute to the uncertainties in the projected changes, that is, the uncertainty in the climate forcing due to different scenarios, the model uncertainty associated with different climate models, and the uncertainty due to the natural variability of the climate system. By coordinating the simulation of future climate scenarios by different research groups in initiatives such as CMIP3, CMIP5 or CORDEX or in the ENSEMBLES project, the importance of some of these sources of uncertainty can be quantified, ultimately leading to estimates of the likelihood at which certain climatic changes can be expected to occur. With the increase in computer power, climate models have been improved in several respects. In particular, components such as vegetation and marine biogeochemical cycles have been added to coupled climate models leading to the development of earth system models (ESMs) and the horizontal and vertical resolutions of both global and regional

climate models have been improved, allowing better representation of certain processes in these models. Furthermore, the ongoing development of regionally coupled model systems with an RCM interactively coupled to an ocean model could improve the presentation of climate processes over the North Sea and, hence, the quality of climate simulations for the North Sea region.

References

Barnes E, Hartman DL (2010) Influence of eddy-driven jet latitude on North Atlantic jet persistence and blocking frequency in CMIP3 integrations. Geophys Res Lett 37:L23802. doi:10.1029/2010GL045700

Barnes E, Polvani L (2013) Response of the midlatitude jets, and of their variability, to increased greenhouse gases in the CMIP5 models. J Clim 26:7117–7135

Barnes E, Slingo J, Woollings T (2012) A methodology for the comparison of blocking climatologies across indices, models and climate scenarios. Clim Dyn 38:2467–2481

Beniston M, Stephenson DB, Christensen OB, Ferro CAT, Frei C, Goyette S, Halsnaes K, Holt T, Jylhä K, Koffi B, Palutikof J, Schöll R, Semmler T, Woth K (2007) Future extreme events in European climate: an exploration of regional climate model projections. Clim Change 81:71–95

Brutel-Vuilmet C, Ménégoz M, Krinner G (2013) An analysis of present and future seasonal Northern Hemisphere land snow cover simulated by CMIP5 coupled climate models. Cryosphere 7:67–80

Cattiaux J, Vautard R, Cassou C, Yiou P, Masson-Delmotte V, Codron F (2010) Winter 2010 in Europe: a cold extreme in a warming climate. Geophys Res Lett 37:L20704. doi:10.1029/2010GL044613

Cattiaux J, Douville H, Peings Y (2013) European temperatures in CMIP5: Origins of present-day biases and future uncertainties. Clim Dyn 41:2889–2907

Cattiaux J, Douville H, Schoetter R, Parey S, Yiou P (2015) Projected changes in diurnal and interdiurnal variations of European summer temperatures. Geophys Res Lett 42:899–907

Chang EKM, Guo Y, Xia X (2012) CMIP5 multimodel ensemble projection of storm track change under global warming. GCMs. J Geophys Res 117:D23118. doi:10.1029/2012JD018578

Christensen JH, Hewitson B, Busuioc A, Chen A, Gao X, Held I, Jones R, Kolli RK, Kwon W-T, Laprise R, Magaña Rueda V, Mearns L, Menéndez CG, Räisänen J, Rinke A, Sarr A, Whetton P (2007) Regional climate projections. In: Solomon S, Qin D, Manning M, Chen Z, Marquis M, Averyt KB, Tignor M, Miller HL (eds) Climate Change 2007: The physical science basis. Contribution of Working Group I to the Fourth Assessment Report of the Intergovernmental Panel on Climate Change. Cambridge University Press

Christensen JH, Krishna Kumar K, Aldrian E, An S-I, Cavalcanti IFA, de Castro M, Dong W, Goswami P, Hall A, Kanyanga JK, Kitoh A, Kossin J, Lau N-C, Renwick J, Stephenson DB, Xie S-P, Zhou T (2013a) Climate phenomena and their relevance for future regional climate change. In: Stocker TF, Qin D, Plattner G-K, Tignor M, Allen SK, Boschung J, Nauels A, Xia Y, Bex V, Midgley PM (eds) Climate Change 2013: The Physical Science Basis. Contribution of Working Group I to the Fifth Assessment Report of the Intergovernmental Panel on Climate Change. Cambridge University Press

Christensen JH, Krishna Kumar K, Aldrian E, An S-I, Cavalcanti IFA, de Castro M, Dong W, Goswami P, Hall A, Kanyanga JK, Kitoh A, Kossin J, Lau N-C, Renwick J, Stephenson DB, Xie S-P, Zhou T (2013b) Climate phenomena and their relevance for future regional climate change; Supplementary Material. In: Stocker TF, Qin D, Plattner GK, Tignor M, Allen SK, Boschung J, Nauels A, Xia Y, Bex V, Midgley PM (eds) Climate Change 2013: The Physical Science Basis. Available from www.climatechange2013.org and www.ipcc.ch

Collins M, Knutti R, Arblaster J, Dufresne J-L, Fichefet T, Friedlingstein P, Gao X, Gutowski WJ, Johns T, Krinner G, Shongwe M, Tebaldi C, Weaver AJ, Wehner M (2013) Long-term climate change: Projections, commitments and irreversibility. In: Stocker TF, Qin D, Plattner GK, Tignor M, Allen SK, Boschung J, Nauels A, Xia Y, Bex V, Midgley PM (eds) Climate Change 2013: The Physical Science Basis. Contribution of Working Group I to the Fifth Assessment Report of the Intergovernmental Panel on Climate Change. Cambridge University Press

Croci-Maspoli M, Schwierz C, Davies H (2007) Atmospheric blocking: space-time links to the NAO and PNA. Clim Dyn 29:713–725

Davini P, Cagnazzo C (2013) On the misinterpretation of the North Atlantic Oscillation in CMIP5 models. Clim Dyn 43:1497–1511

De Winter RC, Sterl A, Ruessink BG (2013) Wind extremes in the North Sea basin under climate change: an ensemble study of 12 CMIP5 GCMs. J Geophys Res 118:1601–1612

Debernard JB, Røed LP (2008) Future wind, wave and storm surge climate in the Northern Seas: a revisit. Tellus 60A:427–438

Deser C, Phillips A, Burdette V, Teng H (2012) Uncertainty in climate change projections: The role of internal variability. Clim Dyn 38:527–546

DMI (2014) Fremtidige klimaændringer I Danmark. Dansk Klimacenter rapport 14-06, DMI, Copenhagen, Denmark

Donat MG, Leckebusch GC, Pinto JG, Ulbrich U (2010) European storminess and associated circulation weather types: future changes deduced from a multi-model ensemble of GCM simulations. Clim Res 42:27–43

Donat MG, Leckebusch GC, Wild S, Ulbrich U (2011) Future changes in European winter storm losses and extreme wind speeds inferred from GCM and RCM multi-model simulations. Nat Hazards Earth Syst Sci 11:1351–1370

Dong B, Sutton RT, Woollings T (2011) Changes of interannual NAO variability in response to greenhouse gases forcing. Clim Dyn 37:1621–1641

Dunn-Sigouin E, Son SW (2013) Northern Hemisphere blocking frequency and duration in the CMIP5 models. J Geophys Res 118:1179–1188

EEA (2012) Climate change, impacts and vulnerability in Europe. European Environment Agency (EEA) Report 12/2012

Feser F, Barcikowska M, Krueger O, Schenk F, Weisse R, Xia L C (2015) Storminess over the North Atlantic and northwestern Europe – A review. Q J Roy Met Soc 141:350–382

Fischer EM, Schär C (2010) Consistent geographical patterns of changes in high-impact European heatwaves. Nat Geosci 3:398–403
Folland CK, Knight J, Linderholm HW, Fereday D, Ineson S, Hurrell JW (2009) The summer North Atlantic Oscillation: past, present, and future. J Clim 22:1082–1103
Frei C, Schöll R, Fukutome S, Schmidli J, Vidale PL (2006) Future change of precipitation extremes in Europe: Intercomparison of scenarios from regional climate models. J Geophys Res 111: D06105. doi:10.1029/2005JD005965
Frich P, Alexander LV, Della-Marta P, Gleason B, Haylock M, Klein Tank AMG, Peterson T (2002) Observed coherent changes in climatic extremes during the second half of the twentieth century. Clim Res 19:193–212
Gaslikova L, Grabemann I, Groll N (2013) Changes in North Sea storm surge conditions for four transient future climate realizations. Nat Hazards 66:1501–1518
Gillett NP, Fyfe JC (2013) Annular mode changes in the CMIP5 simulations. Geophys Res Lett 40:1189–1193
Giorgi F, Jones C, Asrar GR (2009) Addressing climate information needs at a regional level: the CORDEX framework. Bull World Met Org 58:175–183
Haarsma RJ, Selten F, van Oldenborgh GJ (2013) Anthropogenic changes of the thermal and zonal flow structure over Western Europe and Eastern North Atlantic in CMIP3 and CMIP5 models. Clim Dyn 41:2577–2588
Harvey BJ, Shaffrey LC, Wollings TJ, Zappa G, Hodges KI (2012) How large are projected 21st century storm track changes? Geophys Res Lett 39:L18707. doi:10.1029/2012GL052873
Henschel F (2013) Projections of insolation changes for solar energy power production. Master Thesis, Swiss Federal Institute for Technology, Zurich
Hewitson B, Janetos AC, Carter TR, Giorgi F, Jones RG, Kwon W-T, Mearns LO, Schipper ELF, van Alst M (2014a) Regional context. In: Barros VR, Field CB, Dokken DJ, Mastrandrea MD, Mach KJ, Bilir TE, Chatterjee K, Ebi KL, Estrada YO, Genova RC, Girma B, Kissel ES, Levy AN, MacCracken S, Mastrandrea PR, White LL (eds) Climate Change 2014: Impacts, Adaptation, and Vulnerability; Part B: Regional Aspects. Contribution of Working Group II to the Fifth Assessment Report of the Intergovernmental Panel on Climate Change. Cambridge University Press
Hewitson B, Janetos AC, Carter TR, Giorgi F, Jones RG, Kwon W-T, Mearns LO, Schipper ELF, van Alst M (2014b) Regional context: Supplementary material. In: Barros VR, Field CB, Dokken DJ, Mastrandrea MD, Mach KJ, Bilir TE, Chatterjee K, Ebi KL, Estrada YO, Genova RC, Girma B, Kissel ES, Levy AN, MacCracken S, Mastrandrea PR, White LL (eds) Climate Change 2014: Impacts, Adaptation, and Vulnerability; Part B: Regional Aspects. Contribution of Working Group II to the Fifth Assessment Report of the Intergovernmental Panel on Climate Change. Available from www.ipcc-wg2.gov/AR5 and www.ipcc.ch
Hodges KI (1999) Adaptive constraints for feature tracking. Mon Wea Rev 127:1362–1373
Hurrell JW, Deser C (2009) North Atlantic climate variability: The role of the North Atlantic Oscillation. J Mar Syst 78:28–41
Hurrell JW, Kushnir Y, Ottersen G, Visbeck M (2003) An overview of the North Atlantic Oscillation. In: Hurrell JW, Kushnir Y, Visbeck M, Ottersen G (eds), The North Atlantic Oscillation: Climate Significance and Environmental Impact. Geophysical Monograph Series, Vol 134, American Geophysical Union, Washington, DC, 1–35, doi:10.1029/134GM01
IPCC (2012) Managing the risks of extreme events and disasters to advance climate change adaptation. In: Field CB, Barros V, Stocker TF, Qin D, Dokken DJ, Ebi KL, Mastrandrea MD, Mach KJ, Plattner G-K, Allen SK, Tignor M, Midgley PM (eds) Special report of the Intergovernmental Panel on Climate Change. Cambridge University Press
IPCC (2013) Annex I: Atlas of global and regional climate projections. In: Stocker TF, Qin D, Plattner GK, Tignor M, Allen SK, Boschung J, Nauels A, Xia Y, Bex V, Midgley PM (eds) Climate Change 2013: The Physical Science Basis. Cambridge University Press
Itoh H (2008) Reconsideration of the true versus apparent Arctic Oscillation. J Clim 21:2047–2062
Jacob D, Petersen J, Eggert B, Alias A, Christensen OB, Bouwer LM, Braun A, Colette A, Déqué M, Georgievski G, Georgopoulou E, Gobiet A, Menut L, Nikulin G, Haensler A, Hempelmann N, Jones C, Keuler K, Kovats S, Kröner N, Kotlarski S, Kriegsmann A, Martin E, van Meijgaard E, Moseley C, Pfeifer S, Preuschmann S, Radermacher C, Radtke K, Rechid D, Rounsevell M, Samuelsson P, Somot S, Soussana J-F, Teichmann C, Valentini R, Vautard R, Weber B, Yiou P (2014) EURO-CORDEX: new high-resolution climate change projections for European impact research. Reg Environ Change 14:563–578
Kendon EJ, Rowell DP, Jones RG, Buonomo E (2008) Robustness of future changes in local precipitation extremes. J Clim 21:4280–4297
Kendon EJ, Roberts NM, Fowler HJ, Roberts MJ, Chan SC, Senior CA (2014) Heavier summer downpours with climate change revealed by weather forecast resolution model. Nature Clim Change 4:570–576
Kharin S, Zwiers FW, Zhang X, Wehner M (2013) Changes in temperature and precipitation extremes in the CMIP5 ensemble. Clim Change 119:345–357
Kjellström E, Bärring L, Jacob D, Jones R, Lenderink G, Schär C (2007) Modelling daily temperature extremes: recent climate and future changes over Europe. Clim Change 81:249–265
Kjellström E, Nikulin G, Hansson U, Strandberg G, Ullerstig A (2011) 21st century changes in the European climate: uncertainties derived from an ensemble of regional climate model simulations. Tellus 63A:24–40
KNMI (2014) KNMI'14 climate scenarios for the Netherlands: a guide for professionals in climate adaptation. KNMI, De Bilt, The Netherlands
Knutti R, Sedláček J (2012) Robustness and uncertainties in the new CMIP5 climate model projections. Nature Clim Change 3:369–373
Koffi B, Koffi E (2008) Heat waves across Europe by the end of the 21st century: multiregional climate simulations. Clim Res 36:153-168
Kovats RS, Valentini R, Bouwer M, Georgopoulou E, Jacob D, Martin E, Rounsevell M, Soussana J-F (2014a) Europe. In: Barros VR, Field CB, Dokken DJ, Mastrandrea MD, Mach KJ, Bilir TE, Chatterjee K, Ebi KL, Estrada YO, Genova RC, Girma B, Kissel ES, Levy AN, MacCracken S, Mastrandrea PR, White LL (eds) Climate Change 2014: Impacts, Adaptation, and Vulnerability; Part B: Regional Aspects. Contribution of Working Group II to the Fifth Assessment Report of the Intergovernmental Panel on Climate Change. Cambridge University Press
Kovats RS, Valentini R, Bouwer M, Georgopoulou E, Jacob D, Martin E, Rounsevell M, Soussana J-F (2014b) Europe; Supplementary material. In: Barros VR, Field CB, Dokken DJ, Mastrandrea MD, Mach KJ, Bilir TE, Chatterjee K, Ebi KL, Estrada YO, Genova RC, Girma B, Kissel ES, Levy AN, MacCracken S, Mastrandrea PR, White LL (eds), Climate Change 2014: Impacts, Adaptation, and Vulnerability; Part B: Regional Aspects. Contribution of Working Group II to the Fifth Assessment Report of the Intergovernmental Panel on Climate Change. Available from www.ipcc-wg2.gov/AR5 and www.ipcc.ch
Lenderink G, van Meijgaard E (2008) Increase in hourly precipitation extremes beyond expectations from temperature changes. Nature Geosci 1:511–514

Masato G, Hoskins BJ, Wollings T (2013) Winter and summer Northern Hemisphere blocking in CMIP5 models. J Clim 26: 7044–7059

Matsueda M (2011) Predictability of Euro-Russian blocking in summer of 2010. Geophys Res Lett 38:L06801. doi:10.1029/2010GL046557

McInnes KL, Erwin TA, Batholds JM (2011) Global climate model projected changes in 10 m wind speed and direction due to anthropogenic climate change. Atmos Sci Let 12:325–333

Meehl GA, Covey C, Taylor KE, Delworth T, Stouffer RJ, Latif M, McAvaney B, Mitchell JFB (2007a) The WCRP CMIP3 multi-model dataset: a new era in climate change research. Bull Am Met Soc 88:1383–1394

Meehl GA, Stocker TF, Collins WD, Friedlingstein P, Gaye AT, Gregory JM, Kitoh A, Knutti R, Murphy JM, Noda A, Raper SCB, Watterson IG, WeaverAJ, Zhao Z-C (2007b) Global climate projections. In: Solomon S, Qin D, Manning M, Chen Z, Marquis M, Averyt KB, Tignor M, Miller HL (eds) Climate Change 2007: The Physical Science Basis. Contribution of Working Group I to the Fourth Assessment Report of the Intergovernmental Panel on Climate Change. Cambridge University Press

Metzger MJ, Bunce RGH, Jongman RHG, Mücher CA, Watkins JW (2005) A climatic stratification of the environment of Europe. Glob Ecol Biogeogr 14:549–563

Miller RL, Schmidt GA, Shindell DT (2006) Forced annular changes in the 20th century Intergovernmental Panel on Climate Change Fourth Assessment Report models. J Geophys Res 111:D18101. doi:10.1029/2005JD006323

Mizuta R (2012) Intensification of extratropical cyclones associated with the polar jet change in the CMIP5 global warming projections. Geophys Res Lett 39:L19707. doi:10.1029/2012GL053032

Moss RH, Edmonds JA, Hibbard KA, Manning MR, Rose SK, van Vuuren DP, Carter TR, Emori S, Kainuma M, Kram T, Meehl GA, Mitchell JFB, Nakicenovic N, Riahi K, Smith SJ, Stouffer RJ, Thomson AM, Weyant JP, Wilbanks TJ (2010) The next generation of scenarios for climate change research and assessment. Nature 463:747–756

Nakićenović NJ, Alcamo J, Davis G, de Vries B, Fenhann J, Gaffin S, Gregory K, Grübler A, Jung TY, Kram T, Lebre La Rovere E, Michaelis L, Mori S, Morita T, Pepper W, Pitcher H, Price L, Riahi K, Roehrl A, Rogner H-H, Sankovski A, Schlesinger M, Shukla P, Smith S, Swart R, van Rooijen S, Victor N, Dadi Z (2000) IPCC Special Report on Emission Scenarios. Cambridge University Press

Nikulin G, Kjellström E, Hansson U, Strandberg G, Ullerstig A (2011) Evaluation and future projections of temperature, precipitation and wind extremes over Europe in an ensemble of regional climate simulations. Tellus 63A:41–55

Noble IR, Huq S, Anokhin YA, Carmin J, Goudou D, Lansigan FP, Osman-Elasha B, Villamizar A (2014) Adaptation needs and options. In: Barros VR, Field CB, Dokken DJ, Mastrandrea MD, Mach KJ, Bilir TE, Chatterjee K, Ebi KL, Estrada YO, Genova RC, Girma B, Kissel ES, Levy AN, MacCracken S, Mastrandrea PR, White LL (eds) Climate Change 2014: Impacts, Adaptation, and Vulnerability; Part A: Global and Sectoral Aspects. Contribution of Working Group II to the Fifth Assessment Report of the Intergovernmental Panel on Climate Change. Cambridge University Press

Orlowsky B, Seneviratne SI (2012) Global changes in extremes events: Regional and seasonal dimension. Clim Change 110:669–696

Pryor SC, Nikulin G, Jones C (2012) Influence of spatial resolution on regional model derived wind climates. J Geopsys Res 117: D03117. doi:10.1029/2011JD016822

Räisänen J, Eklund J (2012) 21st century changes in snow climate in Northern Europe: a high-resolution view from ENSEMBLES regional climate models. Clim Dyn 38:2575–2591

Räisänen J, Hansson U, Ullerstig A, Döscher R, Graham LP, Jones C, Meier M, Samuelsson P, Willén U (2003) GCM driven simulations of recent and future climate with the Rossby Centre coupled atmosphere – Baltic Sea regional climate model. SMHI Rep Met Climatol 101

Ruosteenoja K, Räisänen P (2013) Seasonal changes in solar radiation and relative humidity in Europe in response to global warming. J Clim 26:2467–2481

Scaife A, Folland CK, Alexander LV, Moberg A, Knight JR (2008) European climate extremes and the North Atlantic Oscillation. J Clim 21:72–83

Schoetter R, Cattiaux J, Douville H (2014) Changes of western European heat wave characteristics projected by the CMIP5 ensemble. Clim Dyn. doi:10.1007/s00382-014-2434-8

Scoccimarro E, Gualdi S, Bellucci A, Zampieri M, Navarra A (2013) Heavy precipitation events in a warmer climate: Results from CMIP5 models. J Clim 26:7902–7911

Seneviratne SI, Nicholls N, Easterling D, Goodess CM, Kanae S, Kossin J, Luo Y, Marengo J, McInnes K, Rahimi M, Reichstein M, Sorteberg A, Vera C, Zhan X (2012) Changes in climate extremes and their impacts on the natural physical environment. In: Field CB, Barros V, Stocker TF, Qin D, Dokken DJ, Ebi KL, Mastrandrea MD, Mach KJ, Plattner G-K, Allen SK, Tignor M, Midgley PM (eds), Managing the Risks of Extreme Events and Disasters to Advance Climate Change Adaptation. A Special Report of Working Groups I and II of the Intergovernmental Panel on Climate Change (IPCC). Cambridge University Press

Sillmann J, Roeckner E (2008) Indices for extreme events in projections of anthropogenic climate change. Clim Change 86:83–104

Sillmann J, Croci-Maspoli M, Kallache M, Katz RW (2011) Extreme cold winter temperatures in Europe under the influence of North Atlantic atmospheric blocking. J Clim 24:5899–5913

Sillmann J, Kharin S, Zwiers FW, Zhang X, Bronough D (2013) Climate extreme indices in the CMIP5 multimodel ensemble: Part 2. Future climate projections. J Geophys Res 118:2473–2493

Sterl A, van den Brink H, de Vries H, Haarsma R, van Meijgaard E (2009) An ensemble study of extreme surge related water levels in the North Sea in a changing climate. Ocean Sci 5:369–378

Sterl A, Bakker AMR, van den Brink HW, Haarsma R, Stepek A, Wijnant IL, de Winter RC (2015) Large-scale winds in the southern North Sea region: the wind part of the KNMI'14 climate change scenarios. Env Res Lett 10:035004. doi:10.1088/1748-9326/10/3

Taylor K, Stouffer RJ, Meehl GA (2012) An overview of CMIP5 and the experiment design. Bull Am Met Soc 93:485–498

Tebaldi C, Hayhoe K, Arblaster JM, Meehl GA (2006) Going to the extremes. An intercomparison of model-simulated historical and future changes in extreme events. Clim Change 79:185–211

Thompson DWJ, Wallace JM (2000) Annular modes in the extratropical circulation. Part I: Month-to-month variability. J Clim 13: 1000–1016

Trenberth KE, Fasullo JT (2009) Global warming due to increasing absorbed solar radiation. Geophys Res Lett 36:L07706. doi:10.1019/2009GL037527

Trigo RM, Trigo IF, DaCamara CC, Osborn TJ (2004) Climate impact of the European winter blocking episodes from the NCEP/NCAR Reanalyses. Clim Dyn 23:17–28

Tyrlis E, Hoskins BJ (2008) Aspects of a Northern Hemisphere atmospheric blocking climatology. J Atmos Sci 65:1638–1652

Ulbrich U, Christoph M (1999) A shift of the NAO and increasing storm track activity over Europe due to anthropogenic greenhouse gas forcing. Clim Dyn 15:551–559

Ulbrich U, Pinto JG, Kupfer H, Leckebusch GC, Spangehl T, Reyers M (2008) Changing Northern Hemisphere storm tracks in an ensemble of IPCC climate change simulations. J Clim 21:1669–1679

Ulbrich U, Leckebusch GC, Grieger J, Schuster M, Akperov M, Bardin MY, Feng Y, Gulev S, Inatsu M, Keay K, Kew SF, Liberato MLR, Lionello P, Mokhov II, Neu U, Pinto JG, Raible CC,

Reale M, Rudeva I, Simmonds I, Tilinina ND, Trigo IF, Ulbrich S, Wang XL, Wernli H and The IMILAST TEAM (2013) Are greenhouse gas signals of Northern Hemisphere winter extra-tropical cyclone activity dependent on the identification and tracking algorithm? Meteorol Z 22:61–68

Van den Hurk B, van Oldenborgh GJ, Lenderink G, Hazeleger W, Haarsma R, de Vries H (2014) Drivers of mean climate change around the Netherlands derived from CMIP5. Clim Dyn 42:1683–1697

Van der Linden P, Mitchell JFB (2009) ENSEMBLES: Climate change and its impacts: Summary of research and results from the ENSEMBLES project. Met Office Hadley Centre, Exeter

Van Vuuren DP, Edmonds J, Kainuma M, Riahi K, Thomson A, Hibbard K, Hurtt GC, Kram T, Krey V, Lamarque J-F, Masui T, Meinshausen M, Nakicenovic N, Smith SJ, Rose SK (2011) Representative concentration pathways: an overview. Clim Change 109:5–31

Wagner S, Berg P, Schädler G, Kunstmann H (2013) High-resolution regional climate simulations for Germany: Part II – projected climate changes. Clim Dyn 40:415–427

Wiedenmann JM, Lupo AR, Mokhov II, Tikhonova EA (2002) The climatology of blocking anticyclones for the Northern and Southern Hemispheres: Block intensity as a diagnostic. J Clim 15:3459–3473

Wild M, Ohmura A, Cubasch U (1997) GCM-simulated surface energy fluxes in climate change experiments. J Clim 10:3093–3110

Winterfeldt J, Weisse R (2009) Assessment of value added for surface marine wind speed obtained from two regional climate models. Mon Wea Rev 137:2955–2965

Woollings T (2010) Dynamical influences on European climate: An uncertain future. Phil Trans Roy Soc 368A:3733–3756

Woollings T, Blackburn M (2012) The North Atlantic jet stream under climate change and its relation to the NAO and EA patterns. J Clim 25:886–902

Zappa G, Sheffrey LC, Hodges KI, Sansom PG, Stephenson DB (2013) A multimodel assessment of future projections of North Atlantic and European extratropical cyclones in the CMIP5 climate models. J Clim 26:5846–5862

Zhang X, Alexander L, Hegerl GC, Jones P, Klein Tank A, Peterson TC, Trewin B, Zwiers FW (2011) Indices for monitoring changes in extremes based on daily temperature and precipitation data. WIREs Clim Change 2:851–870

Zhou L, Dickinson RE, Dirmeyer P, Dai A, Min SK (2009) Spatiotemporal patterns of changes in maximum and minimum temperatures in multi-model simulations. Geophys Res Lett 36: L02702. doi:10.1019/2008GL036141

Projected Change—North Sea

6

Corinna Schrum, Jason Lowe, H.E. Markus Meier, Iris Grabemann, Jason Holt, Moritz Mathis, Thomas Pohlmann, Morten D. Skogen, Andreas Sterl and Sarah Wakelin

Abstract

Increasing numbers of regional climate change scenario assessments have become available for the North Sea. A critical review of the regional studies has helped identify robust changes, challenges, uncertainties and specific recommendations for future research. Coherent findings from the climate change impact studies reviewed in this chapter include overall increases in sea level and ocean temperature, a freshening of the North Sea, an increase in ocean acidification and a decrease in primary production. However, findings from multi-model ensembles show the amplitude and spatial pattern of the projected changes in sea level, temperature, salinity and primary production are not consistent among the various regional projections and remain uncertain. Different approaches are used to downscale global climate change impacts, each with advantages and disadvantages. Regardless of the downscaling method employed, the regional studies are ultimately affected by the forcing global climate models. Projecting regional climate change impacts on biogeochemistry and primary production is currently limited by a lack of consistent downscaling approaches for marine and terrestrial impacts. Substantial natural variability in the North Sea region from annual to multi-decadal time scales is a particular challenge for projecting regional climate change impacts. Natural variability dominates long-term trends in wind fields and strongly wind-influenced characteristics like local sea level, storm

C. Schrum (✉)
Geophysical Institute, University of Bergen, Bergen, Norway
e-mail: corinna.schrum@gfi.uib.no

J. Lowe (✉)
Met Office Hadley Centre, Exeter, UK
e-mail: jason.lowe@metoffice.gov.uk

H.E.M. Meier (✉)
Research Department, Swedish Meteorological and Hydrological Institute, Norrköping, Sweden
e-mail: markus.meier@smhi.se

C. Schrum · I. Grabemann
Institute of Coastal Research, Helmholtz-Zentrum Geesthacht, Geesthacht, Germany
e-mail: corinna.schrum@hzg.de

I. Grabemann
e-mail: iris.grabemann@hzg.de

H.E.M. Meier
Department of Physical Oceanography and Instrumentation, Leibniz-Institute for Baltic Sea Research (IOW), Rostock, Germany
e-mail: markus.meier@io-warnemuende.de

J. Holt · S. Wakelin
National Oceanography Centre, Liverpool, UK
e-mail: jholt@noc.ac.uk

S. Wakelin
e-mail: slwa@noc.ac.uk

M. Mathis
Max Planck Institute for Meteorology, Hamburg, Germany
e-mail: moritz.mathis@mpimet.mpg.de

T. Pohlmann
Institute of Oceanography, CEN, University of Hamburg, Hamburg, Germany
e-mail: Thomas.Pohlmann@uni-hamburg.de

M.D. Skogen
Institute of Marine Research (IMR), Bergen, Norway
e-mail: morten.skogen@imr.no

A. Sterl
Royal Netherlands Meteorological Institute (KNMI), De Bilt, The Netherlands
e-mail: sterl@knmi.nl

M. Quante and F. Colijn (eds.), *North Sea Region Climate Change Assessment*, Regional Climate Studies, DOI 10.1007/978-3-319-39745-0_6

surges, surface waves, circulation and local transport pattern. Multi-decadal variations bias changes projected for 20- or 30-year time slices. Disentangling natural variations and regional climate change impacts is a remaining challenge for the North Sea and reliable predictions concerning strongly wind-influenced characteristics are impossible.

6.1 Introduction

This chapter addresses projected future changes in the North Sea marine system focussing on three major aspects, namely changes in sea level, changes in hydrography and circulation, and changes in lower trophic level dynamics, biogeochemistry and ocean acidification. Future changes in the North Sea marine system will be driven by a combination of changes induced by the globally forced oceanic boundary conditions and by regional atmospheric and terrestrial changes. Regional changes in sea level are forced by changes in ocean water mass, spatial changes in the Earth's gravitational field, geological changes, changes in thermal and haline characteristics and the corresponding volume changes, and by the redistribution of water masses. Only the final two are accounted for directly or can be derived from General Circulation Models (GCMs, global climate models that are based on models for atmospheric and oceanic circulation). The first three contributions, which could have substantial impacts on regional sea level, must be estimated by a combination of expert judgement and additional methods and complementary models. In some cases, information from GCMs also plays a role and helps to ensure the development of an internally consistent scenario.

Current GCMs and ESMs (Earth System Models, here used for global models) typically simulate changes in climate at a resolution of 100 km or more, and thus often fail to deliver reliable information on regional-scale circulation such as for the North Sea (e.g. Ådlandsvik and Bentsen 2007). Moreover, GCMs and ESMs are not optimised for shelf sea hydrodynamics and biogeochemistry, and some key processes relevant to North Sea dynamics, such as tides and physical and biogeochemical coupling at the sediment-water interface, are typically neglected. A systematic climate change assessment for the North Sea using GCM and ESM model data is therefore not available, except for climate change impacts on sea level (see Sect. 6.2). Detailed and spatially resolved studies of climate impacts on the North Sea system typically use dynamic downscaling approaches employing regional dynamic models. In a study of water level extremes, such as through storm surges, it is usually possible to make use of computationally inexpensive 2-dimensional barotropic models for water levels. A simplified approach is also possible for sea surface waves and a model of the generation and dissipation of wave energy is typically employed. However, for a detailed and spatially resolved investigation of regional climate change impacts on physical and biogeochemical variables a more complex and computationally expensive approach is needed. This requires high resolution 3-dimensional coupled physical-biogeochemical models with appropriate atmospheric forcing (i.e. air-sea fluxes of momentum, energy and matter, including the atmospheric deposition of nitrogen and carbon), terrestrial forcing (volume, carbon and nutrient flows from the catchment area) and data at North Atlantic and Baltic Sea lateral boundaries. The far-field oceanic changes in hydrography and circulation are almost exclusively projected using GCMs and their results from boundary conditions for regional North Sea studies. Oceanic boundary conditions from ESMs are used to project local changes in North Sea biogeochemistry. Dynamically consistent climate change scenarios for terrestrial drivers are still lacking, both at global and regional scales. Therefore, regional studies typically use a combination of forcing GCMs and ESMs, regional downscaling and impact models (see Annexes 2 and 3 for a general review of methods), and expert judgement based on available evidence for future impact scenarios for freshwater and nutrient fluxes from terrestrial sources. These regional studies typically employ a wide range of different methods to correct the regional bias in forcing GCMs or ESMs, which are necessary to ensure a correct seasonality and coupling of local ecosystem dynamics.

In recent years, a range of regional scenarios have been published for the North Sea, addressing changes in sea level, hydrodynamics, productivity and biogeochemistry. The methods applied and processes considered vary greatly from study to study and could substantially affect the changes projected. Therefore, a classification of the most important methodological aspects used within the different subsections is provided and the projected impacts are discussed in relation to the study configuration where necessary.

6.2 Sea Level, Storm Surges and Surface Waves

The Intergovernmental Panel on Climate Change (IPCC) concluded in its fifth assessment (AR5; IPCC 2013) that it is very likely that the mean rate of global averaged sea-level rise (SLR) was 1.7 mm year^{-1} between 1901 and 2010, and 3.2 mm year^{-1} between 1993 and 2010, with tide-gauge and satellite altimeter data consistent regarding the higher rate

during the more recent period. While there has been a statistically significant acceleration in SLR since the start of the 20th century of around 0.009 mm year^{-2} (Church and White 2011), rates similar to that of the 1993–2010 period have been observed previously, for instance between 1920 and 1950. In the North Sea, rates of SLR for the 20th century of around 1.5 mm year^{-1} have been estimated (Wahl et al. 2013). Significant future changes in sea level around the world's coastline are expected over the next century and beyond (IPCC 2013). As a global average, and depending on the choice of future greenhouse gas emission scenarios, SLR to 2081–2100 relative to the 1986–2005 baseline period ranges from 0.26 to 0.82 m. Numerous studies (e.g. Bosello et al. 2012; Hinkel et al. 2013) have highlighted the potential impacts in terms of flooding and loss of coastal wetlands, and the potential damage and adaptation costs. This section reviews recent findings on global and European sea-level changes, including the behaviour of storm surges, tides and waves.

6.2.1 Time-Mean Sea Level Change

This sections addresses changes in the time-average sea level, leaving changes in rapidly varying components such as storm surge, tides and sea surface waves to later sections. The current view based on observations from the recent past and future projections by coupled GCMs is a long-term trend of rising sea level with natural variations superimposed on this general trend on a range of time scales and due to a number of physical drivers including atmospheric pressure and wind, and large-scale steric variations (Dangendorf et al. 2014). This variability obscures the detection of regional climate trends (Haigh et al. 2014) both in observations and scenario simulations.

Variations in the time-average sea level can be driven by a number of processes. First, changes in density due to changing temperature and salinity are important for the sea level on a global and regional basis. Thermal expansion occurs as extra heat is added to the water column. Salinity changes in the water column are also important in some regions. In terms of the global average the thermal expansion effect dominates over the salinity effect on sea level. However, both can be important regionally (Lowe and Gregory 2006; Pardaens et al. 2011a). The other major process driving change in time-average sea level is change in total ocean water mass. Over the next century there is likely to be a transfer of water into the ocean from storage on land in mountain glaciers and the Greenland Ice Sheet, and possibly the West Antarctic Ice Sheet. Smaller contributions to sea level change may come from other terrestrial stores, both natural aquifers and man-made reservoirs—although this input is not expected to exceed the contribution from melting land ice. Geological changes, such as changes in the size of ocean basins can also alter global sea level.

Variations in the spatial distribution of sea level are affected by several factors. From an oceanography perspective, changes in the density structure of the ocean and changes in circulation are likely to be associated with changes in the pattern of sea surface height as the ocean seeks to attain a new dynamic balance (e.g. Gregory et al. 2001; Lowe and Gregory 2006; Landerer et al. 2007; Bouttes et al. 2012). From the perspective of geology and solid earth physics, there are also spatial components associated with change in the Earth's gravity field as water moves from storage in land ice into the ocean and movement of the solid Earth as the mass loading on both the land and ocean basins change (e.g. Milne and Mitrovica 1998; Mitrovica et al. 2001). The local and regional deviations from the global mean change can act in both positive and negative directions—in some cases adding to the global mean change and in others offsetting it. Future projections involving changes in water mass distribution must take account of these effects, typically by scaling the global mean change in water mass terms by an appropriate 'fingerprint' (e.g. Slangen et al. 2014). There is also an ongoing change due to the Glacial Isostatic Adjustment (GIA) associated with the last major deglaciation, although this is typically small in most locations compared to most business-as-usual projections for the 21st century. In the southern North Sea, vertical crust movements are negative and correspond to a future sea level increase. In the northern North Sea and along the Norwegian coastline vertical crust movement is positive and leads to a future decrease in sea level. The rate of GIA is roughly linear, with values between −1.5 and +1.5 mm year^{-1} (Shennan and Horton 2002; Shennan et al. 2009), although some higher values may be found (e.g. Simpson et al. 2014). Taking a wide range of physical effects into account the latest IPCC assessment highlighted that, based on the output of predictive models, around 70 % of the global coastline is expected to experience changes within 20 % of the global mean (IPCC 2013). There may also be land movement changes on a more local scale, for instance associated with subsidence caused by ground water or gas extraction.

6.2.2 Range in Global Time-Mean Sea Level Changes

There are three main approaches to considering future global mean sea level changes in current regular use. The first is the use of complex spatially resolved physically based climate models, which attempt to simulate many of the major processes involved in changing sea level. A typical approach

(e.g. Yin 2012) uses a GCM to simulate the large-scale evolution of climate over the next century for a range of alternative pathways of future greenhouse gas forcing. The GCM is able to simulate changes in heat uptake and so thermal expansion can be determined from changes in the in situ simulated ocean temperatures or even simulated directly. The simulated atmospheric temperature and precipitation changes can be used as input to separate physical models of glaciers (e.g. Marzeion et al. 2012; Giesen and Oerlemans 2013; Radić et al. 2014), the Greenland Ice Sheet (e.g. Graversen et al. 2011; Rae et al. 2012; Yoshimori and Abe-Ouchi 2012; Nick et al. 2013) and the Antarctic Ice Sheet (e.g. Vizcaíno et al. 2010; Huybrechts et al. 2011; Bindschadler et al. 2013) to estimate their contributions. The key advantage of this modelling approach is that it can address changes in the relative importance of many different physical processes involved. The disadvantage is that the models may not include all of the important physical processes in the coupled systems or may not represent them with sufficient credibility. This is demonstrated by the latest climate model validation tests (IPCC 2013), which show that although the models clearly have skill at representing many aspects of the real observable climate, other aspects differ sizeably between model and observations. In recent years a significant advance has been to close the global sea level budget (Church et al. 2011). As a result, improved estimates became available for the thermal oceanic contribution, for glaciers and land ice contributions and for terrestrial storage. This credible level of knowledge about the different contributions to SLR in the recent past means it is now possible to model these sufficiently well to make projections of future sea-level change.

The second approach to projecting future global sea level uses climate models with reduced complexity. Here a model that represents the global average climate system is often used. A common approach is to solve the global average heat balance for the upper layer of the ocean, with radiative feedbacks supplying heat upwards from the surface and diffusion of heat downwards into deeper ocean layers (e.g. Raper et al. 2001). In complex models, many key quantities, such as climate sensitivity, are emergent properties. In reduced complexity climate models quantities such as climate sensitivity and mixed-layer depth are set as inputs and provide a means of tuning the simple climate models to emulate the global average behaviour of more complex models. Despite the tuning, there are limitations as to how well the simple model structure is able to achieve this (IPCC 2007). The major advantage of reduced complexity climate models is that they are computationally much less expensive than GCMs and so can be used to explore many more scenarios or to simulate much longer periods. The disadvantage is that they may not capture sufficient physics to be used outside their tuned range. Furthermore, most simple models

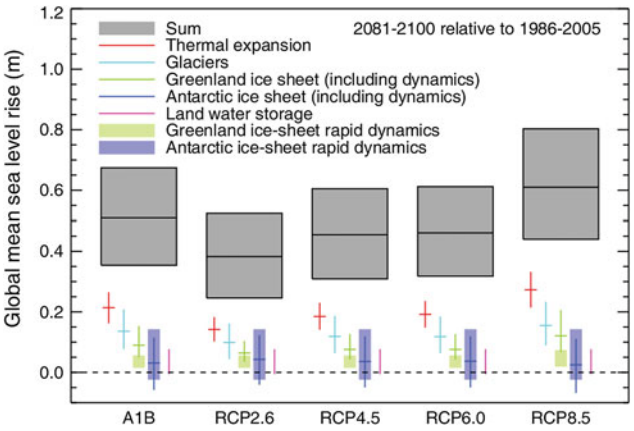

Fig. 6.1 Likely ranges of global mean sea-level rise as reported in the IPCC Fifth Assessment using process based physical models. For comparison, the SRES A1B scenario (the AR4 scenario) has been recalculated using AR5 assessment methods

only simulate long-term trends and do not capture interannual variability. Recent use has also involved combining the simpler models' simulation of global mean values with a scaled spatial pattern of change in sea-surface height from the most complex GCMs (Perrette et al. 2013). This offers the ability to interpolate between the GCM results to generate additional scenarios, although these may be less reliable when addressing stabilised forcing cases. Extra care must be taken if this approach is used for extrapolation.

The IPCC Fifth Assessment (AR5) provides the most comprehensive recent estimates of global SLR from physical models. Figure 6.1 summarises the likely range of 21st century projections. It is important to realise that these ranges are not derived purely from climate models. Expert judgement was used to broaden the range so that model estimates of the 90th percentile range were judged to correspond to the 66th percentile range in the real world. This range is wider than reported in IPCC Fourth Assessment (AR4) although direct comparisons must be undertaken with care, as emission or forcing scenarios, methodologies and even the components of sea level included are different (for emission scenarios see Annex 4). One key difference is that the most recent IPCC assessment (AR5) includes a component from changes in ice dynamics in the likely range of SLR, whereas the previous IPCC assessment (AR4) kept this separate. When this component is included in the AR4 likely range of SLR then for comparable emission or forcing scenarios the two assessments become more similar.

A third class of modelling approach to estimate future global sea level is referred to as semi-empirical and typically uses a relationship derived from observations of sea level and either global temperature (e.g. Rahmstorf 2007) or radiative forcing (e.g. Jevrejeva et al. 2012). By combining the relationship with an estimate of future forcing or surface warming from either a reduced complexity model or a

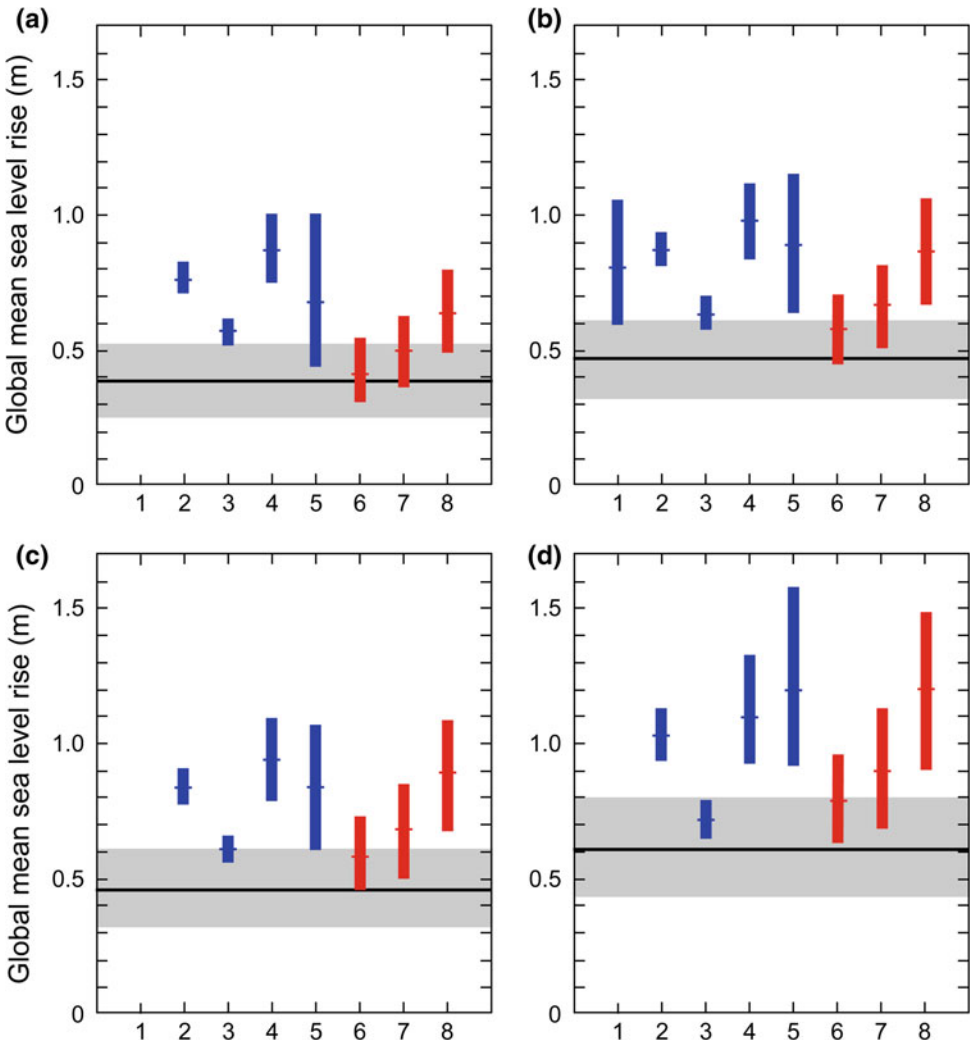

Fig. 6.2 IPCC assessment of the 5–95 % range for projections of global-mean sea level rise (m) at the end of the 21st century (2081–2100) relative to present day (1986–2005) by semi-empirical models for **a** RCP2.6, **b** RCP4.5, **c** RCP6.0, and **d** RCP8.5. *Blue bars* are results from the models using RCP (representative concentration pathway) temperature projections, *red bars* are using RCP radiative forcing. The numbers on the horizontal axis refer to different studies. The likely range (*horizontal grey bar*) from the process-based projections is also shown

complex GCM, an estimate of future sea level can be made. There has been a long debate in the literature (e.g. Lowe and Greogry 2010; Rahmstorf 2010) about the validity of these models. The IPCC AR5 estimate prescribed low confidence in long-term projections from this method (IPCC 2013). However it should be noted that this class of models covers a range of techniques with some likely to be more physically credible than others. Typically semi-empirical methods simulate larger 21st century sea level responses than GCM-based approaches, although there is some recent evidence that ranges estimated from the different approaches are starting to converge (Moore et al. 2013). The range of semi-empirical model estimates in the IPCC AR5 is shown in Fig. 6.2.

It is reasonable to ask if mitigation of emissions will impact significantly on the range of projected future sea level. Recent work has compared the climate response to business-as-usual scenarios, with increasing future emissions and aggressive emission reduction scenarios (Pardaens et al. 2011b; Schaeffer et al. 2012; Koerper et al. 2013). These studies show that mitigation this century (of a size to limit surface warming to no more than 2 °C relative to pre-industrial levels) likely will reduce SLR to 2100 by 25–50 % (Fig. 6.3). Due to the inertia of the climate system larger reductions are expected in the longer term, beyond 2100. However, eventually stabilisation of sea level may not be expected until several hundred years or more after stabilisation of atmospheric greenhouse gas concentrations or radiative forcing (Wigley 2005; Lowe et al. 2006; Levermann et al. 2013). This suggests that to avoid damaging coastal impacts may require both mitigation and adaptation approaches (Nicholls and Lowe 2004). It also raises the question as to whether SLR could be reversed artificially through geo-engineering. Studies such as that by Bouttes et al. (2013) show that the thermal expansion component of SLR can in theory be reversed but that the scenarios of atmospheric greenhouse concentration needed to achieve this are considered unlikely in the next century or so, and possibly even beyond. Land ice melt may be even harder to reverse on a practical time scale because it would take much

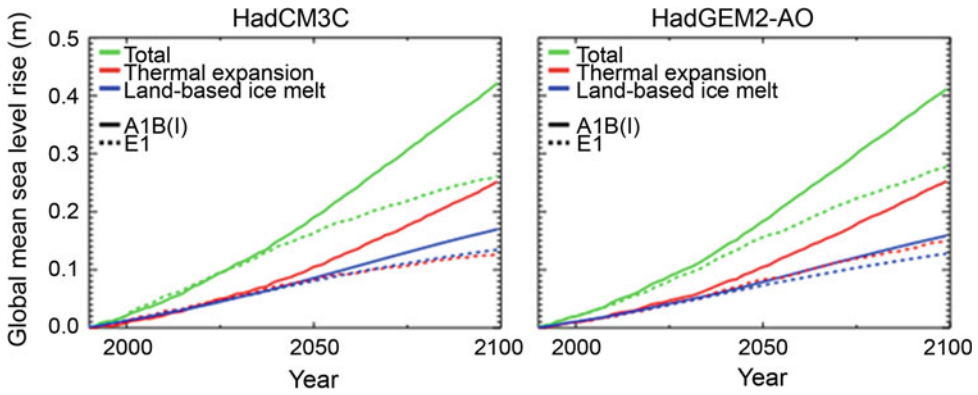

Fig. 6.3 Global mean projections of sea-level rise over the 21st century for the SRES A1B scenario (*solid lines*) and E1 (*dotted lines*) scenarios, together with the thermal expansion and land-based ice melt components. Median projections relative to 1980–1999 are shown for HadCM3C and HadGEM2-AO models (Pardaens et al. 2011b)

longer for the ice sheets to recover, even if greenhouse gas concentrations were significantly reduced (Ridley et al. 2010), than the time needed to reverse thermal expansion.

6.2.3 High-End Estimates of Time-Mean Global Sea Level Change

Another aspect of global mean sea level that has received attention from the adaptation community (e.g. Katsman et al. 2011; Ranger et al. 2013) is the possibility of an increase beyond the likely range projected by physically based climate models. Such a contribution could originate from additional dynamic ice sheet contributions, linked to the movement of fast ice streams and outlet glaciers. Numerous high-end SLR estimates exist (Nicholls et al. 2011) and while the physical processes involved are becoming better understood the global response is still poorly modelled.

Several lines of evidence, such as paleoclimate (Rohling et al. 2008) and consideration of kinematic constraints on ice streams and glaciers (Pfeffer et al. 2008) along with recent consideration of instability of the West Antarctic Ice Sheet suggest it is prudent not to rule out such increases, although the largest increases are considered unlikely. The UK climate assessment in 2009 (UKCP09[1]) (Lowe et al. 2009) concluded that 21st century global sea level increases of up to around 2 m could not be ruled out for design purpose of high risk developments, but clearly stated that rises of under 1 m are much more likely, even in higher emission scenarios. The IPCC AR5 concluded that several tens of centimetres of extra SLR could occur during the 21st century on top of the likely range due to instability of the West Antarctic Ice Sheet, but that other contributions were more unlikely or could not be quantified. When these high-end scenarios are considered, the projected SLR tends to be more similar to that of the semi-empirical method. However, this should not be considered validation of the latter approach because it is unlikely that it is able to capture the physics needed to produce the enhanced rise. Since the publication of the IPCC AR5, evidence has continued to accumulate on the behaviour of the ice sheets and their contribution to future SLR (e.g. Miles et al. 2013; Enderlin et al. 2014; Favier et al. 2014; Khan et al. 2014). This adds further evidence to there being low confidence in the AR5 estimates of the potential contribution of ice sheets to future changes in sea level.

6.2.4 Time-Mean Sea Level Projections for Europe

Numerous studies report the spatial deviation of regional sea level from the global mean values in GCMs (e.g. Gregory et al. 2001), with a considerable spread between models. Pardaens et al. (2011a) noted the lack of reduction in spread between the third and fourth IPCC assessments. Even the latest IPCC assessment (AR5) shows a wide range in the inter-model spread for regional sea level, although there is some convergence in major features, such as changes across the Antarctic Circumpolar Current and the variations associated with some of the large-scale ocean gyres. Moreover, it is now recognised that this is only part of the total pattern of sea-level response and that locally varying components from changes in land-ice loading must also be included and will further affect the spread (e.g. Simpson et al. 2014).

Two pre-AR5 studies of the North Sea resulted in scenarios of future SLR. Lowe et al. (2009) presented a 5th to 95th percentile range based on IPCC AR4, with a number of regional adjustments. By including scenario uncertainty and model uncertainty they found an increase of 5–70 cm

[1] http://ukclimateprojections.defra.gov.uk/.

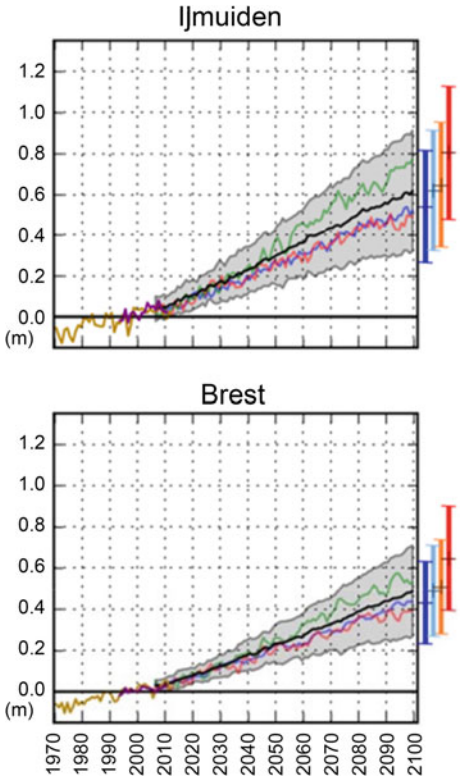

Fig. 6.4 Observed and projected relative net change in sea level for two coastal locations for which long tide-gauge measurements are available. The projected range from 21 RCP4.5 scenario runs (90 % uncertainty) is shown by the shaded region for the period 2006–2100, with the *bold line* showing the ensemble mean. *Coloured lines* represent three individual climate model realisations drawn randomly from three different climate models used in the ensemble. *Vertical bars* at the *right* sides of each panel represent the ensemble mean and ensemble spread (5–95 %) of the likely (medium confidence) change in sea level at each respective location at the year 2100 inferred from RCP2.6 (*dark blue*), RCP4.5 (*light blue*), RCP6.0 (*yellow*), and RCP8.5 (*red*) (IPCC 2013)

relative SLR for Edinburgh and 20–85 cm for the Thames Estuary, both reported for the period 1990–2100 and with the difference between the sites mainly due to different ongoing rates of vertical land movement. Katsman et al. (2008) estimated local increases for the North East Atlantic, for use by planners in the Netherlands. For the moderate climate scenario, they found projected ranges relative to 2005 of 15–25 cm in 2050 and 30–50 cm by 2100. For the warmer climate scenario the corresponding ranges were 20–35 cm in 2050 and 40–80 cm by 2100. In addition to maps of the spatial pattern of change, IPCC AR5 made available some site-specific estimates of future SLR. The time series of the nearest estimates, Ijmuiden in the Netherlands (which is inside the NOSCCA region of interest) and Brest in France (which is outside but near to the NOSCCA region of interest) are shown in Fig. 6.4.

The local time-mean sea-level change values at the end of the 21st century shown in Fig. 6.4 are only slightly different from the global mean estimate for the same scenarios shown in Fig. 6.1. This is not surprising given the IPCC finding that around 70 % of the world's coastline lies within 20 % of the global mean SLR. It also indicates that the global mean estimates for other emission or forcing scenarios can be applied to this European site. Consideration of the spatial patterns also suggests that to a first approximation this value can be applied to the North Sea region.

6.2.5 Future Changes in Extreme Sea Level

Short-lived extreme water levels are often more relevant to many coastal impacts than the time-average changes. A low pressure weather system moving over the North Sea can produce an increase in water level through the inverted barometer effect, and through the winds driving water towards the coastline. The resulting storm surge shows variations on a time scale of a few hours and combines with the tidal water elevations. The highest water levels typically occur with a surge corresponding to the rising limb of the tide rather than the peak of the tide due to non-linear interactions between the tide and surge (Horsburgh and Wilson 2007). The surge is also not a static phenomenon and will move along the coastline as a trapped wave.

Research into future changes in extreme water level uses a range of terminology and sea-surface height metrics, making such estimates difficult to compare. Some studies focus on changes in short-lived extreme water level above present-day mean sea level, while others consider changes in the meteorologically driven surge component only, sometimes expressed as a residual relative to the tidal level but increasingly expressed as changes in the skew surge. Furthermore, some studies refer to return periods while others frame their results as percentiles of the distribution of extreme levels. As the present assessment focuses on identifying the qualitative aspects of past research these complexities should not be a major hindrance.

Changes in extreme coastal water levels can be driven by the time-average sea level changes, which raise the baseline onto which extreme events are added, or by changes in particular atmospheric conditions (e.g. Lowe et al. 2010). There is a strong indication that changes in extreme water levels around the globe during the instrumental record period (about the past 150 years) have been driven predominantly by changes in regional time-mean sea level (Menendez and Woodworth 2010). Similar findings have been published for the English Channel (Haigh et al. 2010). However, there is no way to know a priori whether this will hold in the future,

or whether changes in meteorology will alter the characteristics of storm surges. Furthermore, Woodworth et al. (2007) noted a correlation between some aspects of extreme water levels, such as the winter extreme high water level around the UK measured relative to a fixed datum and the winter North Atlantic Oscillation index (NAO index, see Annex 1), a large-scale measure of the atmospheric circulation regime. The pattern of correlation was found to be very similar to that of the correlation of the time-mean water level and the NAO index, although the magnitude was stronger for the winter extreme high water level. As there is sufficient evidence that the changes in extreme water level due to changes in time-mean sea-level rise and changes in storminess combine approximately linearly (e.g. Kauker and Langenberg 2000; Lowe et al. 2001; Howard et al. 2010) over a sizeable range of future sea levels, it is insightful to consider the two components in isolation.

The recent global analysis of Hunter et al. (2013) and extended in the IPCC AR5, examined change in the return period of extreme water level events for a fixed rise in time-mean sea level and a rise following a policy-relevant scenario. Focusing on the European region for a mean SLR of 50 cm, the frequency of extreme events measured relative to a fixed datum in the present day is projected to increase by around a factor of 10 at many sites in the southern North Sea, and by a factor of more than 100 at some points in the northern North Sea. Although the factors can be applied to a range of different return periods of events, this manner of presenting the results must be placed in perspective. The level of protection increase implied by these changes remains less than an 80 cm increase at most locations.

In the EU-funded Ice2sea project (www.ice2sea.eu), Howard et al. (2014) considered how larger regional time-mean sea level increases from enhanced land ice melting might manifest in terms of changes in extreme sea level along the European coastline. Figure 6.5 shows that most of the projected 21st century change in North Sea extreme water levels is likely to come from the time-mean sea-level change. Considering a central ice melt estimate, Howard et al. (2014) found increases in the 50-year return period surge between about 20 and 40 cm. For a high-end scenario, increases in the 50-year return period surge were estimated at around 60 cm and 1 m. The estimated rise was biggest for Esbjerg and smallest for Bergen.

For potential changes in storm surge heights resulting from future changes in meteorology, both modelling approaches (dynamical downscaling and statistical downscaling) are commonly used. It is clear that the large uncertainties about future storm activity in the North Sea (see Chap. 5) are also reflected in future changes in storm surge heights in the North Sea.

A number of early studies looked at the differences between relatively short near present day and future time periods, typically using either barotropic models (Flather and Smith 1998; WASA-Group 1998; Langenberg et al. 1999; Lowe et al. 2001; STOWASUS-Group 2001) or statistical downscaling approaches (Langenberg et al. 1999). Some of these studies suggested significant changes might occur in various measures of extreme water level, although consistency between different studies was not large.

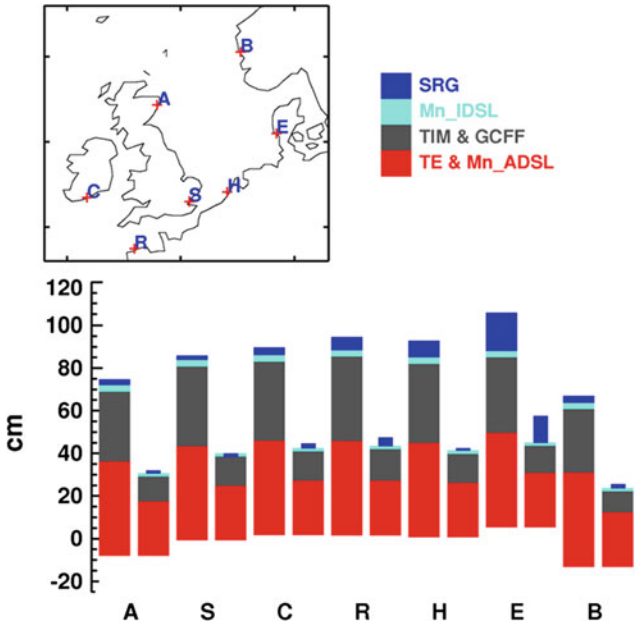

Fig. 6.5 Illustrative addition of high-end and mid-range projections of contributions to changes in the height of the 50-year storm surges in 2100 for seven locations around NW Europe. For each location, the *larger* (*left-hand*) *bar* shows the high-end estimate and the *smaller* (*right-hand*) *bar* shows the mid-range estimate. The projected contribution from Glacial Isostatic Adjustment is shown as an offset to the zero of each bar. The mid-range surge (SRG) projection at Sheerness is negative, and to ensure that this can be seen the mid-range SRG projections are shown as half-width bars. SRG is the change in surge component. Mn_IDSL is the global mean change in dynamic height due to fresh water from ice melt. TIM and GCFF is the ice melt mass component adjusted with a gravitationally consistent fingerprint. TE & Mn_ADSL is the global mean thermal expansion and local dynamic sea surface height pattern. The stations refer to model grid cells, they are close to the following geographical locations: Aberdeen (*A*), Sheerness (*S*), Cork Harbour (*C*), Roscoff (*R*), The Hague (*H*), Esbjerg (*E*) and Bergen (*B*) (Howard et al. 2014)

Later studies continued to use the time-slice approach, but focused more on sources of uncertainty. For instance, Lowe and Gregory (2005) attempted to place the results in context by comparing the uncertainty in surge projections with those from other sources, such as uncertainty in mean sea level projections and uncertainty due to emissions scenario choice. Woth (2005) and Woth et al. (2006) analysed simulations for future North Sea storm surge levels for which the forcing data were derived from simulations of the global and regional climate using different global and regional models and the SRES scenarios A2 and B2 (see Annex 4).

However, separating a robust climate signal from natural variability was still problematic. While use of time-slices was a pragmatic approach to the limits of computer power, which prevented long simulations of high resolution atmospheric models, it risks sampling long-period natural variability rather than picking up aspects of a long-term trend. Reanalysis of the 20th century storminess suggested the need for time-slices much longer than a few years or even a couple of decades. Most of the earlier studies also did not credibly estimate uncertainties in the results.

Lowe et al. (2009) used an ensemble of 11 regional climate models to drive a North Sea storm surge model and investigate uncertainty as part of the UKCP09 study. All of the experiments were transient and began before present day and extended to 2100 to avoid the time-slice problem. Focusing on the southern end of the North Sea near the Thames Estuary they found that only one of the model simulations had a statistically significant increase in the height of the 50-year return period storm surge event. However, in physical terms this change of a few centimetres was small compared to the expected time-mean relative change in sea level. This result disagreed with many earlier studies but had the advantage of not needing to use time-slices. A recent reanalysis of the model results for sites outside the United Kingdom (Howard et al. 2014) suggested larger changes in the surge component at some locations, although for sea level extremes the effect of changes in time-mean SLR still typically dominated. Sterl et al. (2009) undertook a similar study using a global model ensemble and found a similar lack of a clear 21st century trend in the storm surge component, adding further weight to the projections from UKCP09. However, an important caveat is that the atmospheric model used for the UKCP09 ensemble was noted to have a particular storm track response; typically showing a southerly movement but with little evidence of an intensification of the storms. While this is one credible future response the possibility of an intensification of storms should not be completely ruled out, because some of the models used in IPCC assessments do show this (Lowe et al. 2009). A simple scaling argument suggested that if the ensemble of driving models had captured the largest increase in storm intensity from additional GCMs available it may have led to a bigger surge increase at some locations, comparable with changes in the future projected time-mean SLR. However, as such large changes in storm intensity were found in only one GCM (using the storm metric applied) the scaled results should be considered a low confidence projection (Lowe et al. 2009).

Gaslikova et al. (2013) investigated a set of four transient regional projections for the North Sea for which the underlying simulations of the global climate includes combinations of one GCM, two initial states and SRES scenarios A1B and B1. Towards the end of the 21st century (2071–2100) they found an increase in extreme surge heights (mean annual 99th percentiles) in the south-eastern North Sea, which are highest in the German Bight by up to about 15 cm. The authors concluded that the increase in the 99th percentile surge height is mainly due to an increase in the frequency of storm events with intensities already occurring in the respective reference climate and that there are relatively few events with greater intensities. 50-year return values calculated from the 100-year long projection period (2001–2100) were compared to 50-year return values calculated from the 40-year long reference period (1961–2000) and resulted in an increase of between about 10 and 80 cm for the two locations examined off the coast of the German Bight (Fig. 6.6). These return values are comparable to those reported by Lowe and Gregory (2005).

Gaslikova et al. (2013) also investigated internal climate variability in North Sea storm surge conditions and found multi-decadal variability within one projection as well as between the four transient projections, which is of the same order of magnitude as the increase towards 2100. Such multi-decadal variability was also found by Weidemann (2009), based on statistical downscaling of 17 projections for the SRES scenario A1B only differing by varying initial conditions. In this study the linear trend over the years 1958–2100 for the five study locations in the German Bight varied between −8 and 18 cm but most of the projections showed an increase in the surge height corrected for time-mean sea-level changes. The trends presented by Gaslikova et al. (2013) for the SRES A1B and B1 projections are within the range presented by Weidemann (2009).

In a recent assessment of the Dutch coastline, KNMI (2014a, b) reported that changes in wind speed are small and that little change is projected over the next century in northerly winds, which are the ones that tend to cause the largest surges along this stretch of coastline. Extremes of water level are expected to continue to rise, however, driven by the rise in time-mean sea level.

Taken together, the more recent studies suggest the possibility of either no significant increase or a relatively small increase in storm surge height in the North Sea. Where an increase is found it is typically largest at the southern end of the North Sea, especially in the south-east, with changes in the western and northern parts of the North Sea being smaller and non-uniform.

It is also useful to consider possible future changes in the propagation of tides due to changes in time-mean sea level. This could be important from both a flood perspective and a consideration of renewable energy generation. The recent study by Pickering et al. (2012) suggests changes in the tides may result in the North Sea due to altered dynamics. They showed that a 2-m SLR would result in a $\sim$ 5 cm increase in M_2 tidal amplitude in the central North Sea and Southern Bight, and a similar decrease in between. An update by

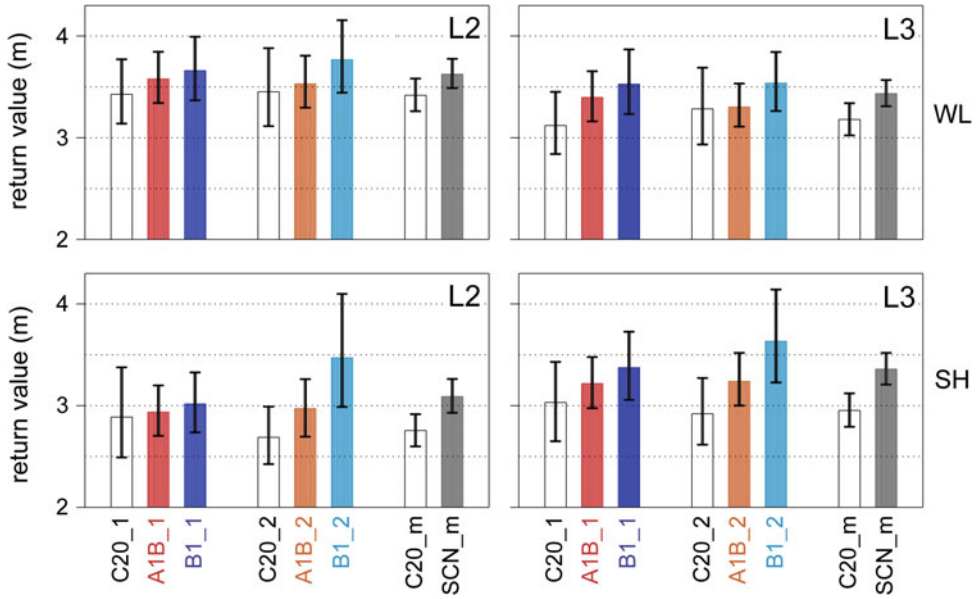

Fig. 6.6 The 50-year return value for water level (WL, *upper panels*) and surge height (SH, *lower panels*) for the control period 1960–2000 from two different ensemble members (C20_1, C20_2) and for four different future scenarios (SRES A1B and B1 scenarios, both simulated using two different GCM ensemble members, for the period 2001–2100). The mean for the control period and the scenario mean are given. The 95 % confidence range for each return value is shown by the *black bars*. L2 and L3 depict locations near the East Frisian and North Frisian coast of the German Bight, respectively (Gaslikova et al. 2013)

Pelling et al. (2013) highlighted a key remaining uncertainty in understanding this response—whether the water is assumed to be contained by a sea wall or allowed to flood the land. Recent work, based on seasonal variations in major tidal constituents (Gräwe et al. 2014; Müller et al. 2014) also suggests the need to consider changes in stratification on the continental shelf in shallow seas, which can alter the eddy viscosity and profile of currents with depth. See Sect. 6.3 for information on how North Sea stratification is projected to change.

6.2.6 Future Changes in Waves

Future changes in waves can be simulated using wind information projected by GCMs and ESMs, sometimes atmospherically-downscaled over the primary region of interest. The studies then typically follow either the statistical approach or the dynamical approach, using models of the generation, transport and dissipation of sea-surface wave energy. Much of the progress in the Northeast Atlantic and the North Sea has used the dynamic wave modelling approach.

Wolf and Woolf (2006) gave a useful overview of how particular aspects of changes in storminess generate changes in the wave climate in the North East Atlantic. The strength of the prevailing westerly winds and the frequency and intensity of storms, the location of storm tracks and the storm propagation speed were all considered. The strength of the westerly winds was found to be most effective at increasing mean and maximum monthly wave height. The frequency, intensity, track and speed of storms have little effect on mean wave height but intensity, track and speed did significantly affect maximum wave height.

The earliest future projection studies, such as those by Rider et al. (1996) of the WASA-Group (1998), used highly idealised climate scenarios, took data from a single or very limited number of climate models and typically used time-slices that were short and did not adequately account for multi-decadal variability. Later studies began to improve their approach, using longer time-slices and modelling policy-relevant future scenarios. The STOWASUS-Group (2001) compared the 30-year time slices 1970–1999 and 2060–2089 for the IPCC scenario IS92a (see Annex 4). For a doubling of carbon dioxide (CO_2) the wave climate responds to projected changes in wind forcing and the mean significant wave height (taken as the mean height of the highest third of waves) increases in the North Sea and north of the British Isles. However, the increase in the mean value throughout the entire year is no more than 15 cm. For extreme waves, expressed as higher percentiles of the distribution of significant wave heights the picture is a more mixed; for the 99th percentile there is an increase of around 0.25–0.5 m in the North Sea, however for the most extreme cases described by the 99th percentile there is little change projected for the North Sea. Debernard et al. (2002) analysed

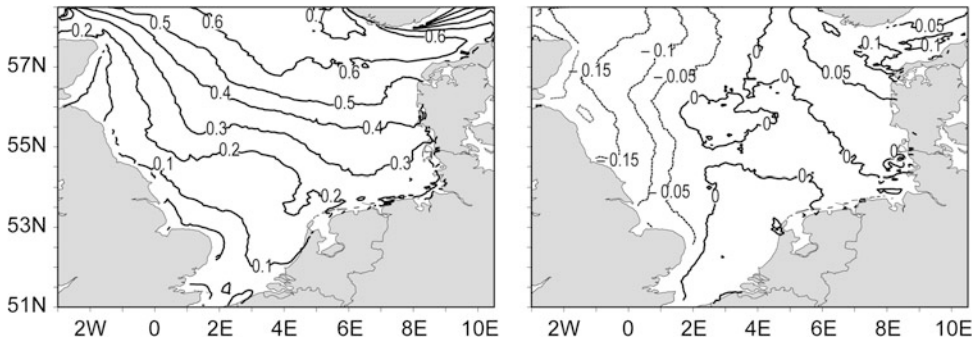

Fig. 6.7 Uncertainties in long-term 99th percentile significant wave height (m) caused by model differences (*left*) and scenario choice (*right*). For the significant wave heights, the uncertainties introduced by different models are generally much larger than those caused by different scenarios. The model uncertainties range from about 0.1 to 0.6 m (adapted from Grabemann and Weisse 2008)

two 20-year time slices for 1980–2000 (reference climate) and 2030–2050 (near future climate). For the global simulations an emission scenario similar to IPCC IS92a was used. The authors reported that the changes in the wave climate for 2030–2050 were mostly small and insignificant.

The next challenge was to try to sample uncertainty in the driving winds by using output from more than one GCM. Debernard and Røed (2008) analysed a set of four climate projections including combinations of SRES scenarios A2, B2, A1B, and three GCMs. The authors compared the results of the 30-year time slices for 1961–1990 (reference climate) and 2071–2100 (future climate) and found changes in the wave conditions for the four climate projections to vary in their spatial pattern and magnitude but that all agree in an increase of severe significant wave heights (99th percentiles) of 6–8 % along the North Sea east coast and in the Skagerrak. Grabemann and Weisse (2008) found comparable changes using a slightly different set of four climate projections, which incorporates two GCMs and SRES scenarios A2 and B2. Comparing the time slices 1961–1990 and 2071–2100 they estimated an increase in extreme wave height (99th percentile) in large parts of the southern and eastern North Sea of about 5–8 % (25–35 cm, average for the four projections). The greatest changes occur in the Skagerrak (an increase of up to 80 cm) in the ECHAM-driven projections. Changes in severe wave height towards the west and north of the North Sea are smaller or even negative. The increase in mean and 99th percentile significant wave height in the eastern North Sea is suggested to result mainly from an increase in the frequency of higher waves. This was also described by Groll et al. (2014). Both Debernard and Røed (2008) and Grabemann and Weisse (2008) reported that model-induced uncertainties and inter-GCM variability are larger than the scenario-related uncertainties (Fig. 6.7). Also Lowe et al. (2009) focused on model uncertainty and used three members of a 17-member GCM ensemble downscaled by a regional model over the North Sea to study future changes in wave heights. Some significant changes in the wave height were noted but further work is needed to understand the patterns. More focus is also needed on how to best select representative ensemble members of the driving GCMs from a larger model ensemble.

Another aspect of uncertainty, the role of natural variability, has been addressed using an 'initial condition ensemble'. De Winter et al. (2012) analysed a 17-member ensemble based on one GCM that was repeatedly started with 17 initial states for the SRES scenario A1B. Again the 30-year time slices 1961–1990 and 2071–2100 were compared. Mean wave heights and wave periods did not change, annual maximum conditions decreased in particular for wave periods and return periods showed no significant change in front of the Dutch coast. Furthermore, the authors found that annual maximum waves propagate more often to easterly directions, which is consistent with an increase in the frequency of extreme westerly winds. The importance of natural variability was investigated by Groll et al. (2014). They used transient projections (1961–2100) to evaluate the internal aspect of climate variability and found strong multi-decadal variability. The changes in median and severe (99th percentile) significant wave heights within a single projection and between projections are of the same order of magnitude as the change (increase in the eastern North Sea) towards the end of the 21st century. Owing to this strong internal variability the largest increase or decrease does not necessarily occur at the end of the 21st century but can occur earlier. Moreover, Groll et al. (2014) noted that the uncertainties from different GCM initial conditions, or arising from the use of different ensemble members are also important.

In a comparative study of ten wave climate projections, including those by Grabemann and Weisse (2008) and Groll et al. (2014) a robust signal was found for the eastern parts of the North Sea where mean and severe wave heights in nine to ten projections tended to increase towards the end of the 21st century (2071–2100). The magnitude of this increase is

much more uncertain. For the western parts of the North Sea a decrease is suggested in more than a half of the projections (Grabemann et al. 2015). These findings are in agreement with the results of other studies (e.g. Debernard and Røed 2008). The changes described are also consistent with a projected increase in the frequency of stronger winds from westerly directions.

6.3 Ocean Dynamics and Hydrography

6.3.1 General Aspects and Methodology

North Sea dynamics are controlled by the interplay of the seasonal heating cycle, atmospheric fluxes, tides, river inputs and exchanges with the open ocean. Most physical processes active in the North Sea are to some extent impacted by global change resulting from anthropogenic increases in greenhouse gas emissions. These impacts are, however, highly dependent on time and space scales and the dominant processes under consideration. The impact of climate change in shelf seas is essentially a boundary value problem, due to the shallow depth and short ocean memory relative to the timescale of climate change. Hence it is necessary to consider the external drivers in some detail. These naturally divide into three vectors: atmospheric, oceanic and terrestrial. A fourth important vector is variability in astronomical forcing (top of atmosphere radiation and tidal potential), but this is not a component of anthropogenic change and so not considered in IPCC assessments. However, it should be noted that changes in sea level and stratification will have some effect on local tidal amplitudes and the implications of this require further investigation (e.g. Pickering et al. 2012; Gräwe et al. 2014; see Sect. 6.2). Direct anthropogenic drivers may result as a consequence of climate change adaptation and mitigation measures. These are not specifically considered here, since human effects on the physical marine environment (e.g. arising from the installation of offshore renewable energy structures, mineral extraction, coastal protection measures etc.) tend to be local and/or coastal, and scenarios of anthropogenic drivers not related to climate change have yet to be developed for the North Sea region and integrated into regional future climate change assessments.

To date, the focus of studies to assess potential climate change impacts on the North Sea dynamic system has been on shelf scales (> 10 km from the coast) and seasonal processes. Finer coastal scales and higher frequency processes remain for future work. The downscaling methods and scenarios used are diverse and so this section begins with a short overview of key approaches and methodology. The use of statistical downscaling (von Storch 1995, see Annexes 2 and 3), applied to assess climate change impacts on sea level, storm surges and wave climate (Sect. 6.2) and also frequently marine biota (e.g. Dippner and Ottersen 2001), is unusual for assessing climate change impacts on ocean dynamics and hydrography and all studies reviewed here were undertaken using the more complex and computationally more expensive dynamical downscaling method (see Annexes 2 and 3) using established and validated regional ocean models (ROMs).

The first climate change downscaling studies for the North Sea were performed as research contributions, which focused on method development and provided first quantitative assessments of the potential regional impacts of future climate change (Kauker 1999; Kauker and von Storch 2000; Ådlandsvik 2008; Madsen 2009). These were followed by more comprehensive assessments performed as part of national regional climate change assessments such as the British UKCP09, the German KLIWAS[2] (Auswirkungen des Klimawandels auf Wasserstraßen und Schifffahrt – Entwicklung von Anpassungsoptionen, German Federal Ministry of Transport, Building and Urban Development) and the EMTOX[3] project from the Netherlands (Impacts of climate change effects on natural toxins in plant and seafood production, Dutch Ministry for Economic Affairs, Agriculture and Innovation). In parallel, a few larger European research projects such as the RECLAIM[4] (REsolving CLimAtic IMpacts on fish stocks), ECODRIVE[5] (Ecosystem Change in the North Sea: Processes, Drivers, Future Scenarios) or MEECE[6] (Marine Ecosystem Evolution in a changing Climate) have produced a suite of regional downscaling studies. Most results are published as contributions to peer reviewed literature, but complementary and additional information is available in the form of project reports (e.g. Drinkwater et al. 2008, 2009; Alheit et al. 2012; Wakelin et al. 2012a; Bülow et al. 2014) or made available to the public via the internet (e.g. MEECE via www.meeceatlas.eu).

A wide range of downscaling methods and models (see Table 6.1 for model acronyms) have been applied to assess regional climate change impacts and a best practice on regional marine downscaling is still a matter of research and consensus has so far not been established. The earliest dynamical downscaling exercise using the OPYC model (Kauker 1999; Kauker and von Storch 2000) was carried out well in advance of the IPCC AR4, and utilised GCM forcing from 5-year time slice experiments for a potential 2 × CO_2 world. Most of the more recent regional projections were carried out for the end of the century (2070–2100) and utilise

[2] www.kliwas.de.
[3] www.deltares.nl/en/project/1172392/emtox.
[4] www.climateandfish.eu.
[5] www.io-warnemuende.de/ecodrive.html.
[6] www.meece.eu.

Table 6.1 Model acronyms together with key references

Acronym	Model type	Key publications
BCM Bergen Climate Model	Global climate model, GCM	Furevik et al. (2003)
CCSM3, Community Climate System Model V3	Global climate model, GCM	Public release: www.cesm.ucar.edu/models/ccsm3.0
Delft3D/BLOOM/GEM	Regional model coupled physical-biological	Lesser et al. (2004), Blauw et al. (2008)
DMI-BSHcmod, Danish meteorological institute	Regional ocean model for the North and Baltic seas	Madsen (2009)
DMI HIRHAM RCM	Regional atmospheric model	Christensen et al. (2007)
ECOSMO ECOSystem Model	Regional model coupled physical-biological	Schrum and Backhaus (1999), Schrum et al. (2006), Daewel and Schrum (2013)
ECHAM3/LSG	Global climate model, GCM, first generation coupled model	Roeckner et al. (1992), Maier-Reimer et al. (1993)
ECHAM5-MPIOM, Max-Planck-Institute, Germany	Global climate model, GCM	Marsland et al. (2003); Roeckner et al. (2003, 2006)
ECOHAM ecosystem model Hamburg	Regional ecosystem model	Pätsch and Kühn (2008)
ERSEM	Ecosystem model	Blackford et al. (2004)
GISS, Goddard Institute for Space Studies	Global climate model, GCM	Schmidt et al. (2006)
HadAM3H, Hadley Center Climate Model	Global climate model, GCM	Jones et al. (2001)
HadCM3, Hadley Center Climate Model 3	Global climate model, GCM	Gordon et al. (2000), Pope et al. (2000)
HadRM3 Hadley Center Regional Model 3	Regional model, RCM	Murphy et al. (2009)
HAMOCC, HAMburg Ocean Carbon Cycle model	Ocean carbon cycle model	Maier-Reimer et al. (2005)
HAMSOM HAMburg Shelf Ocean Model	Regional hydrodynamic model	Pohlmann (1996)
IPSL/IPSL-CM4, Institut Pierre-Simon Laplace, France	Earth system model	Marti et al. (2010)
OPYC	Ocean model, isopycnal coordinates	Oberhuber (1993)
MPIOM, Max Planck Institute for Meteorology	Global ocean model	Marsland et al. (2003)
MPIOM-zoom	Global model with Zoom on the North Sea	Gröger et al. (2013)
NORESM, Norwegian Earth System Model	Earth system model	Bentsen et al. (2012)
NORWECOM, NORWegian ECOlogical Model	Ecosystem model	Skogen et al. (1995), Skogen and Søiland (1998)
POLCOMS Proudman Oceanographic Laboratory Coastal Ocean Modelling System	Regional hydrodynamic model	Holt and James (2001)
RACMO	Regional atmospheric model	van Meijgaard et al. (2008)
RCAO	Regional coupled atmosphere-ocean model	Döscher et al. (2002)
RCA4-NEMO	Regional coupled atmosphere-ocean model	Dieterich et al. (2013)
REMO	Regional atmospheric model	Jacob and Podzun (1997)
ROMS	Regional ocean model	Shchepetkin and McWilliams (2005)
WAM	Wave model	Hasselmann et al. (1988)

the SRES scenario A1B (see Annex 4). These experiments were performed either as time slice experiments of 20–30 years for present-day and future (end-of-the-century or middle-of-the-century) climates (Ådlandsvik 2008; Holt et al. 2010, 2012, 2014, 2016; Friocourt et al. 2012; Wakelin et al. 2012a; Pushpadas et al. 2015) or as continuous integrations (e.g. Mathis 2013; Gröger et al. 2013; Bülow et al. 2014; Mathis and Pohlmann 2014). Only one downscaling was performed for the SRES A2 scenario, which considers stronger radiative forcing (Madsen 2009). To date, only the

regional ECOSMO model was used to project future changes based on the RCP4.5 scenario (see Annex 4) from IPCC AR5 (Wakelin et al. 2012a; Pushpadas et al. 2015). The downscaling setup and the methods applied for the scenario simulations were different with respect to downscaling chain, coupling of the atmosphere-ocean system, bias correction, consideration of terrestrial climate change impacts, open-ocean climate change impacts, Baltic Sea boundary conditions, and forcing GCM (see Tables 6.2, 6.3 and 6.4 for details). All regional models consider tidal forcing by the M_2 partial tide, which is the major forcing tidal constituent in the North Sea. Most models also consider additional tidal constituents, but the actual tidal setup varies between the different models.

To estimate uncertainties in projections of future climate the multi-model ensemble approach has been introduced in Earth system modelling of the North Sea region following the well-established strategy of IPCC assessments (e.g. Friocourt et al. 2012; Wakelin et al. 2012a; Bülow et al. 2014; Holt et al. 2014, 2016; Pushpadas et al. 2015). Both ensembles using one regional model with different global models (e.g. Wakelin et al. 2012a; Holt et al. 2014, 2016; Pushpadas et al. 2015) and ensemble downscaling from one GCM using different regional model systems are available for the North Sea (Bülow et al. 2014). The ensemble simulations allow for a first estimation of uncertainty arising from different GCMs and RCMs (regional climate models). However, it should be noted that the number of ensemble members is typically only two to three and so too small for a sound final assessment of uncertainty ranges.

Complementary understanding of climate change impacts on the North Sea hydrodynamics and ecosystem dynamics is available from so-called 'what-if' or perturbation experiments that consider hypothetical ranges of forcing parameters. For these numerical experiments, forcing atmospheric boundary conditions (wind speed, air temperature, solar radiation) were separately perturbed by a change roughly of the order of the projected climate change (Schrum 2001; Skogen et al. 2011; Drinkwater et al. 2008) or defined by mixing present day with future forcing GCM variables (Holt et al. 2014, 2016). Such perturbation experiments are not dynamically consistent, but do provide some insight into the sensitivity of the regional system to climate change impacts and so improve process understanding.

6.3.2 Changes in Temperature

Despite huge differences in setup, forcing GCM, bias correction and time slice vs continuous simulations, the future projections for sea-surface temperature (SST) in the North Sea are consistent in sign for the different regional model setups, however there are differences in the magnitude of change. Projected annual mean SST increases for the end of the century are in the range 1–3 °C for the A1B scenario (exact numbers are not given here due to differences in spatial averaging and reference periods from the existing literature). Within the given range, projected temperature changes are consistent for the different regional models used. Projected temperature changes are found to be statistically significant using the Kruskal-Wallis test (Wakelin et al. 2012a) or other measures such as the standard deviation (Ådlandsvik 2008; Mathis 2013) so far investigated. Projected changes in SST are typically more pronounced than changes in depth-averaged (or volume-averaged) temperature, which is the ecologically more relevant parameter since it affects vital rates in organisms that are distributed through the entire water column, and are almost completely driven by changes in atmospheric boundary conditions and air-sea fluxes (e.g. Ådlandsvik 2008; Wakelin et al. 2012a).

A few studies were performed using the same GCM forcing but different regional ocean models and configurations. These use the IPSL-CM4.0 ESM (Wakelin et al. 2012a; Chust et al. 2014; Holt et al. 2014, 2016) and MPIOM (Mathis 2013; Gröger et al. 2013) as global forcing. The resulting changes in SST from these experiments are typically very similar for different regional ocean models and differ only by around a tenth of a degree. On the other hand, ensemble studies performed with one regional ocean model and different forcing GCMs clearly show that the magnitude of the projected changes significantly depend on the forcing GCM (Wakelin et al. 2012a; Holt et al. 2010, 2012, 2014, 2016; Pushpadas et al. 2015; Fig. 6.8). Regional projections using different versions of the Max Planck Institute GCM (ECHAM5/MPIOM) and the Norwegian climate models (BCM and NORESM) are typically at the lower end (Kauker 1999; Wakelin et al. 2012a; Gröger et al. 2013; Mathis 2013; Pushpadas et al. 2015). Stronger warming was projected from simulations using the Hadley-Centre climate model (Holt et al. 2010, 2014, 2016; for the SRES A2 scenario Madsen 2009) and the largest changes were projected when using boundary and initial conditions from the French climate model IPSL-CM4.0 (Wakelin et al. 2012a; Holt et al. 2010, 2012, 2014, 2016; Pushpadas et al. 2015); a GCM that projects stronger warming also on the global scale (e.g. Kharin et al. 2007).

Most of the previously reported downscalings were based on uncoupled ocean downscaling neglecting local atmosphere-ocean feedbacks at the regional scale, which were earlier identified to be potentially important for the North Sea region in a present-day hindcast scenario (Schrum et al. 2003a). To account for these regional air-sea feedbacks, a first multi-model ensemble with coupled atmosphere-ocean regional models (AO regional models) was performed as part of the German climate change impact project KLIWAS (Bülow et al. 2014). Three different

Table 6.2 Uncoupled dynamic downscaling experiments for the North Sea for the end of this century

Model chain: GCM-RAM-ROM	Scenario	Time slice	Bias correction	Runoff/Baltic Sea	Considered forcing: atmosphere-only and atmosphere and ocean change	LTL-model/carbonate chemistry	Related publications
ECHAM3/LSG-no-**OPYG**	2 × CO_2	5-year time slice, 2 × CO_2	Flux correction	Resolved/resolved	A only	No	Kauker (1999), Kauker and von Storch (2000)
BCM-no-**ROMS**	A1B	1972–1997 versus 2072–2097	Sea surface salinity relaxation to BCM	Perturbed by future rainfall/no change	AO change/A-only	No	Ådlandsvik and Bentsen (2007), Ådlandsvik (2008)
HadAM3H-DMI-BSHcmod	A2	1960–1990 versus 2070–2100	Direct, no bias correction	No change/resolved	AO change	No	Madsen (2009)
HadCM3-HadRM3-POLCOMS	A1B	1961–1990 versus 2070–2098	Adjusted fluxes	Future change/no change	AO change	No	Lowe et al. (2009), Holt et al. (2010)
HadCM3-no-**POLCOMS**	A1B	1980–1999 versus 2080–2100	Bias corrected temperature	Runoff perturbed by rainfall/no change	AO change/A only	**ERSEM**/no	Wakelin et al. (2012a), Holt et al. (2014)
IPSLCM4-no-**POLCOMS**	A1B	1980–1999 versus 2080–2100	Bias corrected temperature	Perturbed by future rainfall/no change	AO change	**ERSEM**/yes	Artioli et al. (2012, 2013, 2014), Holt et al. (2012, 2014, 2016); www.meeceatlas.eu
IPSLCM4-no-**POLCOMS**	A1B	1980–1999 versus 2080–2100	Delta change	Perturbed by future rainfall/no change	AO change	**ERSEM**/yes	Wakelin et al. (2012a, b), Holt et al. (2014)
ECHAM5/MPIOM-REMO-HAMSOM	A1B	Transient 1951–2100	Bias corrected, all forcing data	No change/changed by discharge from GCM	AO change, except nutrients	**ECOHAM**/yes	Alheit et al. (2012), Mathis (2013), Mathis et al. (2013), Mathis and Pohlmann (2014)
ECHAM5/MPIOM-zoom	A1B	transient 1860–2100	No	future change/resolved, course resolution	AO change	**HAMOCC**/yes	Gröger et al. 2013
IPSLCM4-no-**ECOSMO**	A1B	1970–1999 versus 2070–2099	Delta change	No change/fully resolved	AO change/A only	**ECOSMO**/yes	Wakelin et al. (2012a), Holt et al. (2014, 2016), Pushpadas et al. (2015); www.meeceatlas.eu

(continued)

Table 6.2 (continued)

Model chain: GCM-RAM-ROM	Scenario	Time slice	Bias correction	Runoff/Baltic Sea	Considered forcing: atmosphere-only and atmosphere and ocean change	LTL-model/carbonate chemistry	Related publications
MPIOM-HAMOCC-no-**ECOSMO**	A1B	1970–1999 vs 2070–2099	delta change	no change/fully resolved	AO change/A only	**ECOSMO**/no	Wakelin et al. (2012a); Pushpadas et al. (2015)
BCM-HAMOCC-no-**ECOSMO**	A1B	1970–1999 versus 2070–2099	Delta change	No change/fully resolved	AO change/A only	**ECOSMO**/no	Wakelin et al. (2012a), Pushpadas et al. (2015)
ECHAM5/MPIOM-RCAO-NORWECOM	A1B	1970–1999 versus 2070–2099	Direct	No/no	AO change, except nutrients	**NORWECOM**/no	Eilola et al. (2013), Skogen et al. (2014)
ECHAM5/MPIOM-zoom-no-no	A1B	Continuous 1860–2100	Bias-corrected restoring to forcing GCM	Resolved, coarse scale	AO	**HAMOCC**/yes	Gröger et al. (2013)
NORESM-no-**ECOSMO**	RCP4.5	1970–1999 versus 2070–2099	Delta change	No change/fully resolved	AO change/A only	**ECOSMO**/no	Wakelin et al. (2012a), Pushpadas et al. (2015)
ECHAM5/MPIOM-HAMOCC-no-**ECOSMO**	RCP4.5	1970–1999 versus 2070–2099	Delta change	No change/fully resolved	AO change	**ECOSMO**/no	Pushpadas et al. (2015)
IPSLCM5-no-**ECOSMO**	RCP4.5	1970–1999 versus 2070–2099	Delta change	No change/fully resolved	AO change	**ECOSMO**/no	Pushpadas et al. (2015)

All SRES A1B and A2 scenarios are forced by IPCC-AR4 generation GCMs and ESMs. The RCP4.5 scenarios are forced by IPCC-AR5 generation ESMs

Table 6.3 Coupled atmosphere-ocean downscaling experiments for the North Sea for the end of this century

GCM-RAM-ROM	Scenario	Time slice	Baltic Sea	Restoring/bias correction	LTL-model/carbonate chemistry	Related publications
ECHAM5/MPIOM-REMO-MPIOM-zoom higher resolution	A1B	Continuous 1860–2100	Resolved	No restoring, bias correction of fresh water fluxes globally, not in the North Sea	No	Bülow et al. (2014), Sein et al. (2015)
ECHAM5/MPIOM-RCA4/NEMO	A1B	Continuous 1961–2100	Resolved	No restoring, bias correction in sea level for North Sea inflow	No	Bülow et al. (2014)
ECHAM5/MPIOM-REMO/HAMSOM	A1B	Continuous 1860–2100	Boundary conditions	No restoring or bias correction in the regional model	No	Bülow et al. (2014), Su et al. (2014)

All coupled downscaling experiments are forced by the IPCC-AR4 generation GCM **ECHAM5/MPIOM**

Table 6.4 Dynamic downscaling experiments for the North Sea for the middle of this century

GCM-RAM-ROM	Scenario	Time slice	Bias correction	Runoff/river load/Baltic Sea	A-only versus AO change	LTL-model/carbonate chemistry	Key publications
GISS-no-**ROMS**	A1B	1986–2000 versus 2051–2065	No	No change/na/no change	AO change	No	Melsom et al. (2009), Alheit et al. (2012)
BCM-no-**ROMS**	A1B	1986–2000 versus 2051–2065	Only ocean boundary conditions	No change/na/no change	AO change	No	Ådlandsvik (2008), Alheit et al. (2012)
CCSM-no-**ROMS**	A1B	1986–2000 versus 2051–2065	Only ocean boundary conditions	No change/na/no change	AO change	No	Melsom et al. (2009), Alheit et al. (2012)
ECHAM3-RACOM-Delft3D/BLOOM/GEM	A1B	1985–2004 versus 2031–2050	No	10 % winter increase and 10 % summer decrease/no change/na	AO change	BLOOM/GEM/no	Friocourt et al. (2012)
ECHAM3-RACOM-NORWECOM	A1B	1985–2004 versus 2031–2050	No	10 % winter increase and 10 % summer decrease/no change/no change	A only	NORWECOM/no	Friocourt et al. (2012)
IPSLCM4-no-**POLCOMS**	A1B	1980–1999 versus 2030–2040	Delta change	Various scenarios	AO change	ERSEM	Zavatarelli et al. (2013a, b)
IPSLCM4-no-**ECOSMO**	A1B	1980–1999 versus 2030–2040	Delta change	Various scenarios	AO change	ECOSMO	Zavatarelli et al. (2013a, b)

All scenario simulations are forced by IPCC-AR4 generation GCMs and ESMs

coupled regional AO models were developed, namely MPIOM-REMO (Sein et al. 2015), HAMSOM-REMO (Su et al. 2014) and RCA-NEMO (Dieterich et al. 2013; Wang et al. 2015). The three models have in common that the atmosphere components are all limited area models while their ocean components differ focusing either on the North Sea (HAMSOM), the North and Baltic seas (NEMO) or the global ocean employing a regional zoom to the North Sea (MPIOM-zoom). An ensemble of transient simulations 1960–2100 from all three models driven by the same GCM (ECHAM5-MPIOM) was performed for the SRES A1B scenario (Bülow et al. 2014). All models show an

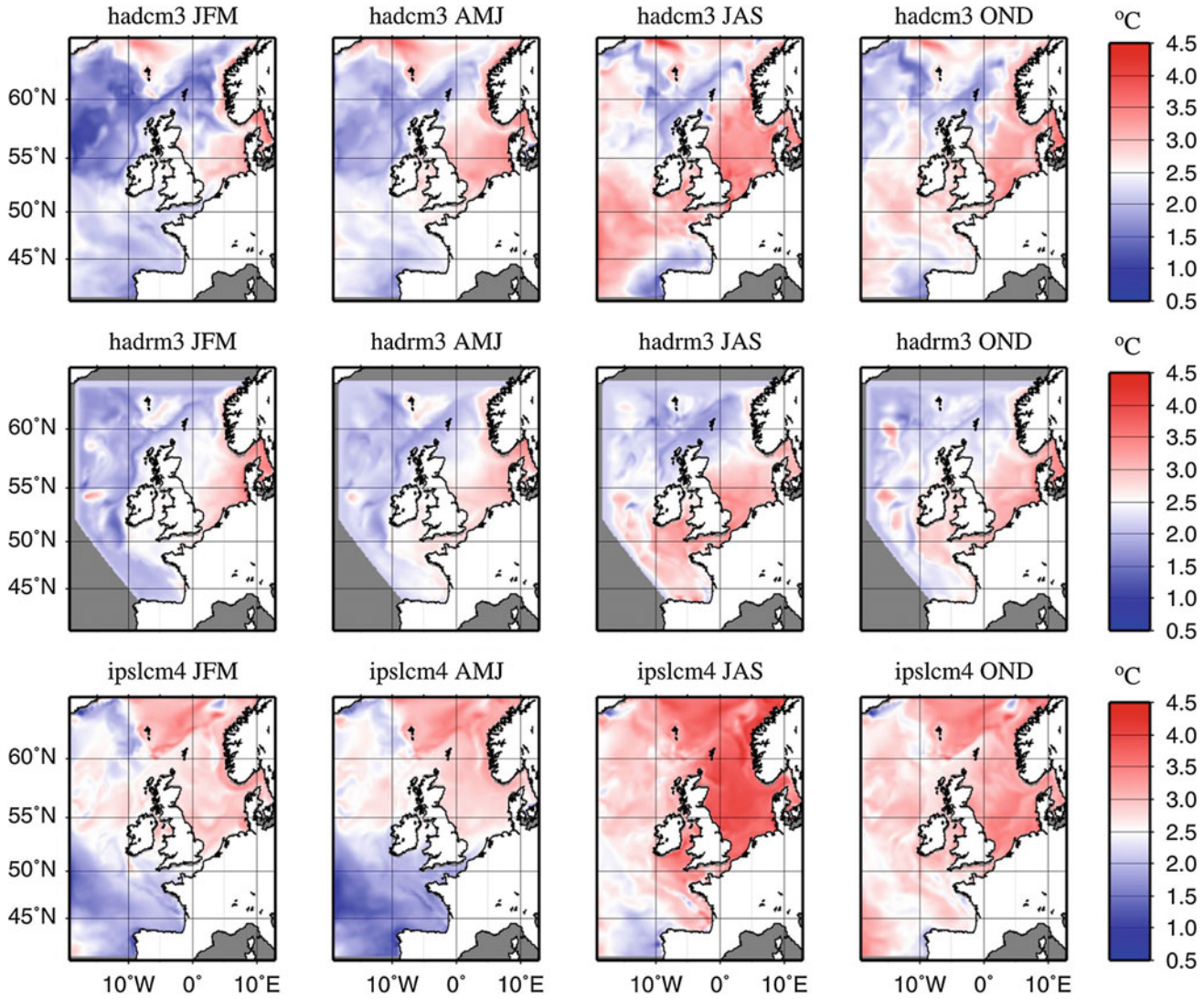

Fig. 6.8 Projected change in seasonal sea-surface temperature from POLCOMS experiments (HADCM3 and IPSL-CM4) and UKCP09 (HADRM3) experiments (redrawn using results from Holt et al. 2010 and Wakelin et al. 2012a)

area-averaged monthly mean SST increase of 1.7–3.0 °C for the end of the century (Fig. 6.9) and annually average SST increases of about 2 °C (Bülow et al. 2014), which is very similar to uncoupled downscalings forced by the ECHAM5/MPIOM model reported by Wakelin et al. (2012a), Mathis (2013) and Mathis and Pohlmann (2014). However, the uncertainty range arising from the different regional models was significantly larger compared to uncoupled model simulations.

An approximately linear trend of about 2 °C per 100 years was projected for SST through continuous simulations (e.g. Mathis 2013: 1.67–1.86 °C). The ensemble projections for the middle of the century were consistent with this trend. When forced by the ECHAM5/MPIOM a change of 0.4–0.8 °C was derived for the near future (2031–2050, Friocourt et al. 2012) and about 0.6–1.3 °C in the coupled simulations (Bülow et al. 2014). The spatial patterns of the projected warming were consistent with time-slice end-of-century projections and increased warming was projected for the coastal zone compared to the northern North Sea. The multi-model ensemble for the near future (+65 years) performed with ROMS, forced by the GISS, BCM, and CCSM GCMs (Alheit et al. 2012; Fig. 6.10), supports the view that the choice of forcing GCM contributes substantial uncertainty to the magnitude of projected warming. The GISS-based downscaling, which has the largest warm bias in the control run, simulates a weak warming. Annual average temperature is rising by 0.3 °C at 25 m in the future scenarios. The BCM downscaling shows an average warming of 0.6 °C. The downscaling based on NCAR CCSM, which has a cold bias in the control simulation, gives the strongest warming at 1.1 °C on average.

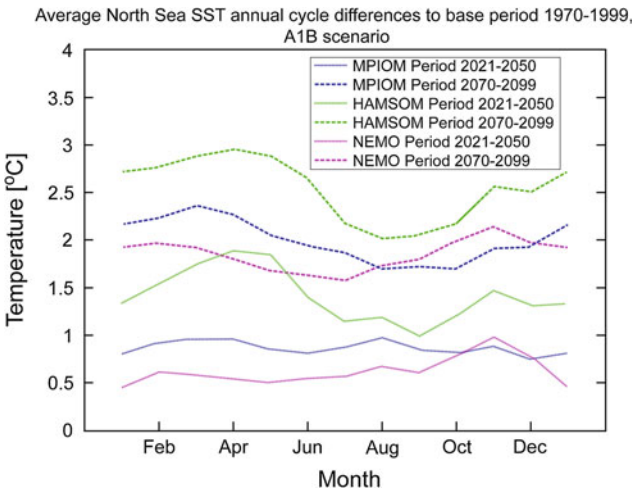

Fig. 6.9 Projected annual cycle of sea surface temperature change for two climate periods and three coupled atmosphere-ocean model downscalings (ocean models: MPIOM, HAMSOM, NEMO) (Bülow et al. 2014)

Simulated future temperature changes are generally seasonally dependent. Many models project larger changes in SST during summer months when a shallow thermocline restricts the incoming heat input to the sea surface (e.g. Figure 6.8) compared to winter, when the North Sea is well mixed and incoming heat is distributed over the entire water column, despite larger changes in heat flux during autumn and winter (e.g. Holt et al. 2010, 2012, 2014). Due to well-mixed conditions during winter, heat flux anomalies result in a larger temperature increase in the shallow south-eastern North Sea than the deeper central and north-western North Sea (e.g. Holt et al. 2010, 2012; Wakelin et al. 2012a; Fig. 6.8). During stratified summer conditions, the southern North Sea also warms more strongly, since mixed-layer thickness is typically shallower than in the northern North Sea (Janssen et al. 1999; Schrum et al. 2003b). However, these regional and seasonal variations in warming are not consistent among the different regional model realisations. Exceptions are those simulated with the HAMSOM model (Mathis 2013), the NORWECOM (Friocourt et al. 2012), and the coupled models (Bülow et al. 2014). These project larger temperature changes in winter, autumn and spring, with significant inter-model differences. From the multi-model ensembles it seems that the strength of the coupling and hence the regional and seasonal pattern of projected changes, are significantly affected by the properties and parameterisations of the regional model. Likely candidates are mixed-layer depth, flux parameterisations and local feedbacks. However, the attribution of a definite cause for the inter-model deviations is not obvious from existing literature.

The ECOSMO model has also been used with forcing from the IPCC AR5 generation models to simulate the RCP4.5 scenario; the first and so far only published attempts to employ the new updated IPCC AR5-scenarios for the North Sea (Wakelin et al. 2012a; Pushpadas et al. 2015).

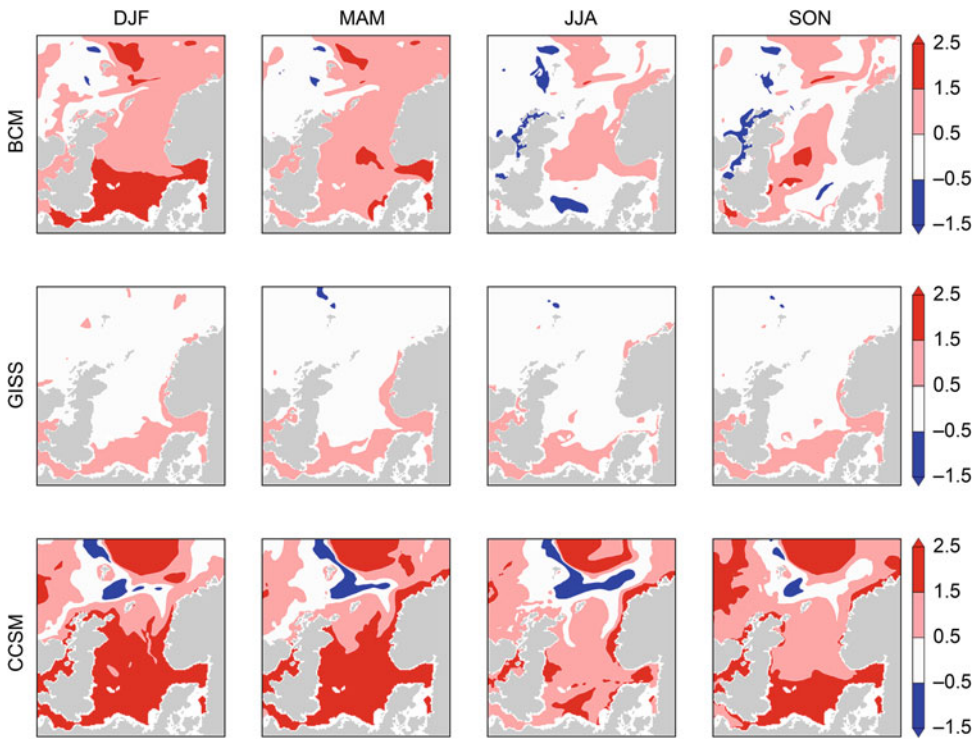

Fig. 6.10 Projected change in temperature (°C) for the near future (2051–2065 vs. 1986–200) for ROMS simulations forced by BCM (*upper*), GISS (*middle*) and CCSM (*lower*) (Alheit et al. 2012)

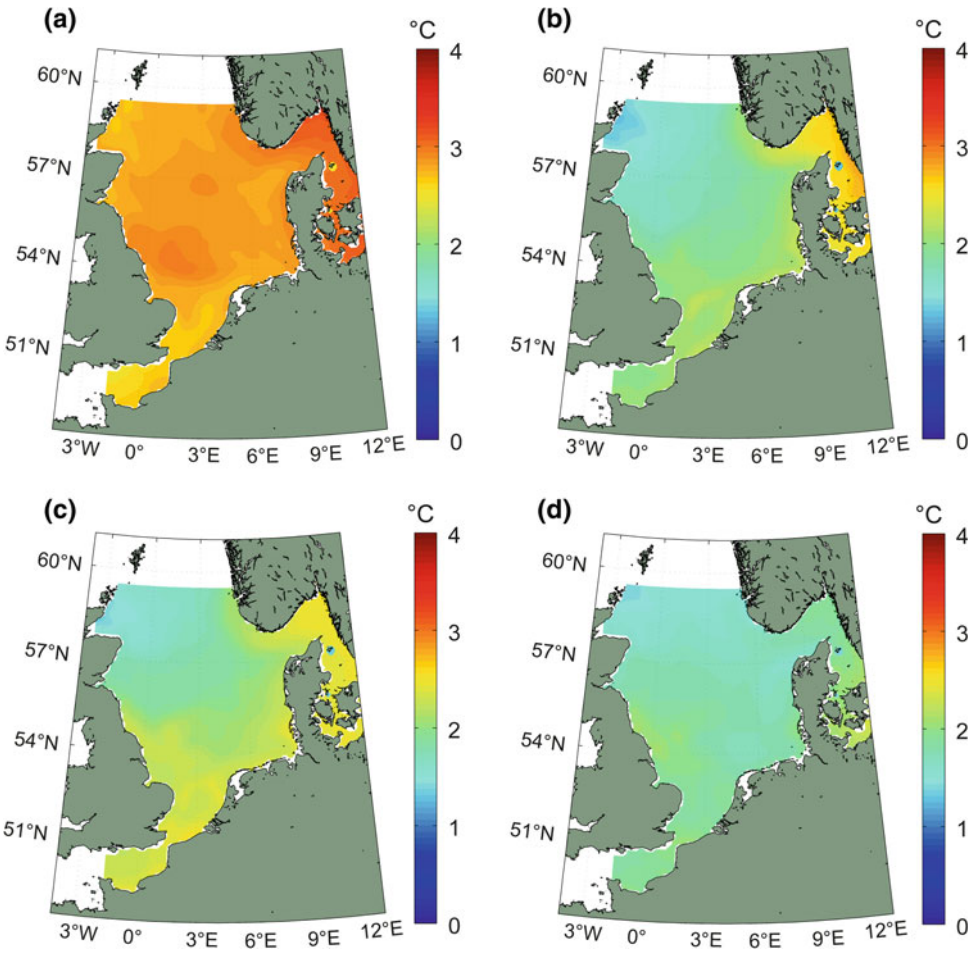

Fig. 6.11 Projected change in temperature (°C) for the end of the century (2070–2100, A1B and RCP4.5 scenario) as projected by the ECOSMO, forced by the IPSL-CM4.0-A1B (**a**), BCM-A1B (**b**), ECHAM5-A1B (**c**) and NORESM-RCP4.5 (**d**) scenarios (Wakelin et al. 2012a)

When comparing the simulation to the older SRES A1B scenario simulations, slightly less warming was found for the simulations forced by the RCP4.5 scenarios and IPCC AR5 generation models (Wakelin et al. 2012a; Pushpadas et al. 2015; Fig. 6.11), which could be largely explained by the fact that both story lines are not fully comparable and the RCP4.5 scenario provides less radiative forcing (see Annex 4). A slight reduction in the ranges of projected SST change was also evident (Pushpadas et al. 2015).

6.3.3 Changes in Salinity

North Sea salinity is influenced by the local balance between precipitation and evaporation, terrestrial runoff and exchange with the North Atlantic and the Baltic Sea. The regional projections of salinity considered in this section utilise full hydrodynamic models. However, their predictive capacity for salt and fresh-water changes is limited and results are biased to an unknown degree by the assumptions and approaches chosen for considering terrestrial fresh-water fluxes (e.g. Wakelin et al. 2012a), Baltic Sea water fluxes (e.g. Mathis 2013), Atlantic boundary conditions (e.g. Friocourt et al. 2012) or the use of a relaxation scheme (e.g. Ådlandsvik 2008), together with the accuracy of cross-shelf circulation and mixing. An attempt to consider all climate change impacts on fresh and salt water sources consistently has only been made for a few studies (e.g. Gröger et al. 2013; Bülow et al. 2014). However, these studies required different global bias- or fresh-water flux corrections in the global forcing model to avoid drift in salinity (see Tables 6.1 and 6.2 for details) and their projections differ despite using the same GCM, possibly due to a regional sensitivity to bias or flux corrections in the GCM.

Gröger et al. (2013) projected substantial freshening of the North Sea manifesting in a reduction in surface salinity of 0.75 (Fig. 6.12), which is coherent with a stronger hydrological cycle and substantial freshening of the North Atlantic under future warming modelled at the global scale. The simulated freshening peaks around 2060–2070, with salinity then increasing towards the end of the century but not to present-day values. A similar freshening of the North Sea is apparent in the HAMSOM regional projections based on the same coarse resolution GCM forcing (Mathis 2013;

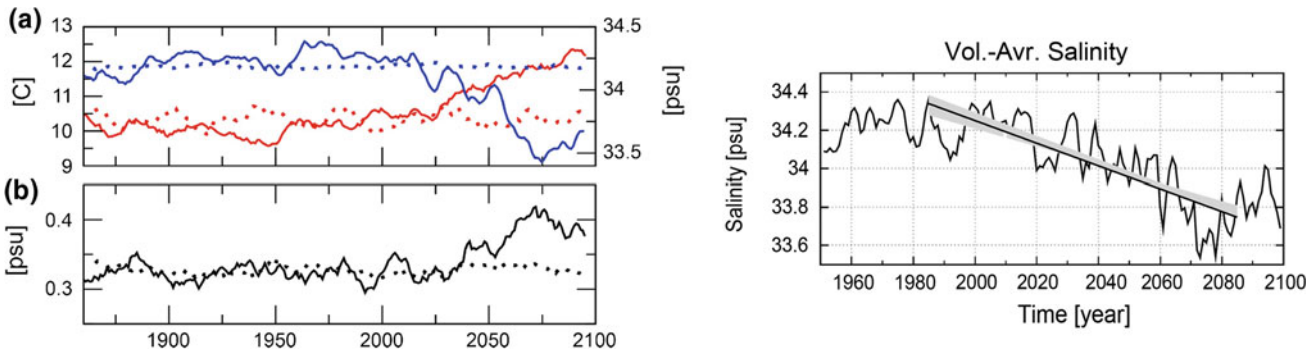

Fig. 6.12 *Left* Time series of projected surface salinity (*a, blue*), sea-surface temperature (*a, red*) and the difference in salinity between the bottom waters and surface waters (*b, black*) in the North Sea simulated by the MPIOM-zoom (Gröger et al. 2013). *Dotted lines* show the results of a control simulation with constant radiative forcing. *Right* Time series of annual (*black*) volume-averaged salinity from HAMSOM uncoupled downscaling (Mathis and Pohlmann 2014)

Mathis and Pohlmann 2014), despite no terrestrial runoff change considered here. In contrast, results from coupled atmosphere-ocean downscaling presented by Bülow et al. (2014), which also used A1B and ECHAM5-MPIOM forcing but with higher resolution, projected salinity to decrease by only about 0.2 (Bülow et al. 2014; Fig. 6.13). This suggests that the projected salinity change is strongly sensitive to the resolution of the atmospheric and oceanic modelling component used and the bias correction or restoring methods used in the global model. Moreover, biases in the flux coupling and internal variability contribute to local deviations and inter-model variability in projected changes. The other regionally coupled AO-projections from NEMO and HAMSOM, which use forcing from the same GCM (but different global realisations, details given by Bülow et al. 2014), project decreases in salinity of the same order of magnitude. However, inter-model differences stemming from the regional models or global runs used are above 0.2 in salinity and significant differences in spatial pattern occur (Fig. 6.14). The differences are particularly strong for the Baltic Sea outflow and the northern boundary inflow.

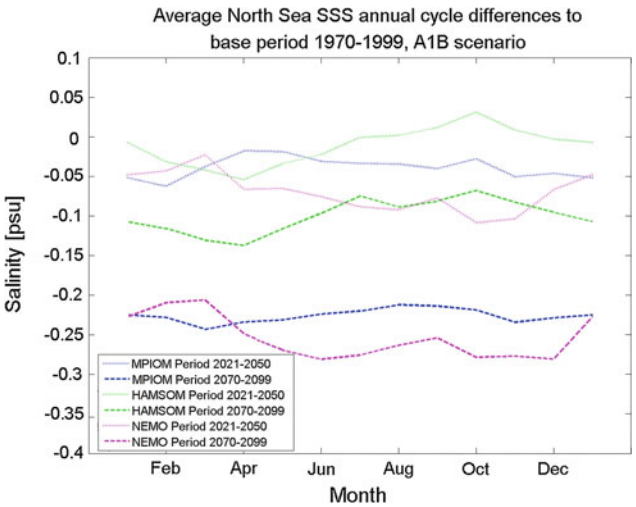

Fig. 6.13 Projected annual cycle of change in sea surface salinity for two periods (2021–2050 vs. 1970–1999, *dotted lines*; and 2070–2099 vs. 1970–1999, *dashed lines*) and three coupled AO-downscalings (ocean models: MPIOM, HAMSOM, NEMO), all with GCM forcing from ECHAM-MPIOM (Bülow et al. 2014)

The projected overall freshening of the North Sea is confirmed by most of the other regional downscaled scenarios (e.g. Kauker 1999; Holt et al. 2010, 2012; Wakelin et al. 2012a; Pushpadas et al. 2015), but the strength of the salinity decrease appeared to be strongly dependent on the choice of GCM (Holt et al. 2014, 2016; Wakelin et al. 2012a; Pushpadas et al. 2015; Fig. 6.15) and inter-GCM related variability in projected surface salinity change is large (≈ O(0.5–1)) and increases from AR4- to AR5-based regional downscaling (Pushpadas et al. 2015). The regional model and assumptions made for runoff and Baltic Sea exchange contribute to inter-model variability. However, these are second order effects compared to GCM-related variability, and projected salinity changes are largely related to North Atlantic salinity changes and the wind-driven inflow to the North Sea. This is confirmed by near future projections: Friocourt et al. (2012) attributed modelled near-future freshening of the North Sea partly to decreasing winter inflow. Potential impacts of circulation changes on salinity were earlier studied by Schrum (2001) in a simple perturbation experiment, which revealed that decreasing westerly wind speed by 25 % would result in a basin-wide freshening of the North Sea of the order of a 0.3–0.4 reduction in average salinity.

6.3.4 Changes in Stratification

During winter the North Sea is generally well mixed due to surface cooling and resulting thermal convection, and winter

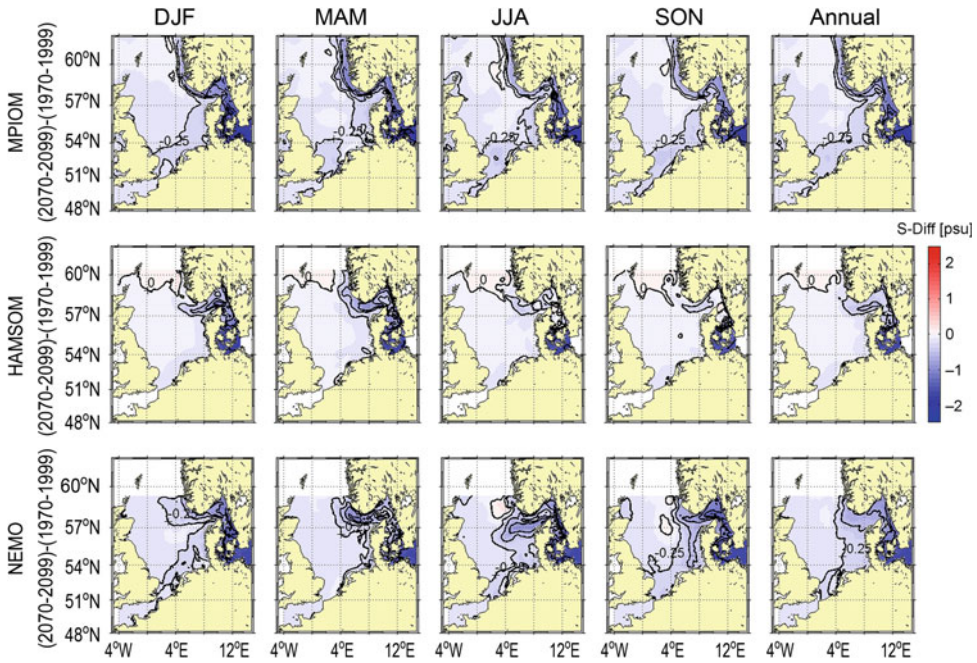

Fig. 6.14 Projected change in sea surface salinity from three regional coupled AO-downscalings (ocean models: MPIOM, HAMSOM, NEMO), all with GCM forcing from ECHAM-MPIOM (Bülow et al. 2014)

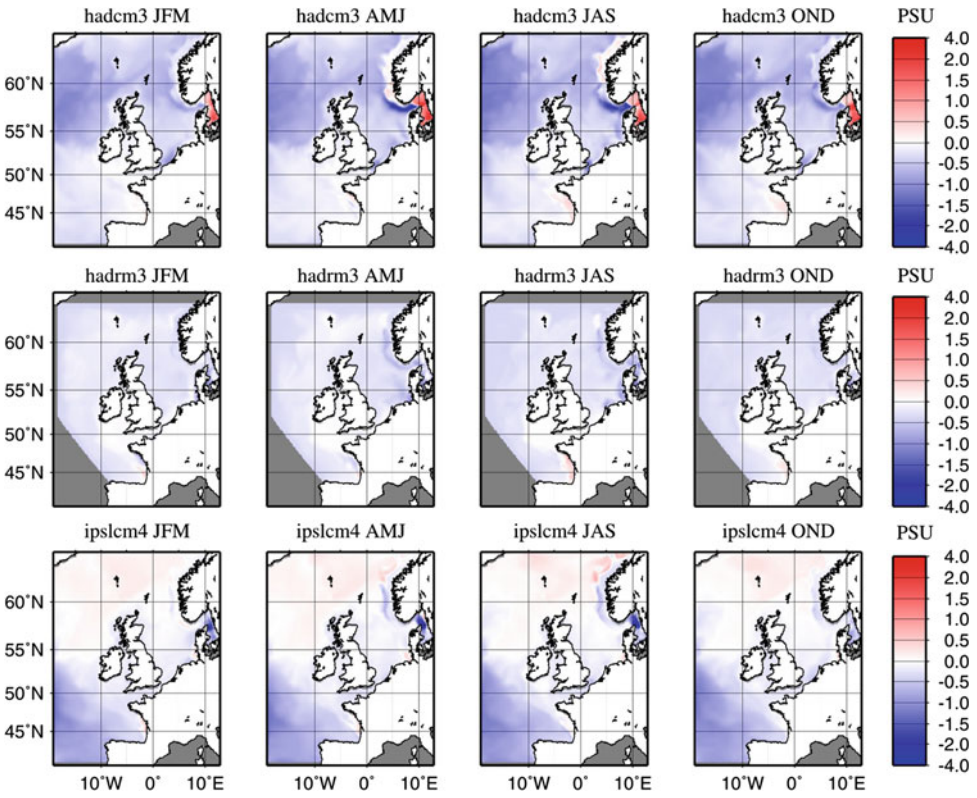

Fig. 6.15 Projected change in sea surface salinity as simulated by the POLCOMS model using forcing from HadCM3, HadRM3 and IPLS-CM4.0 (results combines from Holt et al. 2010, 2012 and Wakelin et al. 2012a, see for time period Table 6.2)

surface temperature generally describes the average temperature of the water column. In late spring, a seasonal thermocline develops (Janssen et al. 1999; Schrum et al. 2003b) and the well-mixed surface layer decouples from the lower layer water. The timing and duration of stratification, thermocline strength and the thickness of the surface mixed layer have implications for air-sea fluxes. Changes in stratification also affect regional ocean characteristics, for example the seasonal variations in tidal constituents through changes in eddy viscosity and current profiles (Sect. 6.2) and sediment transport (Gräwe et al. 2014). Stratification is also an important control of nutrient supply to the euphotic zone

and changes in stratification are therefore a major driver for changes in primary production (e.g. Holt et al. 2014; Sect. 6.4).

A measure of stratification that can be applied to both the shallow shelf and the open ocean is the potential energy anomaly (PEA). This is here defined as the energy required to mix the water column over the top 400 m (see Holt et al. 2010 for further details). For the North Sea, PEA is at minimum in winter, when the water column is well mixed, and increases as soon as seasonal thermal stratification develops. Coastal areas and the Southern Bight are well mixed all year round by intense tidal mixing and show minimal values for PEA throughout the year, as illustrated by the POLCOMS control experiment (Fig. 6.16). The POLCOMS scenario experiments project a substantial increase in stratification in open-ocean regions (e.g. Holt et al. 2010), which is consistent with a future shallowing of the open-ocean mixed layer as modelled by Gröger et al. (2013) and seen in most GCMs (e.g. Allen and Ingram 2002; Wentz et al. 2007).

Projections suggest the shelf will remain generally well mixed during winter, but that stratification in spring, summer and autumn will increase significantly, which could be attributed to earlier onset and later breakdown of seasonal stratification (Holt et al. 2010, stratification is here defined as a sustained surface to bottom density difference equivalent to 0.5 °C and a mixed layer shallower than 50 m) and to stronger stratification during summer. Using the POLCOMS-HadRM3-HadCM3 model scenario, Holt et al. (2010) found that stratification would start 5 days earlier and breakdown 5–10 days later by the end of the century (Fig. 6.17). During summer the greatest increase in ocean stratification is to the south of the domain. Ensemble simulations using different GCMs (POLCOMS-based) are shown in Fig. 6.18 (note the graphic shows fractional changes). All ensemble members simulate a positive fractional change almost everywhere throughout the season. The increase in PEA is strongest in winter in the open ocean and lower in summer and on the shelf. The ensemble simulations also indicate substantial inter-model variability in projected changes in stratification during summer on-shelf and at the shelf break and in the open ocean throughout the year. While there is also a significant fractional change in 'well-mixed' regions, absolute values remain low.

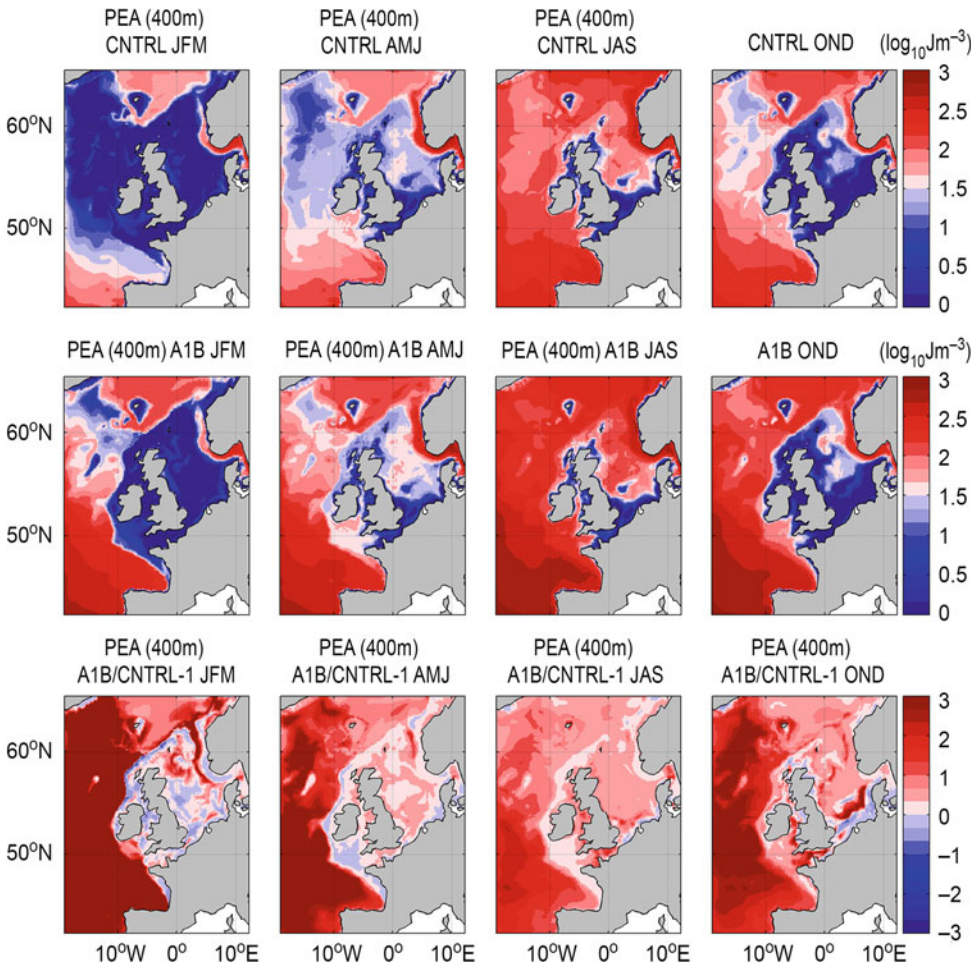

Fig. 6.16 Simulated seasonal mean potential energy anomaly (PEA) with integration limited to 400 m for CNTRL and A1B (note log10 scale, from POLCOMS) and the fractional difference between them. NB this is limited to changes of a factor of 3, maximum change in oceanic regions is a factor of 5.7 (Holt et al. 2012)

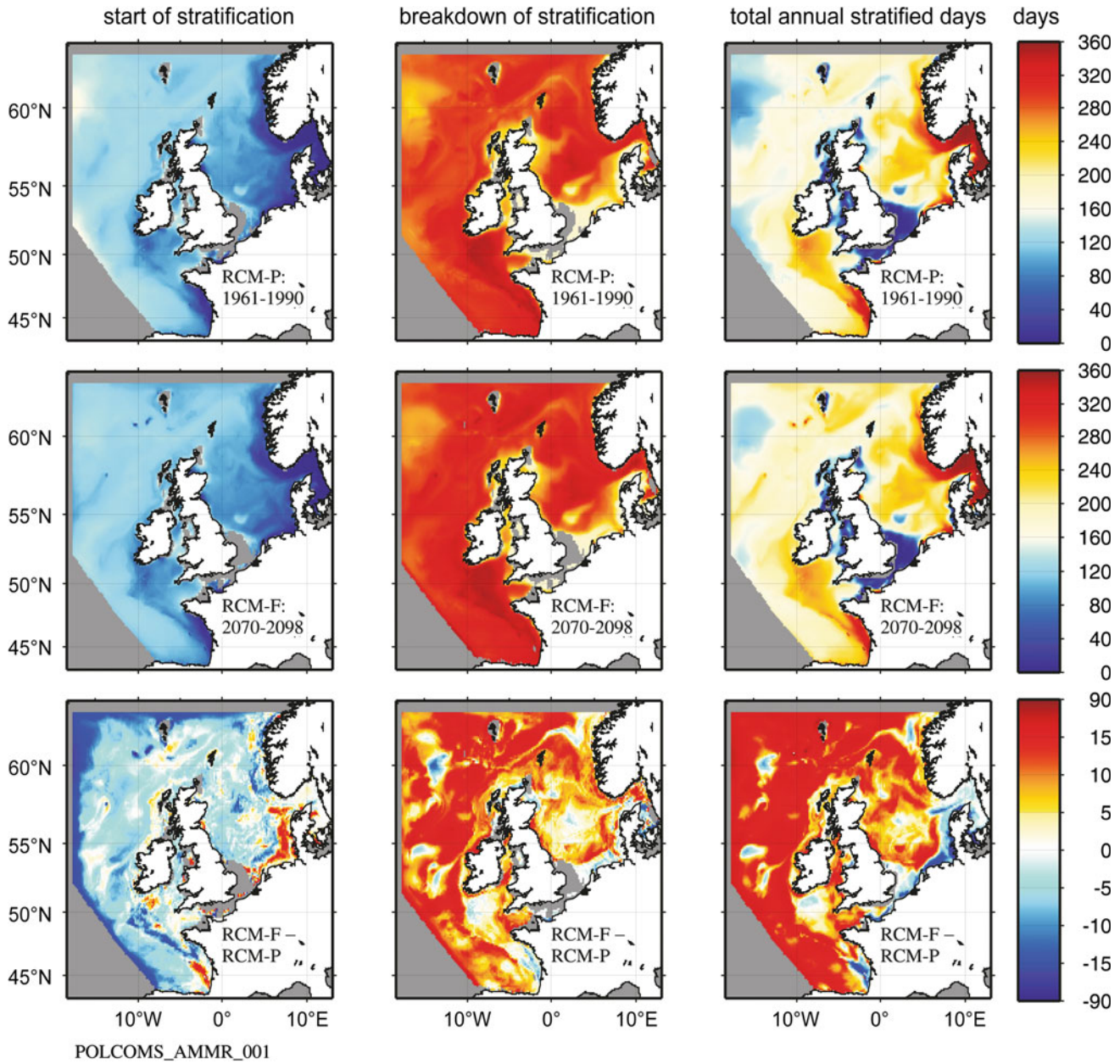

Fig. 6.17 Simulated mean timing of seasonal stratification for present day (RCM-P 1961–1990, *upper*), future climate (RCM-F 2070–2098, *middle*) and the difference between them (i.e. projected change from POLCOMS, *lower*). The graphic shows day of the year (1 January is day 1) when persistent seasonal stratification starts (*left column*) and ends (*middle column*), and the total number of stratified days (*right column*). *Grey shaded* areas are well mixed throughout the year (Holt et al. 2010)

Potential energy anomaly is a metric that does not inform about vertical structure and strength of gradients. Higher PEA could correspond to a deeper thermocline or to a stronger vertical gradient without a change in thermocline depth. Alternative metrics are the depth and strength of the thermocline, which could also provide insight into the nature of the change. Using these metrics Mathis (2013) and Mathis and Pohlmann (2014) identified a weak shallowing of the thermocline in the HAMSOM projection, which they attributed to a weakening of summer wind speeds. In contrast, the seasonal maximum thermocline depth showed a clear and strong deepening trend. Mathis and Pohlmann (2014) attributed this to a delay in thermocline erosion south of the 50 m depth contour in autumn, caused by a decrease in seasonal heat loss and wind speeds in the future (Fig. 6.19).

The spatial extent of stratification is mainly determined by local bathymetry and tidal amplitude and so is not subject to significant change (e.g. Mathis and Pohlmann 2014). Mean and maximum thermocline strength are both

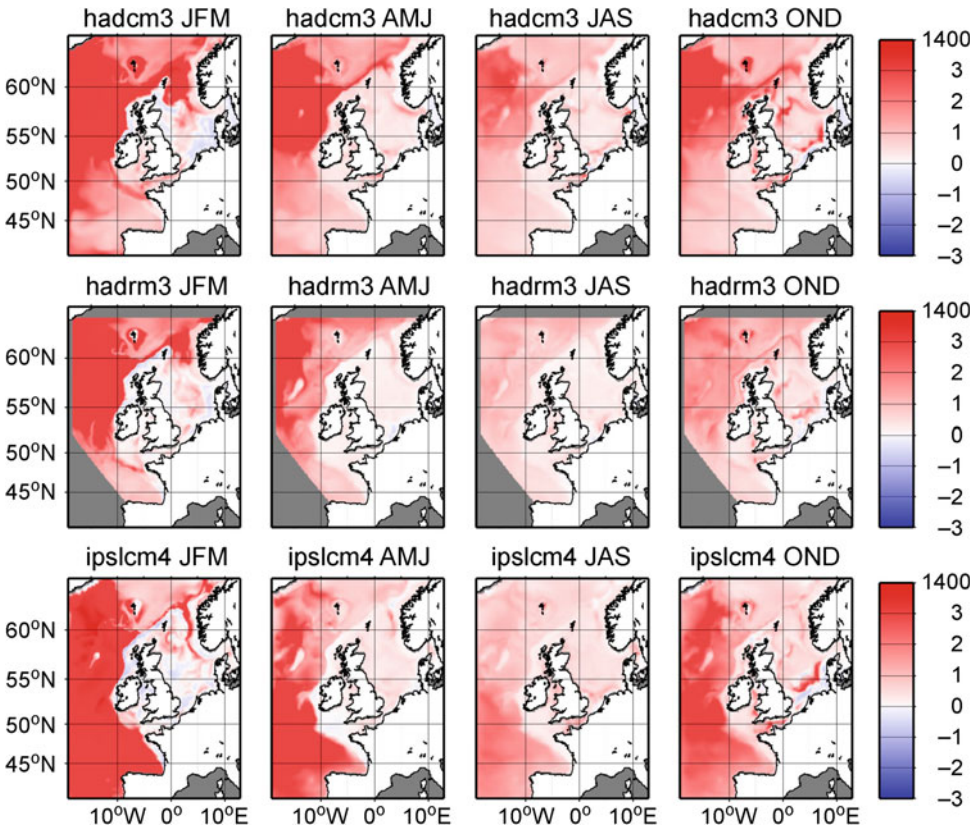

Fig. 6.18 Fractional change (calculated as future/past-1) in potential energy anomaly (PEA) projected by the regional POLCOMS forced by the HadCM3, HadRM3 and IPSL-CM4.0 global climate models. The depth limit for PEA integration is indicated above the colour scale (1400 m) (results combined from Holt et al. 2010, 2012 and Wakelin et al. 2012a)

decreasing, due to stronger warming in winter compared to summer in the HAMSOM projection. Since the temperature of the deeper waters is largely determined by the water temperature of the preceding winter, this results in a progressively smaller temperature difference between surface and bottom waters under a future climate. This conclusion from the HAMSOM simulations is in contradiction to results from Gröger et al. (2013) who found an increasing salinity difference between surface and bottom water and speculated that this is due to enhanced river runoff and a strengthening hydrological cycle through the 21st century. This discrepancy might be explained by different consideration of runoff changes in both downscalings. In contrast to MPIOM simulations, which resolve and consider runoff changes, the HAMSOM-based downscaling experiment is forced by constant climatological river runoff data based on values for the latter half of the 20th century over the entire simulation period. Another reason might be the different downscaling procedures applied, namely bias corrections for HAMSOM downscaling and direct forcing with salinity restoring to the forcing coarse-scale GCM in the coupled atmosphere-ocean model, which have the potential to modulate regional climate change impacts.

6.3.5 Changes in Transport and Circulation

A detailed investigation of transport change was undertaken by Mathis (2013) and Mathis and Pohlmann (2014) based on one regional scenario only. Projected future changes in circulation were analysed for seasonal mean current velocity vectors and trend analyses were applied to depth-averaged current speeds and to volume transports through various lateral sections in the North Sea. Mathis and Pohlmann identified an enhanced general circulation and a stronger northern inflow (Fig. 6.20) in spring, caused by stronger westerly and north westerly winds in the forcing GCM. For the other seasons the slightly decreasing mean wind speeds result in a slightly weaker general circulation. They identified increasing northern inflow in spring (by about +21 %, +0.134 Sv; 1 Sv = 1 million cubic metres per second) as the most significant seasonal 100-year change, which also dominates on annual scales. The other important change is a substantial decreasing inflow through Dover Strait in summer (−38 % or −0.023 Sv). In addition, they found a 12 % (−0.113 Sv) weakening of the Skagerrak recirculation in autumn and a 10 % (−0.055 Sv) reduction of the inflow through the Fair-Isle Passage in winter. A substantial

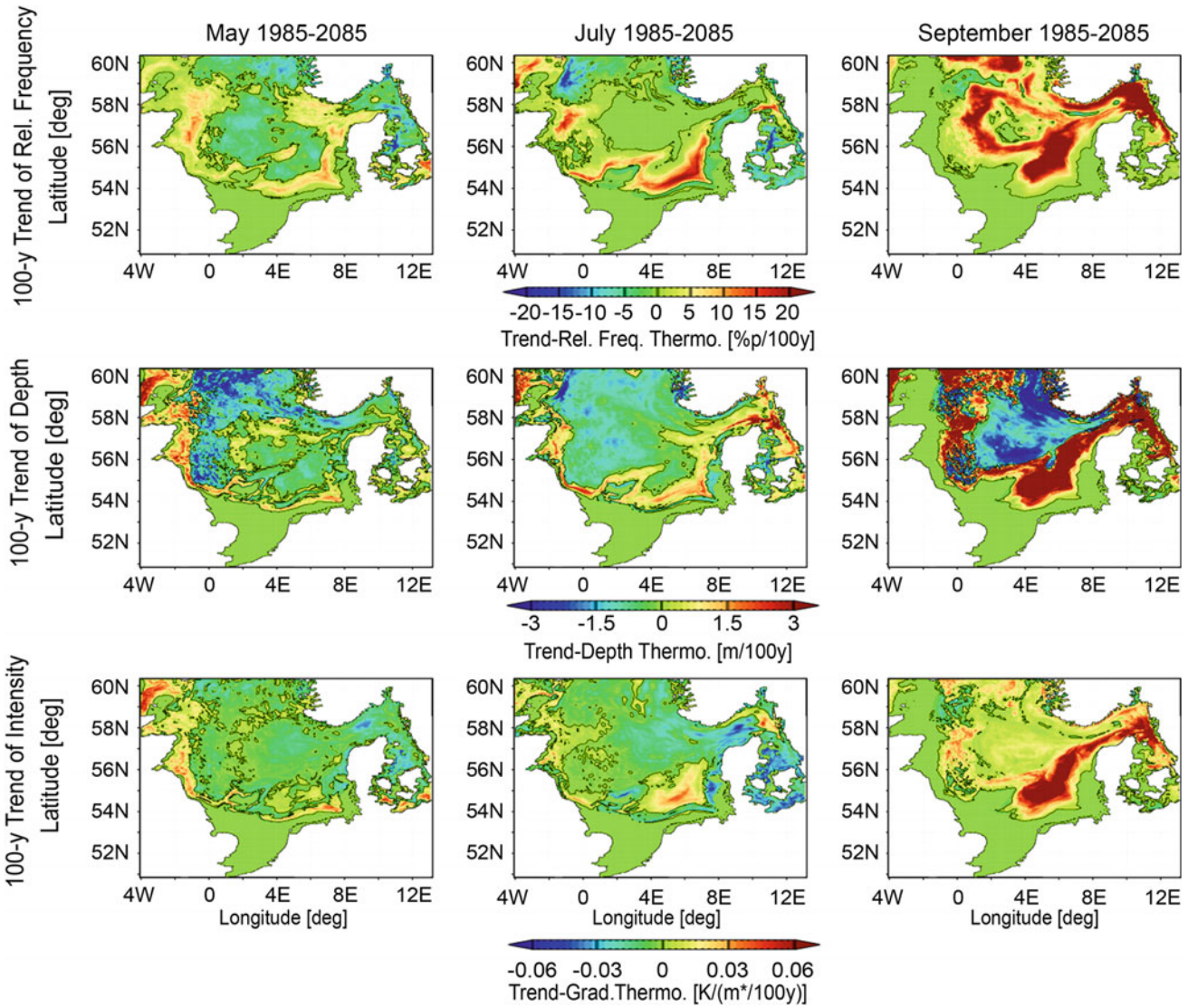

Fig. 6.19 Spatial distribution of modelled representative 100-year trends in the relative frequency of thermocline presence (*upper row*), depth (*middle row*), and intensity (*lower row*) for May (*left column*), July (*middle column*), and September (*right column*) as simulated by the HAMSOM model. The *black contour lines* refer to null trends (Mathis and Pohlmann 2014)

proportion of the northern inflow reverses into the Norwegian Coastal Current shortly after entering the northern North Sea, which consequently increases. Due to a weaker Dooley Current, caused by reduced Fair-Isle inflow, the northern inflow is guided south-eastwards to a lesser extent so that more water of North Atlantic origin is able to enter the central and southern North Sea. A westward strengthening of the northern inflow is indicated through increasing current speed east of the Shetland Islands and in the central North Sea. The changes in depth-averaged current speeds across the entire northern North Sea are statistically significant, as indicated by confidence levels higher than 95 %.

Detailed studies of transport pattern are not available from other regional scenarios and so it remains open how large internal variability and inter-model uncertainty is and whether the projected changes can be considered as robust. However, an overall increasing inflow was also projected by ROMS forced by the global climate model BCM (Ådlandsvik 2008). In contrast to Mathis (2013) and Mathis and Pohlmann (2014), Ådlandsvik projected an increasing inflow for almost the entire seasonal cycle. Only the October and November inflows were projected to decrease slightly. Using a different setup (ECHAM3-RACOM-NORWECOM), Friocourt et al. (2012) simulated for the near future (2031–2050) a decrease in inflow into the North Sea of about 5 %, for almost the entire seasonal cycle (exceptions August and November) with the NORWECOM model.

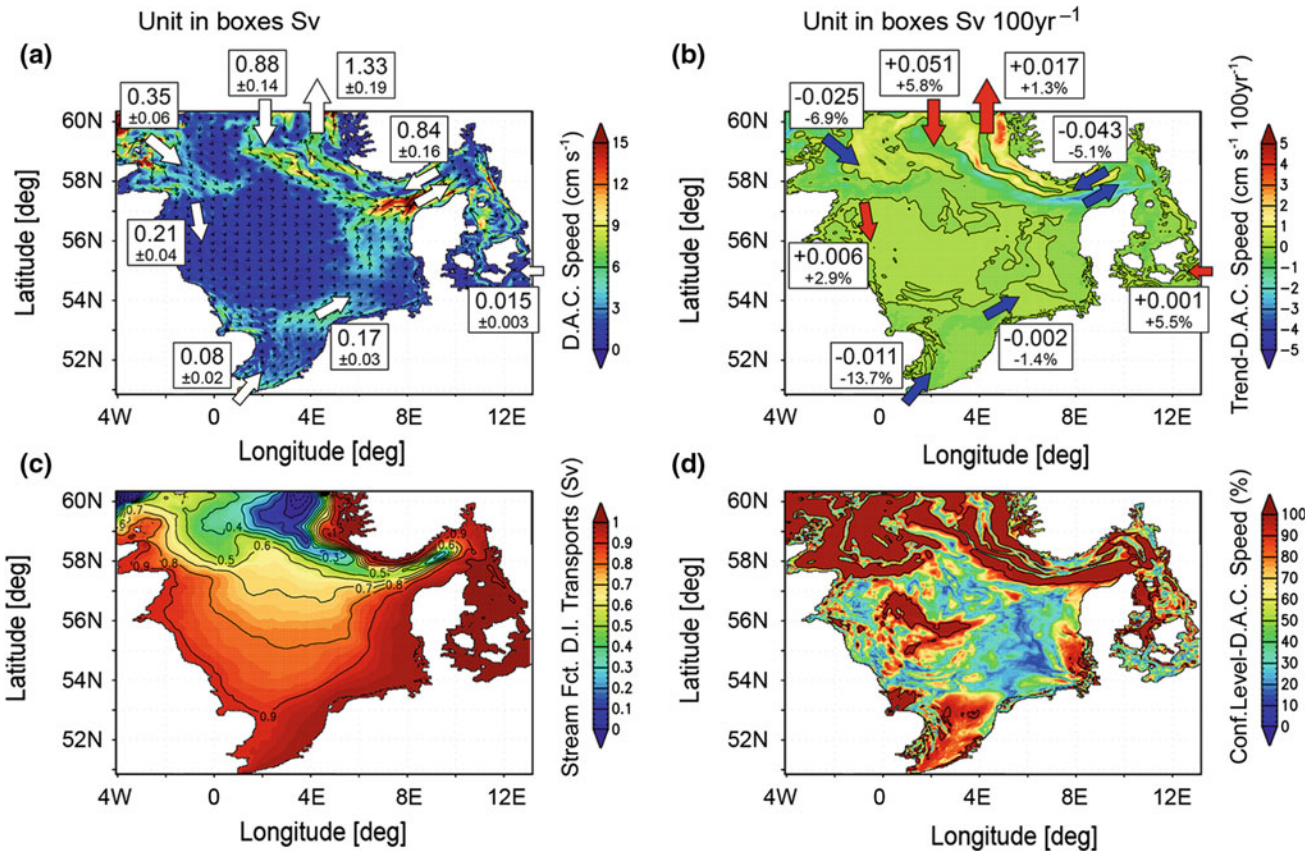

Fig. 6.20 **a** Simulated annual mean depth-averaged current (DAC) speeds and velocity vectors (model results from HAMSOM). Net volume transport at various transverse sections and standard deviations are given in *boxes*. *White arrows* illustrate mean flow direction. **b** Associated linear 100-year trends and relative changes to the magnitudes given in **a**. *Red* (positive) and *blue* (negative) *arrows* indicate trends. **c** Stream function of mean depth-integrated (DI) volume transport. **d** Confidence levels of the linear trends shown in **b** (Mathis and Pohlmann 2014)

6.4 Primary Production, Ocean Biogeochemistry, Ocean Acidification

Climate change impacts on primary production and responsible biogeochemical changes and ocean acidification were studied in a sub-set of the downscaling experiments summarised in Tables 6.2 and 6.4. The POLCOMS, ECOSMO, HAMSOM, Delft3D, NORWECOM and MPIOM simulations were equipped with a lower trophic level model (Alheit et al. 2012; Holt et al. 2012, 2014, 2016; Wakelin et al. 2012a; Gröger et al. 2013; Chust et al. 2014; Skogen et al. 2014; Pushpadas et al. 2015). Some of these downscaling scenarios also considered carbonate chemistry, but published estimates of future ocean acidification are available only from two regional models: POLCOM-ERSEM and ECOSMO (Wakelin et al. 2012a; Artioli et al. 2013, 2014). Although carbonate chemistry was also considered in MPIOM-HAMOCC-zoom (Gröger et al. 2013) and ECOHAM simulations (Alheit et al. 2012), no ocean acidification projections for future climate change have yet been published for these models.

Only the ECOSMO model uses IPCC-AR5 ESM global forcing (Wakelin et al. 2012a; Pushpadas et al. 2015). All other downscaling studies of ocean biogeochemistry and all climate change impact scenarios for ocean acidification are based on global climate change scenarios from the IPCC AR4-generation models (Table 6.2). All regional scenarios lack land-ocean coupling, similar to regional hydrodynamic scenarios (see Annexes 2 and 3 and Sect. 6.3) and climate-driven changes in future river loads are neglected in most regional scenarios in accordance to ESM scenarios (AR4- and AR5-generation models; Regnier et al. 2013). Only for the ECOHAM downscaling scenario was an attempt made to scale river loads by changes in river runoff (Alheit et al. 2012). Different eutrophication scenarios were only considered in a couple of near-future studies undertaken within the MEECE project (Zavatarelli et al. 2013a, b).

6.4.1 Primary Production and Eutrophication

Production of organic carbon through photosynthesis (chemosynthesis is not considered here) is controlled by availability of light and nutrients, and is thus sensitive to climate change. A decrease in annual net primary production (netPP) in the northern North Sea was a consistent impact signal for all scenarios considering North Atlantic impacts and local atmospheric forcing (Holt et al. 2012, 2014, 2016; Wakelin et al. 2012a; Gröger et al. 2013; Pushpadas et al. 2015). The decreasing netPP could be largely attributed to a decrease in cross-shelf nutrient fluxes to the North Sea and a consequent fall in North Sea winter dissolved inorganic nitrogen (DIN; Holt et al. 2012, 2014, 2016; Gröger et al. 2013; Pushpadas et al. 2015). The decrease in nutrient fluxes originates largely from local oceanic stratification changes on the Northwest European Shelf and near the shelf break, but as sensitivity experiments by Holt et al. (2012, 2014) reveal the oceanic far field also contributes. Local stratification changes in the North Sea are less important. Projected decrease in netPP for the end of the century was moderate for the regional models ECOSMO (12 %) and POLCOMS-ERSEM (2 %) when forced by the IPSL-CM4.0 ESM (Wakelin et al. 2012a; Holt et al. 2014, 2016; Fig. 6.21). Projected changes in mean annual netPP from the ECOSMO-IPSL-CM4.0 scenario were significant and could be distinguished from climate-driven variability, although this was not the case for POLCOM-ERSEM results (Wakelin et al. 2012a). Pushpadas et al. (2015) projected greater decreases in netPP for regional model scenarios forced by the ESM MPIOM-HAMOCC (−19 %) and lower primary production decrease for the scenarios forced by BCM-HAMOCC (−2.3 %).

Holt et al. (2012) reported that the North Sea is generally vulnerable to oceanic nutrient changes. However, this is compensated for by on-shelf processes and the actual sensitivity is less than expected. Holt et al. (2014) concluded that, like shelf seas in general, the North Sea is likely to be more robust and less affected by climate change than the global ocean, where the leading process of increasing permanent stratification significantly reduces netPP (e.g. Steinacher et al. 2010). The North Sea is well mixed for almost half the year, and local stratification changes are less important and potentially overridden by other processes (Holt et al. 2014). Strong tidal mixing and a substantial contribution of recycled production, based to a large extent on suspended particulate organic material advected onshore are major controls of ecosystem dynamics in the shallow southern North Sea (Holt et al. 2012). Holt et al. (2014) hypothesised that these properties may shelter the North Sea, similar to other shallow and tidally influenced shelf regions, from some direct impacts of climate change. Consistent with this hypothesis, the regional models ECOSMO and POLCOMS-ERSEM both projected the greatest decreases in production in the deeper northern North Sea and a moderate decrease or even an increase in production in the shallower southern North Sea in most of the scenarios (Holt et al. 2014, 2016; Pushpadas et al. 2015; Figs. 6.21 and 6.22).

Comparing the two regional model scenarios forced by the same ESM (IPSL-CM4.0), shows that the pattern of projected change in netPP and the magnitude of local increases in the southern North Sea are very similar for both regional models, but that the modelled local decreases in other regions are much stronger in the ECOSMO model, which results in a six-fold larger projected decrease in overall netPP for the North Sea with the latter model (Wakelin et al. 2012a; Holt et al. 2014, 2016). A potential cause of this discrepancy is the temperature-dependent metabolic rates in ERSEM, which would speed up growth-and-mortality cycles in a warmer world, and their omission in ECOSMO (Daewel and Schrum 2013). However, according to an assessment by Holt et al. (2014, 2016) this can account for only a small fraction of the discrepancies, mostly along the coast. A more likely candidate is therefore the cross-shelf exchange of nutrients and thus on-shelf production, which is modelled differently by the POLCOMS-ERSEM and IPSL model (Holt et al. 2014). Differences are especially pronounced for the region south and west of Great Britain. These regions appeared to be the most important for nutrient supply to the entire North Sea system (Holt et al. 2012). The different spatial coverage of both regional models is therefore of key importance. ECOSMO, which is forced with boundary nutrients from the global model on the shelf, is more strongly coupled to the global model and its projected changes are more similar to the projected changes by the global model (Chust et al. 2014). In contrast, POLCOMS-ERSEM is forced by boundary conditions from the global model off-shelf and resolves cross-shelf exchange. Hence it can deviate more strongly from the global model and could develop its own regional dynamics. These findings support the hypothesis that the different cross-shelf dynamics in the regional and global model in the shelf break region is a likely cause for deviations in projected climate change impacts between the two regional models. The projected change in the Skagerrak region is also quite different in both regional models. A decrease in netPP is projected by ECOSMO and an increase by POLCOMS-ERSEM. The latter is probably biased by not resolving the Baltic Sea response and artificial boundary assumptions for POLCOMS-ERSEM. Steinacher et al. (2010) reported a drift in the IPSL-CM4.0 ESM A1B simulation. The degree to which the drift affects regional downscaling remains unclear and there has been no attempt

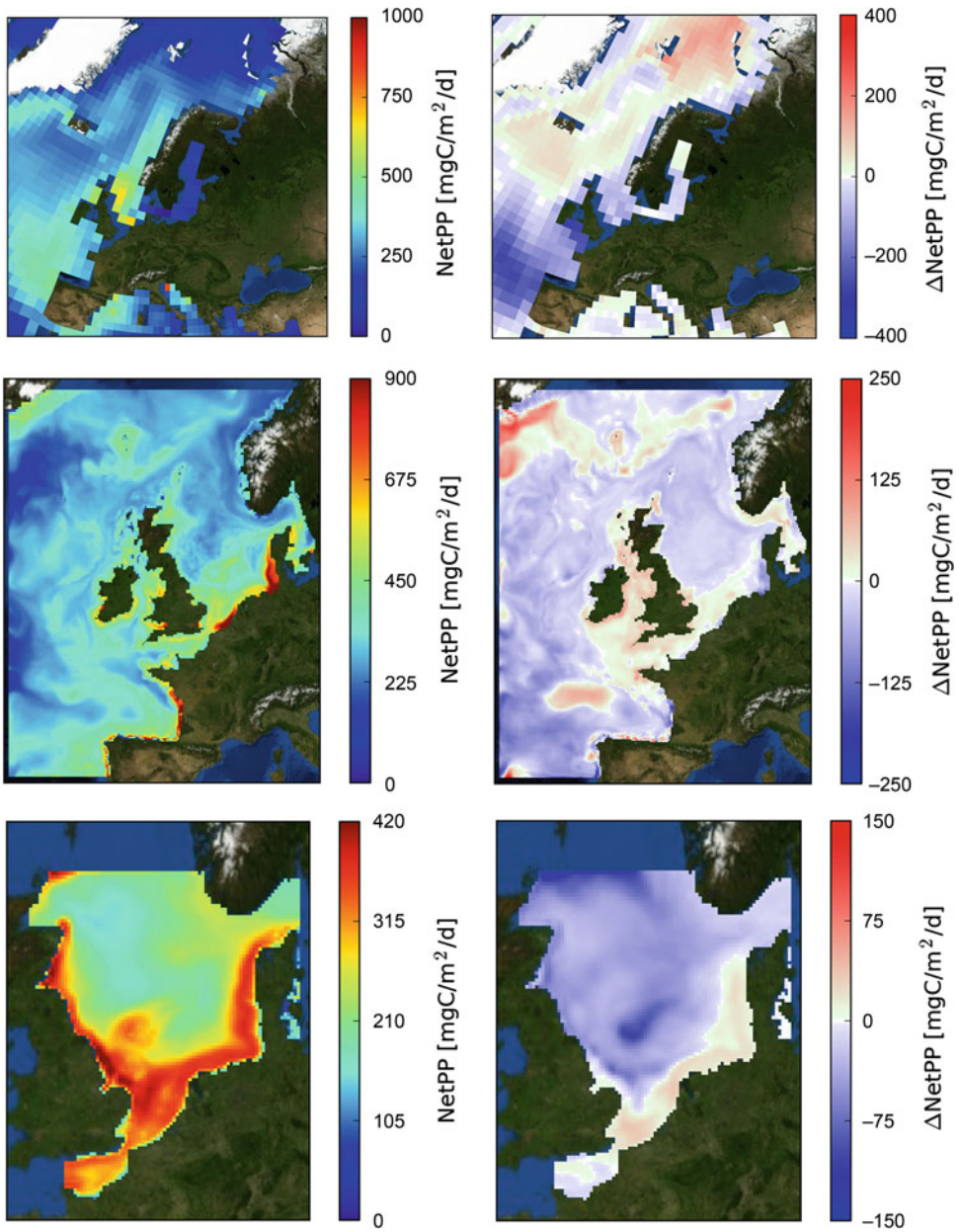

Fig. 6.21 Simulated present-day net primary production (netPP) (*left*, mean 1980–1999) and projected change in daily mean netPP between 1980–1999 and 2080–2099 estimated from the global IPS-CM4 model (*upper*) and from the IPSL-POLCOMS-ERSEM (*middle*) and IPSL-ECOSMO (*lower*) regional downscaling, note the different levels of netPP simulated by both regional models (Holt et al. 2014)

to estimate or remove a potential regional drift in either the POLCOMS-ERSEM or the ECOSMO downscaling.

The projected decrease in netPP from the MPIOM-HAMOCC-zoom model scenarios for the North Sea (Gröger et al. 2013) is 30 % and so substantially larger than estimates from the regional scenarios discussed above. Gröger et al. (2013) concluded that regional impacts on netPP are amplified in the North Sea relative to the global ocean and hypothesised that the shelf is more vulnerable than the open ocean, contradicting the findings and conclusions of Wakelin et al. (2012a), Holt et al. (2014) and Pushpadas et al. (2015). Possible reasons for opposite findings in the regional studies are different sensitivities of the cross-shelf exchange in the global and regional approach caused by different spatial resolution and sensitivity to the GCM bias and bias correction (as shown by Holt et al. 2014), and differences in the regional and global biogeochemical models. That the lower resolution in the MPIOM-HAMOCC zoom configuration (Gröger et al. 2013) compared to the regional models is a major reason for the different sensitivities seems unlikely, since the MPIOM-zoom resolution did not appear to be critical for the representation of hydrodynamics compared to high resolution regional models (not yet published).

More likely factors are differences in the biogeochemical parameterisations and the forcing GCM. The regional multi-ESM ensemble study presented by Pushpadas et al.

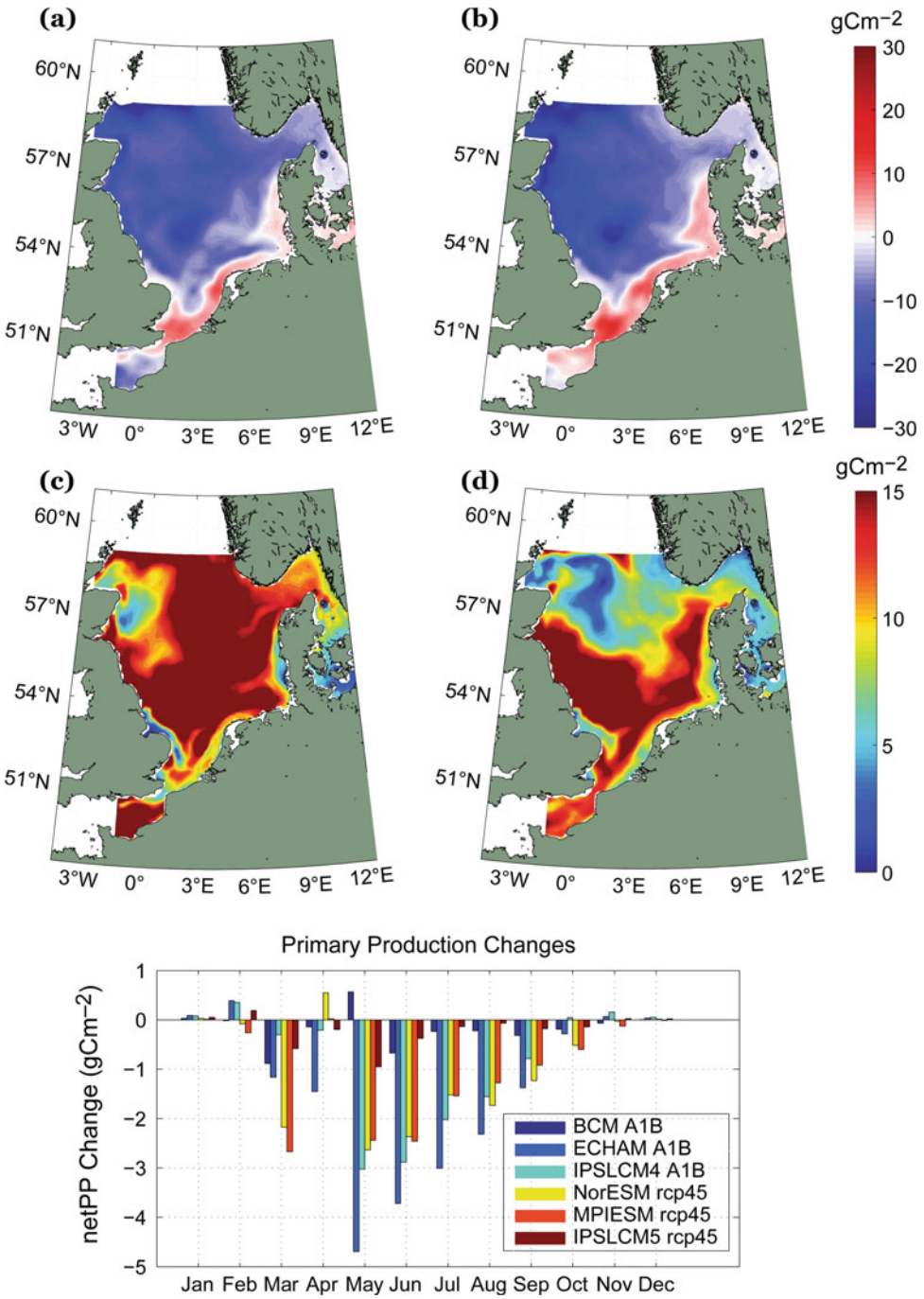

Fig. 6.22 Ensemble mean projected change in net primary production (netPP) from a six-member ensemble simulated with the regional ECOSMO model. *Upper:* **a** ensemble mean for the SRES A1B scenario simulations (forced by BCM-HAMOCC, MPIOM-HAMOCC and IPLS-CM4), **b** ensemble spread for the A1B scenarios, **c** ensemble mean for the RCP4.5 scenarios (forced by NorESM, MPIOM-HAMOCC and IPLS-CM5), and **d** ensemble spread for the RCP4.5 scenarios. *Lower*, projected monthly change in netPP from the different scenarios (redrawn from Pushpadas et al. 2015)

(2015) supported this view, given the large inter-model spread in North Sea projected changes in netPP, caused by the parent ESM (Fig. 6.22). From their six-member ensemble the most pronounced decrease in netPP was modelled by the MPIOM-HAMOCC A1B scenario, however, the projected decrease in the North Sea is weaker (19 %, exact numbers to be used with caution, due to differences in area) when using the regional ECOSMO model compared to the MPIOM-HAMOCC-zoom, which shows that there is also a large sensitivity to the biogeochemical parameterisations on the regional scale. Also, as discussed by Gröger et al. (2013), the global HAMOCC model lacks many processes considered relevant on the shelf, including temperature effects on mineralisation, resolution of the nitrogen cycle and recycled production, realistic benthic remineralisation and re-suspension of organic material. This limits performance of the model in the shallow North Sea and could affect the sensitivity of primary production to climate change. As a result, the North Sea decrease in netPP could be overestimated by the MPIOM-HAMOCC-zoom, which was also

considered possible by Gröger et al. (2013). It is important to note that the correct sensitivity of the North Sea biogeochemistry to climate change is not yet clear, due to the lack of observations preventing an assessment of the different regional and global model approaches. Whether the above mentioned lacking biogeochemical processes are critical to the sensitivity of the regional biogeochemistry of the North Sea is also unknown and MPIOM-HAMOCC-zoom as presented by Gröger et al. (2013) was so far not compared to other biogeochemical models of the North Sea in detailed sensitivity studies. Studies for other seas (such as the Baltic Sea) suggest that even small differences in the parameterisation of biogeochemical processes, and not necessarily only the complexity of biogeochemical models may already be significantly affecting model sensitivity to changes in nutrient availability (Eilola et al. 2011).

The ensemble mean projected change in primary production forced by ESMs scenarios (IPCC AR4- and AR5-generation models) and inter-model spread for both ensembles were compared by Pushpadas et al. (2015; Fig. 6.22). They found a stronger ensemble mean decrease in netPP for the RCP4.5 scenarios than the ensemble mean from the SRES A1B scenario, despite the modelled warming being less in the newer RCP4.5 scenarios. The inter-model spread in projected netPP decrease was significantly lower in most of the area for the RCP4.5 scenarios, with −2.3 to −19 % for the A1B-AR4 scenarios versus 2.5 to −13 % for the RCP4.5-AR5 scenarios. However, generalisation from this finding is premature and not supported by the small number of ensemble members (three) for the A1B and RCP4.5 scenarios, respectively. The projected decrease in netPP and its inter-model ranges in the North Sea are very similar to the projected global decrease and its inter-model range (Bopp et al. 2013).

Holt et al. (2014; Fig. 6.23) showed that the different competing processes have contrasting and spatially structured impacts on primary production on the shelf. Their results demonstrated that the oceanic nutrient changes in the upper water layers due to changes in stratification and the consequent cross-shelf fluxes are the primary cause for projected on-shelf netPP decrease in the central and northern North Sea from the SRES A1B scenario forced by the IPSL-CM4.0 ESM. The increase in netPP in the shallow southern North Sea was attributed to changes in wind forcing and thermal forcing. Wind and thermal forcing contribute to faster on-shelf transport of particulate material and faster recycling of organic material due to increased temperature (Holt et al. 2014). In the central and northern North Sea modelled netPP changes were negative due to more stable thermal stratification, a signal that is weak in the central part and stronger towards the northern boundary and off the shelf. In the southern North Sea, netPP increased due to higher air temperature. In this region, the temperature impact on stratification is inconsequential and the temperature effect on biological recycling dominates. Averaged over the entire North Sea, the contributions from temperature increase leading to increases and decreases in netPP tend to cancel out, which is in accordance with results from perturbation experiments by Drinkwater et al. (2009) and Skogen et al. (2011).

Wakelin et al. (2012a) used the ECOSMO model to assess variations in regional projections arising from the forcing GCM for the combined atmospheric drivers. From these simulations no consistent atmospheric driver signal was projected for the North Sea. Both increasing and decreasing netPP were projected and there is low spatial correlation between the different projections (Fig. 6.24), similar to results presented by Holt et al. (2014, 2016). Overall, the local amplitudes of change stemming from the atmospheric drivers remain in the O(10 %). Average changes for the whole North Sea are much lower and wide areas remain almost unchanged. Comparing the atmosphere-only (Wakelin et al. 2012a) and atmosphere-ocean scenarios forced by ocean boundary nutrients from ESMs (Pushpadas et al. 2015) it can be concluded that decrease in oceanic nutrients is the dominant process in these scenarios and that consideration of changes in oceanic nutrient conditions is critical for reliable projections of future climate impact on the North Sea biological system.

Near-future scenarios performed with the NORWECOM and Delft3D-GEM/BLOOM models show minimal changes in near future netPP, using modelled chlorophyll as a proxy (Friocourt et al. 2012). However, potential effects of changes in top-down control on netPP are not addressed when using chlorophyll as a proxy and could be missed. Seasonal variation in average chlorophyll concentrations does not differ much between the control run and the future climate scenario in either model. Whereas the NORWECOM model shows a slight decrease in chlorophyll over most of the year, this is not the case for the Delft3D model. In the latter, the onset of the spring bloom, as indicated by chlorophyll, occurs earlier for the future climate scenario compared to the control run together with a slightly earlier decline in chlorophyll levels. In the NORWECOM model, the onset of the spring bloom is unchanged in the future scenario but, like the Delft3D model, shows a slightly earlier decline in autumn.

Future changes in eutrophication in the North Sea as a consequence of climate change have been investigated through scenario simulations with NORWECOM for the end of the century (Eilola et al. 2013; Skogen et al. 2014). To assess eutrophication impacts in downscaling scenarios the OSPAR Commission Common Procedure was applied (OSPAR 2005), which distinguishes between parameters in four categories (see Almroth and Skogen 2010): the degree of nutrient enrichment (Cat. I); the direct effect of nutrient enrichment, plankton growth (Cat. II); the indirect effect of

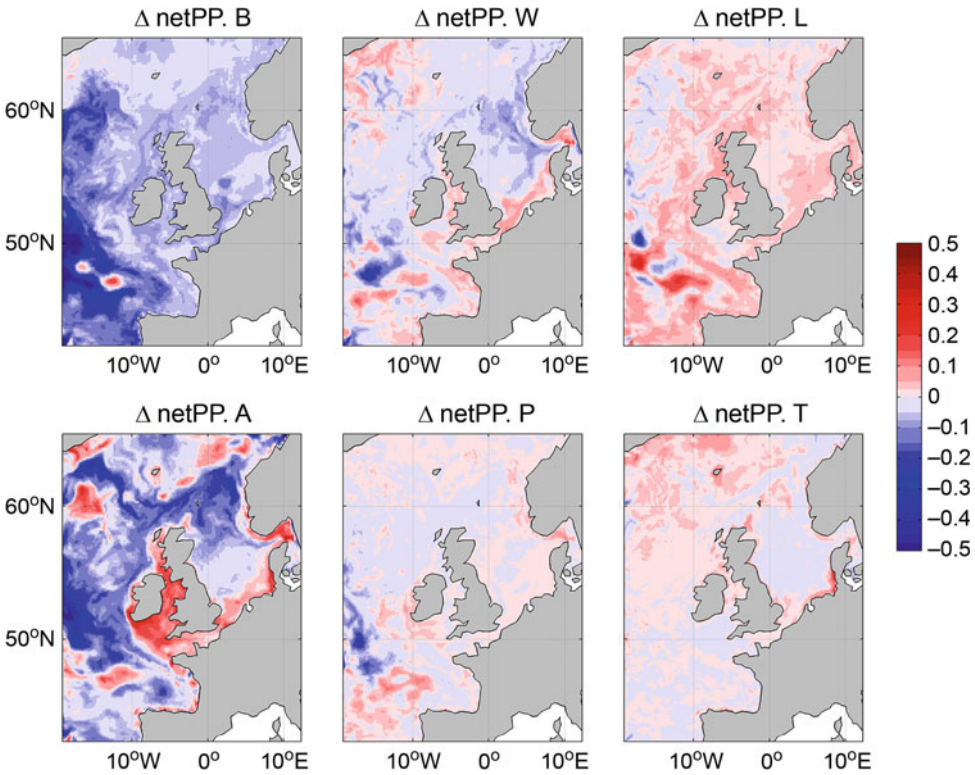

Fig. 6.23 Driver experiments with POLCOMS-ERSEM. Fractional change (estimated as future/past-1) in net primary production (netPP) associated with five external drivers and their non-linear interactions: boundary nutrients (B), wind (W), short-wave radiation (L), air temperature relative humidity (A), precipitation (P), and the direct effects of temperature on growth rates (T) (Holt et al. 2014)

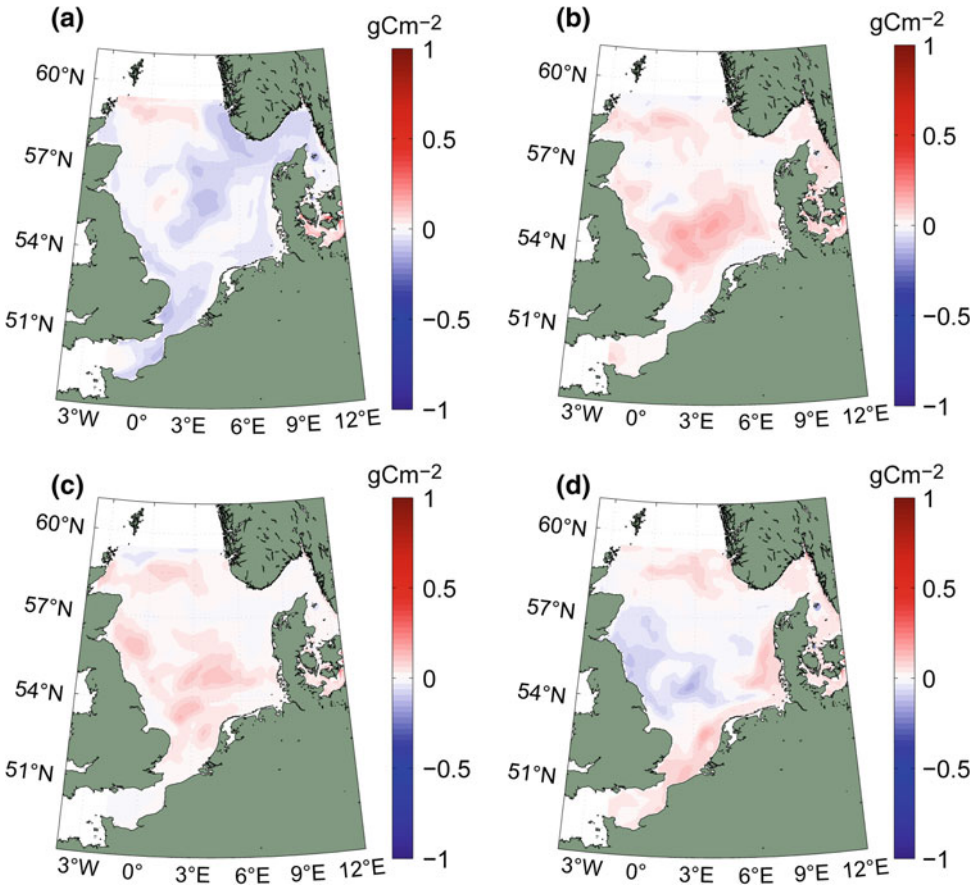

Fig. 6.24 Projected fractional changes (future/past-1) in net primary production (netPP) for the end of the century (1970–1999 vs. 2070–2100). Results from ECOMSO multi-model ensemble, atmosphere-only forced by **a** IPSL-A1B, **b** BCM-A1B, **c** ECHAM5-A1B, **d** NORESM-RCP4.5 (Wakelin et al. 2012a)

nutrient enrichment, increased oxygen consumption (Cat. III); and other possible effects of nutrient enrichment, such as changes in ecosystem structure (Cat. IV). Several eutrophication related parameters, such as winter DIN and dissolved inorganic phosphorous (DIP) and the DIN:DIP ratio, chlorophyll a, and oxygen can be easily explored with models and are used as indicators (in accordance with current management practices). Eilola et al. (2013) found a minor increase in winter nutrient levels for a future climate and projected a slight increase in phosphorus along the continental coast, while nitrogen is unchanged. A slight increase is also seen in summer chlorophyll levels in the German Bight and Kattegat, while the North Sea oxygen minimum is almost unchanged. Using these indicators, Skogen et al. (2014) concluded from one scenario that the overall eutrophication status of the North Sea would remain unchanged under a future climate. However, an increase in the river nutrient load caused by increased runoff, which has the potential to increase winter nutrient levels and eutrophication status near the coast (Zavatarelli et al. 2013a) was not considered in their assessment. The NORWECOM projection was forced by the same GCM as the ECOHAM (Alheit et al. 2012), but using different regional atmospheric, hydrodynamic and biogeochemical models. The projected nutrient levels from ECOHAM are higher near the coast, probably because increasing river loads have been considered in this simulation. A key weakness of both studies is the lack of consideration of North Atlantic nutrient changes, which other studies show have the potential to cause large changes in pre-bloom nutrient levels and thus overall netPP (Holt et al. 2012, 2014, 2016). Near-future change in productivity and nutrients from climate-driven and direct anthropogenic eutrophication were investigated by Zavatarelli et al. (2013b) with two model systems, the POLCOM-ERSEM and ECOSMO models and for two different eutrophication scenarios. These studies confirmed the dominant impact of climate control versus direct anthropogenic eutrophication control for the offshore North Sea system and the larger eutrophication impacts in the coastal zone hypothesised by Zavatarelli et al. (2013a). However, the short assessment period (only ten years) strongly limits the ability to distinguish climate change signals and changes arising from internal variability.

6.4.2 Species Composition and Trophic Coupling

The ecosystem models employed for regional downscaling are limited in terms of their potential to model changes in species composition, community structure and trophic coupling. They typically resolve plankton community structure by addressing a few functional groups such as diatoms, nitrogen-fixing bacteria and flagellates. However, this is a subjective concept and the few groups chosen are arbitrary. Also, fixed parameterisations are used for vital rates (e.g. growth rates, mortality rates), and are often used as a tuning parameter. As a result, these models have very limited potential to resolve changes in species composition, even at the base of the food web and projections are highly uncertain (Follows et al. 2007). Moreover, the models are truncated food-web models, which do not resolve coupling to higher trophic levels and the feedback inherent in this coupling (Fennel 2009).

Holt et al. (2014) investigated the sensitivity of diatoms relative to the rest of the phytoplankton community using the POLCOMS-ERSEM model. They found that both functional groups are sensitive to the projected changes, but that the amplitude of the projected changes is significantly smaller for diatoms than for the other phytoplankton functional groups. The changes are largest during the spring bloom and in the southern North Sea, when an increase in production was modelled to be supported by an accelerated growth rate. The changes were positive for all periods in both groups, except for summer, when production decreased significantly for the non-diatom groups.

Examining changes in the near future with the Delft3D-BLOOM/GEM model (four phytoplankton groups), Friocourt et al. (2012) found substantial differences in the average distribution of the different phytoplankton groups over the year, despite negligible changes in overall chlorophyll concentrations. The spring diatom bloom occurred slightly but consistently earlier in the future climate scenario. The general trend is for an increase in dinoflagellates and an earlier onset of growth for this group. In terms of factors limiting dinoflagellate growth (light-, nitrogen- and phosphorus-limitation), bloom probability and duration are higher for the future climate scenario than for the present day, irrespective of the type of growth limitation. The relative increase is largest for the nitrogen-limited type of dinoflagellates.

Wakelin et al. (2012a), Chust et al. (2014) and Pushpadas et al. (2015) found trophic amplification of the climate impact on productivity in the North Sea, based on ECOSMO and POLCOMS-ERSEM downscaling (Fig. 6.25). The relative decrease in production for the second trophic level is stronger than for the first trophic level, a phenomenon which is also widely seen in downscaling studies for other regions and in the response from the forcing ESM (Chust et al. 2014).

6.4.3 Ocean Acidification

Rising atmospheric CO_2 concentrations result in higher ocean uptake of CO_2. This in turn is driving a decrease in

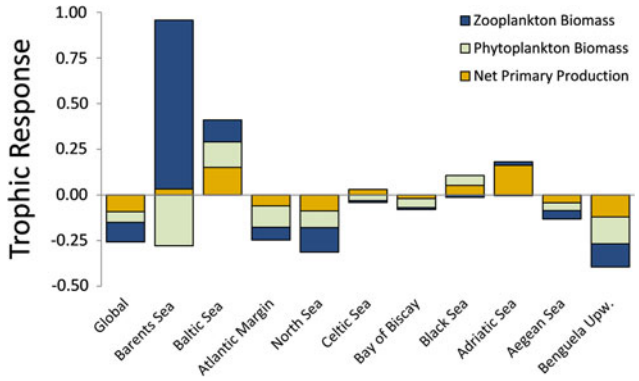

Fig. 6.25 Plankton response to the SRES A1B scenario as projected by different regional models forced by the IPSLCM4 earth system model. The graphic shows fractional change (calculated as future/past-1) for the end of the century (2080–2100) relative to present day (1980–2000) (Chust et al. 2014)

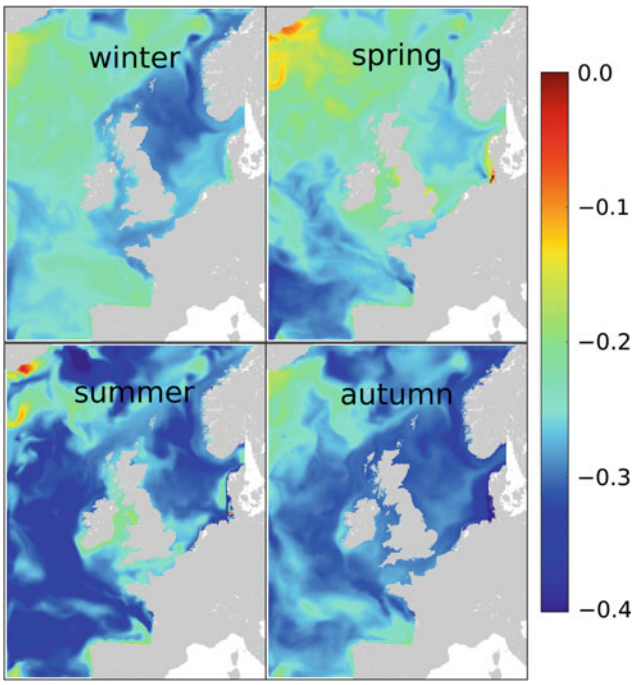

Fig. 6.26 Impacts of climate change and ocean acidification (OA) in the carbonate system as projected by the SRES A1B scenario, the graphic shows absolute difference in surface pH compared to the present-day by season (Artioli et al. 2013, 2014)

ocean pH and thus an increase in ocean acidification (OA) (also known as 'the other CO_2 problem'). However, OA is a complex process and is also influenced by climatic and biogeochemical processes. Artioli et al. (2013, 2014) investigated climate-driven impacts on OA in the North Sea using the POLCOMS-ERSEM model forced by the IPSL-CM4.0 ESM. For the end of the century, they found a significant change in annual mean pH of the order of −0.27, which is consistent in magnitude to the projected change in the annual global mean pH. The major driver for this decrease in pH was clearly the increasing atmospheric CO_2 concentration. The projected temperature rise had contrasting effects on OA in their downscaling experiment; both decreasing the solubility of CO_2, which leads to increased outgassing and lower OA, and increasing dissociation constants, which supports OA. Another but more minor effect is the decrease in total alkalinity due to the projected freshening which reduces the buffering capacity of the system. As Artioli et al. (2013) discussed, this feedback stems from assuming a simple correlation between total alkalinity and salinity (Millero 1995). Uncertainty might therefore be large and the total-alkalinity feedback remains unclear.

Biological processes were identified to be responsible for a strong modulation of the spatial and seasonal patterns of climate-driven impacts on OA, with average local variations of more than 0.4 in pH (Fig. 6.26). In highly productive areas and during the spring bloom less OA was projected. Acidification generally peaks in autumn and aragonite under-saturation was simulated in the present climate for bottom waters in the central North Sea in spring and summer, caused by community respiration and simultaneous stratification, which prohibits ventilation (Artioli et al. 2013, 2014). Artioli et al. (2014) projected an increase in the seasonal aragonite under-saturation in bottom waters in a future climate due to increased respiration in deep waters and benthic systems. The largest seasonal variations in projected pH change occurred in coastal areas; the projected local increase in netPP in this area may also have helped to reduce the projected OA increase by up to 0.1 according to projections by Artioli et al. (2013, 2014). However, uncertainty in the near-coastal projections for OA is large, since river runoff and loads have significant potential to override the OA changes and consistent scenarios and projections for river nutrients and total alkalinity loads are not available. The POLCOMS-ERSEM results are consistent with projections from the ECOSMO model using the same ESM forcing (Wakelin et al. 2012a). The ECOSMO downscaling reveals a decrease in mean North Sea pH from 8.09 to 7.87 (1980–1999 to 2080–2099; Fig. 6.27), indicating slightly weaker OA as projected by Artioli et al. (2013, 2014), and a continuation of the present almost linear trend of OA in the North Sea. The small differences in projected change in pH potentially arise from neglected seasonality in total alkalinity due to biological processes and total alkalinity changes in the ECOSMO study, as well as from different coupling sensitivity to the climate model for both models.

Increasing research efforts in recent years have improved understanding of OA and raised evidence for the broad impacts of OA on the marine ecosystem (e.g. Riebesell et al. 2007; Gattuso et al. 2011). Two such impacts namely the supporting effect of OA on primary production (Riebesell

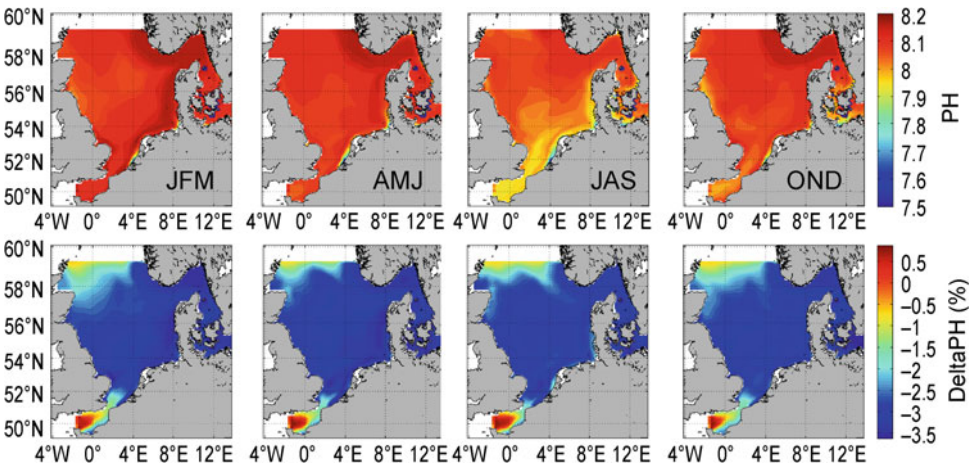

Fig. 6.27 Simulated seasonal mean pH (1980–1999) (*upper panels*) and percentage change (fractional change × 100) simulated by ECOSMO for a future climate (2080–2099) (Wakelin et al. 2012a)

and Tortell 2011) and the effect of OA on the nitrogen cycle (Gehlen et al. 2011) were studied by Artioli et al. (2013). While using a simplified parameterisation of increased growth rates for all phytoplankton functional groups, they found the potential effect of OA on primary production to be similar in magnitude to the climate-driven impact on primary production and to enhance spring production and decrease summer production. This supports a shift from flagellates to diatoms, a signal which was found to move up the trophic chain and support mesozooplankton over microzooplankton. Artioli et al. (2014) concluded that OA and climate change impacts on primary production could cancel out but could also amplify, and that regional hydrodynamics and productivity dynamics need to be taken into consideration. However, it should be mentioned that these are first attempts to model the OA impact on primary production and that a very simple parameterisation was applied to extrapolate available knowledge on a species level to the entire plankton community. This is very likely to be an oversimplification, which could strongly overestimate the potential OA effect on productivity as discussed by Artioli et al. (2013, 2014). The effect of OA on the nitrogen cycle was found to be small compared to the climate-driven impact on the nitrogen cycle via increased mineralisation due to higher temperatures (Artioli et al. 2013).

6.5 Conclusions and Recommendations

Increasing numbers of regional climate change scenario assessments became available for the North Sea and the new developments have contributed important understanding of regional processes mediating climate change impacts in the North Sea. Improved understanding of processes contributing to global sea level rise over the last decade has led to better regional projections of future changes in sea level. Better projections of future storm surges and waves are mainly due to better awareness of the factors driving change in the atmospheric storm track, and a better appreciation of the relative roles of long-term change and natural variability. Assessing climate-driven impacts on hydrography, circulation and biogeochemistry has benefited from new and advanced downscaling methods. Among these are the regional fully-coupled RCMs, initiated by the German KLIWAS project and physical-biological regional downscaling models, which were coupled with ESMs as part of the EU project MEECE. The large number of regional studies now available enables a critical review of current knowledge on climate change impacts in the North Sea region and allows the identification of challenges, robust changes, uncertainties and specific recommendations for future research.

6.5.1 Robustness and Uncertainties

Coherent findings from the climate change impact studies reviewed in this chapter include overall increases in sea level and ocean temperature, a freshening of the North Sea, an increase in ocean acidification and a decrease in primary production. In terms of the drivers of these changes, the impact of natural variability on sea surface temperature and ocean acidification is less dominant compared to projected anthropogenic changes, and their projected future changes appear to be relatively consistent among the different downscaling scenarios. This is also evident when considering GCM simulated time-series of future annual average steric sea level. Unlike atmospheric quantities such as rainfall or temperature, the climate change signal exceeds the simulated natural variability for mean sea level even for future scenarios with a high degree of emissions mitigation. Thus a rise in future global sea level is a robust result, although the precise amount remains uncertain. A projected regional temperature increase towards the end of the century

also appears to be a robust result from the multi-model ensemble projections reviewed in this chapter. However, the range in projected future temperature change depends on the choice of GCM and as the range in projected changes is of the order of the amplitude of the projected change itself, the magnitude of the change cannot therefore be considered robust. On smaller spatial scales a lower signal to noise ratio is typically expected. Projected regional patterns and seasonal modulation of temperature increase are variable and their future development is uncertain. The spatial patterns of sea level rise are also more diverse among the different regional projections (Pardaens et al. 2011a) but in the latest IPCC assessment some of the spread across normalised modelled sea level change patterns appears to have been eliminated.

A general decrease in ocean pH was a consistent signal from two regional climate change projections of OA. Offshore inter-model differences in projected future ocean pH appear to be small compared to the magnitude of projected changes, which could be attributed to the strong impact of changes in atmospheric CO_2 levels on ocean pH in comparison to other internal physical and biogeochemical effects. The projected increase in regional OA for the North Sea can thus be considered robust for offshore waters, despite the small number of studies available. In contrast, the importance of terrestrial impacts near the coast is increasing and the projections are adversely affected by the lack of terrestrial coupling and lack of information on river loads and total alkalinity changes.

Wind changes have a strong impact, *inter alia*, on local sea level, storm surges, surface waves, primary production, circulation, advection of salt- and nutrient-rich water from the North Atlantic, mixing, stratification, and offshore transport of river plumes. The North Sea is located in the land-ocean transition zone of the Northwest European shelf, which is characterised by very high variability due to the alternating dominance of the maritime climate of the North Atlantic and the continental climate (e.g. Backhaus 1989; Hawkins and Sutton 2009). There are several modes of variability that are particularly important for the North Sea; the North Atlantic Oscillation (NAO), the Atlantic Multi-decadal Oscillation (AMO) and the Atlantic Meridional Mode (AMM, e.g. Grossmann and Klotzbach 2009). The large natural variability has a greater impact on the local North Sea wind field than potential anthropogenic-induced trends, and strong natural climate variability from annual to multi-decadal scales (e.g. Arguez et al. 2009) is a particular challenge when developing projections of climate change in the North Sea. Regional projections for changes in wind in existing scenario simulations are not robust for the North Sea (e.g. Lowe et al. 2009; see also Chap. 5), with many GCMs still unable to accurately capture features such as the placing and timing of atmospheric pressure systems in the UK region (IPCC 2013). The long-term climate trends are superimposed on the natural modes of variability and distinguishing between the two in order to identify the anthropogenic climate change signal is one of the 'grand challenges' of climate change impact studies in marine regions. This is of particular relevance for the North Sea region where reliable predictions concerning strongly wind-influenced characteristics such as local sea level, storm surges, surface waves and thermocline depth are still impossible.

Substantial multi-decadal variability in projected climate change impacts was identified from atmospheric and sea level studies (e.g. Gaslikova et al. 2013). These multi-decadal variations bias projected changes estimated for 20- or 30-year time slices. Whether this is also relevant for ocean hydrodynamics and biogeochemistry has so far not been addressed. However, variability in wind fields appears a strong driver in hydrodynamic and biogeochemical changes in the North Sea (Skogen et al. 2011; Holt et al. 2014, 2016) and substantial multi-decadal variations are also to be expected for hydrodynamics and biogeochemistry (Daewel and Schrum, 2013).

A common regional finding for those scenarios considering future variations in oceanic nutrient conditions is a decrease in future levels of primary production (which are not always statistically significant). However, the projected decrease varies widely (from −2 to −30 %) depending on the driving ESM and the regional model used (Gröger et al. 2013; Holt et al. 2014; Pushpadas et al., 2015). Projections of future regional primary production are therefore less robust than for sea level, temperature and OA, which was also concluded by Bopp et al. (2013) for changes in global primary production projected by recent ESMs. Uncertainties in regional projections from multi-model ensembles are still large for offshore nutrient and salt fluxes and the consequent changes in netPP. Local atmospheric impacts on netPP remain dominated by natural variability and a common response in scenario simulations for lower trophic level dynamics was hardly identified for atmospheric drivers. Moreover, extending the regional models into the Baltic Sea and across the shelf break appears to be critical for the North Sea. The downscaling studies of Holt et al. (2012, 2014, 2016), Wakelin et al. (2012a), Gröger et al. (2013) and Bülow et al. (2014), showed the projected change in cross-shelf exchange probably depends on model resolution and is critically influenced by GCM biases and by the bias correction strategies used in the GCM and regional ocean climate models.

Close to the shelf, the boundary values from ESMs are impaired by a lack of consistent terrestrial coupling for nutrient loads (Regnier et al. 2013) and simplified parameterisation of physics and biogeochemical cycling in some ESMs (such as unconsidered re-suspension and tidal

mixing). The reliability of the near shelf and near coastal boundary conditions from ESMs is therefore unclear, and more research is needed to improve understanding of land-ocean coupling and the regional impacts and feedbacks to the global scale. Another source of uncertainty is regional atmosphere-ocean coupling and the advantages and disadvantages of using coupled atmosphere-ocean downscaling versus uncoupled regional atmospheric models to force regional ocean models.

6.5.2 Future Challenges

The lack of consideration given to terrestrial climate change impacts and their coupling to the ocean through runoff and terrestrial carbon and nutrient loads is a major issue. Projecting terrestrial impacts on salinity and especially on nutrients, carbon chemistry and alkalinity is a challenge at both the global and regional scale. Consideration of terrestrial impacts is critical for a shelf sea like the North Sea and improved understanding of the coupled dynamics in the land-ocean transition zone is essential. Many downscaling studies for the North Sea assume that runoff from the catchment area and freshwater outflow from the Baltic Sea will not change under a future climate (e.g. Wakelin et al. 2012a). Only the MPIOM-REMO simulation (see Bülow et al. 2014) closes the water cycle, although a freshwater flux-correction is also used here at the global scale (Sein et al. 2015), which could introduce artificial sources and sinks and bias the projected changes to an unknown degree. To date, no attempt has been made to include changes in terrestrial nutrient loads or alkalinity at the regional scale, nor is this standard for ESMs (Regnier et al. 2013). Although the impact of changes in runoff and river loads and in Baltic Sea outflow properties is probably restricted to the southern coastal North Sea and the Skagerrak, respectively, a more consistent approach is needed to address the water and nutrient budget of the North Sea, one which should consider the entire land-ocean continuum. A new hydrological model, HYPE (HYdrological Predictions for the Environment; Lindström et al. 2010; Arheimer et al. 2012), was recently developed to calculate river flow and river-borne nutrient loads from all European catchment areas; this is known as E-HYPE. In the future, scenario simulations using HYPE should generate more consistent changes in water and nutrient budgets. But despite these recent efforts, the uncertainties in runoff for the end of the 21st century will still be considerable due to precipitation biases in regional atmospheric models, as illustrated by Donnelly et al. (2014) for the Baltic Sea. Projections of nutrient loads are even more uncertain than projections of river flow due to unknown future land use and socio-economic scenarios (Arheimer et al. 2012). Plus, the carbon cycle and carbon loads are still not considered in the present version of HYPE and coupled land-ocean carbon scenarios remain for future work.

Other relevant factors include biogeochemical parameterisations, which have substantial impacts on structuring the ecosystem. For the North Sea system, sediment-water exchange and its parameterisation are particularly important. Further limitations are inherent in present-day regional biogeochemistry models. Changes in plankton community structure (e.g. Follows et al. 2007) and consistent trophic coupling also including higher trophic levels (e.g. Fennel 2009) are not yet incorporated and current models are too simple to provide reliable estimates of changes in community structure or trophic coupling. To date, they are only able to provide first indications of climate change impacts on trophic controls and community structure (e.g. Chust et al. 2014; Holt et al. 2014). Projecting future OA impacts on the regional scale requires better understanding of OA impacts on productivity, which could affect first-order impacts from changes in atmospheric CO_2 levels (Artioli et al. 2013, 2014).

Regardless of the specific methods employed, the downscaled simulations and regional studies are ultimately affected by the driving GCM or ESM. Despite improvements (e.g. Scaife et al. 2010), the latest generation of GCMs and ESMs still has significant biases and the spread in projected global warming among GCMs has not changed from IPCC AR4 to AR5 (e.g. Knutti and Sedláček 2012). Moreover, additional uncertainties arise from the downscaling methods and regional models used (e.g. Holt et al. 2014). From the simulations presented in this chapter it is clear that identifying best practice in climate downscaling is far from trivial and not yet achieved. A range of different approaches is currently used, each with advantages and disadvantages. A review of the literature shows that choice of regional model is not critical for the projected mean change, but is crucial for the projected spatial and seasonal patterns of regional climate change impacts. Regional models are sensitive to climate model biases and bias corrections are necessary for many applications, such as in modelling seasonal cycles of stratification and biological productivity. But bias correction also affects the sensitivity of regional systems to climate change impacts and might shift a critical change in one variable to a non-critical range and vice versa (Holt et al. 2014). Future work is required on the effects of global and regional model bias on regional dynamics and sensitivities to climate change impacts.

While models and observations have long been used together for validation, bias correction and re-analysis there is a movement in general circulation modelling and earth system science towards the use of observations as a constraint on the future change projected by climate models (e.g. Murphy et al. 2004; Stott and Kettleborough 2002; Cox et al.

2013). In some cases (e.g. Stott and Kettleborough 2002), the approach is closely related to optimal detection of past climate change and uses the model's ability to simulate past change in order to derive a distribution of signal weights that are assumed to apply in the future. In other approaches (e.g. Murphy et al. 2004), different model versions, using a range of different parameterisations, are used to simulate the future but the distribution of possible future scenarios is weighted according to each model's ability to simulate recent climatology. While these methods are still evolving they present an exciting opportunity for improving the projection of North Sea climate change. First, the methods could allow a weighting of the boundary conditions to regional simulations. Later they might also be applied directly to regional simulations. Considerable further work is required to understand the relevant constraints and optimum statistical framework for applying them. The result could be a narrowing of the uncertainty range of future projections as the observed signal of climate change becomes ever stronger.

Regional climate change impact assessment in the coastal area requires a greater degree of accuracy and more detailed process consideration than is currently available from GCMs and ESMs. GCM resolution is constantly improving, but so is resolution at the regional scale and the demand for detailed knowledge is expanding. Local planning in relation to climate change impacts might in future require unstructured grids or further local downscaling, as shown by Gräwe and Burchard (2012) for the western Baltic Sea or Zhang et al. (2015) for the North Sea and Baltic Sea. Combined assessment of climatic and direct human impacts such as eutrophication, fisheries, offshore construction, mining and dredging is increasingly required. Downscaling methods are therefore as necessary now as in the future and coupling regional downscaling models to down-stream impact models (such as for inundation or biological production at higher trophic levels; e.g. Daewel et al. 2008) is becoming increasingly important. Regional and seasonal patterns are very important for down-stream impact models and the application of such models requires the identification of robust patterns and estimates of uncertainty, making ensemble simulations, including larger sets of GCMs and regional models mandatory for the North Sea. Comparing results from different models to identify the presence or absence of robust change requires, as a minimum, harmonisation of experiment design, along the lines of the Coupled Model Intercomparison Project (CMIP, http://cmip-pcmdi.llnl.gov), to set standards that endure beyond the length of individual projects. This in turn requires a greater degree of organisation and resources in regional downscaling for the ocean.

References

Ådlandsvik B (2008) Marine downscaling of a future climate scenario for the North Sea. Tellus A 60:451–458

Ådlandsvik B, Bentsen M (2007) Downscaling a twentieth century global climate simulation to the North Sea. Ocean Dyn. 57:453–466

Alheit J, Ådlandsvik B, Boersma M, Daewel U, Diekmann R, Flöter J, Hufnagl M, Johannessen T, Kong S-M, Mathis M, Möllmann C, Peck M, Pohlmann T, Temming A, Shchekinova E, Skogen M, Sundby S, Wagner C (2012) ERANET MarinERA: Verbundprojekt 189592 ECODRIVE. Förderkennzeichen: 03F603, Schlußbericht. Bundesministerium für Bildung und Forschung, Bonn

Allen MR, Ingram WSJ (2002) Constraints on future changes in climate and the hydrologic cycle. Nature 419:224

Almroth E, Skogen MD (2010) A North Sea and Baltic Sea Model Ensemble Eutrophication Assessment. AMBIO 39:59–69

Arguez A, O'Brien JJ, Smith SR (2009) Temperature impacts over Eastern North America and Europe associated with low-frequency North Atlantic SST variability. Int J Climatol 29:1–10

Arheimer B, Dahne J, Donnelly C (2012) Climate change impact on riverine nutrient load and land-based remedial measures of the Baltic Sea Action Plan. AMBIO 41:600–612

Artioli Y, Blackford JC, Butenschön M, Holt J, Wakelin SL, Thomas H, Borges AV, Allen JI (2012) The carbonate system in the North Sea: Sensitivity and model validation. J Mar Sys 102-104:1–13

Artioli Y, Blackford JC, Nondal G, Bellerby RGJ, Wakelin SL, Holt JT, Butenschön M, Allen JI (2013) Heterogeneity of impacts of high CO_2 on the North Western European Shelf. Biogeosci Discuss 10:9389–9413

Artioli Y, Blackford JC, Nondal G, Bellerby RGJ, Wakelin SL, Holt JT, Butenschön M (2014) Heterogeneity of impacts of high CO_2 on the North Western European Shelf. Biogeosciences 11:601–612

Backhaus J (1989) The North Sea and the climate. Dana 8:69–82

Bentsen M, Bethke I, Debernard JB, Iversen T, Kirkevåg A, Seland Ø, Drange H, Roelandt C, Seierstad IA, Hoose C, Kristjánsson JE (2012) The Norwegian Earth System Model, NorESM1-M – Part 1: Description and basic evaluation. Geosci Model Dev Discuss 5:2843–2931

Bindschadler RA, Nowicki S, Abe-Ouchi A, Aschwanden A, Choi H, Fastook J, Granzow G, Greve R, Gutowski G, Herzfeld U, Jackson C, Johnson J, Khroulev C, Levermann A, Lipscomb WH, Martin MA, Morlighem M, Parizek BR, Pollard D, Price SF, Ren D, Saito F, Sato T, Seddik H, Seroussi H, Takahashi K, Walker R, Wang WL (2013) Ice-sheet model sensitivities to environmental forcing and their use in projecting future sea level (the SeaRISE project). J Glaciol 59:195–224

Blackford JC, Allen JI, Gilbert FJ (2004) Ecosystem dynamics at six contrasting sites: A generic modelling study. J Mar Sys 52:191–215

Blauw AN, Los FJ, Bokhorst M, Erftemeijerm PLA (2008) GEM: a generic ecological model for estuaries and coastal waters. Hydrobiologia 618:175–198

Bopp L, Resplandy L, Orr JC, Doney SC, Dunne JP, Gehlen M, Halloran P, Heinze C, Ilyina T, Séférian R, Tjiputra J, Vichi M (2013) Multiple stressors of ocean ecosystems in the 21st century: projections with CMIP5 models. Biogeosciences 10:6225–6245

Bosello F, Nicholls RJ, Richards J, Roson R, Tol RSJ (2012) Economic impacts of climate change in Europe: sea-level rise. Clim Chan 112:63–81

Bouttes N, Gregory JM, Kuhlbrodt T, Suzuki T (2012) The effect of windstress change on future sea level change in the Southern Ocean. Geophys Res Lett 39: L23602, doi:10.1029/2012GL054207.

Bouttes N, Gregory JM, Lowe JA (2013) The reversibility of sea level rise. J Clim 26:2502–2513

Bülow K, Dieterich C, Heinrich H, Hüttl-Kabus S, Klein B, Mayer B, Meier HEM, Mikolajewicz U, Narayan N, Pohlmann T, Rosenhagen G, Sein D, Su J (2014) Comparison of 3 coupled models in the North Sea region under todays and future climate conditions. KLIWAS Schriftenreihe. www.bsh.de/de/Meeresdaten/Beobachtungen/Klima-Anpassungen/Schriftenreihe/27-2014.pdf

Christensen OB, Drews M, Christensen JH, Dethloff K, Ketelsen K, Hebestadt I, Rinke A, Weidman JP (2007) The HIRHAM Regional Climate Model: Version 5 (β). Tech Rep 06-17, Danish Meteorological Institute

Church JA, White NJ (2011) Sea-level rise from the late 19th to the early 21st century. Surv Geophys 32:585–602

Church JA, White NJ, Konikow LF, Domingues CM, Cogley G, Rignot E, Gregory JM, van den Broeke MR, Monaghan AJ, Velicogna I (2011) Revisiting the Earth's sea-level and energy budgets from 1961 to 2008. Geophys Res Lett 38, L18601, doi:10.1029/2011GL048794

Chust G, Allen I, Bopp L, Schrum C, Holt J, Tsiaras K, Zavatarelli M, Chifflet M, Cannaby H, Dadou I, Daewel U, Wakelin SL, Machu E, Pushpadas D, Butenschon M, Artioli Y, Petihakis G, Smith C, Garçon V, Goubanova K, Le Vu B, Fach BA, Salihoglu B, Clementi E, Irigoien X (2014) Biomass changes and trophic amplification of plankton in a warmer ocean. Glob Chan Biol 20:2124–2139

Cox PM, Pearson D, Booth BB, Friedlingstein P, Huntingford C, Jones CD, Luke CM (2013) Sensitivity of tropical carbon to climate change constrained by carbon dioxide variability. Nature 494:341–344

Daewel U, Schrum C (2013) Simulating long-term dynamics of the coupled North and Baltic Sea ecosystem with ECOSMO II: model description and validation. J Mar Sys 119–120:30–49

Daewel U, Peck MA, Alekseeva I, St. John MA, Kühn W, Schrum C (2008) Coupling ecosystem and individual-based models to simulate the influence of climate variability on potential growth and survival of larval fish in the North Sea. Fish Oceanogr 17-5:333–351

Dangendorf S, Rybski D, Mudersbach C, Müller A, Kaufmann E, Zorita E, Jensen J (2014) Evidence for long-term memory in sea level. Geophys Res Lett 41:5530–5537

de Winter RC, Sterl A, de Vries JW, Weber SL, Ruessink G (2012) The effect of climate change on extreme waves in front of the Dutch coast. Ocean Dyn 62:1139–1152

Debernard J, Røed L (2008) Future wind, wave and storm surge climate in the Northern Seas: a revisit. Tellus 60:427–438

Debernard J, Sætra Ø, Røed L (2002) Future wind, wave and storm surge climate in the Northern Seas. Clim Res 23:39–49

Dieterich C, Schimanke S, Wang S, Väli G, Liu Y, Hordoir R, Axell L, Höglund A, Meier HEM (2013) Evaluation of the SMHI coupled atmosphere-ice-ocean model RCA4-NEMO. SMHI Rep Oceanogr 47

Dippner JW, Ottersen G (2001) Cod and climate variability in the Barents Sea. Clim Res 17:73–82

Donnelly C, Yang W, Dahné J (2014) River discharge to the Baltic Sea in a future climate. Clim Chan 122:157–170

Döscher R, Willén U, Jones C, Rutgersson A, Meier HEM, Hansson U, Graham LP (2002) The development of the regional coupled ocean-atmosphere model RCAO. Boreal Env Res 7:183–192

Drinkwater K, Skogen M, Hjøllo S, Schrum C, Alekseeva I, Huret M, Léger F (2008) The effects of a future climate on the physical oceanography and comparisons of the mean and variability of the physical properties with present day conditions. RECLAIM deliverable 4.1.

Drinkwater K, Skogen M, Hjøllo S, Schrum C, Alekseeva I, Huret M, Woillez M (2009) Report on the effects of future climate change on primary and secondary production as well as ecosystem structure in lower trophic to mid- trophic levels. RECLAIM deliverable 4.2.

Eilola K, Gustafsson BG, Kuznetsov I, Meier HEM, Neumann T, Savchuk OP (2011) Evaluation of biogeochemical cycles in an ensemble of three state-of-the-art numerical models of the Baltic Sea. J Mar Syst 88:267–284

Eilola K, Hansen J, Meier HEM, Molchanov MS, Ryabchenko, Skogen, MD (2013) Eutrophication Status Report of the North Sea, Skagerrak, Kattegat and the Baltic Sea: A model study. Present and future climate. Tech Rep Oceanogr XX/2013, SMHI

Enderlin EM, Howat IM, Jeong S, Noh MJ, van Angelen JH, van den Broeke MR (2014) An improved mass budget for the Greenland ice sheet. Geophys Res Lett 41:866–872

Favier L, Durand G, Cornford SL, Gudmundsson GH, Gagliardini O, Gillet-Chaulet F, Zwinger T, Payne AJ, Le Brocq AM (2014) Retreat of Pine Island Glacier controlled by marine ice-sheet instability. Nat Clim Chan 4:117–121

Fennel W (2009) Parameterizations of truncated food web models from the perspective of an end-to-end model approach. J Mar Sys 76:171–185

Flather RA, Smith JA (1998) First estimates of changes in extreme storm surge elevations due to the doubling of CO_2. Glob Atmos Ocean Sys 6:193–208

Follows MJ, Dutkiewicz S, Grant S, Chisholm SW (2007) Emergent biogeography of microbial communities in a model ocean. Science 315:1843–1846

Friocourt YF, Skogen M, Stolte W, Albretsen J (2012) Marine downscaling of a future climate scenario in the North Sea and possible effects on dinoflagellate harmful algal blooms. Food Addit Contam A 29:1630–1646

Furevik T, Bentsen M, Drange H, Kindem IKT, Kvamstø NG, Sorteberg A (2003) Description and validation of the Bergen Climate Model: ARPEGE coupled with MICOM. Clim Dyn 21:27–51

Gaslikova L, Grabemann I, Groll N (2013) Changes in North Sea storm surge conditions for four transient future climate realizations. Nat Hazards 66:1501–1518

Gattuso JP, Bijma J, Gehlen M, Riebesell U, Turley C (2011) Ocean acidification: knowns, unknowns and perspectives. In: Gattuso JP, Hansson L (eds) Ocean Acidification. Oxford University Press

Gehlen M, Gruber N, Gangstø R, Bopp L, Oschlies A (2011) Biogeochemical consequences of ocean acidification and feedbacks to the earth system. In: Gattuso JP, Hansson L (eds) Ocean Acidification. Oxford University Press

Giesen RH, Oerlemans J (2013) Climate-model induced differences in the 21st century global and regional glacier contributions to sea-level rise. Clim Dyn 41:3283–3300

Gordon C, Cooper C, Senior CA, Banks H, Gregory JM, Johns TC, Mitchell JFB, Wood RA (2000) The simulation of SST, sea ice extents and ocean heat transports in a version of the Hadley Centre coupled model without flux adjustments. Clim Dyn 16:147–168

Grabemann I, Weisse R (2008) Climate change impact on extreme wave conditions in the North Sea: an ensemble study. Ocean Dyn 58:199–212

Grabemann I, Groll N, Möller J, Weisse R (2015) Climate change impact on North Sea wave conditions: a consistent analysis of ten projections. Ocean Dyn 65:255–267

Graversen RG, Drijfhout S, Hazeleger W, van de Wal R, Bintanja R, Helsen M (2011) Greenland's contribution to global sea-level rise by the end of the 21st century. Clim Dyn 37:1427–1442

Gräwe U, Burchard H (2012) Storm surges in the Western Baltic Sea, the present and a possible future. Clim Dyn 39:165–183

Gräwe U, Burchard H, Müller M, Schuttelaars HM (2014) Seasonal variability of M_2 and M_4 tidal constituents and its implications for the coastal residual sediment transport. Geophys Res Lett 41: 5563–5570

Gregory JM, Church JA, Boer GJ, Dixon KW, Flato GM, Jackett DR, Lowe JA, O'Farrell SP, Roeckner E, Russell GL, Stouffe, RJ, Winton M (2001) Comparison of results from several AOGCMs for global and regional sea-level change 1900-2100. Clim Dyn 18: 225–240

Gröger M, Maier-Reimer E, Mikolajewicz U, Moll A, Sein D (2013) NW European shelf under climate warming: implications for open ocean – shelf exchange, primary production, and carbon absorption. Biogeosciences 10:3767–3792

Groll N, Grabemann I, Gaslikova L (2014) North Sea wave conditions: an analysis of four transient future climate realizations. Ocean Dyn 64:1–12

Grossmann I, Klotzbach PJ (2009) A review of North Atlantic modes of natural *variability* and their driving mechanisms. J Geophys Res, Atmos 114: D24107, doi:10.1029/2009JD012728

Haigh I, Nicholls R, Wells N (2010) Assessing changes in extreme sea levels: Application to the English Channel, 1900-2006. Cont Shelf Res 30:1042–1055

Haigh ID, Wahl T, Rohling EJ, Price RM, Pattiaratchi CB, Calafat FM, Dangendorf S (2014) Timescales for detecting a significant acceleration in sea level rise. Nat Commun 5:3635. doi:10.1038/ncomms4635

Hasselmann S, Hasselmann K, Bauer E, Janssen PAEM, Komen GJ, Bertotti L, Lionello P, Guillaume A, Cardone VC, Greenwood JA, Reistad M, Zambresky L, Ewing JA (1988) The WAM model - A third generation ocean wave prediction model. J Phys Oceanog 18:1775–1810

Hawkins E, Sutton R (2009) The potential to narrow uncertainties in regional Climate predictions. Bull Am Met Soc 90:1095–1107

Hinkel J, van Vuuren DP, Nicholls RJ, Klein RJT (2013) The effects of adaptation and mitigation on coastal flood impacts during the 21st century. An application of the DIVA and IMAGE models. Clim Chan 117:783–794

Holt JT, James ID (2001) An s-coordinate density evolving model of the North West European Continental Shelf. Part 1 Model description and density structure. J Geophys Res 106:14015–14034

Holt J, Wakelin S, Lowe J, Tinker J (2010) The potential impacts of climate change on the hydrography of the northwest European Continental shelf. Prog Oceanogr 86:361–379

Holt J, Butenschon M, Wakelin SL, Artioli Y, Allen JI (2012) Oceanic controls on the primary production of the northwest European continental shelf: model experiments under recent past conditions and a potential future scenario. Biogeosciences 9:97–117

Holt J, Schrum C, Cannaby H, Daewel U, Allen I, Artioli Y, Bopp L, Butenschon M, Fach B, Harle J, Pushpadas D, Salihoglu B, Wakelin S (2016) Potential impacts of climate change on the primary production of regional seas: a comparative analysis of five European seas. Prog Oceanogr 140:91–115

Horsburgh KJ, Wilson C (2007) Tide-surge interaction and its role in the distribution of surge residuals in the North Sea. J Geophys Res, Oceans:112:C08003, doi:10.1029/2006JC004033

Howard T, Lowe J, Horsburgh K (2010) Interpreting century-scale changes in southern North Sea storm surge climate derived from coupled model simulations. J Clim 23:6234–6247

Howard T, Pardaens AK, Lowe JA, Ridley J, Hurkmans R, Bamber J, Spada G, Vaughan D (2014) Sources of 21st century regional sea level rise along the coast of North-West Europe. Ocean Sci Discuss 10:2433–2459

Hunter JR, Church JA, White NJ, Zhang X (2013) Towards a global regionally varying allowance for sea-level rise. Ocean Engin 71: 17–27

Huybrechts P, Goelzer H, Janssens I, Driesschaert E, Fichefet T, Goosse H, Loutre MF (2011) Response of the Greenland and Antarctic ice sheets to multi-millennial greenhouse warming in the Earth System Model of Intermediate Complexity LOVECLIM. Surv Geophys 32:397–416

IPCC (2007) Contribution of Working Group I to the Fourth Assessment Report of the Intergovernmental Panel on Climate Change, 2007. Solomon S, Qin D, Manning M, Chen Z, Marquis M, Averyt KB, Tignor M, Miller HL (eds) Cambridge University Press

IPCC (2013) Climate Change 2013: The Physical Science Basis. Contribution of Working Group I to the Fifth Assessment Report of the Intergovernmental Panel on Climate Change. Stocker TF, Qin D, Plattner GK, Tignor M, Allen SK, Boschung J, Nauels A, Xia Y, Bex V, Midgley PM (eds). Cambridge University Press

Jacob D, Podzun R (1997) Sensitivity studies with the regional climate model REMO. Meteorol Atmos Phys 63:119–129

Janssen F, Schrum C, Backhaus JO (1999) A climatological data set of temperature and salinity for the Baltic Sea and the North Sea. Dt Hydrogr Z 51:5–245

Jevrejeva S, Moore JC, Grinsted A (2012) Sea level projections to AD2500 with a new generation of climate change scenarios. Glob Planet Chan 80-81:14–20

Jones R, Murphy J, Hassell D, Taylor R (2001) Ensemble mean changes in a simulation of the European climate of 2071-2100 using the new Hadley Centre regional modelling system: HadAM3H/HadRM3H. Hadley Centre, Met Office, UK. http://prudence.dmi.dk/public/publications/hadley_200208.pdf

Katsman C, Hazeleger W, Drijfhout S, Oldenborgh G, Burgers G (2008) Climate scenarios of sea level rise for the northeast Atlantic Ocean: a study including the effects of ocean dynamics and gravity changes induced by ice melt. Clim Chan 91:351–374

Katsman CA, Sterl A, Beersma JJ, van den Brink HW, Church JA, Hazeleger W, Kopp RE, Kroon D, Kwadijk J, Lammersen R, Lowe J, Oppenheimer M, Plag H-P, Ridley J, von Storch H, Vaughan DG, Vellinga P, Vermeersen LLA, van de Wal RSW, Weisse R (2011) Exploring high-end scenarios for local sea level rise to develop flood protection strategies for a low-lying delta-the Netherlands as an example. Clim Chan 109:617–645

Kauker F (1999) Regionalization of Climate Model Results for the North Sea. PhD thesis. University of Hamburg

Kauker F, Langenberg H (2000) Two models for the climate change related development of sea levels in the North Sea - a comparison. Clim Res 15:61–67

Kauker F, von Storch H (2000) Statistics of "Synoptic Circulation Weather" in the North Sea as derived from a multiannual OGCM simulation. J Phys Oceanogr 30:3039–3049

Khan SA, Kjaer KH, Bevis M, Bamber JL, Wahr J, Kjeldsen KK, Bjork AA, Korsgaard NJ, Stearns LA, van den Broeke MR, Liu L, Larsen NK, Muresan IS (2014) Sustained mass loss of the northeast

Greenland ice sheet triggered by regional warming. Nat Clim Chan 4:292–299
Kharin V, Zwiers FW, Zhang X, Hegerl GC (2007) Changes in temperature and precipitation extremes in the IPCC ensemble of global coupled model simulations. J Clim 20:1419–1444
KNMI (2014a) Climate Change scenarios for the 21st Century: A Netherlands perspective. Scientific Report WR2014-01, KNMI, DeBilt, The Netherlands
KNMI (2014b) KNMI'14 climate scenarios for the Netherlands: A guide for professionals in climate adaptation. KNMI, De Bilt, The Netherlands
Knutti R, Sedláček J (2012) Robustness and uncertainties in the new CMIP5 climate model projections. Nature Clim change 3:369–373
Koerper J, Höschel I, Lowe JA, Hewitt CD, Salas y Melia D, Roeckner E, Huebener H, Royer J-F, Dufresne J-F, Pardaens A, Giorgetta MA, Sanderson MG, Otterå OH, Tjiputra J, Denvil S (2013) The effects of aggressive mitigation on steric sea level rise and sea ice changes. Clim Dyn 40:531–550
Landerer FW, Jungclaus JH, Marotzke J (2007) Regional dynamic and steric sea level change in response to the IPCC-A1B scenario. J Phys Oceanogr 37:296–312
Langenberg H, Pfizenmayer A, von Storch H, Sundermann J (1999) Storm-related sea level variations along the North Sea coast: natural variability and anthropogenic change. Cont Shelf Res 19:821–842
Lesser GR, Roelvink JA, van Kester JATM, Stelling GS (2004) Development and validation of a three-dimensional morphological model. Coast Eng 51:883–915
Levermann A, Clark PU, Marzeion B, Milne GA, Pollard D, Radic V, Robinson A (2013) The multimillennial sea-level commitment of global warming. Proc Nat Acad Sci USA 110:13745–13750
Lindström G, Pers C, Rosberg J, Strömqvist J, Arheimer B (2010) Development and test of the HYPE (Hydrological Predictions for the Environment) model – A water quality model for different spatial scales. Hydrol Res 41:295–319
Lowe JA, Gregory JM (2005) The effects of climate change on storm surges around the United Kingdom. Phil Trans Roy Soc A 363:1313–1328
Lowe JA, Gregory JM (2006) Understanding projections of sea level rise in a Hadley Centre coupled climate model. J Geophys Res, Oceans 111:C11014, doi:10.1029/2005JC003421
Lowe JA, Greogry JM (2010) A sea of uncertainty. Nature Reports Clim Change doi:10.1038/climate.2010.30
Lowe JA, Gregory JM, Flather RA (2001) Changes in the occurrence of storm surges around the United Kingdom under a future climate scenario using a dynamic storm surge model driven by the Hadley Centre climate models. Clim Dyn 18:179–188
Lowe JA, Gregory JM, Ridley J, Huybrechts P, Nicholls RJ, Collins M (2006) The role of sea-level rise and the Greenland ice sheet in dangerous climate change: implications for the stabilisation of climate. In: Schellnhuber J, Cramer W, Nakicenovic N, Wigley T, Yohe G (eds) Avoiding Dangerous Climate Change. Cambridge University Press
Lowe JA, Howard TP, Pardaens A, Tinker J, Holt J, Wakelin S, Milne G, Leake J, Wolf J, Horsburgh K, Reeder T, Jenkins G, Ridley J, Dye S, Bradley S (2009) UK Climate Projections science report: Marine and coastal projections. Hadley Centre, Met Office, UK
Lowe JA, Woodworth PL, Knutson T, McDonald RE, McInnes KL, Woth K, von Storch H, Wolf J, Swail V, Bernier NB, Gulev S, Horsburgh KJ, Unnikrishnan AS, Hunter JR, Weisse R (2010) Past and Future Changes in Extreme Sea Levels and Waves, in Understanding Sea-Level Rise and Variability. Wiley-Blackwell
Madsen KS (2009) Recent and future climatic changes in temperature, salinity, and sea level of the North Sea and the Baltic Sea. PhD thesis, Niels Bohr Institute, University of Copenhagen
Maier-Reimer E, Mikolajewicz U, Hasselmann K (1993) Mean circulation of the Hamburg LSG OGCM and its sensitivity to the thermohaline surface forcing. J Phys Oceanogr 23:731–757
Maier-Reimer E, Kriest I, Segschneider J, Wetzel P (2005) The Hamburg oceanic carbon cycle circulation model HAMOCC5.1—Technical Description Release 1.1, Tech Rep 14, Reports on Earth System Science, Max Planck Institute for Meteorology, Hamburg
Marsland SJ, Haak H, Jungclaus JH, Latif M, Roeske F (2003) The Max-Planck-Institute global ocean/sea ice model with orthogonal curvilinear coordinates. Ocean Model 5:91–127
Marti O, Braconnot P, Dufresne J-L, Bellier J, Benshila R, Bony S, Brockmann P, Cadule P, Caubel A, Codron F, de Noblet N, Denvil S, Fairhead L, Fichefet T, Foujols M-A, Friedlingstein P, Goosse H, Grandpeix J-Y, Guilyardi E, Hourdin F, Idelkadi A, Kageyama M, Krinner G, Lévy C, Madec G, Mignot J, Musat I, Swingedouw D, Talandier C (2010) Key features of the IPSL ocean atmosphere model and its sensitivity to atmospheric resolution. Clim Dyn 34:1–26
Marzeion B, Jarosch AH, Hofer M (2012) Past and future sea-level change from the surface mass balance of glaciers. Cryosphere 6:1295–1322
Mathis M (2013) Projected Forecast of Hydrodynamic Conditions in the North Sea for the 21st Century. Dissertation, University of Hamburg
Mathis M, Pohlmann T (2014) Projection of physical conditions in the North Sea for the 21st century. Clim Res 61:1–17
Mathis M, Mayer B, Pohlmann T (2013) An uncoupled dynamical downscaling for the North Sea: Method and evaluation. Ocean Model 72:153–166
Melsom A, Lien VS, Budgell WP (2009) Using the Regional Ocean Modeling System (ROMS) to improve the ocean circulation from a GCM 20th century simulation. Ocean Dyn 59:969–981
Menendez M, Woodworth PL (2010) Changes in extreme high water levels based on a quasi-global tide-gauge data set. J Geophys Res, Oceans 115:C10011, doi:10.1029/2009JC005997
Miles BWJ, Stokes CR, Vieli A, Cox NJ (2013) Rapid, climate-driven changes in outlet glaciers on the Pacific coast of East Antarctica. Nature 500:563–566
Millero FJ (1995) Thermodynamics of the carbon dioxide system in the oceans. Geochmic Cosmochim Ac 59:661–677
Milne GA, Mitrovica, JX (1998) Postglacial sea-level change on a rotating Earth. Geophys J Int 133:1-19
Mitrovica JX, Milne GA, Davis JL (2001) Glacial isostatic adjustment on a rotating earth. Geophys J Int 147:562-578
Moore JC, Grinsted A, Zwinger T, Jevrejeva S (2013) Semi-empirical and process-based global sea level projections. Rev Geophys 51:484–522
Müller M, Cherniawsky JY, Foreman MGG, von Storch JS (2014) Seasonal variation of the M_2 tide. Ocean Dyn 64:159–177
Murphy JM, Sexton DMH, Barnett DN, Jones GS, Webb MJ, Collins M, Stainforth DA (2004) Quantification of modelling uncertainties in a large ensemble of climate change simulations. Nature 430:768–772
Murphy JM, Sexton DMH, Jenkins GJ, Boorman PM, Booth BBB, Brown CC, Clark RT, Collins M, Harris GR, Kendon EJ, Betts RA, Brown SJ, Howard TP, Humphrey KA, McCarthy MP, McDonald RE, Stephens A, Wallace C, Warren R, Wilby R, Wood RA (2009) UK Climate Projections Science Report: Climate change projections. Hadley Centre, Met Office, UK
Nicholls RJ, Lowe JA (2004) Benefits of mitigation of climate change for coastal areas. Glob Environ Change 14:229–244
Nicholls RJ, Marinova N, Lowe JA, Brown S, Vellinga P, de Gusmão D, Hinkel J, Tol RSJ (2011) Sea-level rise and its possible impacts given a 'beyond 4 degrees C world' in the twenty-first century. Phil Trans Roy Soc A 369:161–181

Nick FM, Vieli A, Andersen ML, Joughin I, Payne A, Edwards TL, Pattyn F, van de Wal RSW (2013) Future sea-level rise from Greenland's main outlet glaciers in a warming climate. Nature 497:235–238

Oberhuber J (1993) Simulating of the Atlantic circulation with a coupled sea ice-mixed layer-isopycnical General Circulation Model. Part 1: Model Description. J Phys Oceanogr 23:808–829

OSPAR (2005) Common Procedure for the Identification of the Eutrophication Status of the OSPAR Maritime Area. OSPAR, Ref 2005-3. OSPAR Commission, London

Pätsch J, Kühn W (2008) Nitrogen and carbon cycling in the North Sea and exchange with the North Atlantic – a model study. Part I. Cont Shelf Res 28:767–787

Pardaens AK, Gregory JM, Lowe JA (2011a) A model study of factors influencing projected changes in regional sea level over the twenty-first century. Clim Dyn 36:2015–2033

Pardaens AK, Lowe JA, Brown S, Nicholls RJ, de Gusmao D (2011b) Sea-level rise and impacts projections under a future scenario with large greenhouse gas emission reductions. Geophys Res Lett 38: L12604, doi:10.1029/2011GL047678

Pelling HE, Green JAM, Ward SL (2013) Modelling tides and sea-level rise: To flood or not to flood. Ocean Modell 63:21–29

Perrette M, Landerer F, Riva R, Frieler K, Meinshausen M (2013) A scaling approach to project regional sea level rise and its uncertainties. Earth Sys Dyn 4:11–29

Pfeffer WT, Harper JT, O'Neel S (2008) Kinematic constraints on glacier contributions to 21st-century sea-level rise. Science 321:1340–1343

Pickering MD, Wells NC, Horsburgh KJ, Green JAM (2012) The impact of future sea-level rise on the European Shelf tides. Cont Shelf Res 35:1–15

Pohlmann T (1996) Calculating the annual cycle of the vertical eddy viscosity in the North Sea with a three-dimensional baroclinic shelf sea circulation model. Cont Shelf Res 16:147–161

Pope VD, Gallani ML, Rowntree PR, Stratton RA (2000) The impact of new physical parameterizations in the Hadley Centre climate model – HadAM3. Clim Dyn 16:123–146

Pushpadas D, Schrum C, Daewel U (2015) Projected climate change effects on North Sea and Baltic Sea: CMIP3 and CMIP5 model-based scenarios. Biogeosciences Discuss 12:12229–12279

Radić V, Bliss A, Beedlow AC, Hock R, Miles E, Cogley JG (2014) Regional and global projections of twenty-first century glacier mass changes in response to climate scenarios from global climate models. Clim Dyn 42:37–58

Rae JGL, Aðalgeirsdóttir G, Edwards TL, Fettweis X, Gregory JM, Hewitt HT, Lowe JA, Lucas-Picher P, Mottram RH, Payne AJ, Ridley JK, Shannon SR, van de Berg WJ, van de Wal RSW, van den Broeke MR (2012) Greenland ice sheet surface mass balance: evaluating simulations and making projections with regional climate models. Cryosphere 6:1275–1294

Rahmstorf S (2007) A semi-empirical approach to projecting future sea-level rise. Science 315:368–370

Rahmstorf S (2010) A new view on sea-level rise. Nature Rep Clim Change doi:10.1038/climate.2010.29

Ranger N, Reeder T, Lowe JA (2013) Addressing 'deep' uncertainty over long-term climate in major infrastructure projects: four innovations of the Thames Estuary 2100 Project. EURO J Decis Process 1:3–4

Raper SCB, Gregory JM, Osborn TJ (2001) Use of an upwelling-diffusion energy balance climate model to simulate and diagnose A/OGCM results. Clim Dyn 17:601–613

Regnier P, Friedlingstein P, Ciais P, Mackenzie FT, Gruber N, Janssens IA, Laruelle GG, Lauerwald R, Luyssaert S, Andersson AJ, Arndt S, Arnosti C, Borges AV, Dale AW, Gallego-Sala A, Goddéris Y, Goossens N, Hartmann J, Heinze C, Ilyina T, Joos F, LaRowe DE, Leifeld J, Meysman FJR, Munhoven G, Raymond PA, Spahni R, Suntharalingam P, Thullner M (2013) Anthropogenic perturbation of the carbon fluxes from land to ocean. Nat Geosci 6:597–607

Rider KM, Konen GJ, Beersma J (1996) Simulation of the response of the ocean waves in the North Atlantic and North Sea to CO_2 doubling in the atmosphere. KNMI Scientific Rep WR 96-05

Ridley J, Gregory JM, Huybrechts P, Lowe JA (2010) Thresholds for irreversible decline of the Greenland ice sheet. Clim Dyn 35: 1065–1073

Riebesell U, Tortell PD (2011) Effects of ocean acidification on pelagic organisms and ecosystems. In: Gattuso JP, Hansson L (eds) Ocean Acidification. Oxford University Press

Riebesell U, Schulz KG, Bellerby R, Botros M, Fritsche P, Meyerhofer M, Neill C, Nondal G, Oschlies A, Wohlers J, Zollner E (2007) Enhanced biological carbon consumption in a high CO_2 ocean. Nature 450:545–548

Roeckner E, Arpe K, Bengtsson L, Brinkop S, Dümenil L, Esch M, Kirk E, Lunkeit F, Ponater M, Rockel B, Sausen R, Schlese U, Schubert S, Windelband M (1992) Simulation of the present-day climate with the ECHAM model: impact of model physics and resolution. Max-Planck-Institut für Meteorologie, Hamburg. Rep 93

Roeckner E, Bauml G, Bonaventura L, Brokopf R, Esch M, Giorgetta M, Hagemann S, Kirchner I, Kornblueh L, Manzini E, Schlese U, Schulzweida U (2003) The atmospheric general circulation model ECHAM5: Part 1: Model description. Max-Planck-Institut für Meteorologie, Hamburg. Rep 349

Roeckner E, Brokopf R, Esch M, Giorgetta M, Hagemann S, Kornblueh L, Manzini E, Schlese U, Schulzweida U (2006) Sensitivity of simulated climate to horizontal and vertical resolution in the ECHAM5 atmosphere model. J Clim 19:3771–3791

Rohling EJ, Grant K, Hemleben C, Siddall M, Hoogakker BAA, Bolshaw M, Kucera M (2008) High rates of sea-level rise during the last interglacial period. Nat Geosci 1:38–42

Scaife AA, Woollings T, Knight J, Martin G, Hinton T (2010) Atmospheric blocking and mean biases in climate models. J Clim 23:6143–6152

Schaeffer M, Hare W, Rahmstorf S, Vermeer M (2012) Long-term sea-level rise implied by 1.5 degrees C and 2 degrees C warming levels. Nature Clim Chan 2:867–870

Schmidt GA, Ruedy R, Hansen JE, Aleinov I, Bell N, Bauer M, Bauer S, Cairns B, Canuto V, Cheng Y, Del Genio A, Faluvegi D, Friend AD, Hall TM, Hu Y, Kelley M, Kiang NY, Koch D, Lacis AA, Lerner J, Lo KK, Miller RL, Nazarenko L, Oinas V, Perlwitz Ja, Perlwitz Ju, Rind D, Romanou A, Russell GL, Sato M, Shindell DT, Stone PH, Sun S, Tausnev N, Thresher D, Yao M-S (2006) Present day atmospheric simulations using GISS ModelE: Comparison to in-situ, satellite and reanalysis data. J Clim 19: 153–192

Schrum C (2001) Regionalization of climate change for the North Sea and the Baltic Sea. Clim Res 18:31–37

Schrum C, Backhaus JO (1999) Sensitivity of atmosphere-ocean heat exchange and heat content in North Sea and Baltic Sea. A comparative assessment. Tellus 51A:526–549

Schrum C, Hübner U, Jacob D, Podzun R (2003a) A coupled atmosphere/ice/ocean model for the North Sea and the Baltic Sea. Clim Dyn 21:131–151

Schrum C, Siegismund F, St. John M (2003b) Decadal variations in the stratification and circulation patterns of the North Sea. Are the 90's unusual? ICES Symposium of Hydrobiological Variability in the ICES area 1990-1999. ICES J Mar Sci 219:121–131

Schrum C, Alekseeva I, St. John M (2006) Development of a coupled physical–biological ecosystem model ECOSMO Part I: Model description and validation for the North Sea. J Mar Sys 61: 79-99

Sein DV, Mikolajewicz U, Gröger M, Fast I, Cabos W, Pinto JG, Hagemann S, Semmler T, Izquierdo A, Jacob D (2015) Regionally coupled atmosphere ocean sea ice, marine biogeochemistry model ROM: 1. Description and validation. JAMES 7:268–304

Shchepetkin AF, McWilliams JC (2005) The Regional Ocean Modeling System (ROMS): A split-explicit, free-surface, topography-following coordinates ocean model. Ocean Mod 9:347–404

Shennan I, Horton BP (2002) Holocene land- and sea-level changes in Great Britain. J Quat Sci 17:511–526

Shennan I, Milne G, Bradley S (2009) Late Holocene relative land- and sea-level changes: Providing information for stakeholders. GSA Today 19:doi:10.1130/GSATG50GW.1

Simpson MJR, Breili K, Kierulf HP (2014) Estimates of twenty-first century sea-level changes for Norway. Clim Dyn 42:5–6

Skogen MD, Søiland H (1998) A User's Guide to NORWECOM v2.0, a coupled 3-dimensional physical chemical biological ocean model. Tech. Rept. Fisken og Havet 18/98. Institute of Marine Research, Norway. www.imr.no/~morten/norwecom/userguide2_0.ps.gz

Skogen M, Svendsen D, Berntsen E, Aksnes JD, Ulvestad KB (1995) Modelling the primary production in the North Sea using a coupled three-dimensional physical-chemical-biological ocean model. Estuar Coast Shelf Sci 41:545–5658

Skogen MD, Drinkwater K, Hjøllo S, Schrum C (2011) North Sea sensitivity to atmospheric forcing. J Mar Sys 85:106–114

Skogen MD, Eilola K, Hansen JLS, Meier HEM, Molchanov MS, Ryabchenko VA (2014) Eutrophication Status of the North Sea, Skagerrak, Kattegat and the Baltic Sea in present and future climates: A model study. J Mar Sys 132:174–184

Slangen ABA, Carson M, Katsman C, van de Wal RSW, Köhl A, Vermeersen LLA, Stammer D (2014) Projecting twenty-first century regional sea-level changes. Clim Chan 124:317–332

Steinacher M, Joos F, Fröhlicher T, Bopp L, Cadule P, Cocco V, Doney S, Gehlen M, Lindsay K, Moore JK, Schneider B, Segschneider J (2010) Projected 21st century decrease in marine productivity: a multi-model analysis. Biogeosciences 7:979–1005

Sterl A, van den Brink H, de Vries H, Haarsma R, van Meijgaard E (2009) An ensemble study of extreme storm surge related water levels in the North Sea in a changing climate. Ocean Sci 5:369–378

Stott PA, Kettleborough JA (2002) Origins and estimates of uncertainty in predictions of twenty-first century temperature rise. Nature 416:723–726

STOWASUS-Group (2001) Synthesis of the STOWASUS-2100 project: regional storm, wave and surge scenarios for the 2100 century. www.pd.infn.it/AOD/immagini_projects/Stowasus_final.pdf

Su J, Yang H, Pohlmann T, Ganske A, Klein B, Klein H, Narayan N (2014) A regional coupled atmosphere-ocean model system REMO/HAMSOM for the North Sea. KLIWAS Schriftenreihe, KLIWAS-60/2014

Van Meijgaard E, van Ulft LH, van de Berg WJ, Bosveld FG, van den Hurk BJJM, Lenderink G, Siebesma AP (2008) The KNMI regional atmospheric climate model RACMO version 2.1. Tech. Rep TR-302.

Vizcaíno M, Mikolajewicz U, Jungclaus J, Schurgers G (2010) Climate modification by future ice sheet changes and consequences for ice sheet mass balance. Clim Dyn 34:301–324

von Storch H (1995) Inconsistencies at the interface of climate impact studies and global climate research. Meteor Z 4:72–80

Wahl T, Haigh ID, Woodworth PL, Albrecht F, Dillingh D, Jensen J, Nicholls RJ, Weisse R, Wöppelmann G (2013) Observed mean sea level changes around the North Sea coastline from 1800 to present. Earth-Sci Rev 124:51–67

Wakelin S, Daewel U, Schrum C, Holt J, Butenschön M, Artioli Y, Beecham J, Lynam C, Mackinson S (2012a) MEECE deliverable D3.4: Synthesis report for Climate Simulations Part 3: NE Atlantic / North Sea, www.meece.eu/documents/deliverables/WP3/D3%204_Part3_NE%20Atlantic.pdf

Wakelin SL, Holt J, Blackford JC, Allen JI, Butenschön M, Artioli Y (2012b) Modeling the carbon fluxes of the northwest European continental shelf: Validation and budgets. J Geophys Res 117, C05020 doi:10.1029/2011JC007402

Wang S, Dieterich C, Döscher R, Höglund A, Hordoir R, Meier HEM, Samuelsson P, Schimanke S (2015) Development and evaluation of a new regional coupled atmosphere-ocean model in the North Sea and the Baltic Sea. Tellus A 67:24284, http://dx.doi.org/10.3402/tellusa.v67.24284

WASA-Group (1998) Changing waves and storms in the Northeast Atlantic? Bull Am Met Soc 79:741–760

Weidemann H (2009) Statistisch regionalisierte Sturmflutszenarien für Cuxhaven. Thesis. Christian-Albrechts-Universität Kiel

Wentz FJ, Riccaiardulli L, Hilburn K, Mears C (2007) How much more rain will global warning bring? Science 317:233–235

Wigley TML (2005) The climate change commitment. Science 307:1766–1769

Wolf J, Woolf DK (2006) Waves and climate change in the north-east Atlantic. Geophys Res Lett 33 doi:10.1029/2005GL025113

Woodworth PL, Flather RA, Williams JA, Wakelin SL, Jevrejeva S (2007) The dependence of UK extreme sea levels and storm surges on the North Atlantic Oscillation. Cont Shelf Res 27:935–946

Woth K (2005) North Sea storm surge statistics based on projections in a warmer climate: How important are the driving GCM and the chosen emission scenario? Geophys Res Lett 32:122708 doi:10.1029/2005GL023762

Woth K, Weisse R, von Storch H (2006) Climate change and North Sea storm surge extremes: an ensemble study of storm surge extremes expected in a changed climate projected by four different regional climate models. Ocean Dyn 56:3–15

Yin JJ (2012) Century to multi-century sea level rise projections from CMIP5 models. Geophys Res Lett 39: L17709, doi:10.1029/2012GL052947

Yoshimori M, Abe-Ouchi A (2012) Sources of spread in multimodel projections of the Greenland Ice Sheet surface mass balance. J Clim 25:1157–1175

Zavatarelli M, Akoglu E, Artioli Y, Beecham J, Butenschon M, Cannaby H, Chifflet M, Chust G, Clementi E, Daewel U, Fach B, Holt J, Machu E, Petihaks G, Salihoglu B, Schrum C, Shin Y, Smith C, Travers M, Tsiaras K, Wakelin S, Allen JI (2013a) D4.1. Hindcast simulations of isolated direct anthropogenic drivers. MEECE deliverable, www.meece.eu/Deliv.html

Zavatarelli M, Artioli Y, Beecham J, Butenschon M, Chifflet M, Christensen A, Chust G, Daewel U, Holt J, Neuenfeldt S, Schrum C, Skogen M, Wakelin S, Allen JI (2013b) D4.3. Synthesis report on the comparison of WP3 and WP4 simulations: Part 2a Multiple Driver Scenarios, NE Atlantic, North Sea, Baltic Sea and Biscay. MEECE deliverable, www.meece.eu/Deliv.html

Zhang YJ, Stanev E, Grashorn S (2015) Unstructured-grid model for the North Sea and Baltic Sea: Validation against observations. Ocean Model 97:91–108

Projected Change—River Flow and Urban Drainage

7

Patrick Willems and Benjamin Lloyd-Hughes

Abstract

Hydrological extremes, largely driven by precipitation, are projected to become more intense within the North Sea region. Quantifying future changes in hydrology is difficult, mainly due to the high uncertainties in future greenhouse gas emissions and climate model output. Nevertheless, models suggest that peak river flow in many rivers may be up to 30 % higher by 2100, and in some rivers even higher. The greatest increases are projected for the northern basins. Earlier spring floods are projected for snow-dominated catchments but this does not always cause an increase in peak flows; peak flows may decrease if higher spring temperatures lead to reduced snow storage. An increase in rain-fed flow in winter and autumn may change the seasonality of peak flows and floods. The proximity of a river basin to the ocean is also important; the closer the two the greater the potential damping of any climate change effect. In urban catchments, the specific characteristics of the drainage system will dictate whether the net result of the climate change effect, for example the projected increase in short-duration rainfall extremes, is to damp or amplify the impact of this change in precipitation. The response in terms of sewer flood and overflow frequencies and volumes is highly non-linear. The combined impact of climate change and increased urbanisation in some parts of the North Sea region could result in as much as a four-fold increase in sewer overflow volumes.

7.1 Introduction

The hydrological cycle is an intrinsic part of the climate system. Changes within the climate directly and indirectly influence the components of the hydrological cycle. As an illustration, climate change may alter river regimes directly through changes in rainfall, and indirectly through changes in temperature, which may change evaporation and affect snow melt. Differences in rainfall intensity may alter flood hazards through changes in peak discharge and erosion. Additionally, temperature changes, especially during summer, affect the soil water content and groundwater recharge, and thus water input (from ground water and base flow) to rivers. As a result, the risk of low flow alters, which can also impact on water quality, navigation and water availability for agricultural and industrial purposes. In short, climate change affects or controls inputs, losses, storage and transfer into the hydrological system (IPCC 2014). Whether and in what way this is the case for the North Sea region is the focus of this chapter, based on a review of available studies on climate change impacts on river flow in the North Sea region. Impacts in urban catchments are also considered.

To assess the potential impacts of climate change on river flow, methods are applied that make use of both climate models and hydrological models. Climate models simulate

Electronic supplementary material Supplementary material is available in the online version of this chapter at 10.1007/978-3-319-39745-0_7.

P. Willems (✉)
Department of Civil Engineering, KU Leuven, Leuven, Belgium
e-mail: patrick.willems@bwk.kuleuven.be

B. Lloyd-Hughes (✉)
Walker Institute for Climate System Research,
University of Reading, Reading, UK
e-mail: B.LloydHughes@reading.ac.uk

M. Quante and F. Colijn (eds.), *North Sea Region Climate Change Assessment*,
Regional Climate Studies, DOI 10.1007/978-3-319-39745-0_7

the climate system to determine the response to changes in greenhouse gases in the atmosphere (see Chap. 5) while hydrological models simulate the climate change effect on the water cycle. To assess the potential impact of climate change on river flow, climate change signals are used to alter the input to hydrological models that aim to simulate the climate-driven response in the hydrological environment. The strength of the changes depends on the temporal and spatial scales being examined.

River flow may be affected by changes in land use, ground water abstraction, hydraulic structures (such as reservoirs) along the river course, and urbanisation (see Sect. 7.3.3), among others; none of which are directly linked to climate change. Such features mean not all climate-driven hydrological impacts are easily discernible, and so caution is necessary when attributing hydrological change to 'climate change impact'; see also Chap. 5.

7.2 Methodology

7.2.1 Temporal and Spatial Scales

Uncertainties in climate and hydrological models mean caution must be applied in using the model output to project climate-driven impacts on river flow. This is especially the case for studying local hydrological impacts. Local climates are represented in regional climate models (RCMs) at the spatial resolution of the RCMs, and are less reliable than the coarser resolution climate data obtained from the same RCMs or from global climate models (GCMs). However, the reliability of climate models is improving due to the ongoing research in climate science (see the Supplement S7 to this chapter). The highest resolution RCMs are now in the range of a few tens of kilometres which reduces the mismatch with hydrological models that often operate at resolutions of a few kilometres or less. High resolution models, however, do not completely resolve the physics of the climate system so climate model output still requires further scrutiny before use in regional climate studies.

Although the natural processes addressed in climate and hydrological models are closely linked, because climate science and hydrology are separate disciplines the technical aspects of these different disciplines require an interface linking the respective models. This interface allows a realistic transfer of information between climatic and hydrologic simulations. Methods at the interface range from the direct use of climate model output to correct for bias (systematic over- or underestimations) before use. However, direct use is rarely implemented due to the bias in climate models. Another major interfacing issue is the need for high resolution data in many hydrological applications, both in space and time. Finer-resolution climate models imply a developmental and computational burden which translates to higher resources, in time and money. While efforts to increase the resolution of GCMs and RCMs continue (e.g. HiGEM, Shaffrey et al. 2009; Kendon et al. 2012) the current state-of-the-art is well short of the requirements for local hydrological modelling.

These two main interfacing problems are met by applying statistical downscaling to the climate model output, ultimately in combination with bias correction. The aims of the bias correction and statistical downscaling are to eliminate systematic errors between the climate model output and the corresponding meteorological variables at the finer hydrological impact scales and/or to convert the climate model output to the finer-scale variables using statistical methods (Maraun et al. 2010; Gudmundsson et al. 2012a). More discussion on the mismatch of scales, statistical downscaling and bias correction is available in the Supplement S7. These downscaling and bias correction methods have increased data availability for hydrological assessments. Different approaches have been developed. Several have been applied in the North Sea region, depending on the area, type of hydrological impact, approach and experience of the modeller and available resources, among others.

7.2.2 Analysis

Determining the climate-driven change in river flow typically includes four steps: evaluating the climate models; downscaling/bias correction of the hydrological variables from the climate scenarios; converting climate change signals/perturbations to hydrological parameters; and simulating the hydrological climate change effect.

Different types of hydrological models have been used for studying the impact of climate change, depending on the scale and the processes. Conceptual rainfall-runoff models have been widely applied to individual catchments because of their ease of use and calibration (limited number of model parameters) and because they provide overall runoff estimates at the scale of a catchment or sub-catchment (see Supplement S7 for examples). In order to capture the spatial variability of the hydrological response in larger river basins or regions, spatially-distributed hydrological balance models have been applied. These can be of a conceptual nature or more detailed, depending on the types of impacts studied (e.g. Shabalova et al. 2003; Lenderink et al. 2007; Thompson et al. 2009; Bell et al. 2012; Huang et al. 2013). At the continental and global scale, land surface models and coarse-scale global water balance models are used, such as at the scale of Europe (e.g. Dankers and Feyen 2008; Feyen and Dankers 2009; Prudhomme et al. 2012) or the entire globe (e.g. Arnell and Gosling 2016; Dankers et al. 2014).

Hydrological impact results are typically evaluated for mean annual or seasonal volumes, but also for flow extremes

(peak flows and low flows). The latter are of particular relevance for water management, given that they are fundamental to flood and water scarcity risks. Peak and low flow extremes for current and future climatic conditions are typically compared for quantiles, hence for given exceedance probabilities or return periods. Such quantiles, for example the 100-year peak flow, form the basis of water engineering design statistics. They can be obtained empirically from the independent extreme flows extracted from the simulated time series (possible only up to the length of the time series), or after extreme-value analysis (required for extrapolating beyond the length of the time series). Bastola et al. (2011), Arnell and Gosling (2016), Dankers et al. (2014), and Smith et al. (2014), for example, defined peak flows as annual maximum flows and extrapolated these based on the Generalized Extreme Value (GEV) distribution. Lawrence and Hisdal (2011) did the same but used the Gumbel distribution as a special case of the GEV, and Kay and Jones (2012) made use of a generalised logistic distribution. Willems (2013a) selected independent peak flows from a time series by means of hydrological independence criteria to obtain a peak-over-threshold or partial-duration-series. These typically follow the Generalized Pareto Distribution (GPD), or the exponential distribution as a special case. The statistical uncertainty in estimates of large return periods (e.g. 100 years) may be considerable, however, especially when based on relatively short time series (typically 30 years for climate model results) (Brisson et al. 2015). Using information on flood thresholds or hydraulic flood modelling, the flow extremes can be related to flood hazard (e.g. return period of flooding) or even flood risk after considering functions describing the regional or local relationship between flood flow or depth and the flood consequences (Feyen et al. 2012; Ward et al. 2013; Arnell and Gosling 2016).

For impact analysis on urban drainage (sewer floods), because of the quick response of such systems to rainfall, changes in short-duration extremes (hourly to sub-hourly) are considered. These changes are propagated to changes in sewer flow by full hydrodynamic or conceptual sewer models; a recent state-of-the-art review of methods, difficulties/pitfalls, and impact results was made by Willems et al. (2012a, b).

As well as changes in rainfall and evaporation, for impact analysis on water quality in urban drainage systems and along rivers, changes in other variables must also be considered. Impacts on water quality are not only controlled by changes in rainfall, but also by (changes in the length of) dry periods. In the case of longer dry periods in north-western Europe, river pollution will be less diluted and river water quality will deteriorate. Some sources of river pollution might even increase, such as pollution originating from sewer overflows.

Along sewer systems, longer dry periods cause water and wastewater to stay for longer in the sewer pipes. Particularly in the low and flat North Sea region, this will lead to higher sewer solids sedimentation (Bates et al. 2008). An increase in short-duration rainfall extremes will not only increase peak runoff discharges but will also increase wash off from surfaces (impermeable and permeable) in the sewer catchment. An increase in runoff and sewer peak flows, would increase the frequency of sewer overflows or the spilling of storm- and/or waste-water into the receiving river. These effects are studied by integrated urban drainage models comprising the sewer system, wastewater treatment plant and receiving river. Using such a model, Astaraie-Imani et al. (2012) studied the impact of climate change (and urbanisation) on the receiving water quality of an urban river for dissolved oxygen and ammonium using a semi-real case study in the UK. Another application, but for a catchment in Belgium and limited to the flow impacts of sewer systems on receiving rivers was reported by Keupers and Willems (2013). Other types of climatic change effect along sewer systems include changes in temperature, which affect sewer quality processes (Ashley et al. 2008), risk of sulphide production in the sewer pipes, and increased odour problems; as well as increased sewer floods and sewer overflows because of changes in snowmelt patterns in mountainous regions, sea-level rise in low-lying coastal areas, inflow of groundwater during the wet season, and increased leakage of wastewater into the soil during the dry season, among others.

Whatever model type is applied, it is necessary to be aware that parameters calibrated for historical periods may not be valid under a changing climate. For instance, it is known that under dry conditions, soil moisture parameters are likely to change, which may affect the hydrological processes by introducing other complex mechanisms (Diaz-Nieto and Wilby 2005). One way of understanding the changes is to assess longer hydrological and meteorological records with significantly different changes in climate and land use (Refsgaard et al. 2014). However, sufficiently long time series (e.g. over 100 years) are often not available to evaluate this assumption.

It is also necessary to be aware of the limitations of the models in modelling particular types of extremes (e.g. high flow, low flow). For that reason, methods have been developed that explicitly validate model performance for high and low extremes; see Seibert (2003), Willems (2009), and Karlsson et al. (2013). Van Steenbergen and Willems (2012) proposed a data-based method to validate the performance of hydrological models in describing changes in peak flow under changes in rainfall extremes, prior to their use for climate change impact investigations. Vansteenkiste et al. (2013, 2014) compared different hydrological models and concluded that the impact results of climate scenarios might significantly differ depending on the model structure and

underlying assumptions, especially for low flow. Gosling et al. (2011) applied two types of distributed hydrological model to different catchments, including the Harper's Brook catchment in the UK, to analyse the impact uncertainty from seven GCM runs. Both models simulated similar climate change signals, but differences occurred in the mean annual runoff, the seasonality of runoff, and the magnitude of changes in extreme monthly runoff. Also, Bastola et al. (2011) emphasised the importance of incorporating hydrological model structure and parameter uncertainty in estimating climate change impacts on flood quantiles. They found that the highest model uncertainty is associated with low frequency flood quantiles and with models that use nonlinear surface storage structures. Lawrence et al. (2009) investigated model parameter calibration uncertainty for the Nordic HBV model calibrated to 115 Norwegian catchments. This was done by selecting 25 parameter sets that lead to almost equal model performance. In general, however, hydrological model related uncertainty is low compared to climate model uncertainty (Minville et al. 2008; Kay et al. 2009). The latter is shown by comparing evaluations of climate and hydrological model performance against observations; however limited to historical (climate) conditions. For drought, Prudhomme et al. (2014) concluded that global hydrological models show a higher uncertainty than global climate models. At the catchment scale, it appears that hydrological model impact uncertainties are greater for low flow than for peak flow (Vansteenkiste et al. 2013, 2014), but are still less than from climate models.

7.2.3 Scenarios

Owing to the high uncertainties involved in the parameterisations of the climate models and the future greenhouse gas scenarios (see Supplement S7), it is better to apply a broad ensemble set of climate model simulations. Uncertainty in the future projections can thus be partly accounted for (Palmer and Räisänen 2002; Tebaldi et al. 2005; Collins 2007; Smith et al. 2009; Semenov and Stratonovitch 2010). Use of ensemble-based probabilistic projections has been proposed but would raises questions and difficulties for impact modellers (New et al. 2007). Linking probabilities to future scenarios is a commendable idea, but it is not clear how the use of probabilities would maintain internal consistency, which is a key requirement for impact analysis. It is pragmatic, therefore, to make use of existing climate change impact methods, albeit with improvements.

Any ensemble of climate model runs best includes a broad set of different climate models and greenhouse gas scenarios (SRES, RCP; see Supplement S7). Note in this respect that hydrological impact analyses of climate change to date have largely ignored the most pessimistic projections for climate change such as the SRES A1FI scenario. It has been argued that emission trends since 2000 are in line with the A1FI projections made in the 1990s (Raupach et al. 2007), which means that the A1FI scenario is becoming more plausible and the most likely projected high flows could be even higher than those reported here. Recent evidence also suggests that GCM projections underestimate the amount of warming that is already being observed in western Europe (van Oldenborgh et al. 2009).

The hydrological impact results reported in this chapter are primarily based on the SRES scenarios. Hydrological impact results for the newer RCP-based climate scenarios were still limited at the time this chapter was drafted (first global results exist: Dankers et al. 2014; Prudhomme et al. 2014), but it would be worth more extensively testing the change and consistency in impact results between the SRES and RCP-based scenarios.

In addition to uncertainties in the climate process modelling and greenhouse gas scenarios, the downscaling method used adds to uncertainty in the climate scenarios (see more discussion in the Supplement S7). Impact modelling based on large ensembles of climate model simulations under different downscaling assumptions remains difficult in practice because of the high computational costs associated with hydrological and hydraulic modelling. A pragmatic approach would be to summarise the different meteorological impact results of climate change in a limited set of (tailored) scenarios. Examples include the UKCIP02 (Hulme et al. 2002), UKWIR06 (Vidal and Wade 2008), and UKCP09 scenarios in the UK (Murphy et al. 2009), the KNMI'06 scenarios in the Netherlands (Van den Hurk et al. 2006; de Wit et al. 2007), and the CCI-HYDR scenarios in Belgium (Willems 2013a; Ntegeka et al. 2014).

Figure 7.1 illustrates how the CCI-HYDR high, mean and low scenarios for one particular season are based on the highest, average and lowest climate factors for the entire set of potential scenarios considered. The changes for different seasons are combined in different versions such that they lead to high, mean, and low impacts for specific (tailored) hydrological applications, for example winter floods, summer flash floods and summer low flows. This is the opposite of the KNMI'06 scenarios that are based on meteorological considerations only (Fig. 7.2, where scenarios W and G refer to higher or lower changes in temperature, and the scenarios W+ and G+ to stronger changes in atmospheric circulation).

7.3 Projections

7.3.1 North Sea Region

Numerous studies indicate that in north-western Europe a warmer climate may lead to an increase in intense rainfall

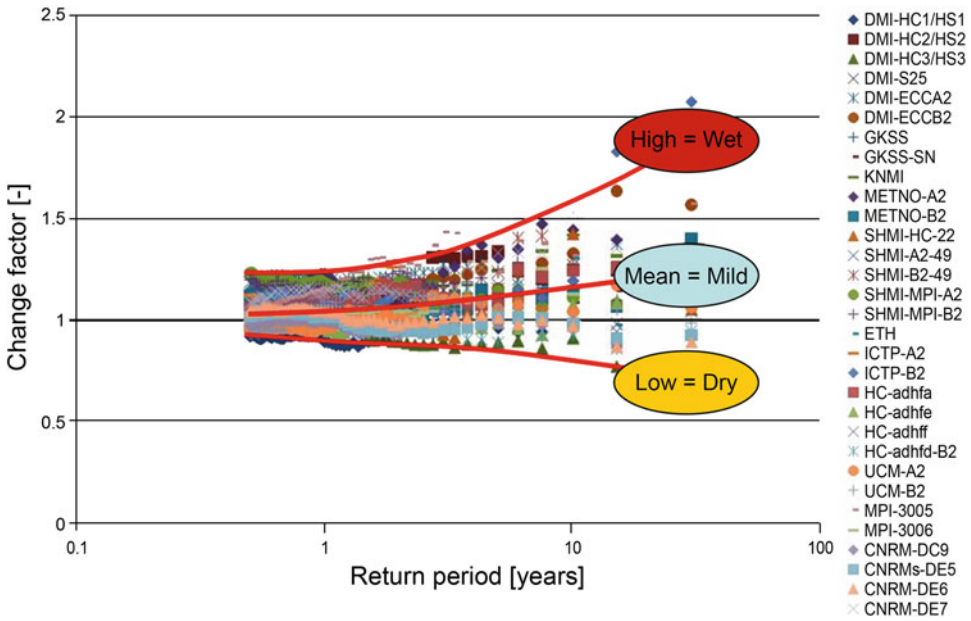

Fig. 7.1 High-mean-low tailored climate scenarios to simplify the flood impact analysis based on an ensemble set of climate model simulations (here: factor change in daily rainfall quantiles from 1961–1990 to 2071–2100 for A2 and B2 SRES scenarios and all RCM runs available for Belgium from the EU PRUDENCE project; Ntegeka et al. 2014)

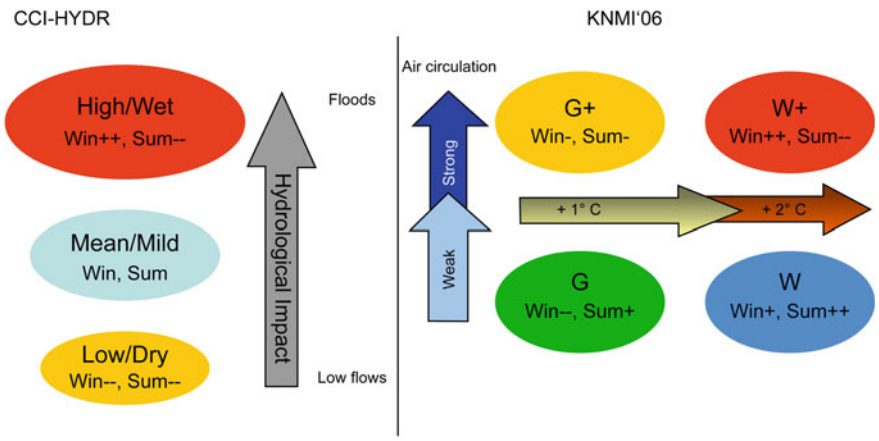

Fig. 7.2 Tailored climate scenarios: hydrological impact based (*left* CCI-HYDR, Ntegeka et al. 2014) versus meteorological based (*right* KNMI'06, van den Hurk et al. 2006)

(e.g. Kundzewicz et al. 2006; Hanson et al. 2007) and to longer dry periods (e.g. Good et al. 2006; May 2008), and consequent changes in river flows, as is shown in Table 7.1 based on a review by the European Environment Agency (EEA 2012) and the Intergovernmental Panel on Climate Change in its Fifth Assessment (IPCC 2014). The projections indicate an intensification of rainfall during both winter and summer, but for summer, although the heavy rainfall events may become more intense the intensity of the light and moderate events will decrease. How these meteorological changes will affect river flow shows strong seasonal and regional differences. For north-western Europe, the intensity and frequency of winter and spring river floods are generally expected to increase (EEA 2012).

Based on climate projections from three GCMs and impact analysis in three relatively coarse resolution global hydrological models, Prudhomme et al. (2012) found that river flow in north-western Europe (e.g. Great Britain) would increase in winter with concurrent increases in regional high flow anomalies, and would decrease in summer. Giving particular attention to daily peak flow and related flood risk, Hirabayashi et al. (2013), Arnell and Gosling (2016) and Dankers et al. (2014) found strong sub-regional variations in Europe with both increases (mostly for the UK, France and Ireland) and decreases in the size of the flood-prone populations. Giving particular attention to hydrological droughts, Prudhomme et al. (2014) found significant increases in the frequency of droughts of more than 20 % in central and western Europe. Also based on a coarse-scale hydrological model, but this time with a focus on the main rivers in Europe, Feyen and Dankers (2009) found stream flow droughts will become more severe and persistent in most parts of Europe by the end of the century, except in the most northern and-north eastern regions.

However, it should be noted that these results are based on only one RCM run (HIRHAM 12-km resolution model;

Table 7.1 Typical change in inland river flows for northern and north-western Europe (EEA 2012; IPCC 2014)

Variable	Northern Europe		North-Western Europe	
	Observed	Projected	Observed	Projected
River flow	+	+	(+)	+
River flood		±	+	+
River low flow (drought)	0	+	0	−

+ increase; − decrease; ± increase and decrease; 0 little change

A2 and A1B SRES scenarios). Based on the same RCM runs and the same hydrological model, Dankers and Feyen (2008) and Rojas et al. (2011) focused on the flood hazard climate change impact and found that extreme discharge levels may increase in magnitude and frequency in parts of western and eastern Europe. In several rivers, the return period of what is currently a 100-year flood may decrease to 50 years or less. Rojas et al. (2012) extended the analysis by applying the same hydrological model to 12 RCM runs, and concluded that results show large discrepancies in the magnitude of change in the 100-year flood for the different RCM runs. Some regions even show an opposite signal of change, but for many regions the projected changes are not statistically significant due to the low signal-to-noise ratio. Western Europe and the British Isles show a robust increase in future flood hazard, mainly due to a pronounced increase in extreme rainfall. A decrease in the 100-year flood, on the other hand, is projected in southern Sweden because the signal is dominated by a strong reduction in snowmelt-induced spring floods, which offsets the increase in average and extreme precipitation. This is also valid for other snowmelt dominated areas of the North Sea region.

Another Europe-wide hydrological impact study was undertaken by Schneider et al. (2013) who applied the global hydrological model WaterGAP3 on a 50′ × 50′ European grid. Climate change impacts were based on three GCMs after bias correction. Looking at their results for the North Sea region, they found that flow magnitude was more affected in the northern parts of the North Sea region, such as Sweden and Norway, with strong increases projected in winter precipitation. The lowest impacts across Europe were found in western Europe (i.e. the UK, Ireland, Benelux, Denmark, Galicia and France). The difference is due to the additional impact of temperature on snow cover in the northern region. The greatest impact on peak flows in Scandinavia occurred in April, rather than May, one month earlier in the future. Earlier snowmelt in spring and sporadic melt events in winter will reduce snow storage. However, in Sweden and Norway, these effects were more than compensated for by higher precipitation. During summer (June to September), increased precipitation is offset by greater evapotranspiration. Scandinavia is the only region in Europe where elevated low flows are projected.

7.3.2 Sub-region or Country-Scale

7.3.2.1 Belgium

Using finer scale hydrological models (c.f. Sect. 7.3.1), more local European climate studies have projected similar climate change impacts. For 67 catchments in the Scheldt river basin in Flanders, Boukhris et al. (2008) found that extreme peak flows in rivers may increase or decrease depending on the climate scenario used. Winter rainfall volumes increase but evapotranspiration volumes also increase. Depending on the balance between rainfall increase versus evapotranspiration increase, the change in net runoff may switch from positive to negative. From a set of 31 statistically downscaled RCM simulations and more than 20 GCM simulations available for Belgium, the most negative change led to an increase in the river peak flows of about 30 % for the 2080s (Fig. 7.3).

Impacts on river low flows were more uniform. All of the climate model simulations projected a decrease in river low flow extremes during summer. For Belgian rivers, the change in low flow extremes projected for the 2080s ranged between −20 and −70 % (Fig. 7.3). The drier summer conditions for Belgium lead to lower groundwater levels, as shown by Brouyére et al. (2004) and Goderniaux et al. (2009) for the Geer catchment, and by Dams et al. (2012) and Vansteenkiste et al. (2013, 2014) for the Nete catchment.

7.3.2.2 Northern France

Within the main river basins in France, Boé et al. (2009) found a decrease in mean discharge for summer and autumn. They also simulated a decrease in soil moisture, and a decrease in snow cover, which was especially pronounced at low and middle altitudes. The low flows in France become more frequent. This was also found by Habets et al. (2013) for the rivers Seine and Somme in northern France, based on seven hydrological models ranging from lumped rainfall-runoff to distributed hydrogeological models, and three downscaling methods. A general decrease in river flow of at least 14 % occurred at the outlets of the Seine and Somme basins by the 2050s and at least 22 % by the 2080s. More than 90 % of projections showed a decrease in summer flow at these outlets. For the winter high flows, about

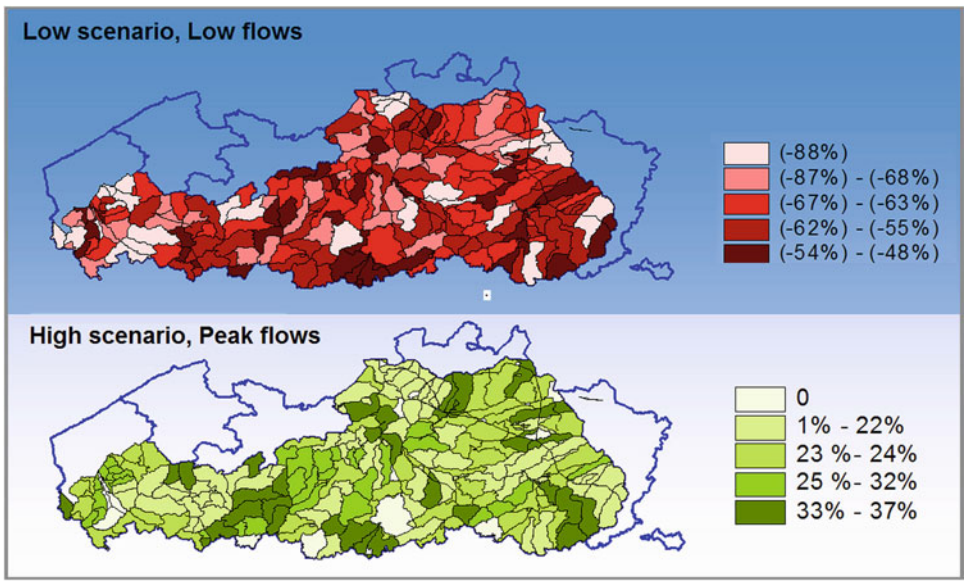

Fig. 7.3 Percentage change in low flows for a low/dry CCI-HYDR climate scenario (*upper*) and peak flows for a high/wet CCI-HYDR climate scenario (*lower*), averaged for return periods of 1–30 years, for 2071–2100 and 67 catchments in Flanders, Belgium (Boukhris et al. 2008)

10 % of projections showed the possibility of increased flow in winter in the River Seine and throughout the year in the River Somme, while 10 % projected a decrease of more than 40 % in river discharge at the basin outlets. For the same basins, Ducharne et al. (2011) found little change in the risk of floods for the 10- and 100-year return periods.

7.3.2.3 Germany

For various river basins in Germany, including the Ems, Weser, Elbe and Rhine (up to the Rees gauge station), based on two RCM simulations Huang et al. (2013) found an increase of about 10–20 % in the 50-year flood levels in the rivers Weser, Rhine, Main, Saale and Elbe. The Ems showed no clear increase and the Neckar a 20 % decrease. In contrast, the Wettreg statistical downscaling method projected a decrease in flood level for the Ems and Weser (10 %), and Saale (20 %) river basins, and no distinct change for the Main and Neckar. For the River Rhine, Shabalova et al. (2003) found future climate scenarios to result in higher mean discharges in winter (about +30 % by the end of the century), but lower mean discharges in summer (about −30 %), particularly in August (about −50 %). Temporal variability in the 10-day discharge increased significantly, even if temporal variability in the climatic inputs remains unchanged. The annual maximum discharge increases in magnitude throughout the Rhine and tends to occur more frequently in winter, suggesting an increasing risk of winter floods. At the Netherlands-German border, the magnitude of the 20-year maximum discharge event increased by 14–29 %; the present-day 20-year event tends to reappear every 3 to 5 years. The frequency of low and very low flows increases, in both scenarios alike. Studying changes in 10-day precipitation sums for return periods in the range 10 to 1000 years in the Rhine basin (within the scope of the RheinBlick2050 project), van Pelt et al. (2012) found changes of up to about +30 %. Pfister et al. (2004) projected increased flooding probably due to higher winter rainfall for the Rhine and Meuse river basins. Most hydrological simulations suggest a progressive shift of the Rhine from a 'rain-fed/meltwater' river to a mainly 'rain-fed' river. Studying projected change in the 1250-year peak flows in the Rhine and Meuse rivers, which are used as the basis for dike design along these rivers, de Wit et al. (2007) found the 1250-year peak flow to increase from 16000 to 18000 $m^3 s^{-1}$ by 2100 for the Rhine and from 3800 to 4600 $m^3 s^{-1}$ for the Meuse. For low flow, they found stronger seasonality in the discharge regime of the Meuse: increased low discharge in winter and decreased low discharge in summer. The same findings were obtained by van Huijgevoort et al. (2014).

7.3.2.4 Ireland

For catchments in Ireland, Bastola et al. (2011) simulated monthly changes derived from 17 GCM runs to the input of four hydrological models, and quantified the impact on flood quantiles up to 100-year return periods. They also studied the sensitivity of the impact results within and between hydrological models. The results show a considerable residual risk associated with allowances of +20 % when uncertainties are accounted for and that the risk of exceeding design allowances is greatest for more extreme, low frequency events (Fig. 7.4) with major implications for critical infrastructure such as culverts, bridges, and flood defences.

7.3.2.5 Scandinavia

In the Scandinavian countries, the increase in peak flows is higher than in other North Sea countries due to the higher

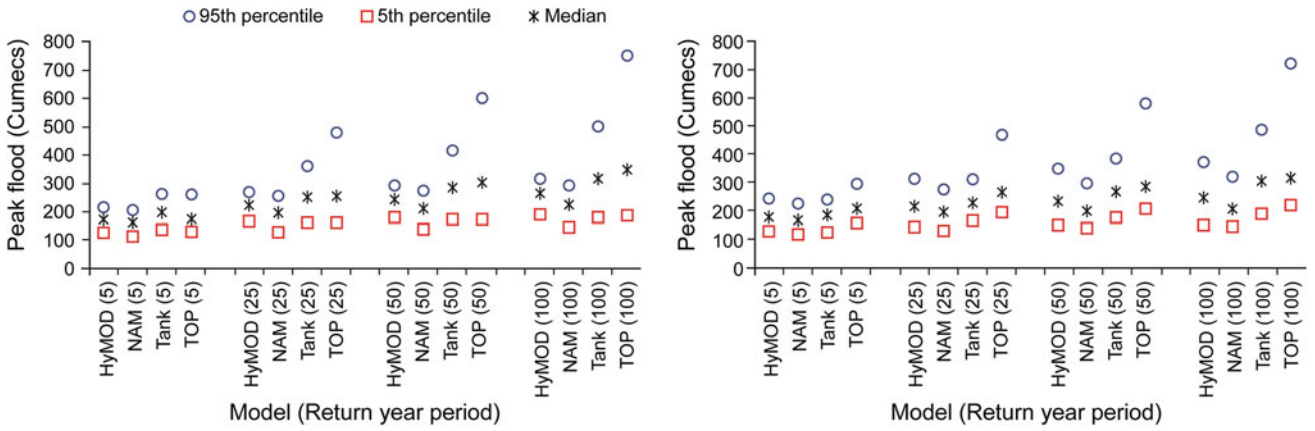

Fig. 7.4 The 95th percentile, 5th percentile and median value for modelled flood quantiles (5-, 25-, 50- and 100-year return periods) for the Moy river basin (*left*) and Boyne river basin (*right*) in Ireland (Bastola et al. 2011)

increase in winter rainfall. In Norway, Lawrence and Hisdal (2011) studied the changes in flood discharges for 115 unregulated catchments. Projected changes in peak flow quantiles for return periods of 200, 500 and 1000 years show strong regional differences (Fig. 7.5). These regional differences are explained by the role of snowmelt versus rainfall and how they increase the peak flows. This is, however, different for catchments where peak flows are mainly due to snow melt in spring. In this case, increased winter temperature will cause reduced snow storage, and thus decreased peak flows. An exception is catchments at higher elevations in areas where winter precipitation continues to fall predominantly as snow and higher spring temperatures produce more rapid snowmelt (SAWA 2012). In addition to changes in snowmelt-induced peak flows, the timing of the peak flows becomes earlier (i.e. spring rather than summer). Changes in the seasonality of peak flows occurs in catchments where flows driven by snowmelt decrease but flows driven by winter and autumn rainfall increase. The median projected change in the ensemble of hydrological projections for Norway at 2071–2100 varied from +10 to +70 % in catchments located in western and south-western regions (Vestlandet), coastal regions of southern and south-eastern Norway (Sørlandet and Østlandet) and in Nordland, and decreased down to −30 % for northernmost areas (Finnmark and parts of Troms) and middle and southern inland areas (Hedmark, Oppland, and parts of Buskerud, Telemark and Trøndelag).

Similar results to eastern Norway were obtained by Andréasson et al. (2011) for Sweden; see the regional differences in 100-year peak flows in Fig. 7.6. They are based on spatial interpolation, without taking into account the influence of river regulation effects. The northern catchments in Sweden mostly show decreasing peak flows towards the end of the century, whereas the southern basins show increasing 100-year flows. The changes in peak flows vary

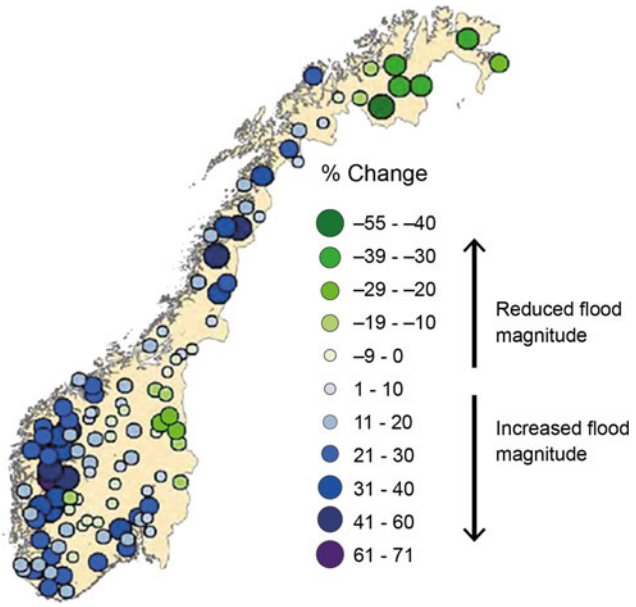

Fig. 7.5 Median projected change in peak flows for 200-year return period and 2071–2100 for 115 unregulated catchments across Norway (Lawrence and Hisdal 2011; SAWA 2012)

from −45 to +45 %. A similar range was found by Teutschbein et al. (2011) and Teutschbein and Seibert (2012) for five catchments in Sweden.

Andersen et al. (2006) studied the climate change impact for six sub-catchments within and for the entire Gjern river basin in Denmark, but only based on one RCM simulation. Mean annual runoff from the river basin increased by 7.5 %, whereas greater changes were found for the extremes. The modelled change in the seasonal hydrological pattern is most pronounced in first- or second-order streams draining loamy catchments, which currently have a low base-flow during summer. Reductions of 40–70 % in summer runoff are projected for this stream type. Similar conclusions were obtained

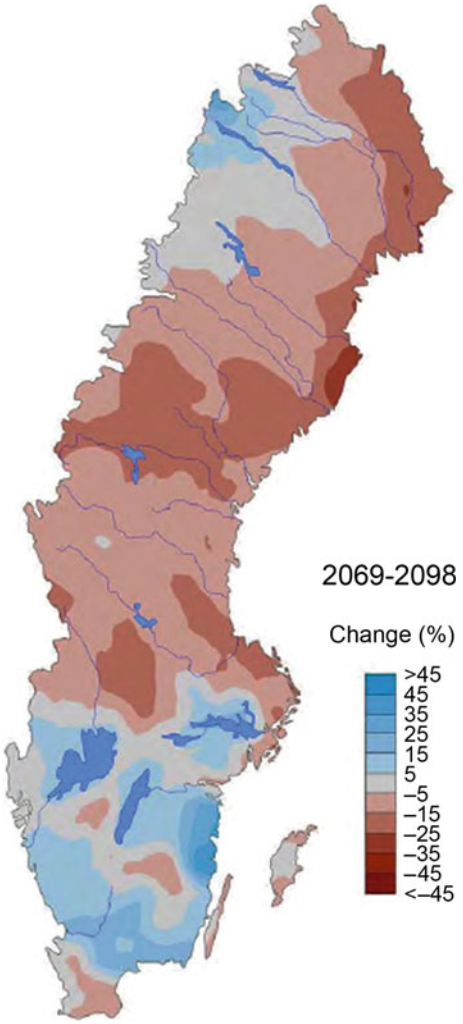

Fig. 7.6 Median projected change in spatially interpolated peak flows for 100-year return period and 2069–2098 for Sweden (Andréasson et al. 2011; SAWA 2012)

based on the same RCM run for five major Danish rivers divided into 29 sub-catchments by Thodsen (2007). The river discharge that exceeded 0.1 % of all days increases approximately 15 %, and the 100-year flood is modelled to increase 11 % on average. Andersen et al. (2006) also studied the climate change impact on diffuse nutrient losses (i.e. losses from land to surface waters). Simulated changes in annual mean total nitrogen load were about +8 %. Even though an increase in nitrogen retention in the river system of about 4 % was simulated in the scenario period, an increased in-stream total nitrogen export occurred due to the simulated increase in diffuse nitrogen transfer from land to surface water.

7.3.2.6 UK

For eight catchments in northwest England, Fowler and Kilsby (2007) used an ensemble set of simulation results with the HadRM3H RCM (UKCIP02 scenarios) and undertook a comprehensive treatment of climate modelling uncertainty. They concluded that annual runoff is projected to increase slightly at high elevation catchments, but to reduce by ~16 % for the 2080s at lower elevations. Impacts on monthly flow distribution are significant, with summer reductions of 40–80 % of mean flow, and winter increases of up to 20 %. The changing seasonality has a large impact on low flows, with 95 %-percentile flows projected to decrease in magnitude by 40–80 % in summer months (Fig. 7.7). In contrast, high flows (>5 %-percentile flows) are projected to increase in magnitude by up to 25 %, particularly at high elevation catchments, providing an increased risk of flooding during winter. Based on the same RCM and with a focus on river flood hazards in winter, Kay et al. (2006) found increased flood hazard particularly in East Anglia and the Upper Thames, with flood peaks in some places increasing by more than 50 % for the 50-year return level. Clear regional differences were also found by Arnell (2011) and Christierson et al. (2012) after analysing many UK catchments and several climate models or scenarios. Based on six catchments across the UK, Arnell (2011) found clear differences between northern and southern catchments, with large climate change effects in winter in the north and summer in the south. After analysing 70 UK catchments, Christierson et al. (2012) found major differences between the western and northern mountainous part of the UK and the rest of the UK, with an increase in winter river flow over the western part but less clear results or a decrease in mean monthly river flows all year round. In summer, most catchments showed negative or very slightly positive changes, with the largest flow decrease in the Thames, Anglian and Severn river basin districts, with decreases of 10 % or more in mean monthly flows all year round and even more in summer.

A specific study for the River Thames by Diaz-Nieto and Wilby (2005) concluded that substantial reductions in summer precipitation accompanied by increased potential evaporation throughout the year, lead to reduced river flow in late summer and autumn. Kay et al. (2006) found the same situation even in winter for some catchments in the south and east of England despite an increase in extreme rainfall events. This was explained by higher soil moisture deficits in summer and autumn that may have an influence up to the start of winter. Also for the Thames basin, but based on the more recent UKCP09 scenarios, Bell et al. (2012) found a 10–15 % increase in winter rainfall by the end of the century. This might potentially lead to higher flows than the River Thames can accommodate. Towards the downstream end, they estimated an average change in modelled 20-year return period flood peaks by the 2080s of 36 % (range −11 to +68 %).

For the River Avon catchment, Smith et al. (2014) obtained changes in the 25-year return period flows of +15,

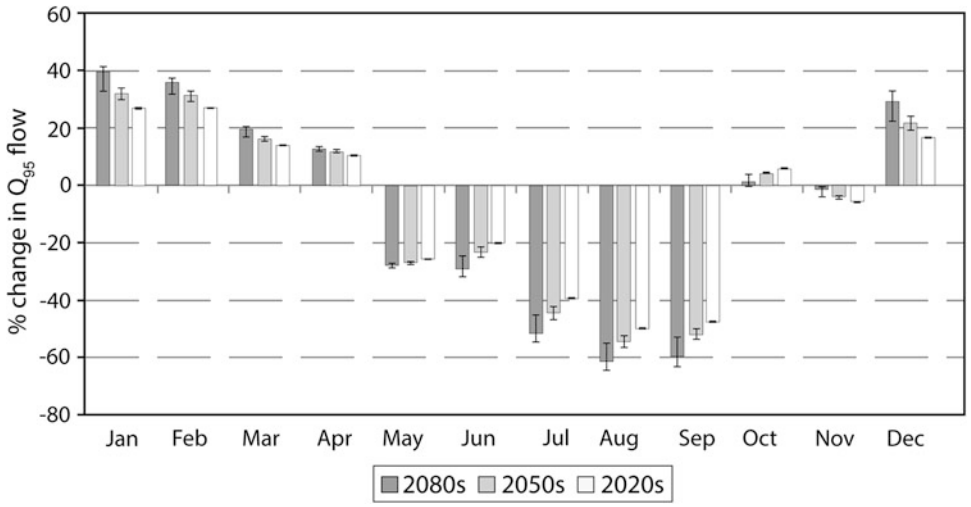

Fig. 7.7 Change in 95 %-percentile flow between the HadRM3H control and future scenarios for 2020s, 2050s and 2080s time-slices. The uncertainty bounds are for the different SRES scenarios (Fowler and Kilsby 2007)

+2 or +7 % based on three different methods for transferring the climate model output to hydrological model input. For 200-year peak flows, these percentages increased to +22 +19 and +6 %. For the River Medway catchment, Cloke et al. (2010) found a significant lowering of summer flow with a more than 50 % reduction for 2050–2080 and up to 70 % in some months. For six other UK catchments, Arnell (2011) simulated changes in summer runoff of between −40 and +20 %.

In terms of groundwater recharge, Herrera-Pantoja and Hiscock (2008) concluded that by the end of the century decreases in recharge of between 7 and 40 % are expected across the UK, leading to increased stress on local and regional groundwater supplies that are already under pressure to maintain both human and ecosystem needs.

The impacts that these hydrological changes may have in terms of flood and water availability risk were assessed by the UK-Government funded initiative AVOID (Warren et al. 2010; MetOffice 2011). Based on an ensemble set of 21 GCMs, it is shown that nearly three-quarters of the models project an increase in flood risk. For the 2030s and averaged over the UK as a whole, the change ranges from −20 to +70 %, with a mean of +4 % (Fig. 7.8). Larger increases are shown for longer time horizons. Overall, the models show a tendency for a large increase in flood risk for the UK as a whole.

The water availability threat in the UK (calculated using the Human Water Security Threat indicator by Vörösmarty et al. 2010) ranges from very high in the south-east to moderate in the south, Midlands, and southern Scotland (Fig. 7.9). For southern England, the loss in deployable water output due to climate change and population growth is estimated to be 3 % by 2035 (Charlton and Arnell 2011). Increased irrigation requirements were also found for the south-east and north-west of England (Henriques et al. 2008).

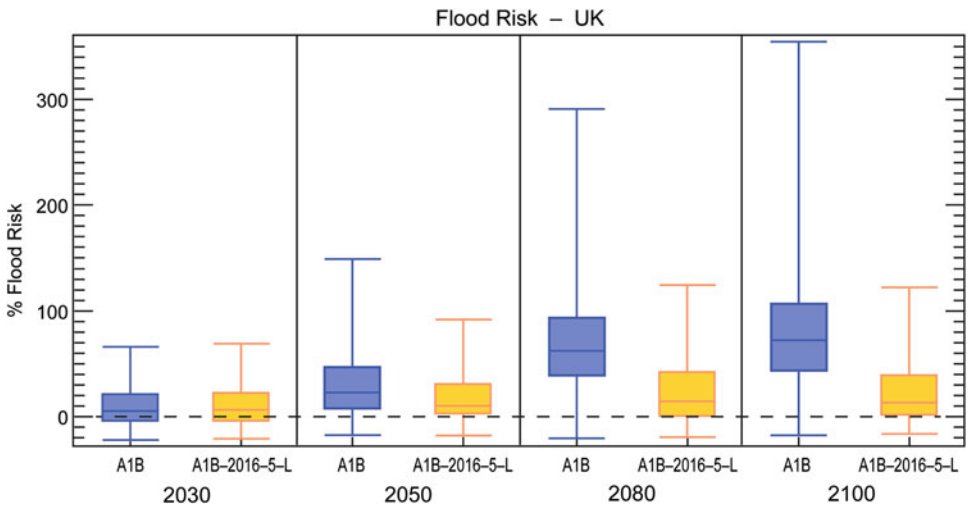

Fig. 7.8 Change in average annual flood risk for the UK, based on 21 GCMs under two emission scenarios (A1B and A1B-2016-5-L), for four time horizons (MetOffice 2011). The plots show the 25th, 50th, and 75th percentiles (represented by the *boxes*), and the maximum and minimum values (shown by the extent of the *whiskers*)

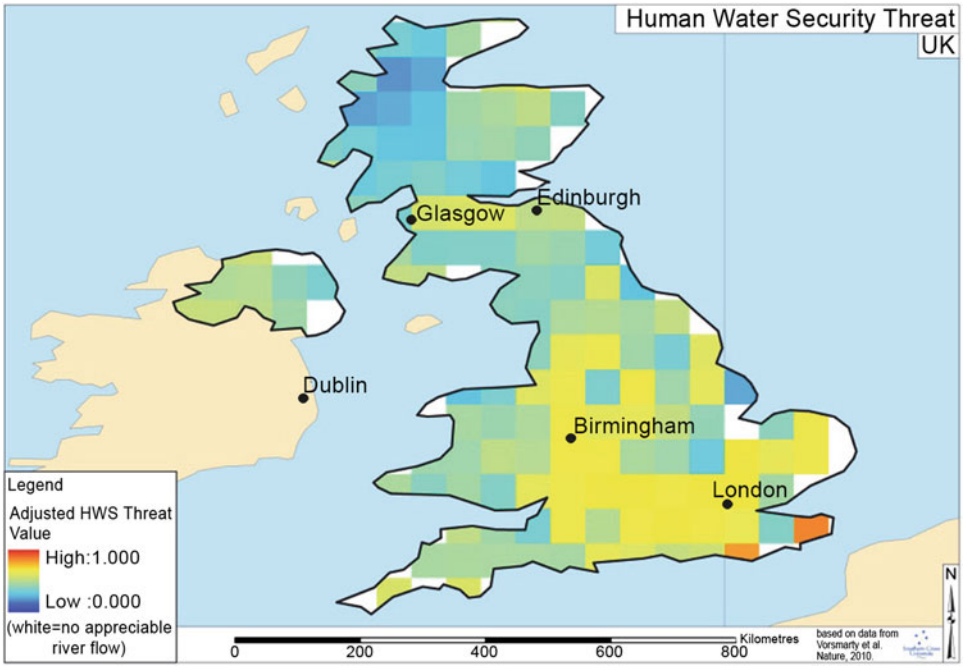

Fig. 7.9 The human water security threat for the UK (MetOffice 2011)

7.3.2.7 Comment on Low Flows

Although models project that climate change will cause a decrease in low flows in north-western European rivers over the coming decades, it should be noted that most models have low accuracy in the simulation of low flow extremes. Evidence for this is provided by Gudmundsson et al. (2012b) based on nine large-scale hydrological models after comparison to observed runoff from 426 small catchments across Europe. Further evidence is provided by Vansteenkiste et al. (2013, 2014) for a catchment in Belgium. Low accuracy for low flows is associated with the representation of hydrological processes, such as the depletion of soil moisture stores (Vansteenkiste et al. 2013, 2014).

7.3.2.8 Estuaries

In addition to changes in inland rainfall, temperature and reference evapotranspiration, which lead to changes at the upstream boundaries of estuaries, it is also important to consider changes in the downstream coastal boundary. In relation to the Scheldt estuary (Fig. 7.10), Ntegeka et al. (2011, 2012) studied projected changes in mean sea level, storm surge levels, wind speed and wind direction, and their correlation with changes in inland rainfall (see also Monbaliu et al. 2014 and Weisse et al. 2014). The changes in storm surge levels were derived from changes in sea-level pressure (SLP) in the Baltic Sea, the Atlantic Ocean area west of France, and the Azores, and a correlation model between SLP and storm surge level. The model was derived after analysing SLP composite maps and SLP-surge correlation maps (Fig. 7.11) for days where the surge exceeds given thresholds (for different return periods). Correlations were identified between the inland (rainfall, runoff) and coastal climatic changes. Based on the ensemble set of change factors, tailored climate scenarios (tailored for the specific application of flood impact analysis along the Scheldt) were developed to the 2080s. After statistical analysis, a reduced set of climate scenarios ('high', 'mean' and 'low') was derived for each boundary condition (runoff upstream, mean sea level, and surge downstream). Smart combinations of the scenarios account for the correlation between boundary changes (Monbaliu et al. 2014; Weisse et al. 2014).

7.3.2.9 Overview

Table 7.2 summarises the hydrological impact studies reviewed in this assessment. Because many of the studies report climate change impacts on peak river flows, the impacts were reported as percentage change by the end of the century. Many other hydrological variables are also of relevance, such as mean or low flows, but fewer studies report percentage change in these variables or the various study results are not directly comparable (e.g. derived at different time scales: annual vs. seasonal or monthly). It should also be noted that in several regions, the sign and order of magnitude of change are not consistent when results from different studies are compared. This reflects differences in methodology (number and type of climate model and greenhouse gas scenario, type of hydrological-hydraulic impact model, and statistical downscaling and analysis approach; see the Supplement S7 for more discussion on such issues), as well as uncertainties in the numerical projections of changes in hydrology. That results on changes in

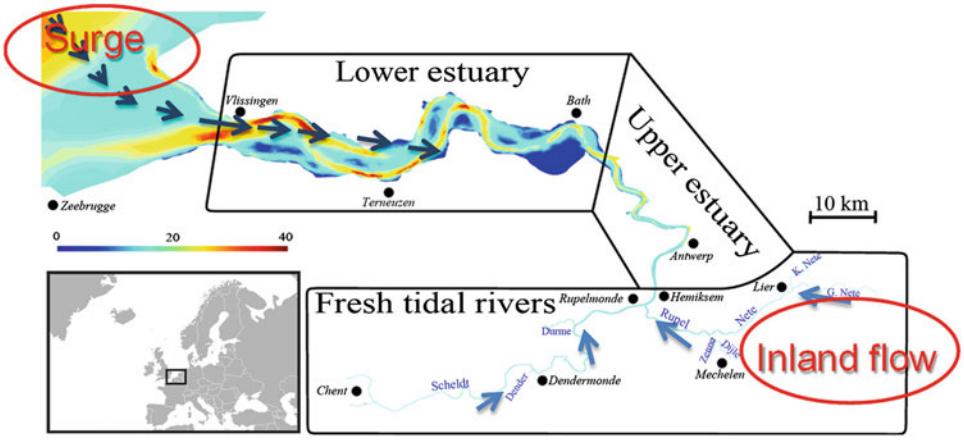

Fig. 7.10 Case study on the Scheldt Estuary: boundary conditions are the downstream surge (North Sea) and the upstream river flows (different rivers) for which correlation in the changes needs to be taken into account (Ntegeka et al. 2012)

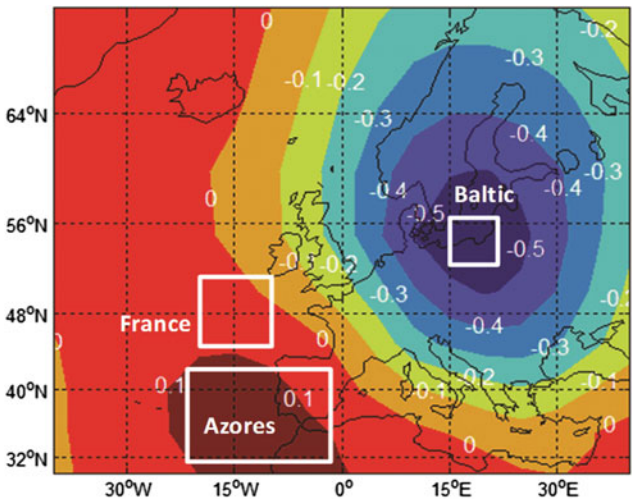

Fig. 7.11 Correlation between storm surges along the Belgian North Sea coast at Ostend and sea-level pressure over the North Atlantic region (mean based on historical events) (Ntegeka et al. 2012)

flood magnitude and frequency resulting from climate change are unclear was also concluded by the international review of Kundzewicz et al. (2013). It makes clear—as stressed in Sect. 7.2—that great care must be taken when conducting model-based impact analyses of climate change and in interpreting the results. Typical issues include consideration of only one or few climate models, greenhouse gas scenarios and/or hydrological models; poor calibration and validation of models; and inaccuracies of the models in extrapolating beyond historical conditions.

7.3.3 Urban Catchments

Hydrological analyses of urban catchments are based on studies with a particular focus on fine-scale meteorological and hydrological processes (as explained in Sect. 7.2.2).

A recent review by Willems et al. (2012a, b) and Arnbjerg-Nielsen et al. (2013) of the impacts of climate change on short-duration rainfall extremes and urban drainage showed that short-duration rainfall extremes were projected to increase by 10–60 % in 2100 relative to the baseline period (1961–1990). An urban drainage system may damp or amplify changes in precipitation, depending on the system characteristics. For the sewer network of Lund, Sweden, Niemczynowicz (1989) found the relative change in urban runoff volume to be higher than for the rainfall input. They found that a 30 % increase in the 40-min rainfall intensity would lead to a 66–78 % increase in sewer overflow volume (depending on a return period of between 1 and 10 years and the type of design storm). In Sweden, Olsson et al. (2009) found an increase in the number of urban drainage system surface floods of 20–45 % for Kalmar in 2100. For Odense in Denmark, Mark et al. (2008) found flood depth and the number of buildings currently affected once in every 50 years would correspond to a return period of 10 years in the future (based on the impacts discussed by Larsen et al. 2009 and Arnbjerg-Nielsen 2012). For Roskilde, also in Denmark, Arnbjerg-Nielsen and Fleischer (2009) found that a 40 % increase in design rainfall intensities would lead to a factor of 10 increase in the current level of damage costs related to sewer flooding. The actual change in cost will depend on catchment characteristics. In a similar study for another location with the same increase in rainfall intensity, Zhou et al. (2012) reported a factor 2.5 increase in annual costs. A common conclusion, however, is that the main impact of an increase in precipitation extremes is not primarily related to the additional cost associated with the most extreme events, but rather with the damage occurring far more frequently.

A higher factor increase in sewer impacts compared to the factor increase in rainfall was also reported by Nie et al. (2009) for Fredrikstad, Norway. They concluded that the total volume of water spilling from overflowing manholes is

Table 7.2 Summary of impact results on river flows available for the North Sea region

Region	Source	GCM-RCM(s) considered	Greenhouse gas scenario(s)	Hydrological-hydraulic impact model(s)	Change in river peak flow by 2100
Belgium	Boukhris et al. (2008), Ntegeka et al. (2014); Vansteenkiste et al. (2013, 2014), Tavakoli et al. (2014)	31 PRUDENCE RCM runs, 18 ENSEMBLES RCM runs	SRES A1, A1B, A2, B1, B2	Lumped conceptual NAM, PDM, VHM spatially distributed MIKE-SHE, WetSpa	Up to +30 %
Denmark	Andersen et al. (2006), Thodsen (2007)	HIRHAM RCM nested in ECHAM4/OPYC GCM	SRES A2	NAM rainfall runoff model /Mike 11–TRANS modelling system	Up to 12.3 %
France	Boé et al. (2009), Habets et al. (2013), Ducharne et al. (2011)	6 IPCC AR4 GCM runs	SRES A1B and A2	Hydrological models MARTHE, MODCOU, SIM, CLSM, EROS, GARDENIA and GR4 for Seine and Somme	No significant change
Germany	Huang et al. (2013)	REMO & CCLM RCMs	SRES A1B, A2, B1	SWIM eco-hydrological model	−20 to +20 %
Germany–Netherlands	van Pelt et al. (2012)	5 RCMs mainly ENSEMBLES + 13 CMIP3 GCMs	SRES A1B	HBV model Rhine basin	
Ireland	Bastola et al. (2011)	17 GCMs AR4	SRES A1B, A2, B1	4 conceptual models (HyMOD, NAM, TANK, TOPMODEL) for 4 catchments	Most up to +20 %
Netherlands	Shabalova et al. (2003), Lenderink et al. 2007	HadRM2 and HadRM3H RCMs	SRES A2 (for Lenderink et al. 2007)	RhineFlow distributed hydrological model	Up to +30 %
	de Wit et al. (2007)	KNMI'06 scenarios		Rhineflow and Meuseflow distributed hydrological models	
	Leander et al. (2008)	3 PRUDENCE RCMs	SRES A2	HBV model Meuse basin	
Norway	Lawrence and Hisdal (2011)	13 RCM runs RegClim & ENSEMBLES	SRES A1B, A2, B2	HBV rainfall runoff model 'Nordic' version	−30 to +70 %
Sweden	Andréasson et al. (2011), Teutschbein et al. (2011), Teutschbein and Seibert (2012)	12 RCM runs SMHI & ENSEMBLES	SRES A1, A2, B1, B2	HBV rainfall runoff model	−45 to +45 %
UK	Cameron (2006)	UKCIP02 climate change scenarios: HadRM3 RCM nested in HadCM3 GCM		TOPMODEL	
	Kay et al. (2006)	1 RCM: HadRM3H (UKCP02)	SRES A2	Simplified PDM lumped conceptual rainfall runoff model	Some up to +50 %
	Fowler and Kilsby (2007)	Ensemble of runs for 1 RCM: HadRM3H (UKCP02)	SRES A2	ADM model	Up to +25 %
	Chun et al. (2009)	7 GCMs & RCMs		pd4-2par conceptual rainfall-runoff model for 6 catchments	
	Cloke et al. (2010)	HadRM3 RCM: subset of UKCP09 scenarios	SRES A1B	CATCHMOD semi-distributed conceptual model for Medway catchment	
	Arnell (2011)	21 CMIP3 GCMs		Cat-PDM conceptual model for 6 catchments	
	Charlton and Arnell (2011)	UKCP09 climate change scenarios		Cat-PDM conceptual model for 6 catchments	
	Christierson et al. (2012)	UKCP09 climate change scenarios	SRES A1B	PDM lumped conceptual rainfall runoff model and CATCHMOD semi-distributed conceptual model for 70 catchments	
	Bell et al. (2012)	UKCP09 climate change scenarios	SRES A1B	G2G model Thames basin	−11 to +68 %
	Kay and Jones (2012)	Perturbed parameter ensemble of 1 RCM		Nationwide grid-based runoff and routing model UK	
	Smith et al. (2014)	18 RCMs from ENSEMBLES and UKCP09	SRES A1B	HBV-light lumped conceptual rainfall runoff model Avon catchment	−1 to +23 %

(continued)

Table 7.2 (continued)

Region	Source	GCM-RCM(s) considered	Greenhouse gas scenario(s)	Hydrological-hydraulic impact model(s)	Change in river peak flow by 2100
UK and NW Europe	Prudhomme et al. (2012)	3 GCMs: ECHAM5, IPSL, CNRM		Global hydrological models JULES, MPI-HM, WaterGAP (WaterMIP project)	
Larger rivers in Europe	Dankers and Feyen (2008), Feyen and Dankers (2009), Rojas et al. (2011, 2012)	HIRHAM5 and 12 ENSEMBLES RCM runs	SRES A2, A1B	Coarse scale spatially distributed model LISFLOOD	Dependent on sub-region
Europe	Schneider et al. (2013)	3 GCMs	SRES A2	Global hydrological model WaterGAP3	Dependent on sub-region
Globe	Arnell and Gosling (2016)	1 GCM: HadCM3	SRES A1B	Water balance model Mac-PDM.09	Dependent on sub-region
	Dankers et al. (2014)	5 GCMs	RCP8.5	9 global water balance models (from WaterMIP)	Dependent on sub-region
	Prudhomme et al. (2014)	5 GCMs	RCP2.6, 8.5	9 global water balance models	
	Hirabayashi et al. (2013)	11 GCMS	RCPs	global river routing model with inundation scheme	Dependent on sub-region

two- to four-fold higher than the increase in precipitation, and that the total sewer overflow volume is 1.5- to three-fold higher. They also found that the number of overflowing manholes and number of surcharging sewers may change dramatically, but the precise magnitude of change in response to the change in precipitation is uncertain.

Willems (2013a) found that for sewer systems in Flanders, Belgium, built for design storms with return periods of two to 20 years, that the present-day design storms would increase for the high-tailored climate scenario by +15 to +50 % depending on the return period (range 1 month to 10 years) (Fig. 7.12). For the mean-tailored scenario, the changes were less: from +4 to +15 %. For the high scenario, the return period of sewer flooding increases by about a factor 2.

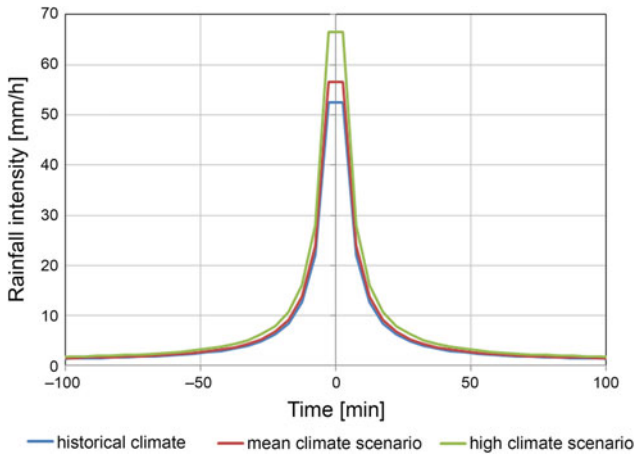

Fig. 7.12 Change in the design storm for sewer systems in Flanders, Belgium, for a 2-year return period for high and mean climate scenarios (Willems 2013a)

For the Windermere drainage area in NW England, Abdellatif et al. (2014) concluded based on the UKCP09 scenarios that an increase in the design storm of as little as 15 % is projected to cause an increase of about 40 % in flood volume due to surface flooding. However, impacts on house basements showed a damping effect (a 35 % increase in design storm leads to 16 % in the number of basements at risk of flooding). This confirms that the precise effects of climate change strongly depend on the type of impacts studies and the specific properties of the sewer system.

The impacts of climate change on sewer flood and overflow frequencies and volumes show wide variation. Studies indicate a range from a four-fold increase to as low as a 5 % increase, depending on the system characteristics (Willems et al. 2012a, b). Floods and overflows occur when runoff or sewer flow thresholds are exceeded. Given that the response of the sewer system to rainfall may be highly non-linear, the changes in the sewer response may be much stronger than the changes in rainfall. And the impact ranges can even by wider when studying the impacts of sewer overflows on receiving rivers. Sewer overflow mainly occurs in summer and as models project the likelihood of lower river flow in summer in north-western Europe, dilution effects in the receiving water might be less, thus increasing impacts on river water quality and aquatic life. Astaraie-Imani et al. (2012) found for a semi-real case study in the UK that changes in rain storm depth and peak rainfall intensity of up to +30 % by the 2080s could cause strong deterioration in river water quality; an increase in rain storm depth of 30 % led to an increase in river ammonium concentration of about 40 % and a decrease in dissolved oxygen concentration of about 80 %. This was found to correspond with a strong increase in the frequency of breaching given concentration thresholds (i.e. immission standards). The

frequency of breaching the dissolved oxygen threshold of 4 mg l^{-1} increased from 49 to 99 %; the frequency of exceeding the ammonium threshold of 4 mg l^{-1} increased from 45 to 79 %. The effect of changes in peak rainfall intensity was found to be an order of magnitude lower.

Climate-driven changes in large-scale atmospheric circulation and related wind fields may cause significant changes in the amount and type of sediment on catchment surfaces available for wash-off into urban drainage systems. Higher deposition during prolonged dry periods will increase pollution concentrations in first flushes. This will lead to higher pollution loads in sewer overflows and in inflow to wastewater treatment plants; the latter leading to higher solids loads to clarifiers, different treatment efficiencies and higher pollution loads. Downstream of the treatment plants, receiving rivers during long dry spells in future summers may have reduced capacity to assimilate the more concentrated effluent. Prolonged dilute loading of wastewater treatment plants due to low-intensity long-duration precipitation events can also affect wastewater treatment with potential for major impacts on overall treatment (Plosz et al. 2009).

Changes other than those related to climate may also occur in urban areas and affect or strengthen urban drainage impacts. For example, changes in pavement surfaces, and these should not be seen in isolation but as related to population growth and increase in welfare, and thus partly interrelated with anthropogenic climate change. Semadeni-Davies et al. (2008) analysed the combined impact of climate change and increased urbanisation in Helsingborg, Sweden, and found that this could result in a four-fold increase in sewer overflow volumes. Using a similar approach, Olsson et al. (2010) analysed future loads on the main combined sewer system in Stockholm, Sweden, due to climate change and population increase. They estimated annual total inflow to the treatment plant to increase by 15–20 %, sewer overflow volumes to increase by 5–10 % and critically high water levels to increase by 10–20 % in the first half of the century. For the latter half of the century, they found no further increase in total inflow, but a 20–40 % increase in sewer overflow volumes and a 30–40 % increase in high water levels (within the sewer system). Both studies highlighted the importance of addressing climate change impacts in combination with other key non-stationary drivers of equal importance (e.g. urbanisation trends, sewer system or management changes). In fact, the study by Semadeni-Davies et al. (2008) clearly showed that climate change is not the most important driver of increased pollution levels, and that increases in damage may be effectively counterbalanced by measures not solely related to urban drainage.

Tait et al. (2008) confirmed that increased urbanisation (related to increased population and economic growth) also had a significant impact on urban runoff. For a typical urban area in the UK, in addition to climate change they assumed that paved areas would increase by about 25 % of their current value and roof areas by about 10 %. Model simulations showed that sewer overflow volumes would increase by about 15–20 % when only the increase in paved areas is considered. These changes are comparable to those expected from climate change.

Climatic variability at multi-decadal time scales has been detected by several authors (Stahl et al. 2010, 2012; Hannaford et al. 2012; Boé and Habets 2013; Willems 2013b). This must also be considered, given that it could temporarily limit, reverse or even increase the long-term impacts of climate change (Boé and Habets 2013).

7.4 Conclusion

Hydrological extremes are projected to become more intense. These changes are largely driven by changes in precipitation, which RCM rainfall projections for the North Sea region suggest will become significantly more intense (see Chap. 5; Van der Linden and Mitchell 2009). Future winters are expected to see both an increase in the volume and intensity of precipitation. The intensity of summer extremes may also increase albeit with a reduction in overall volume. These findings are consistent with recent observations at some monitoring stations that show winter extremes in high river flow are already increasing (see Chap. 4).

Quantifying future changes in hydrology is difficult. This reflects the high uncertainties in model output: mainly due to uncertainties in the climate processes, and—to a lesser extent—in knowledge of the hydrological processes and their schematisation in hydrological impact models. The impact uncertainties also reflect the level of uncertainties in future greenhouse gas emissions and concentrations.

Taking the uncertainties into account, the reported overview of impact results for rivers in the North Sea region in Table 7.2, indicates increases in river peak flow by 2100 of up to +30 % for many rivers and even higher for some. An increase in river peak flows is more evident for the northern basins of the North Sea region. The greatest increases are projected for catchments in south-western Norway, up to +70 % for 200-year peak flows. In snow-dominated catchments of Norway and southern Sweden, earlier spring flooding is projected. These spring floods do not always increase, however, peak flows from snowmelt may decrease when higher spring temperatures lead to reduced snow storage. Decreasing snowmelt-induced spring flow, and increased rain-fed flow in winter and autumn may change the seasonality of peak flows and floods. In northern France and Belgium, an increase in river peak flow is less clear in that not all models project an increase. Hence, the spatial differences mainly occur in a north-south direction. The

position of a river basin relative to the ocean is also important. Allan et al. (2005) found that the greater the proximity the greater the potential damping of any climate change effect.

The impacts of climate change on sewer flood and overflow frequencies and volumes vary widely. The specific characteristics of an urban drainage system will dictate whether the net result of the projected increase in, for example, short-duration rainfall extremes is to damp or amplify these changes in precipitation. The precise amplitude of response is highly uncertain and non-linear. The combined impact of climate change and increased urbanisation in some parts of the North Sea region could result in as much as a four-fold increase in sewer overflow volumes.

References

Abdellatif M, Atherton W, Alkhaddar R, Osman Y (2014) Application of the UKCP09 WG outputs to assess performance of combined sewers system in a changing climate. J Hyd Eng, doi:10.1061/(ASCE)HE.1943-5584.0001129

Allan JD, Palmer MA, Poff NL (2005) Climate change and freshwater ecosystems. In: Climate Change and Biodiversity. Yale University Press

Andersen HE, Kronvang B, Larsen SE, Hoffmann CC, Jensen TS, Rasmussen EK (2006) Climate-change impacts on hydrology and nutrients in a Danish lowland river basin. Sci Total Environ 65:223–237

Andréasson J, Bergström S, Gardelin M, German J, Gustavsson H, Hallberg K, Rosberg J (2011) Dimensionerande flöden för dammanläggningar för ett klimat i förändring - metodutveckling och scenarier [Design floods for dams in a changing climate – methods and scenarios]. Elforsk rapport 11:25, Stockholm

Arnbjerg-Nielsen K (2012) Quantification of climate change effects on extreme precipitation used for high resolution hydrologic design. Urban Water J 9:57–65

Arnbjerg-Nielsen K, Fleischer HS (2009) Feasible adaptation strategies for increased risk of flooding in cities due to climate change. Water Sci Technol 60:273–281

Arnbjerg-Nielsen K, Willems P, Olsson J, Beecham S, Pathirana A, Bülow Gregersen I, Madsen H, Nguyen VTV (2013) Impacts of climate change on rainfall extremes and urban drainage systems: a review. Water Sci Technol 68:16–28

Arnell NW (2011) Uncertainty in the relationship between climate forcing and hydrological response in UK catchments. Hyd Earth Sys Sci 15:897–912

Arnell NW, Gosling SN (2016) The impacts of climate change on river flood risk at the global scale. Climatic Change 134(3):387–401

Ashley RM, Clemens FHLR, Tait SJ, Schellart A (2008) Climate change and the implications for modeling the quality of flow in combined sewers. Proceedings of the 11th International Conference on Urban Drainage, 31 August - 5 September 2008, Edinburgh, Scotland

Astaraie-Imani M, Kapelan Z, Fu G, Butler D (2012) Assessing the combined effects of urbanisation and climate change on the river water quality in an integrated urban wastewater system in the UK. J Environ Manage 112:1–9

Bastola S, Murphy C, Sweeney J (2011) The sensitivity of fluvial flood risk in Irish catchments to the range of IPCC AR4 climate change scenarios. Sci Total Environ 409:5403–5415.

Bates BC, Kundzewicz ZW, Wu S, Palutikof JP (eds) (2008) Climate change and water. Technical Paper of the Intergovernmental Panel on Climate Change, IPCC Secretariat, Geneva

Bell VA, Kay AL, Cole SJ, Jones RG, Moore RJ, Reynard NS (2012) How might climate change affect river flows across the Thames Basin? An area-wide analysis using the UKCP09 Regional Climate Model ensemble. J Hydrol 442-443:89–104

Boé J, Habets F (2013) Multi-decadal river flows variations in France. Hydrol Earth Syst Sc Disc 10:11861–11900

Boé J, Terray L, Martin E, Habets F (2009) Projected changes in components of the hydrological cycle in French river basins during the 21st century. Water Resour Res 45:W08426 doi:10.1029/2008WR007437

Boukhris O, Willems P, Vanneuville W (2008) The impact of climate change on the hydrology in highly urbanized Belgian areas. Proceedings International Conference on 'Water & Urban Development Paradigms: Towards an integration of engineering, design and management approaches', Leuven, 15-17 September

Brisson E, Demuzere M, Willems P, van Lipzig N (2015) Assessment of natural climate variability using a weather generator. Clim Dynam 44:495–508

Brouyére S, Carabin G, Dassargues A (2004) Climate change impacts on groundwater resources: modelled deficits in a chalky aquifer, Geer basin, Belgium. Hydrogeol J 12:123–134

Cameron (2006) An application of the UKCIP02 climate change scenarios to flood estimation by continuous simulation for a gauged catchment in the northeast of Scotland, UK (with uncertainty). J Hydrol 328:212–226

Charlton MB, Arnell NW (2011) Adapting to climate change impacts on water resources in England - An assessment of draft Water Resources Management Plans. Global Environ Chang 21:238–248

Christierson BV, Vidal JP, Wade SD (2012) Using UKCP09 probabilistic climate information for UK water resource planning. J Hydrol 424-425:48–67

Chun KP, Wheater HS, Onof CJ (2009) Streamflow estimation for six UK catchments under future climate scenarios. Hydrol Res 40:96–112

Cloke HL, Jeffers C, Wetterhall F, Byrne T, Lowe J, Pappenberger F (2010) Climate impacts on river flow: projections for the Medway catchment, UK, with UKCP09 and CATCHMOD. Hydrol Process 24:3476–3489

Collins M (2007) Ensembles and probabilities: a new era in the prediction of climate change. Phil Trans R Soc A 365:1957–1970

Dams J, Salvadore E, Van Daele T, Ntegeka V, Willems P, Batelaan O (2012) Spatio-temporal impact of climate change on the groundwater system. Hydrol Earth Syst Sc 16:1517–1531

Dankers R, Feyen L (2008) Climate change impact on flood hazard in Europe: An assessment based on high-resolution climate simulations. J Geophys Res 113:D19105. doi:10.1029/2007JD009719

Dankers R, Arnell NW, Clark DB, Falloon PD, Fekete BM, Gosling SN, Heinke J, Kim H, Masaki Y, Satoh Y, Stacke T, Wada Y, Wisser D (2014) First look at changes in flood hazard in the Inter-Sectoral Impact Model Intercomparison Project ensemble. PNAS 111:3257–3261

de Wit M, Buiteveld H, van Deursen W (2007) Klimaatverandering en de afvoer van Rijn en Maas [Climate change and the discharge of the Rhine and Meuse]. Memo WRR/2007-006, RIZA, Netherlands

Diaz-Nieto J, Wilby RL (2005) A comparison of statistical downscaling and climate change factor methods: Impacts on low flows in the River Thames, United Kingdom. Climatic Change 69: 245–268

Ducharne A, Sauquet E, Habets F, Deque M, Gascoin S, Hachour A, Martin E, Oudin L, Page C, Terray L, Thiery D, Viennot P (2011) Evolution potentielle du régime des crues de la Seine sous changement climatique. Houille Blanche 1:51–57

EEA (2012) Climate change, impacts and vulnerability in Europe 2012: An indicated based report – Summary. European Environment Agency, Copenhagen

Feyen L, Dankers R (2009) Impact of global warming on streamflow drought in Europe. J Geophys Res 114:D17116. doi:10.1029/2008JD011438

Feyen L, Dankers R, Bódis K, Salamon P, Barredo JI (2012) Fluvial flood risk in Europe in present and future climates. Climatic Change 112:47–62

Fowler HJ, Kilsby CG (2007) Using regional climate model data to simulate historical and future river flows in northwest England. Climatic Change 80:337–367

Goderniaux P, Brouyére S, Fowler HJ, Blenkinsop S, Therrien R, Orban P, Dassargues A (2009) Large scale surface-subsurface hydrological model to assess climate change impacts on groundwater reserves. J Hydrol 373:122–138

Good P, Barring L, Giannakopoulos C, Holt T, Palutikof J (2006) Non-linear regional relationships between climate extremes and annual mean temperatures in model projections for 1961-2099 over Europe. Clim Res 31:19–34

Gosling S, Taylor RG, Arnell N, Todd MC (2011) A comparative analysis of projected impact of climate change on river runoff from global and catchment-scale hydrological models. Hydrol Earth Syst Sc 15:279–294

Gudmundsson L, Bremnes JB, Haugen JE, Engen-Skaugen T (2012a) Technical Note: Downscaling RCM precipitation to the station scale using statistical transformations - a comparison of methods. Hydrol Earth Syst Sc 16:3383–3390

Gudmundsson L, Tallaksen LM, Stahl K, Clark DB, Dumont E, Hagemann S, Bertrand N, Gerten D, Heinke J, Hanasaki N, Voss F, Koirala S (2012b) Comparing large-scale hydrological model simulations to observed runoff percentiles in Europe. J Hydrometeorol 13:604–620

Habets F, Boé J, Déqué M, Ducharne A, Gascoin S, Hachour A, Martin E, Pagé C, Sauquet E, Terray L, Thiéry D, Oudin L, Viennot P (2013) Impact of climate change on the hydrogeology of two basins in Northern France. Climatic Change 121:771–785

Hannaford J, Buys G, Stahl K, Tallaksen LM (2012) The influence of decadal-scale variability on trends in long European streamflow records. Hydrol Earth Syst Sc Disc 10:1859–1896

Hanson CE, Palutikof JP, Livermore MTJ, Barring L, Bindi M, Corte-Real J, Durao R., Giannakopoulos C, Good P, Holt T, Kundzewicz Z, Leckebusch GC, Moriondo M., Radziejewski M, Santos J, Schlyter P, Schwarb M, Stjernquist I, Ulbrich U (2007) Modelling the impact of climate extremes: an overview of the MICE project. Climatic Change 81:163–177

Henriques C, Holman IP, Audsley E, Pearn K (2008) An interactive multiscale integrated assessment of future regional water availability for agricultural irrigation in East Anglia and North West England. Climatic Change 90:89–111

Herrera-Pantoja M, Hiscock KM (2008) The effects of climate change on potential groundwater recharge in Great Britain. Hydrol Process 22:73–86

Hirabayashi Y, Mahendran R, Koirala S, Konoshima L, Yamazaki D, Watanabe S, Kim H, Kanae S (2013) Global flood risk under climate change. Nat Climate Chang 3:816–821

Huang S, Hattermann FF, Krysanova V, Bronstert A (2013) Projections of climate change impacts on river flood conditions in Germany by combining three different RCMs with a regional eco-hydrological model. Climatic Change 116:631–663

Hulme M, Jenkins GJ, Lu X, Turnpenny JR, Mitchell TD, Jones RG, Lowe J, Murphy JM, Hassell D, Boorman P, McDonald R, Hill S (2002) Climate Change Scenarios for the United Kingdom: The UKCIP02 Scientific Report. Tyndall Centre for Climate Change Research, School of Environmental Sciences, University of East Anglia, Norwich, UK

IPCC (2014) Climate Change 2014: Impacts, Adaptation, and Vulnerability. Part A: Global and Sectoral Aspects. Contribution of Working Group II to the Fifth Assessment Report of the Intergovernmental Panel on Climate Change - Chapter 3: Freshwater Resources. Intergovernmental Panel on Climate Change, University Press

Karlsson IB, Sonnenborg TO, Jensen KH, Refsgaard JC (2013) Evaluating the influence of long term historical climate change on catchment hydrology – using drought and flood indices. Hydrol Earth Syst Sc Disc 10:2373–2428

Kay AL, Jones DA (2012) Transient changes in flood frequency and timing in Britain under potential projections of climate change. Int J Climatol 32:489–502

Kay AL, Jones RG, Reynard NS (2006) RCM rainfall for UK flood frequency estimation. II. Climate change results. J Hydrol 318:163–172

Kay AL, Davies HN, Bell VA, Jones RG (2009) Comparison of uncertainty sources for climate change impacts: flood frequency in England. Climatic Change 92:41–63

Kendon EJ, Roberts NM, Senior CA, Roberts MJ (2012) Realism of rainfall in a very high-resolution regional climate model. J Climate 25:5791–5806

Keupers I, Willems P (2013) Urbanization versus climate change: impact analysis on the river hydrology of the Grote Nete catchment in Belgium. Water Sci Technol 67:2670–2676

Kundzewicz ZW, Radziejewski M, Pinskwar I (2006) Precipitation extremes in the changing climate of Europe. Clim Res 31:51–58

Kundzewicz ZW, Kanae S, Seneviratne SI, Handmer J, Nicholls N, Peduzzi P, Mechler R, Bouwer LM, Arnell N, Mach K, Muir-Wood R, Brakenridge GR, Kron W, Benito G, Honda Y, Takahashi K, Sherstyukov B (2013) Flood risk and climate change: global and regional perspectives. Hydrolog Sci J 59:1–28

Larsen AN, Gregersen IB, Christensen OB, Linde JJ, Mikkelsen PS (2009) Potential future increase in extreme one-hour precipitation events over Europe due to climate change. Water Sci Technol 60:2205–2216

Lawrence D, Hisdal H (2011) Hydrological projections for floods in Norway under a future climate. Report no. 5-2011, Norwegian Water Resources and Energy Directorate

Lawrence D, Haddeland I, Langsholt E (2009) Calibration of HBV hydrological models using PEST parameter estimation. Report no. 1-2009, Norwegian Water Resources and Energy Directorate

Leander R, Buishand TA, van den Hurk BJJM, de Wit MJM (2008) Estimated changes in flood quantiles of the river Meuse from resampling of regional climate model output. J Hydrol 351:331–343

Lenderink G, Buishand A, van Deursen W (2007) Estimates of future discharges of the river Rhine using two scenario methodologies: direct versus delta approach. Hydrol Earth Syst Sc 11:1145–1159

Maraun D, Wetterhall F, Ireson AM, Chandler RE, Kendon EJ, Widmann M, Brienen S, Rust HW, Sauter T, Themeßl M, Venema VKC, Chun KP, Goodess CM, Jones RG, Onof C, Vrac M, Thiele-Eich I (2010) Precipitation downscaling under climate change: Recent developments to bridge the gap between dynamical models and the end user. Rev Geophys, AGU, 48: RG3003. doi:10.1029/2009RG000314

Mark O, Svensson G, König A, Linde JJ (2008) Analyses and adaptation of climate change impacts on urban drainage systems. Proceedings of the 11th International Conference on Urban Drainage, 31 August – 5 September 2008, Edinburgh, Scotland

May W (2008) Potential future changes in the characteristics of daily precipitation in Europe simulated by the HIRHAM regional climate model. Clim Dynam 30:581–603

MetOffice (2011) Climate: Observations, projections and impacts, Subreports for United Kingdom, France, Germany. UK MetOffice

Minville M, Brissette F, Leconte R (2008) Uncertainty of the impact of climate change on the hydrology of a Nordic watershed. J Hydrol 358:70–83

Monbaliu J, Chen Z, Felts D, Ge J, Hissel F, Kappenberg J, Narayan S, Nicholls RJ, Ohle N, Schuster D, Sothmann J, Willems P (2014) Risk assessment of estuaries under climate change: lessons from Western Europe. Coast Eng 87:32–49

Murphy JM, Sexton DMH, Jenkins GJ, Booth BBB, Brown CC, Clark RT, Collins M, Harris GR, Kendon EJ, Betts RA, Brown SJ, Humphrey KA, McCarthy MP, McDonald RE, Stephens A, Wallace C, Warren R, Wilby R, Wood RA (2009) Climate change projections. UK Climate Projections Science Report. UK Met Office Hadley Centre

New M, Cuellar M, Lopez A (2007) Probabilistic regional and local climate projections: false dawn for impacts assessment and adaptation? In: Integrating Analysis of Regional Climate Change and Response Options, Nadi, Fiji

Nie L, Lindholm O, Lindholm G, Syversen E (2009) Impacts of climate change on urban drainage systems – a case study in Fredrikstad, Norway. Urban Water J 6:323–332

Niemczynowicz J (1989) Impact of the greenhouse effect on sewerage systems – Lund case study. Hydrolog Sci J 34:651–666

Ntegeka V, Willems P, Monbaliu J (2011) Incorporating the correlation between upstream inland, downstream coastal and surface boundary conditions into climate scenarios for flood impact analysis along the river Scheldt. Geophysical Research Abstracts, EGU2011-6554: EGU General Assembly 2011, Vienna, April 2011

Ntegeka V, Decloedt LC, Willems P, Monbaliu J (2012) Quantifying the impact of climate change from inland, coastal and surface conditions. In: Comprehensive Flood Risk Management – Research for Policy and Practise (Klijn F, Schweckendiek T, eds), CRC Press

Ntegeka V, Baguis P, Roulin E, Willems P (2014) Developing tailored climate change scenarios for hydrological impact assessments. J Hydrol 508:307–321

Olsson J, Berggren K, Olofsson M, Viklander M (2009) Applying climate model precipitation scenarios for urban hydrological assessment: A case study in Kalmar City, Sweden. Atmos Res 92:364–375

Olsson J, Dahné J, German J, Westergren B, von Scherling M, Kjellson L, Ohls F, Olsson A (2010) A study of future discharge load on Stockholm's main sewer system, SMHI Reports Climatology 3 (in Swedish)

Palmer TN, Räisänen J (2002) Quantifying the risk of extreme seasonal precipitation events in a changing climate. Nature 415:512–514

Pfister L, Kwadijk J, Musy A, Bronstert A, Hoffmann L (2004) Climate change, land use change and runoff prediction in the Rhine-Meuse basins. River Res Appl 20:229–241

Plosz BG, Liltved H, Ratnaweera H (2009) Climate change impacts on activated sludge wastewater treatment: a case study from Norway. Water Sci Technol 60:533–541

Prudhomme C, Williamson J, Parry S, Hannaford J (2012) Projections of flood risk in Europe. In: Changes in Flood Risk in Europe, CRC Press

Prudhomme C, Giuntoli I, Robinson EL, Clark DB, Arnell NW, Dankers R, Fekete BM, Franssen W, Gerten D, Gosling SN, Hagemann S, Hannah DM, Kim H, Masaki Y, Satoh Y, Stacke T, Wada Y, Wisser D (2014) Hydrological droughts in the 21st century, hotspots and uncertainties from a global multimodel ensemble experiment. PNAS 111:3262–3267

Raupach MR, Marland G, Ciais P, Le Quéré C, Canadell JG, Klepper G, Field CB (2007) Global and regional drivers of accelerating CO_2 emissions. Proc Nat Acad Sci 104:10288–10293

Refsgaard JC, Madsen H, Andréassian V, Arnbjerg-Nielsen K, Davidson TA, Drews M, Hamilton D, Jeppesen E, Kjellström E, Olesen JE, Sonnenborg TO, Trolle D, Willems P, Christensen JH (2014) A framework for testing the ability of models to project climate change and its impacts. Climatic Change 122:271–282

Rojas R, Feyen L, Dosio A, Bavera D (2011) Improving pan-European hydrological simulation of extreme events through statistical bias correction of RCM-driven climate simulations. Hydrol Earth Syst Sc 15:2599–2620

Rojas R, Feyen L, Bianchi A, Dosio A (2012) Assessment of future flood hazard in Europe using a large ensemble of bias corrected regional climate simulations. J Geophys Res 117:D17109. doi:10.1029/2012JD017461

SAWA (2012) Climate change impacts and uncertainties in flood risk management: Examples from the North Sea Region. Report no. 05 – 2012 of SAWA Interreg IVB Project, Norwegian Water Resources and Energy Directorate

Schneider C, Laizé CLR, Acreman MC, Flörke M (2013) How will climate change modify river flow regimes in Europe? Hydrol Earth Syst Sc 17:325–339

Seibert J (2003) Reliability of model predictions outside calibration conditions. Nordic Hyd 34:477–492

Semadeni-Davies A, Hernebring C, Svensson G, Gustafsson LG (2008) The impacts of climate change and urbanisation on drainage in Helsingborg, Sweden: Combined sewer system. J Hydrol 350:100–113

Semenov MA, Stratonovitch P (2010) Use of multi-model ensembles from global climate models for assessment of climate change impacts. Clim Res 41:1–14

Shabalova MV, van Deursen WP, Buishand TA (2003) Assessing future discharge of the river Rhine using regional climate model integrations and a hydrological model. Clim Res 23:233–246

Shaffrey LC, Stevens I, Norton WA, Roberts MJ, Vidale PL, Harle JD, Jrrar A, Stevens DP, Woodage MJ, Demory ME, Donners J, Clark DB, Clayton A, Cole JW, Wilson SS, Connolley WM, Davies TM, Iwi AM, Johns TC, King JC, New AL, Slingo JM, Slingo A, Steenman-Clark L, Martin GM, (2009) UK HiGEM: The new UK High-resolution Global Environment Model - Model description and basic evaluation. J Climate 22:1861–1896

Smith JB, Schneider SH, Oppenheimer M, Yohe GW, Hare W, Mastrandrea MD, Patwardhan A, Burton I, Corfee-Morlot J, Magadza CHD, Füssel HM, Pittock AB, Rahman A, Suarez A, van Ypersele JP (2009) Assessing dangerous climate change through an update of the Intergovernmental Panel on Climate Change (IPCC) "reasons for concern". PNAS 106:4133–4137

Smith A, Freer J, Bates P, Sampson C (2014) Comparing ensemble projections of flooding against flood estimation by continuous simulation. J Hydrol 511:205–219

Stahl K, Hisdal H, Hannaford J, Tallaksen LM, van Lanen HAJ, Sauquet E, Demuth S, Fendekova M, Jódar J (2010) Streamflow trends in Europe: evidence from a dataset of near-natural catchments. Hydrol Earth Syst Sc 14:2367–2382

Stahl K, Tallaksen LM, Hannaford J, van Lanen HAJ (2012) Filling the white space on maps of European runoff trends: estimates from a multi-model ensemble. Hydrol Earth Syst Sc 16:2035–2047

Tait SJ, Ashley RM, Cashman A, Blanksby J, Saul AJ (2008) Sewer system operation into the 21st century, study of selected responses from a UK perspective. Urban Water J 5:77–86

Tavakoli M, De Smedt F, Vansteenkiste Th, Willems P (2014) Impact of climate change and urban development on extreme flows in the Grote Nete watershed, Belgium. Nat Hazards 71:2127–2142

Tebaldi C, Smith R, Nychka D, Mearns L (2005) Quantifying uncertainty in projections of regional climate change: a Bayesian approach to the analysis of multi-model ensembles. J Climate 18:1524–1540

Teutschbein C, Seibert J (2012) Bias correction of regional climate model simulations for hydrological climate-change impact studies: Review and evaluation of different methods. J Hydrol 456-457:12–29

Teutschbein C, Wetterhall F, Seibert J (2011) Evaluation of different downscaling techniques for hydrological climate-change impact studies at the catchment scale. Clim Dynam 37:2087–2105

Thodsen H (2007) The influence of climate change on stream flow in Danish rivers. J Hydrol 333:226–238

Thompson JR, Gavin H, Refsgaard A, Refstrup Sørenson H, Gowing DJ (2009) Modelling the hydrological impacts of climate change on UK lowland wet grassland. Wetl Ecol Manag 17:503–523

van den Hurk B, Tank AK, Lenderink G, van Ulden A, van Oldenborgh GJ, Katsman C., van den Brink H, Keller F, Bessembinder J, Burgers G, Komen G, Hazeleger W, Drijfhout S (2006) KNMI Climate Change Scenarios 2006 for the Netherlands, KNMI Scientific Report WR 2006-01, KNMI, De Bilt, The Netherlands

Van der Linden P, Mitchell JFB (2009) ENSEMBLES: Climate Change and its Impacts: Summary of research and results from the ENSEMBLES project, UK Met Office Hadley Centre

van Huijgevoort MHJ, van Lanen HAJ, Teuling AJ, Uijlenhoet R (2014) Identification of changes in hydrological drought characteristics from a multi-GCM driven ensemble constrained by observed discharge. J Hydrol 512:421–434

van Oldenborgh GJ, Drijfhout S, Ulden A, Haarsma R, Sterl A, Severijns C, Hazeleger W, Dijkstra H (2009) Western Europe is warming much faster than expected. Clim Past 5:1–12

van Pelt SC, Beersma JJ, Buishand TA, van den Hurk, BJJM, Kabat P (2012) Future changes in extreme precipitation in the Rhine basin based on global and regional climate model simulations. Hydrol Earth Syst Sc 16:4517–4530

Van Steenbergen N, Willems P (2012) Method for testing the accuracy of rainfall-runoff models in predicting peak flow changes due to rainfall changes, in a climate changing context. J Hydrol 414-415:425–434

Vansteenkiste Th, Tavakoli M, Ntegeka V, Willems P, De Smedt F, Batelaan O (2013) Climate change impact on river flows and catchment hydrology: a comparison of two spatially distributed models. Hydrol Process 27:3649–3662

Vansteenkiste Th, Tavakoli M, Ntegeka V, De Smedt F, Batelaan O, Pereira F, Willems P (2014) Intercomparison of hydrological model structures and calibration approaches in climate scenario impact projections. J Hydrol 519:743–755

Vidal JP, Wade SD (2008) Multimodel projections of catchment-scale precipitation regime. J Hydrol 353:143–158

Vörösmarty CJ, McIntyre PB, Gessner MO, Dudgeon D, Prusevich A, Green P, Glidden S, Bunn SE, Sullivan CA, Liermann CR, Davies PM (2010) Global threats to human water security and river biodiversity. Nature 467:555–561

Ward PJ, Jongman B, Weiland FS, Bouwman A, van Beek R, Bierkens PFP, Ligtvoet W, Winsemius HC (2013) Assessing flood risk at the global scale: model setup, results and sensitivity. Env Res Lett 8:044019. doi:10.1088/1748-9326/8/4/044019

Warren R, Arnell N, Berry P, Brown S, Dicks L, Gosling S, Hankin R, Hope C, Lowe J, Matsumoto K, Masui T, Nicholls R, O'Hanley J, Osborn T, Scriecru S (2010) The economics and climate change impacts of various greenhouse gas emissions pathways: A comparison between baseline and policy emissions scenarios. Work stream 1, Deliverable 3, Report 1 of the AVOID programme (AV/WS1/D3/R01)

Weisse R, Bellafiore D, Menendez M, Mendez F, Nicholls R, Umgiesser G, Willems P (2014) Changing extreme sea levels along European coasts. Coast Eng 87:4–14

Willems P (2009) A time series tool to support the multi-criteria performance evaluation of rainfall-runoff models. Environ Modell Softw 24:311–321

Willems P (2013a) Revision of urban drainage design rules after assessment of climate change impacts on precipitation extremes at Uccle, Belgium. J Hydrol 496:166–177

Willems P (2013b) Multidecadal oscillatory behaviour of rainfall extremes in Europe. Climatic Change 120:931–944

Willems P, Arnbjerg-Nielsen K, Olsson J, Nguyen VTV (2012a) Climate change impact assessment on urban rainfall extremes and urban drainage: methods and shortcomings. Atmos Res 103:106–118

Willems P, Olsson J, Arnbjerg-Nielsen K, Beecham S, Pathirana A, Bülow Gregersen I, Madsen H, Nguyen VTV (2012b) Impacts of Climate Change on Rainfall Extremes and Urban Drainage. IWA Publishing

Zhou Q, Mikkelsen PS, Halsnæs K, Arnbjerg-Nielsen K (2012) Framework for economic pluvial flood risk assessment considering climate change effects and adaptation benefits. J Hydrol 414-415:539–549

Part III

Impacts of Recent and Future Climate Change on Ecosystems